TECHNISCHE UNIVERSITÄT MÜNCHEN

TUM School of Life Sciences der Technischen Universität München

Lehrstuhl für Technische Mikrobiologie

Interaction of modified atmosphere packaging gases and meat-spoiling bacteria

Sandra Kolbeck

Vollständiger Abdruck der von der TUM School of Life Sciences der Technischen Universität München zur Erlangung des akademischen Grades einer

Doktorin der Naturwissenschaften (Dr. rer. nat.)

genehmigten Dissertation.

Vorsitzender:	Prof. Dr. Jürgen Geist
Prüfer der Dissertation:	1. Prof. Dr. Rudi F. Vogel
	2. Prof. Dr. Wolfgang Liebl
	3. Prof. Dr. Jochen Weiss

Die Dissertation wurde am 18.05.2021 bei der Technischen Universität München eingereicht und durch die TUM School of Life Sciences am 31.08.2021 angenommen.

Interaction of modified atmosphere packaging gases and meat-spoiling bacteria

Sandra Kolbeck

„Nicht nörgeln und schnörkeln, sondern lachen und machen!“

- Cäsar Flaischlen –

Doctoral thesis

Freising, 2021

Vorwort und Danksagung:

Die vorliegende Arbeit wurde gefördert vom Bundesministerium für Wirtschaft und Energie (BMWi) über die Arbeitsgemeinschaft industrieller Forschungsvereinigungen (AiF) und die Industrievereinigung für Lebensmitteltechnologie und Verpackung e. V. (IVLV) im Rahmen des Projektes AiF 19993N.

Ich möchte mich bei einigen Personen sehr herzlich bedanken, welche meine Erfahrungen und meinen positiven Rückblick auf die Promotionszeit maßgeblich geprägt haben:

- Mein persönlicher Dank gilt **Prof. Dr. Rudi F. Vogel** für die Antragstellung des Promotionsthemas und der Finanzierung, sowie der umfassenden Betreuung und Unterstützung während der gesamten Promotionszeit.
- Des Weiteren möchte ich **Dr. Maik Hilgarth** für sein offenes Ohr und der hervorragenden Betreuung während der letzten Jahre danken.
- Ein herzliches Dankeschön gilt auch meinen Kolleginnen der „Fleisch"-Gruppe: **Sandra Fuertes Perez**, **Philippa Hauschild** und **Viktoria Werum** für die tolle Zusammenarbeit in inter-Projekt spezifischen Fragestellungen sowie der entstandenen freundschaftlichen Beziehungen.
- **Allen Angestellten des Lehrstuhls**, besonders aber meinem Büro 36 **(Magdalena Mann, Lisa Frisch und Esther Rogalski)**, die zu einem hervorragenden Arbeitsklima beigetragen haben, möchte ich ebenfalls von Herzen Danke sagen.
- Zuletzt gilt mein Dank **meiner Familie und meinem Freund**, welche mich stets in meinem Handeln unterstützt und ermutigt haben.

Ein herzlicher Dank euch allen!

Abbreviations

°C	Degree Celsius	**ml**	Milliliter
µ	Micro (10^{-6})	**mm**	Millimeter
A	Surface	**ms**	Meter per second
ADI	Arginine deiminase	**MS**	Mass spectrometer
ANOVA	Analysis of variance	**MS-media**	Meat simulation media
ATP	Adenosine triphosphate	**MSP**	Mass spectrometry profiles
B.	*Brochothrix*	**n**	Nano (10^{-9})
BCA	Bicinchoninic acid	**N_2**	Nitrogen
BCFA	Branched chain fatty acids	**NCBI**	National Center for Biotechnology Information
BHI	Brain-heart-infusion	**O_2**	Oxygen
BLAST	Basic local alignment search tool	**$OD_{600\ nm}$**	Optical density at 600 nm
bp	Base pairs	**OUR**	Oxygen uptake rate
C.	*Carnobacterium*	**p**	Probability value
CFU	Colony forming units	***P.***	*Pseudomonas*
CL	Cardiolipin	**PA**	Phosphatic acid
cm	Centimeter	**PBS**	Phosphate buffer saline
CO_2	Carbon dioxide	**PC**	Phosphatidylcholine
C_T	Cycle threshold	**PCR**	Polymerase chain reaction
Da	Dalton	**PE**	Phosphatidylethanolamine
diH_2O	De-ionized water	**PG**	Phosphatidylglycerol
DNA	Deoxyribonucleic acid	**PGAP**	NCBI prokaryotic genome annotation pipeline
dNTP	Deoxy nucleoside triphosphate	**pH**	Negative decimal logarithm of hydrogen ion activity
DO	Dissolved oxygen	**PI**	Phosphatidylinositol
DSMZ	Deutsche Sammlung von Mikroorganismen und Zellkulturen	**PP**	Polypropylene
E	Primer efficiency	**PS**	Phosphatidylserine
E.	*Escherichia*	**PVC**	Polyvinylchloride
ED	Entner-Doudoroff	**qRT**	Quantitative real-time
EDTA	Ethylenediaminetetraacetic acid	**RAPD**	Random-amplified polymorphic DNA
EMP	Embden Meyerhof Parnas	**RAST**	Rapid annotations using subsystems technology
ESOs	Ephemeral spoilage organisms	**RGB**	Red green blue
EVOH	Ethylene vinyl alcohol	**RNA**	Ribonucleic acid
FA	Fatty acid	**ROS**	Reactive oxygen species
g	Gram	**rpm**	Rotations per minute
GC	Gas chromatography	**RT**	Relative transcription
GP	General polarization	**s**	Second (")
h	Hour	**SCFA**	Short chain fatty acids
HCA	Hierarchical cluster analysis	**SDS**	Natriumdodecylsulfat
HPLC	High-performance liquid chromatography	**SE**	Standard error
iBAQ	Intensity based absolute quantification	**SFA**	Saturated fatty acids
KEGG	Kyoto encyclopedia of genes and genomes	**SSOs**	Specific-spoilage organisms
K_La	Volumetric mass transfer coefficient	**subsp.**	Subspecies
l	Liter	**Taq**	*Thermus aquaticus*
L.	*Leuconostoc*	**TBE**	Tris-HCl boric acid EDTA buffer
LAB	Lactic acid bacteria	**TCA**	Tricarboxylic acid
Lc.	*Lactococcus*	**TIGR**	The Institute for Genomic Research
LCFA	Long chain fatty acids	**TMW**	Technical microbiology Weihenstephan
LFQ	Label-free quantification	**Tris**	Tris(hydroxymethyl)-aminomethan
M	Molar	**UBFA**	Unbranched fatty acids
mA	Milliampere	**UFA**	Unsaturated fatty acids

MA	Modified atmosphere	**UPGMA**	Unweighted pair group method with arithmetic mean
MALDI-TOF MS	Matrix assisted laser desorption/ionization – time of flight mass spectrometry	**V**	Volt
MAP	Modified atmosphere packaging	**VOCs**	Volatile organic compounds
mg	Milligram	**vs.**	*Versus*
MIC	Minimal inhibitory concentration	**W**	Watt
min	Minute (')	**w / v**	Weight per volume

Table of contents

List of tables

List of figures

1. Introduction

1.1. Meat consumption, composition and losses

The world total meat production is increasing constantly since decades with more than 342 million tons of carcass weight being produced in 2018 (FOA, 2020). This is due to the enormous growth of the world population (PRB, 2020) but also to rising living standards, achievable prices and improved trading connections of countries (FOA, 2020). Meat is a highly sensitive food product, which is prone to fast spoilage due to its constituents. The detailed chemical composition of meat is strongly depending on the animal tissue, age and part of the body (Franzke *et al.*, 2008; Cobos *et al.*, 2015). In this work the extensive term “meat” was divided into two groups based on the color type of muscle fibers: Red meat (beef, pork, rabbit, sheep, lamb) and white meat (chicken, turkey). Main difference between both types is the content of myoglobin, which is high in red muscle fibers and low in white muscle fibers. Furthermore, red muscle fibers have a lot of mitochondria thus mainly performing oxidative phosphorylation within the respiratory chain, whereas white muscle fibers rather perform a glycolytic metabolism (Cobos *et al.*, 2015). This study further focuses on the meat types turkey breast, chicken breast and beef steaks as used for several experiments. Table 1 summarizes main components of this meat types.

Table 1. Average chemical composition of different meat types.

	Turkey breast (Cobos *et al.*, 2015; Çelen *et al.*, 2016; Oblakova *et al.*, 2016)	**Chicken breast** (Chmiel *et al.*, 2019)	**Beef steaks** (Cobos *et al.*, 2015)
Water [%]	74%	74%	60%
Protein [%]	23%	23%	15%
Fat [%]	2%	2%	23%
Ash [%]	1%	1%	2%
Carbohydrates [%]	0%	0%	0%

Besides a high water content, the main fraction of meat is represented by proteins including myoglobin, actin, myosin, collagen and elastin (Cobos *et al.*, 2015). Some of these proteins are *post mortem* oxidized or digested by proteolytic activity of meat proteases e.g. calpains resulting in the production of free peptides and amino acids. This proteolytic activity is also thought to contribute to meat tenderization. The (intramuscular) fat content of meat can vary greatly even within the same species type, depending on the diet but also on the fitness level of the slaughtered animal (Toldrá and Hui, 2014). The term fat can be divided into depot fat (mainly consisting of triglycerides) and structural lipids, which are in membranes of muscle cells. Main constituents of structural lipids are phospholipids e. g. phosphatidylcholine (40%), phosphatidylethanolamine (15%), phosphatidylserine (10%) and sphingomyelin (5%) (Willian,

2013). Ash summarizes ions like potassium, phosphorus, sodium, chlorine, magnesium, calcium, and iron. Carbohydrates are present lower than <1% in meat and mainly exist of glycogen, which is transformed into lactic acid *post mortem* (Cobos *et al.*, 2015). Taken together, meat presents a nutrient rich substrate, which offers a perfect habitat for the growth of bacteria. Due to its moderate pH (5.5 ±0.3) and a high-water activity (0.99) growth of microorganisms is further promoted.

As a consequence, tremendous meat losses during slaughtering, processing, distribution and consumption processes are often traced back to microbial growth with concomitant spoilage. According to Gustavsson *et al.* (2011), approx. 20% of total food losses in Europe and Northern America are meat and meat products with the highest amount being lost at household level. This is due to wrong storage temperature leading to rapid spoilage of meat products but also to exceeding the expiration date. Latter is also one of the main causes for high meat losses in distribution sectors (Kranert *et al.*, 2012). Furthermore, preventable meat losses can also occur during transport processes, as a short break in the cooling chain result in massive food losses due to rapid microbial growth. Considering the high amounts of meat losses due to wrong handling and passing expiration dates on consumer and retailer level, worlds meat demand can be counteracted by improving methods preserving meat quality and safety and thus prolonging the shelf life of products.

1.2. Meat preservation by modified atmosphere packaging and refrigerated storage

Chilling and modified atmosphere packaging (MAP) are the two most effective preservation methods applied in industry to prolong the shelf life of meat products. Cold storage of modified atmosphere (MA) packages effectively suppresses a broad variety of bacteria found on fresh slaughtered meat (Table 2). In detail, meat is commercially stored at 4 °C to inhibit the growth of mesophilic species, which exhibit a temperature optimum of 20 °C-45 °C and restricted growth at temperatures <20 °C (Margesin and Schinner, 1994; Sun and Holley, 2012). It has been demonstrated that temperatures above 4 °C would enhance microbial growth and consequently significantly shorten the shelf life of meat (Koutsoumanis *et al.*, 2006). Additionally to cold storage, MAP is applied to meat, which is defined as controlled enclosure of a meat product into a gas-barrier material with exchanging the gaseous environment by a defined atmosphere (Suman and Joseph, 2013). Similar to cold storage, MAP suppresses the growth of specific gas-intolerant bacteria (Table 2), but further also retains the color of meat (Jakobsen and Bertelsen, 2000). Thus, commercial retailing of refrigerated MAP meat was introduced in the early 1970s (Djenane and Roncalés, 2018). Today more than 60% of the

fresh slaughtered meat in the United States and 43% in European is packaged under a modified atmosphere (MA) and stored at chilled temperatures (Belcher, 2006; McMillin, 2008).

Industrial applied modified atmospheres. The conventional gases used for MAP are oxygen (O_2), carbon dioxide (CO_2) and nitrogen (N_2) (McMillin, 2008) but also other gases such as carbon monoxide (if applied <1%) are used for MAP in the United states and Norwegian (Cornforth and Hunt, 2008; Djenane and Roncalés, 2018). Commonly a mixture of two gases is applied in MAP, as the usage of one gas does not fulfill all requirements for industry. Thus, red meat such as beef or pork are usually packaged under a high oxygen atmosphere containing 30% CO_2 / 70% O_2 (Djenane *et al.*, 2003; Eilert, 2005; Belcher, 2006; Djenane and Roncalés, 2018), whereas white meat such as chicken or turkey is packaged under a low oxygen atmosphere containing 30% CO_2 / 70% N_2 or 100% N_2 (Brenes and Roura, 2010; Rossaint *et al.*, 2015). However, nowadays especially European meat-processing plants also apply high oxygen MAP for white meats, due to the reported inhibitory effect of high oxygen on some pathogens (Meredith *et al.*, 2014; Rossaint *et al.*, 2015).

The main reason for the application of 30% CO_2 in all of those MA packages, is the demonstrated inhibitory effect of CO_2 on the growth of several meat spoilers (Table 2). Even though it has been demonstrated that higher CO_2 concentrations would more efficiently inhibit meat spoilers, this is unbeneficial for industry, as > 30% CO_2 impairs the meat color due to formation of the brownish color pigment metmyoglobin and further accelerates lipid oxidation leading to texture losses (Smith *et al.*, 1990; Martínez *et al.*, 2005; Esmer *et al.*, 2011). Additionally, high CO_2 concentrations often result in packaging collapses due to CO_2 absorbance by the meat tissue (McMillin *et al.*, 1999). Thus, the potential of CO_2 to control microbial spoilage of meat is restricted by preserving meat quality criteria such as color and texture, which were shown to be best at CO_2 concentrations of 30% (Esmer *et al.*, 2011).

Oxygen is either excluded from industrial MA packaging or used in high concentrations of approximately 70%. Both can lead to an effective inhibition of certain meat bacteria, depending on their oxygen metabolism as demonstrated in Table 2. Whereas the absence of O_2 inhibits strict aerobic bacteria, high levels of O_2 can supress the growth of both anaerobic and aerobic bacteria, since the optimal oxygen level for growth (21% for aerobes, 0-2% for anaerobes) is surpassed (Farber, 1991). However, beside microbial control, the main advantage of high oxygen atmosphere packaging is the stabilization and maintenance of the bright red color of meat due to the formation of the color pigment oxymyoglobin (Jakobsen and Bertelsen, 2000; Jayasingh *et al.*, 2002; Mancini and Hunt, 2005). It has been demonstrated that red meat, which is packaged under normal air atmosphere has a color shelf life of less than one week (McMillin, 2008), whereas under controlled high oxygen atmosphere acceptable red color is retained for up to 14 days (Suman and Joseph, 2013). Nevertheless, there are also reports

about deteriorative reactions of meat due to the application of 70% O_2, comprising fat and pigment oxidation both of which significantly impairing meat quality (Djenane and Roncalés, 2018). White meat, which is less prone to discoloration due to a reduced amount of myoglobin, has thus commonly been packaged under an oxygen free atmosphere to prevent those oxidative quality losses. Based on this, high oxygen packaging of white meat as applied in Europe is controversially debated in science, as it is not necessary for maintaining color stability, accelerates meat oxidation processes but, on the other hand, inhibits important human pathogens (Dhananjayan *et al.*, 2006; Chmiel *et al.*, 2019).

Sensitivity and occurrence of single meat bacteria to / on refrigerated MAP meat. Due to extensive scientific work, there is a great knowledge today about single organisms occurring as initial contaminants on fresh slaughtered meat, their sensitivity to O_2, CO_2 and cold temperatures as well as their occurrence and predominance on different refrigerated MAP meat. Table 2 summarizes this knowledge in order to illustrate the power of refrigerated MA packaging for preserving microbial safety of meat.

Table 2. Meat organisms and their sensitivity to cold storage, O_2 and CO_2 exposure as well as their occurrence on refrigerated MAP meat. List of most prominent Gram-negative and Gram-positive bacteria found as initial contaminants on fresh slaughtered meat and their tolerance to refrigerated temperatures and the MAP gas CO_2, based on a reduction (not complete inhibition) of growth. Furthermore, the potential to completely inhibit the growth of those bacteria by the application of O_2 or exclusion of O_2 in MAP as well as their basic oxygen metabolism is given. "-" no or minimal inhibition by the corresponding gas/temperature, "+" partial or total inhibition by the corresponding gas/temperature, "()" inhibition is depending on the species. Isolation sources on different MA packaged meat types for each genus / species are provided. Grey highlighted genus / species are predominating and were frequently isolated on the corresponding meat type.

	Partial or total inhibition by		**Total inhibition by**			**Isolation from refrigerate meat stored under**			
	Refrigeration at 4 °C	**Presence of CO_2**	**Presence of O_2 (<21%)**	**Absence of O_2**	**Oxygen metabolism**	**>20% CO_2 / >70% O_2**	**30% CO_2 / 70% N_2**	**Vacuum**	**Sources**
Gram-negative bacteria									
Acinetobacter	+	+	-	+	Obligate aerobe				(Farber, 1991; Bowman, 2006)
Aeromonas hydrophila	-	+	-	-	Facultative anaerobe			Pork Beef	(Molin, 1983; Gill and Reichel, 1989; de Fernando *et al.*, 1995; Roberts *et al.*, 1996; Palumbo *et al.*, 2006)
Bacillus cereus	+	+	-	-	Facultative anaerobe			Beef steaks	(Enfors and Molin, 1981; Devlieghere and Debevere, 2000; Rosenfeld *et al.*, 2005; Thippareddi and Phebus, 2007; Pichner *et al.*, 2014)

Campylobacter jejuni	+	+	-	+	Micro aerophile				(Hoffman and Goodman, 1982; Farber, 1991; Chan *et al.*, 2001; Sellars *et al.*, 2002)
Escherichia coli	+	+	-	-	Facultative anaerobe		Chicken	Beef	(Shaw *et al.*, 1971; Farber, 1991; Chaves *et al.*, 2012; Höll *et al.*, 2016; Finn *et al.*, 2017)
Hafnia alvei	-	?	-	-	Facultative anaerobe	Chicken Beef Pork Minced beef	Chicken Broiler Turkey Marinated pork Marinated beef	Beef	(Ridell and Korkeala, 1997; Nychas *et al.*, 2008; Chaves *et al.*, 2012; Hernández-Macedo *et al.*, 2012; Säde *et al.*, 2013; Höll *et al.*, 2016; Hilgarth *et al.*, 2018a; Höll *et al.*, 2019; Imran *et al.*, 2019)
Klebsiella pneumoniae	+	?	-	-	Facultative anaerobe			Beef	(Shirey and Bissonnette, 1992; Brisse *et al.*, 2006; Chaves *et al.*, 2012)
Moraxella spp.	+	+	-	(+)	(Obligat) aerobe				(Nortjé *et al.*, 1990; Santos *et al.*, 1999; Bowman, 2006; Sun, 2012; LaCroce *et al.*, 2019)
Pantoea agglomerans	+	+	-	-	Facultative anaerobe	Beef steaks			(Gill and Tan, 1980; Board, 1998; Amanatidou *et al.*, 1999; Francis *et al.*, 2000; Cruz *et al.*, 2007; Esmer *et al.*, 2011; Sawsan *et al.*, 2018)
***Photobacterium* spp.**	-	?	-	-	Facultative aerobe	Poultry Minced meat Pork Chicken	Chicken	Beef Pork	(Pennacchia *et al.*, 2011; Stoops *et al.*, 2015; Hilgarth *et al.*, 2018b; Fuertes-Perez *et al.*, 2019; Höll *et al.*, 2019)
Proteus spp.	+	+	-	-	Facultative anaerobe			Beef	(Farber, 1991; Rossi *et al.*, 2011; Wang and Pan, 2014)
***Pseudomonas* spp.**	-	+	-	+	Obligate aerobe	Chicken Minced beef Beef Poultry	Chicken	Lamb Beef Poultry	(Lambert *et al.*, 1991; Kakouri and Nychas, 1994; Ercolini *et al.*, 2006; Ercolini *et al.*, 2009; Esmer *et al.*, 2011; Rossaint *et al.*, 2015; Höll *et al.*, 2016; Kaur *et al.*, 2017; Hilgarth *et al.*, 2018a; Hilgarth *et al.*, 2019; Imran *et al.*, 2019)
***Psychrobacter* spp.**	-	?	-	+	Obligate aerobe	Minced meat			(Bowman, 2006; Yang, 2014; Stoops *et al.*, 2015)
***Rahnella* spp.**	-	-	-	-	Facultative anaerobe	Minced pork Minced beef	Broiler Turkey	Pork Beef	(Farber, 1991; Chang *et al.*, 1999; Ercolini *et al.*, 2006; Ercolini *et al.*, 2009; Pennacchia *et al.*, 2011; Säde *et al.*, 2013; Godziszewska *et al.*, 2017)
Salmonella typhimurium	+	+	-	-	Facultative anaerobe				(Yamamoto and Droffner, 1985; Farber, 1991; Morey and Singh, 2012)
Serratia liquefaciens	-	+	-	-	Facultative anaerobe	Beef Pork Chicken Minced pork Minced beef	Chicken Broiler Turkey Marinated pork Marinated beef	Beef	(Farber, 1991; Ridell and Korkeala, 1997; Ahmad and Marchello, 2006; Ercolini *et al.*, 2006; Ercolini *et al.*, 2009; Säde *et al.*, 2013; Schuerger *et al.*, 2013; Hilgarth *et al.*, 2018a; Höll *et al.*, 2019)
Shewanella putrefaciens	(+)	+	-	-	Facultative anaerobe			Lamb	(Boskou and Debevere, 1997; DiChristina *et al.*, 2006; Nychas *et al.*, 2008; Karpinets *et al.*, 2010; Kaur *et al.*, 2017)
Vibrio parahaemolyticus	+	+	-	-	Facultative anaerobe				(Thomson and Thacker, 1973; Farber, 1991; Nychas *et al.*, 2008; Qian *et al.*, 2020)
Yersinia enterocolitica	-	+	-	-	Facultative anaerobe	Minced pork Minced beef	Chicken Broiler Turkey	Lamb Beef	(Stern *et al.*, 1980; Gill and Reichel, 1989; Farber, 1991; de Fernando *et al.*, 1995; Thippareddi and Phebus, 2007; Chaves *et al.*, 2012; Hernández-Macedo *et al.*, 2012; Säde *et al.*, 2013; Ćirić *et al.*, 2014; Höll *et al.*, 2016; Kaur *et al.*, 2017)
Gram-positive bacteria									
Bacillus cereus	+	+	-	-	Facultative anaerobe				(Molin, 1983; Farber, 1991; Duport *et al.*, 2016; Juneja *et al.*, 2018)
Brochothrix thermosphacta	-	+	-	-	Facultative anaerobe	Chicken Beef Minced beef Pork	Chicken Cooked Ham	Lamb poultry	(Eklund and Jarmund, 1983; Molin, 1983; Blickstad and Molin, 1984; Lambert *et al.*, 1991; Ordonez *et al.*, 1991; Kakouri and Nychas, 1994; Nychas *et al.*, 2008; Vasilopoulos *et al.*, 2008; Esmer *et al.*, 2011; Gribble *et al.*, 2014; Rossaint *et al.*, 2015; Höll *et al.*, 2016; Säde *et al.*, 2017; Hilgarth *et al.*, 2019; Höll *et al.*, 2019)
***Carnobacterium* spp.**	-	-	-	-	Facultative anaerobe	Chicken Minced meat	Chicken Cooked Ham	Lamb Beef Pork Ham Turkey	(Laursen *et al.*, 2005; Chenoll *et al.*, 2007; Leisner *et al.*, 2007; Nychas *et al.*, 2008; Vasilopoulos *et al.*, 2008; Ercolini *et al.*, 2009; Jiang *et al.*, 2010; Stoops *et al.*, 2015; Höll *et al.*, 2016; Kaur *et al.*, 2017; Höll *et al.*, 2019)

Clostridium spp.	**(+)**	**-**	**+**	**-**	Obligate anaerobe			Lamb beef	(Doyle, 1983; Foegeding and Busta, 1983; Farber, 1991; Lambert *et al.*, 1991; Whiting and Naftulin, 1992; Broda *et al.*, 1996; Doyle, 2002; Hernández-Macedo *et al.*, 2012; Kaur *et al.*, 2017)
Corynebacterium spp.	**+**	**+**	**-**	**(+)**	Facultative anaerobe to aerobe				(Farber, 1991; Liebl, 2006; Tauch and Sandbote, 2014)
Enterococcus faecalis	**+**	**+**	**-**	**-**	Facultative anaerobe		Cooked Ham		(Farber, 1991; Panoff *et al.*, 1997; Vasilopoulos *et al.*, 2008; Portela *et al.*, 2014)
Lactococcus piscium	**-**	**-**	**-**	**-**	Facultative anaerobe	Beef Minced beef Chicken	Chicken	Pork Beef	(Sakala *et al.*, 2002; Nychas *et al.*, 2008; Jiang *et al.*, 2010; Saraoui *et al.*, 2016; Hilgarth *et al.*, 2018a; Hilgarth *et al.*, 2019; Höll *et al.*, 2019)
Latilactobacillus curvatus	**-**	**?**	**-**	**-**	Facultative anaerobe			Beef Pork	(Farber, 1991; Fadda *et al.*, 2008; Jiang *et al.*, 2010; Hernández-Macedo *et al.*, 2012)
Latilactobacillus sakei	**-**	**-**	**-**	**-**	Facultative anaerobe	Beef Chicken Beef steaks	Chicken	Beef Pork	(Devlieghere *et al.*, 1998; Devlieghere and Debevere, 2000; Ercolini *et al.*, 2006; Vihavainen and Björkroth, 2007; Fadda *et al.*, 2008; Jiang *et al.*, 2010; Hernández-Macedo *et al.*, 2012; Höll *et al.*, 2016; Zagorec and Champomier-Vergès, 2017; Hilgarth *et al.*, 2018a; Höll *et al.*, 2019)
Lactiplantibacillus plantarum	**-**	**?**	**-**	**-**	Facultative anaerobe			Beef	(Eklund and Jarmund, 1983; Fadda *et al.*, 2008; Zotta *et al.*, 2017)
Lactobacillus algidus	**-**	**-**	**-**	**-**	Facultative anaerobe	Minced meat Beef steaks		Beef	(Farber, 1991; Kato *et al.*, 2000; Vihavainen and Björkroth, 2007; Stoops *et al.*, 2015)
***Leuconostoc* spp.**	**-**	**-**	**-**	**-**	Facultative anaerobe	Beef Minced beef Pork	Cooked ham	Bacon Beef Ham Turkey	(Savell *et al.*, 1981; Hamasaki *et al.*, 2003; Feiner, 2006; Chenoll *et al.*, 2007; Vihavainen and Björkroth, 2007; Cavett, 2008; Nychas *et al.*, 2008; Vasilopoulos *et al.*, 2008; Chaves *et al.*, 2012; Rahkila *et al.*, 2012; Säde *et al.*, 2017; Hilgarth *et al.*, 2018a; Hilgarth *et al.*, 2019)
Listeria monocytogenes	**-**	**+**	**-**	**-**	Facultative anaerobe			Beef	(Gill and Reichel, 1989; Walker *et al.*, 1990; Farber, 1991; Amanatidou *et al.*, 1999; Borges *et al.*, 2007; Thippareddi and Phebus, 2007; Roberts *et al.*, 2020)
Microbacterium spp.	**(-)**	**?**	**-**	**(-)**	Facultative anaerobe to obligate aerobe	Chicken	Chicken		(Evtushenko and Takeuchi, 2006; Höll *et al.*, 2016; Bellassi *et al.*, 2020)
Micrococcus luteus	**+**	**?**	**-**	**+**	Obligate aerob				(Evans *et al.*, 1955; Garip *et al.*, 2007)
Staphylococcus aureus	**+**	**+**	**-**	**-**	Facultative anaerobe				(Farber, 1991; Jofré *et al.*, 2008; Balasubramanian *et al.*, 2017)
Streptococcus spp.	**+**	**+**	**-**	**-**	Facultative anaerobe				(Lee and Collins, 1976; Farber, 1991; Patterson, 1996; Davies, 2003)
Weisella viridescens	**-**	**?**	**-**	**-**	Facultative anaerobe			Pork	(Jiang *et al.*, 2010; Dušková *et al.*, 2013; Fusco *et al.*, 2015)

Table 2 illustrates that a huge variety of organisms can be found as initial spoilers on fresh slaughtered meat. Those bacteria can be traced back to the environment the animal was in contact with during transport and slaughtering as well as to its intestinal tract (Nychas *et al.*, 2007; Nychas *et al.*, 2008; Doulgeraki *et al.*, 2012). Furthermore, several of the listed organisms are important human pathogens, which can cause serious infections and are thus undesired on meat products. Applying MAP technologies in combination with refrigerated temperatures, enables to partially control the occurrence of those pathogenic bacteria and selectively shift the initial microbiota to certain less harmful species, which subsequently dominate on meat.

Even though only a combination of refrigeration and atmospheric packaging frequently results in a complete inhibition of those organisms, the contribution of each single environmental parameter (O_2, CO_2 and temperature) could be dissected species-specific in Table 2. For example, growth of some (human pathogen) organisms can be completely suppressed by the presence or absence of O_2, comprising *Campylobacter jejuni*, *Clostridium* spp., *Corynebacterium* spp., *Micrococcus luteus* and *Weisella viridescens*. Furthermore, the application of CO_2 suppresses a wide range of organisms such as *Pseudomonas* species, which are well adapted to cold temperatures (King and Nagel, 1967; Gill and Tan, 1979). Contrary, *Salmonella typhimurium* or *Klebsiella pneumoniae* are both not sensitive to MAP gases but markedly inhibited at refrigerated temperatures < 4 °C (Brisse *et al.*, 2006; Morey and Singh, 2012). Summing up, certain inhibition of bacteria can be obtained by either refrigerated storage or atmospheric packaging of meat, but effective control of microbial spoilage and product safety can only be obtained by combining both parameters.

Inhibitory mechanisms of action of MAP gases and refrigerated temperatures on microbial metabolism. As highlighted in Table 2, the protective action of industrial applied MAP gases against the growth of microorganisms has been described and proven in several studies. However, knowledge about the mechanisms of action of theses MAP gases on bacterial metabolism is limited and only few well analyzed mechanisms are accepted in science yet. The main inhibitory effect of O_2 on microorganisms is based on formation of reactive oxygen species (ROS) such as O_2^-, OH^- and H_2O_2, which induce oxidative stress within the cell. If not detoxified, the accumulation of those ROS causes massive damage of DNA, lipids and proteins of bacteria, finally leading to cell death (Feng and Wang, 2020). Furthermore, oxygen is described to inhibit enzymes containing Fe-S cluster such as dehydrogenases, which are present in many strict anaerobic bacteria (Klees *et al.*, 1992; Hofmeister *et al.*, 1994; Scherf *et al.*, 1994). Contrary the absence of oxygen can also lead to remarkable suppression of bacteria, especially of those, which gain energy from aerobic respiratory activity (Crowley *et al.*, 2010).

Compared to O_2, the inhibitory effect of CO_2 on bacterial metabolism has not been elucidated in detail yet (Casaburi *et al.*, 2015), despite the bacteriostatic action of CO_2 has been proven in several studies (Gill and Tan, 1980; Blickstad and Molin, 1983). It is known that CO_2 lowers the pH of media, consequently inducing acid stress within the cell, which reduces the growth rate of bacteria (King and Nagel, 1967; Daniels *et al.*, 1985). Another mechanism of action of CO_2 is expected to be an alteration of the membrane permeability due to destroying the structural integrity of cell membranes. This was supposed by Sears and Eisenberg (1961), who investigated the effect of CO_2 on the interfacial tensions between water and oil phases (benzene). Nevertheless, more studies supporting this assumption by analyzing the detailed

effect of CO_2 exposure to changes in the fatty acid composition of bacteria are missing yet. Furthermore, a mass action effect inhibiting especially decarboxylation enzymes of microorganisms is supposed for CO_2 (King Jr and Nagel, 1975). However, studies concerning this assumption give controversial results, as Foster and Davis (1949) reported CO_2 to inhibit the oxaloacetate decarboxylase, while King Jr and Nagel (1975) demonstrated no inhibitory effect of CO_2 on this enzyme but a markedly inhibition of the isocitrate and malate dehydrogenase. Another less studied mechanism of action of CO_2 is supposed to be an inhibition of enzymes of the oxidative metabolism as demonstrated by Gill and Tan (1980). They measured a reduction in bacterial respiration due to CO_2 exposure for some meat spoilers. However, this mechanistic way of action is controversially discussed in science as displacement of oxygen by carbon dioxide is rather unlikely (Daniels *et al.*, 1985). Thus, further studies have to be done investigating the effect of CO_2 on the respiration rates of different bacteria.

The gas nitrogen is thought to have no antimicrobial or bacteriostatic effect and further does not influence meat quality criteria (Church, 1994). Thus, it is often used as inert filling gas to prevent collapse of meat packages (Lambert et al., 1991). Consequently, the main protective effect of MAP is based on the presence or absence of the gases O_2 and CO_2. The synergistic effect of both protective gases is reported to enable a 7-10 days shelf life extension of meat (Clark and Lentz, 1973; Vihavainen and Björkroth, 2007).

The mechanistic way of action of temperatures below bacteria´s minimal tolerance on their metabolism has also been well studied in the past. It is commonly accepted that low temperatures decrease membrane fluidity and increase damage by ice crystal formation within the cell (Graumann and Marahiel, 1996). Consequently, membrane diffusion is slowed down, resulting in a reduction of nutrient and waste product alteration (D'Amico *et al.*, 2006). Furthermore, proteins become too rigid for catalyzing reactions, thus lose their affinity to substrates and can even undergo denaturation (Gerday *et al.*, 1997). Furthermore D'Amico *et al.* (2006) stated that temperatures below the optimum decrease rates of DNA translation and RNA transcription as well as enhance inappropriate protein folding. All of those factors finally result in reduced cell division and can even lead to cell death.

1.3. Ephemeral spoilage organisms and their spoilage potential

Based on the specific interference of O_2, CO_2 and cold temperatures on the metabolism of bacteria, predominating species found in the microbial consortium of refrigerated MAP meat must be able to perform well upon metabolic adaptation to these environmental factors. Those species able to adapt their metabolism and grow on refrigerated MAP meat, but also spoil MAP meat, have been defined as specific-spoilage organisms (SSOs) by Gram and Dalgaard

(2002). Later on, Nychas *et al.* (2007) specified a smaller group of SSOs, which finally predominate and spoil MAP meat, as “ephemeral spoilage microorganisms” (ESOs). Bacteria, classified as ESOs according to Nychas *et al.* (2007) are highlighted in Table 2. However, even within the ESOs, one can distinguish between strong spoilers such as *B. thermosphacta* and species, which are recognized as less strong spoilers or even putative protective cultures such as *Lactococcus* (*Lc.) piscium* (Matamoros *et al.*, 2009; Fall *et al.*, 2010; Macé *et al.*, 2013; Leroi *et al.*, 2015). This study investigates ESOs, which are proven to significantly contribute to meat spoilage and thus are highly relevant for meat quality assessment. In the following, information about the spoilage potential of those bacteria is given.

***Leuconostoc (L.) gelidum* subspecies.** Several species of the ESOs are phylogenetically grouped to the lactic acid bacteria (LAB), whose basic energy metabolism is due to hetero- or homolactic acid fermentation (Gopal, 2020). Among those are the psychrotrophic bacteria *L. gelidum* subsp. *gelidum* and *L. gelidum* subsp. *gasicomitatum* (Rahkila *et al.*, 2014). The spoilage potential of both subspecies has been analyzed by Vihavainen and Björkroth (2007), who highlighted their contribution to green surface discoloration of raw MAP beef steaks. This can be traced back to H_2O_2 or H_2S production, leading to the formation of the greenish color pigment sulfmyoglobin (Nicol *et al.*, 1970; Borch *et al.*, 1996). Furthermore, both subspecies contribute to a strong unpleasant buttery/diacetyl-like odor (Vihavainen and Björkroth, 2007; Johansson *et al.*, 2011). Later on, Jääskeläinen *et al.* (2015) identified *L. gelidum* subsp. *gasicomitatum* to produce diacetyl and acetoin especially when glucose is depleted in the medium and inosine and ribose are utilized.

Carnobacterium (C.). Two frequently occurring MAP meat-spoiling species within the group of LAB comprise *C. divergens* and *C. maltaromaticum*. Both are known to produce the biogenic amine tyramine on MAP shrimp (Laursen *et al.*, 2006) as well as on cold-smoked salmon (Duffes *et al.*, 1999; Jørgensen *et al.*, 2000), beef (Edwards *et al.*, 1987) and in a meat-fat mixture (Masson *et al.*, 1999). Furthermore, the ability to produce volatile organic compounds (VOCs) such as 3-methyl-1-butanal has also been demonstrated for both *Carnobacterium* species (Leisner *et al.*, 1995; Larrouture *et al.*, 2000; Laursen *et al.*, 2006; Vihavainen and Björkroth, 2007; Casaburi *et al.*, 2011). Nevertheless, production of VOCs appears to be a strain-specific characteristic for those species.

Brochothrix (B.) thermosphacta. One main spoiler within the ESOs is the species *B. thermosphacta,* which is phylogenetically classified as closely related to *Listeria monocytogenes,* thus not belonging to the group of LAB (Ordonez *et al.*, 1991; Kakouri and Nychas, 1994; Samelis, 2006; Nychas *et al.*, 2008; Hilgarth *et al.*, 2018a). Several spoilage metabolites, considered as putrid and stinky, have been identified for *B. thermosphacta*, comprising acetoin, diacetyl, acetic acid, isobutyric acid, 2-methylbutyric, isovaleric acids and

3-methylbutanol (Dainty and Hibbard, 1980; Dainty and Hibbard, 1983). While those are predominantly produced under oxic conditions, olfactory neutral metabolites such as lactic acid and ethanol could be identified under anoxic conditions for this species. Thus, the contribution of *B. thermosphacta* to anaerobic meat spoilage is considered as lower compared to aerobic meat spoilage.

***Pseudomonas (P.)* spp**. Within the huge genus *Pseudomonas*, the bacteria *P. lundensis*, *P. fragi*, *P. weihenstephanensis*, *P. fluorescens* and *P. putida* are considered as main ESOs of oxically stored MAP meat. In most cases, spoilage is induced by production of slime and off-odors (Skandamis and Nychas, 2002; Nychas *et al.*, 2007; Raposo *et al.*, 2017). It has been shown that these characteristics become dominant after glucose and lactate are metabolized and amino acids are used as subsequent substrate (Nychas *et al.*, 2007). Nevertheless, production of VOCs is strongly strain and species-specific. Production of extensive amounts of 1-undecene, 5-methyl-2-hexanone and methyl-2-butenoic acid were identified for *P. lundensis* strains, whereas some *P. fragi* strains produce large amounts of methyl and ethyl acetate as well as methyl esters. Besides production of VOCs, *Pseudomonas* species are described as high proteolytic (Drosinos and Board, 1995; Koutsoumanis *et al.*, 2006). While this feature is advantageous to these bacteria due to a better access to nutrients on meat, it causes massive product deterioration, which is unwanted by producers (Wickramasinghe *et al.*, 2019). Furthermore, high lipolytic activity leading to massive fat degradation of chicken skin and thus rancidity of meat has been described for *P. fluorescens* (Mellor *et al.*, 2011). Regarding meat discoloration, *P. fluorescens* and *P. fragi* both accelerate oxymyoglobin oxidation on beef resulting in meat browning (Bala *et al.*, 1977; Chan *et al.*, 1998; Motoyama *et al.*, 2010). Taken together, *Pseudomonas* species contribute in various ways to a deterioration of MAP meat and thus can be considered as main spoiling microorganisms within the ESOs.

1.4. Microbial consortia on MAP meat

As demonstrated, the microbiota of MAP meat comprises several diverse ESOs, which as a consortium synergistically contribute to spoilage of the product. The knowledge about the occurrence of those microorganisms on MAP meat (chapter 1.2, Table 2) and their spoilage potential (chapter 1.3) is extensive, as both factors are of high interest for meat industry in concern of microbial safety assessment (Dainty and Mackey, 1992; Skandamis and Nychas, 2002; Balamatsia *et al.*, 2006; Ercolini *et al.*, 2006; Doulgeraki *et al.*, 2012; Casaburi *et al.*, 2015; Höll *et al.*, 2016; Hilgarth *et al.*, 2018a). However, all of those studies are quite descriptive, focusing on the abundance of different bacteria on MAP meat as well as putrid metabolites found by high-performance liquid chromatography (HPLC) and gas chromatography (GC). No investigations have been done yet, attempting to mechanistically explain the general adaptation of those ESOs to their gaseous environment as well as their ability to coexist on MAP meat, which is both based on their capability to cope with the applied modified atmospheres and synchronously handle substrate competition. This might be due to less relevance for meat industry but also due to missing practicable analyze methods. However, gas adaptation and coexistence are both obligate for ESOs to survive and grow on MAP meat surfaces and knowledge about their adaptation mechanisms enables to understand their occurrence on MAP meat.

To investigate this neglected questions, recently upcoming advanced “omic”-technologies are of great value, as those non-targeted approaches enable insights into the whole metabolism and metabolic processes taking place in bacteria, consequently uncovering new or unnoticed metabolic adaptation mechanisms. Furthermore, due to encompassed metabolic insights, conclusions about the mechanistic action of O_2 and CO_2 on bacterial metabolism can be done. The applicability and power of those methods has been demonstrated in recent studies, analyzing proteomic changes of *Staphylococcus xylosus* to anaerobiosis (Quintieri *et al.*, 2018) or acid stress (Kolbeck *et al.*, 2019). Until now, there are only few studies applying this advanced techniques on ESOs comprising a transcriptomic study on *P. fragi* NMC25 to MAP stress (30% CO_2 / 70% N_2), revealing a downregulation of enzymes of the electron transport chain due to MAP (Wang *et al.*, 2018a) and a comparative genomic study on the anaerobic respiration of some food-spoiling bacteria belonging to *Enterobacteriaceae* and *Vibrinaceae,* uncovering new regulon members functioning in respiration and carbohydrate metabolism (Ravcheev *et al.*, 2007). Furthermore, Höll *et al.* (2019) performed a meta-transcriptomic study, comparing the transcriptomic profile of the whole microbial consortium of meat packaged under two different atmospheres. Beside insights into the basic lifestyle of ESOs under MAP atmospheres, this study also uncovered the presence of, until then, non-culturable *Photobacterium* species on MAP meat. Concluding, all of these studies demonstrate the power

and potential of advanced “omic”-technologies to obtain new insights into bacterial metabolism, thus highlighting the need to also apply these methods to explore the adaptation and coexistence of typical ESOs to/on MAP meat.

1.5. Headspace changes during storage of MAP meat and possible causes

As a mutual interaction of MAP gases and bacteria, the influences of microorganisms on headspace changes of MA packages were analyzed in this study. It has been known for a long time that the headspace gas composition of initially packaged MAP trays is not static, but rather changing during storage period. Several studies detected a decrement in the headspace oxygen content with a concomitant increase in carbon dioxide levels during the storage time of MAP meat (O'Grady *et al.*, 2000; Ercolini *et al.*, 2006; Koutsoumanis *et al.*, 2008; Höll *et al.*, 2016; Hilgarth *et al.*, 2018a). An example for the headspace development of naturally spoiled high oxygen MAP beef steak stored at 4 °C by Hilgarth *et al.* (2018a) is given in Figure 1.

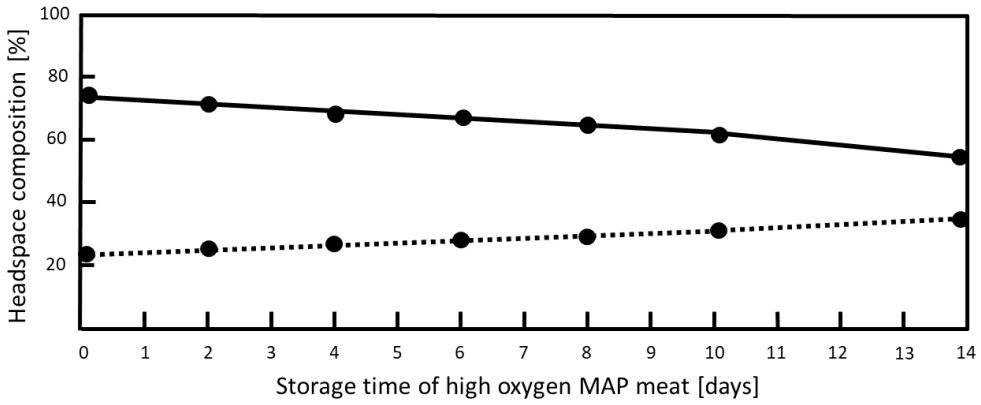

Figure 1. Headspace development of MAP beef steak during storage at 4 °C. The headspace gas development of high oxygen MAP beef steak stored at 4 °C for 14 days is shown. Curves were adapted from the study of Hilgarth *et al.* (2018a). Solid line: headspace O_2 content. Dotted line: headspace CO_2 content.

Different causes for the observed shelf development of the headspace compositions during MAP storage have been discussed in science, comprising microbial metabolism, permeability of MA packages, mitochondrial respiration of meat cells, oxidation of fat and proteins as well as oxidation of myoglobin (Koutsoumanis *et al.*, 2008; Esmer *et al.*, 2011; Chaix *et al.*, 2014). Among those, microbial metabolism is the most consistent and accepted explanation in science as it induces both, a decrement in headspace O_2 and an increase in CO_2. However, a direct comparison of the oxygen consumption capacity of each single cause has not been done yet, as the amount of oxygen consumed by fat and protein oxidation as well mitochondrial respiration cannot directly be quantified on meat. Thus, the only available oxygen consumption values for this causes derive from *in vitro* experiments and can only be highly speculatively counted back to real meat. Nevertheless, in the following, important considerations regarding each possible cause and their contribution to headspace changes are discussed.

Microbial metabolism. Microorganisms living on the surface of meat can consume oxygen by performing aerobic respiration. Thereby electrons, origin from oxidation of redox equivalents (NADH), are shuttled through membrane bound enzyme along their redox potential. The involved enzymes *vice versa* pump protons out of the cell, thereby generating a proton gradient over the membrane. When protons influx into the cell, adenosine triphosphate (ATP) is produced by another membrane bound enzyme, thus enabling growth of bacteria (Pedersen *et al.*, 2012). At the end of respiratory chain, electrons have to be shuttled to a terminal acceptor molecule, which is known to be O_2 under oxic conditions. Oxygen is consequently reduced to water and thus consumed by bacteria. A study from Lechardeur *et al.* (2011) demonstrated that several LABs exhibit the ability to perform this respiratory chain activity when exogenous hemin is applied, thus assuming also ESOs to contribute to an O_2 decrement in the headspace of MAP meat. The amount of O_2 consumed by a single cell of ESOs over a specific time period is unclear yet, but it might be comparable to data available for *Escherichia (E.) coli*. In detail, Riedel *et al.* (2013) demonstrated that one cell of exponentially growing *E. coli* K-12 is able to consume 0.24 pmol O_2/ *day in artificial media. Applying this oxygen uptake rate to ESOs, and considering an initial cell count of $\log_{10}$(CFU) = 10^4 per gram of fresh meat (Aljasass, 2013; Hilgarth *et al.*, 2018a), the initial contribution to oxygen consumption by meat-spoiling bacteria might not be high, but exponentially increasing with increasing cell counts upon storage. Furthermore, some members of the ESOs, especially LAB and *B. thermosphacta* are known to produce CO_2 by either heterofermentative lactic acid fermentation or by secondary decarboxylation reactions (Hitchener *et al.*, 1979; De Bruyn *et al.*, 1988; Schillinger and Holzapfel, 1995). Microbial CO_2 production can even be such strong that bulging of packages due to CO_2 accumulation is observed, as described for *L. gelidum* species (Vihavainen *et al.*, 2008). Thus, there appears to be a direct linkage of microbial growth on meat and the observed changes in the headspace of MAP meat. Studies done by Höll *et al.* (2016) and Hilgarth *et al.* (2018a) further confirm this thesis. They detected a rise in microbial counts on beef and poultry, which was concomitant with an enhanced decrease of O_2 and enhanced increase in CO_2 in the headspace of MAP chicken and beef.

Permeability of the packaging material. Gas permeability of MAP trays is considered as another reason for headspace changes. Especially high oxygen MAP trays, exhibiting a high gradient of gas concentrations of the external and internal atmosphere, are prone to gas losses due to permeable packaging material. However, advances in packaging processes enable production of polyphasic packaging materials with extremely low oxygen permeability, guaranteeing a constant and stable oxygen content of MAP trays (McMillin, 2008). In this manner, cheap but oxygen permeable (O_2 transmission rate = 100-6000 cc/m^2/24h) polymers such as polystyrene, polypropylene (PP), polyethylene and polyvinylchloride (PVC) (Belcher,

2006; Duffy *et al.*, 2006) are sealed with an O_2 impermeable barrier film such as ethylene vinyl alcohol (EVOH) exhibiting an extremely low O_2 transmission rate of 0.5 cc/m^2/24h (McMillin, 2008). Due to this high gas permeable polyphasic materials, gas losses of MAP trays due to diffusion can be neglected as main causative of headspace changes.

Mitochondrial respiration of meat cells. Another explanation for the observed O_2 decrement of MA packages is thought to be metabolic activity of mitochondria from meat cell after slaughtering (Esmer *et al.*, 2011). As mentioned before, it is not possible to calculate the oxygen uptake rate of mitochondria directly on meat, thus values from *in vitro* studies have to be taken. Tang *et al.* (2005) calculated an oxygen consumption rate for mitochondria of 164 nmol O_2/min for one milligram of isolated mitochondrial protein from bovine cardiac muscle two hours *post mortem* at 25 °C. Although this value appears quite high compared to microbial respiration, one can expect a significantly lower oxygen consumption rate for MAP beef stored at 4 °C instead of 25 °C, whereas the amount of mitochondria in non-heart related meat types is also expected to be lower. Furthermore, diffusion of oxygen into the meat surface is limited to 2-4 millimeters (Zaritzky and Bevilacqua, 1988; Tofteskov *et al.*, 2017), thus only a minor part of mitochondria in relation to total meat weight is assumed to be oxidized in MA packages. At least, the activity of mitochondria is also known to decrease strongly during meat storage due to a decrease in meat pH (Tang *et al.*, 2005), with no remaining activity being detected after 6 days *post mortem* for ox muscle (Cheah and Cheah, 1971; 1974; Gao *et al.*, 2013). Summing up, it appears that at the beginning of MAP storage O_2 consumption is mainly due to mitochondrial respiration, whereas the contribution can be neglected after few days.

Meat oxidation processes. Oxidation of unsaturated fats and proteins as well as myoglobin from meat has also been discussed as causative for O_2 consumption in MA packages. Similar to mitochondrial respiration, a direct measurement of the amount of O_2 consumed by fat and protein oxidation processes on meat is almost impossible due to the complexity of chain reactions taking place in the process of autocatalysis (Frayn, 1983; Chaix *et al.*, 2014). However, an *in vitro* study from Frayn (1983) came up with 0.04 mol O_2 and 0.09 mol O_2 being consumed per gram of full oxidized protein or fat ($C_{55}H_{104}O_6$). A more precise calculation can be conducted for the process of myoglobin oxidation based on the assumption that the molarity of O_2 bound by myoglobin to form oxymyoglobin is equivalent. Considering a myoglobin content of 4.86 mg/g for Indian beef (Babji *et al.*, 1989), 100 g of beef would consume approximately 0.9 mg of O_2 (Chaix *et al.*, 2014), which is comparable high to the other causes discussed for headspace O_2 consumption. Nevertheless, as mentioned above, O_2 diffusion into the meat surface is limited to few millimeters, thus proteins, lipids and myoglobin are not expected to be fully oxidized during storage. Furthermore, several studies demonstrated that lipid and protein oxidation is a rather constant processes occurring during whole storage period

of MAP meat (Olivares *et al.*, 2012; Fu *et al.*, 2014; Kang *et al.*, 2014). Taken together, even though the contribution of oxidation processes to headspace O_2 consumption cannot be quantified directly on meat, these calculations demonstrated that meat oxidation is a crucial factor, which have to be considered when talking about the shelf development of the headspace atmosphere of MAP meat.

Concluding, all of this considerations led to the assumption that directly after slaughtering headspace O_2 consumption is mainly due to mitochondrial respiration as well as oxidation processes of fat, proteins and myoglobin and less due to bacterial metabolism. However, during storage of MAP meat O_2 consumption by microorganisms increases exponentially, while the contribution of all other factors to headspace O_2 consumption decrease or remains constant at a lower level. Furthermore, microbial metabolism is the only causative resulting in a concomitant increase in CO_2, thus fitting to the observed shelf development of long-time stored MAP meat. Thus, microbial respiration can be seen as main causative for the observed headspace changes during long-time storage of high oxygen MAP meat.

Based on this assumption, several questions can be derived concerning microbial O_2 consumption in MA packages. For instance, it is still unclear, which and how many species of the ESOs contribute to the observed headspace changes and whether those species are considered as meat spoilers or protective cultures as discussed above. Furthermore, studies are missing, to quantify the oxygen consumption rate of those organisms *in situ* and *in vitro* in order to validate whether their contribution to headspace O_2 reduction in MA packages is equal or significantly different. This would be crucial to understand headspace development of single MA packages, which all differ in their microbial composition of ESOs. Further on, investigations are missing uncovering metabolic pathways responsible for O_2 consumption, as it is still unclear whether other enzymatic reactions despite respiration can also significantly contribute to measurable O_2 consumption. Only by addressing those knowledge gaps, the microbial contribution of headspace changes in high oxygen MAP meat can be fully understood.

1.6. Oxygen sensors for monitoring headspace changes in MA packages

Intelligent food packaging systems. In recent years new technologies have been invented, which aimed to monitor product safety in concern of microbial meat spoilage and packaging damage. Those technologies are called “intelligent food packaging systems”, as they are based on small sensors, which are frequently integrated into the food wrapper during the packaging process. Great efforts have been done, especially to perform real-time monitoring and recording of high throughput data by simultaneously avoiding interfering with the food product (Fuertes *et al.*, 2016). Parameters measured by those technologies due to their association with food spoilage are e.g. temperature, gases such as O_2 and CO_2, pH, humidity and volatile amines. For example, there are time and temperature indicators monitoring temperature changes during transport of food products (Kim *et al.*, 2016), pH sensors detecting changes of the pH value due to microbial metabolism (Chun *et al.*, 2014; Kuswandi *et al.*, 2014) and gas sensors indicating leaking of food packages (Matindoust *et al.*, 2016).

Oxygen sensors. Concerning gas sensors, investigations made to record O_2 and CO_2 development in food packages where mainly focused on biosensors that can be integrated or even directly printed on single meat packaging trays (McEvoy *et al.*, 2003) allowing a non-destructive validation of the product quality. Among those are optical and electrochemical sensors, which are either based on fluorescence or infrared light (Werle *et al.*, 2002; McEvoy *et al.*, 2003; Nopwinyuwong *et al.*, 2010). Optical O_2 sensors are highly discussed for their appliance in MAP of meat due to their low price, easy miniaturization, simple usage, low chemical interference and O_2 loss (Meng *et al.*, 2014). Most commonly, those optical sensors measure intensity changes in the luminescence emitting from an O_2 sensitive probe molecule. This probe molecule is sprayed on a small sensor spot, which can be integrated in the food package. Finally, luminescence signals can be readout by a fiber-optic phase detector (Fitzgerald *et al.*, 2001). As O_2 can reversibly quench the luminescence, sensors can be re-used several times (Mills, 1997; Meng *et al.*, 2014). Despite the fact that sensor technologies are known for more than two decades, less research has been done yet regarding the application of those O_2 sensors in MAP meat. There are only few studies investigating this technology to e. g. validate the potential of identifying product wrapping damages (Fitzgerald *et al.*, 2001) or to correlated residual O_2 with the level of lipid oxidation in vacuum or anoxic MA packaged beef and poultry (Smiddy *et al.*, 2002a; Smiddy *et al.*, 2002b). No study has been conducted yet, validating the application of optical sensor technologies for monitoring headspace O_2 changes in high oxygen (>70%) MAP meat.

Application of oxygen sensors in MAP meat for detecting meat spoilage. As discussed above, a decrement of O_2 in the headspace of high oxygen MA meat packages is an indicator for microbial cell load (Höll *et al.*, 2016; Hilgarth *et al.*, 2018a) as well as meat oxidation processes (Frayn, 1983; Chaix *et al.*, 2014). Both factors are crucial for the shelf life of meat, as increased production of spoilage compounds and meat degradation by oxidation of lipids and proteins are responsible for the quality loss of MAP meat (Kang *et al.*, 2014; Ana Beatriz *et al.*, 2018). Thus, the content of O_2 in the headspace of MA packages provides information about the spoilage process of meat. This raises the question, whether meat spoilage can be predicted prior to its onset, by monitoring the O_2 content of MA packages applying the described O_2 sensor spot technology. This would enable sorting within retail by declaring lower prices for fast spoiling meat products, and consequently reduce the amount of discarded meat.

1.7. The lifestyle of *Pseudomonas* species on anoxic packaged meat

In a previous study, Hilgarth *et al.* (2019) demonstrated that microbial O_2 consumption can even lead to complete anoxic conditions within high oxygen MAP minced beef when stored for 8 days at 10 °C. In this study, he observed a high abundance of certain *Pseudomonas* strains belonging to the species *P. lundensis*, *P. weihenstephanensis* and *P. fragi* at a late storage time of 10-14 days, when O_2 was already depleted within the meat packages. Even though the total cell count on minced beef was stationary at this time point, some strains of the isolated *Pseudomonas* species exhibited the potential to grow under anoxic conditions *in vitro* on BHI agar plates, thus suggesting also anaerobic growth *in situ* on minced beef (Hilgarth *et al.*, 2019). This was rather surprising, as almost all *Pseudomonas* species including *P. lundensis*, *P. weihenstephanensis* and *P. fragi* are described as strict aerobic bacteria, unable to perform a fermentative metabolism (Hussong *et al.*, 1937; Molin *et al.*, 1986; Von Neubeck *et al.*, 2016). In accordance to Hilgarth *et al.* (2019), other studies also reported the presence and sometimes even growth of meat-spoiling *Pseudomonas* strains in vacuum packs containing lamb, beef and poultry (Table 2) (Kakouri and Nychas, 1994; Ercolini *et al.*, 2009; Kaur *et al.*, 2017). However, it has been assumed that the observed growth of those *Pseudomonas* species was based on residual O_2 within vacuum packs (Kaur *et al.*, 2017). Actually, due to results from Hilgarth *et al.* (2019), doubts arise regarding this explanation, as growth of certain *Pseudomonas* strains on anoxic incubated BHI agar plates indicate a true anaerobic metabolism of those strains. As those meat-spoiling species are known to produce putrid metabolites and VOCs (Dainty *et al.*, 1989; Drosinos and Board, 1995; Koutsoumanis *et al.*, 2006; Stanborough *et al.*, 2018), even long-term survival or restricted growth of *Pseudomonas* cells under strict anoxic conditions could contribute to perceptible meat spoilage. Consequently, it appears like the contribution of *Pseudomonas* species to spoilage of anoxic packaged meat has been underestimated in the past, especially in vacuum packs and high oxygen MAP trays where cell counts of *Pseudomonas* were enriched due to an initial oxic atmosphere prior to a switch to anoxic atmospheres. Therefore, *in situ* studies on strictly anoxic packaged meat are missing to demonstrate whether certain *Pseudomonas* strains as those isolated from Hilgarth *et al.* (2019) are actually able to persist/ grow *in situ* on anoxic MAP meat, or whether the described growth of *Pseudomonas* on MAP meat and vacuum packs is due to residual O_2.

Furthermore, analyses of the anaerobic metabolism of certain meat-spoiling *Pseudomonas* strains are missing to support and explain the assumption of an anaerobic lifestyle of those species. Beyond the huge genera of *Pseudomonas*, only certain organisms are able to perform an anaerobic metabolism comprising *P. denitrificans*, *P. stutzeri*, *P. aeruginosa* and *P. putida.* However, the naturally occurring habitat of those species are less related to meat but rather to human, marine or soil environments as well as other food products such as tofu (Carlson and

Ingraham, 1983; Yoon *et al.*, 2002; Wu *et al.*, 2005; Lalucat *et al.*, 2006; Stoops *et al.*, 2012). However, due to phylogenetic relationship, similarities between the energy metabolism of putative anaerobic meat-spoiling *Pseudomonas* species and those well studied anaerobic *Pseudomonas* species can be assumed. In detail, the possibility to perform denitrification or dissimilatory nitrate reduction of *P. denitrificans*, *P. stutzeri* and *P. aeruginosa* under anoxic conditions has been described by Carlson and Ingraham (1983). Thereby, nitrate is used as an alternative electron acceptor to oxygen, thus keeping the respiratory chain running under anoxic conditions what provides ATP for growth. Furthermore, *P. aeruginosa* is able to perform pyruvate fermentation converting pyruvate to acetate by generating one molecule of ATP under anoxic conditions. It has been demonstrated that pyruvate fermentation does provide long-term survival of *P. aeruginosa* under anoxic conditions (Eschbach *et al.*, 2004). As a third, arginine fermentation via the arginine deiminase pathway (ADI) enables anaerobic growth of *P. aeruginosa* by production of one molecule of ATP (Vander Wauven *et al.*, 1984). No such anaerobic metabolism has yet been discovered for meat-spoiling *Pseudomonas* species such as *P. lundensis*, *P. weihenstephanensis* and *P. fragi*. Thus, it remains unclear, weather the observed anaerobic growth of certain *Pseudomonas* strains on BHI plates or vacuum packaged meat is due to a similar anaerobic metabolism as described for *P. aeruginosa*. Consequently, metabolic studies of anaerobic growing meat-spoiling *Pseudomonas* species are needed to answer this knowledge gaps.

2. Hypotheses and Objectives

This study aimed to understand the lifestyle and formation of the consortium of meat-spoiling bacteria in MA packages by applying advanced mass spectrometry technologies, which enable to uncover the hitherto unexplored metabolism as well as metabolic adaptations of these organisms on MAP meat. Thus, knowledge about meat-spoiling organisms should be complemented, which was hitherto focused on the abundance of meat-spoiling bacteria on meat as well as their production of putrid metabolites. In detail, proteomic data should be used to explain the influence of MAP gases on microbial growth and metabolism as well as help to mechanistically explain microbial coexistence on meat. Contrary, the influence of bacterial metabolism on headspace changes of MA packages should be studied. Therefore, single microbial induced headspace oxygen consumption should be quantified and referred to metabolic differences as derived from “omic” analysis. The obtained results should be used to validate a new prediction method for the onset of meat spoilage based on the O_2 content in MA packages. This would enable individual sorting of MA packages at retail level and thus reduce the amount of discarded meat. Furthermore, previously isolated putative anaerobic meat-spoiling *Pseudomonas* species should be characterized regarding their ability to grow and metabolically adapt to anoxic conditions on meat, estimating their role as meat spoilers on vacuum and anoxic MAP meat. Therefore, this thesis is divided into three chapters:

I. Metabolic adaptation of meat organisms to MAP gases

In this chapter, the growth and metabolic adaptation of the typical Gram-positive meat-spoiling bacteria *B. thermosphacta*, *C. divergens*, *C. maltaromaticum*, *L. gelidum* subsp. *gelidum* and *L. gelidum* subsp. *gasicomitatum* in response to different MAs should be analyzed. By understanding single bacterial metabolism, this study aimed to mechanistically explain the species-specific dominance as well as co-existence of the whole microbial consortium on MAP meat.

<u>Working hypotheses and approaches taken:</u>

- Microbial resistance to MA gases and their coexistence on MAP meat is provided by a multifactorial adaptation of their metabolism
    - Establishment of differential proteomes and growth curves for these bacteria growing under three different gas atmospheres as applied in MAP and normal air
    - Analysis of membrane fatty acids upon growth under different gas atmospheres

- Recording of the growth of bacteria on MAP meat, packaged under increasing CO_2 concentrations

- The measured *in vitro* behavior of bacteria cultivated in meat simulation (MS)-media can be used to predict the behavior in real meat systems

  - Correlation of proteomic data obtained from bacteria growing on meat and bacteria growing in MS-media

II. Change of the headspace atmospheres by microbial metabolism

The aim of this chapter was to attribute O_2 consumption in the headspace of MAP meat to microbial metabolic activity. The contribution of the single meat spoilers *B. thermosphacta*, *C. divergens*, *C. maltaromaticum*, *L. gelidum* subsp. *gelidum* and *L. gelidum* subsp. *gasicomitatum* to O_2 consumption should be quantified and explained by uncovering their corresponding species-specific O_2 consuming reactions. Concomitant to microbial O_2 consumption, microbial spoilage should be analyzed, in order to validate, whether the time point of meat spoilage can be predicted based on the O_2 content in the headspace of MAP meat.

Working hypotheses and approaches taken:

- The contribution of meat-spoiling bacteria to O_2 consumption in the headspace of MAP meat is species-specific and depends on specific microbial pathways / enzymatic reactions

  - Quantification of bacterial O_2 consumption in MS-media

  - Comparison of microbial respiratory activity to genomic settings and proof of respiratory activity by physiological analysis

  - Quantification of the contribution of single O_2-consuming enzymes to oxygen consumption by qPCR

  - Determination of the differential expression of O_2-consuming enzymes under different gas atmospheres

- The MAP-gas CO_2 inhibits microbial growth by reducing the activity of enzymes, which are active in O_2 consumption

  - Determination of bacterial O_2 consumption in media gassed with 70% O_2 / 30% CO_2 or 70% O_2 / 30% N_2.

- There is a correlation between microbial O_2 consumption and meat spoilage, which can be used to predict the onset of meat spoilage of individual meat products prior to sensorial perception

    - Monitoring O_2 consumption in deliberately contaminated MAP meats, followed by sensory analysis of the meat

III. Role and lifestyle of *Pseudomonas* species on anoxic MAP meat

This chapter aimed to analyze the ability of the typical meat-spoiling *Pseudomonas* species *P. lundensis*, *P. weihenstephanensis* and *P. fragi* to grow or persist on anoxically packaged meat. Putative anaerobic growth should be explained by analyzing bacterial metabolism.

Working hypotheses and approaches taken:

- Meat-spoiling *Pseudomonas* species are able to grow on anoxically packaged meat

    - Determination of growth of *Pseudomonas* on anoxic packaged chicken breast filet

- Anaerobic growth is enabled by metabolic adaptation of their energy metabolism

    - Establishment and evaluation of comparative proteomics for *Pseudomonas* under air and 100% N_2

    - Performance of physiological experiments to determine any influence of $NaNO_3$ and arginine on the anaerobic growth of *Pseudomonas*

3. Material and methods

3.1. Basic cultivation methods

3.1.1. Species and strains

Bacteria used in this study, originated from the strain collection of the institution “Technical Microbiology Weihenstephan” (TMW). They were collected and isolated in previous studies done by Dr. Maik Hilgarth and Dr. Linda Höll, from high oxygen MAP minced beef, beef steak, turkey or chicken breast (Höll *et al.*, 2016; Hilgarth *et al.*, 2018a; Hilgarth *et al.*, 2019). This includes 8 strains of *L. gelidum* subspecies *gelidum*, 11 strains of *L. gelidum* subspecies *gasicomitatum*, 10 strains of *C. divergens*, 6 strains of *C. maltaromaticum* and 10 strains of *B. thermosphacta*, 2 strains of *P. lundensis,* 2 strains of *P. weihenstephanensis* and 2 strains of *P. fragi*. Additionally, the species *P. aeruginosa* form the institution of “German collection of microorganisms and cell cultures” (DSMZ) was used as a positive control. A list of all species and strains used in this study and their isolation sources are given in Table 3.

Table 3. Summary of all strains used in this study as well as their origin of isolation.

L. gelidum* subsp. *gelidum		
Nr.	**strain**	**source**
1	TMW2.2319	beef steak
2	TMW2.2320	beef steak
3	TMW2.2321	beef steak
4	TMW2.2322	beef steak
5	TMW2.2323	beef steak
6	TMW2.1998	beef steak
7	TMW2.1618	beef steak
8	TMW2.1620	beef steak

L. gelidum* subsp. *gasicomitatum		
Nr.	**strain**	**source**
1	TMW2.2324	beef steak
2	TMW2.2325	beef steak
3	TMW2.2326	beef steak
4	TMW2.2327	beef steak
5	TMW2.2328	beef steak
6	TMW2.2329	beef steak
7	TMW2.2330	beef steak
8	TMW2.1507	beef steak
9	TMW2.1616	chicken breast
10	TMW2.1617	beef steak
11	TMW2.1619	beef steak

B. thermosphacta		
Nr.	**strain**	**source**
1	TMW2.1906	beef steak
2	TMW2.2331	beef steak
3	TMW2.2332	beef steak
4	TMW2.2101	beef steak
5	TMW2.2333	beef steak
6	TMW2.1565	chicken breast
7	TMW2.1567	chicken breast
8	TMW2.1564	chicken breast
9	TMW2.1570	chicken breast
10	TMW2.1569	chicken breast

C. divergens		
Nr.	**strain**	**source**
1	TMW2.1510	chicken breast
2	TMW2.1869	turkey
3	TMW2.1871	beef steak
4	TMW2.1907	beef steak
5	TMW2.1575	chicken breast
6	TMW2.1577	chicken breast
7	TMW2.1580	chicken breast
8	TMW2.1574	chicken breast
9	TMW2.1863	chicken breast
10	TMW2.1866	chicken breast

C. maltaromaticum		
Nr.	**strain**	**source**
1	TMW2.1509	chicken breast
2	TMW2.1581	chicken breast
3	TMW2.1582	chicken breast
4	TMW2.1583	chicken breast
5	TMW2.1624	chicken breast
6	TMW2.1867	poultry

P. lundensis		
Nr.	**strain**	**source**
1	TMW2.1732	beef steak
2	TMW2.2076	minced beef

P. weihenstephanensis		
Nr.	**strain**	**source**
1	TMW2.1728	beef steak
2	TMW2.2077	minced beef

P. fragi		
Nr.	**strain**	**source**
1	TMW2.2081	minced beef
2	TMW2.2082	minced beef
P. aeruginosa DSM 1117		

3.1.2. Basic media for precultures

Brain-heart-infusion (BHI) broth medium (Roth, Karlsruhe, Germany) was used for preparing solid and liquid precultures as well as cryo-conserved cultures. Therefore, 37 g BHI was mixed with one liter of deionized water (diH_2O). For preparing solid agar plates, 20 g/l agar-agar (Roth, Karlsruhe, Germany) was added. The pH-value was adjusted to 7.4 and medium was autoclaved at 121 °C for 20 minutes.

3.1.3. Cryo-stock conservation

Media for experiments were inoculated either from freshly prepared liquid cultures, plate cultures or cryo-conserved cultures. Latter were prepared mixing fresh grown cells suspended in BHI with 34% (w/v) glycerol. Cryo-stocks were frozen at -80 °C until usage. For experiments where inoculation was performed directly from cryo-stocks, the colony forming unit (CFU) of one representative cryo-stock was determined after 3 days at -80 °C. After this time period, the CFU values were assumed to be constant.

3.1.4. Development of a meat simulation (MS)-medium

As real meat is a complex system, which often interferes with molecular analysis, a MS-medium was developed, enabling a simple performance and analysis of experiments. Based on the growth requirements of different bacteria, the MS-medium was adapted for each species. Meat extract was the basic component of the MS-medium, which was supplemented with different additives: glycerol (Gerbu Biotechnik GmbH, Heidelberg, Germany), tween80 (Gerbu Biotechnik GmbH, Heidelberg, Germany), hemin chloride (Roth, Karlsruhe, Germany) dissolved in dimethyl sulfoxide (99.8%) (Roth, Karlsruhe, Germany), menaquinone-4 (Sigma-Aldrich, St. Louis, MO, United States) dissolved in ethanol (100%) (Roth, Karlsruhe, Germany) and glucose monohydrate (Merck, Darmstadt, Germany). Additives were supplemented as they represent main components of real meat but are hard to extract (e.g. fat) or destroyed by autoclaving (e.g. heme, menaquinone and glucose). According to previous studies, fat was substituted by glycerol and tween80 (Man *et al.*, 2008; Reitermayer *et al.*, 2018). The concentration of meat extract was defined for each species individually, whereas the concentration of additives was uniform for all species. Therefore, amounts were chosen due to literature or if not available, due to growth experiments testing different concentrations of each additive (Table 4). Therefore, two strains, one from beef and one from chicken were selected for each species and tested for their growth in 100 g/l meat extract (Merck, Darmstadt,

Germany). The strain exhibiting highest growth was chosen for development of MS-media, comprising *C. divergens* TMW2.1577, *C. maltaromaticum* TMW2.1583, *B. thermosphacta* TMW2.2331, *L. gelidum* subsp. *gelidum* TMW2.1618, *L. gelidum* subsp. *gasicomitatum* TMW2.1507 and *P. lundensis* TMW2.1732. All growth experiments were performed in sterile microtiter plates as described in chapter 3.1.5.

3.1.5. Microtiter plate assays monitoring bacterial growth

Growth of bacteria with and without addition of specific ingredients (Table 4) was monitored in 96-well microtiter plates (Sarstedt, Nümbrecht, Germany). Therefore, the optical density at 600 nm ($OD_{600\ nm}$) was measured and recorded by a FLUOstar Omega microplate reader (BMG Labtech, Ortenberg, Germany). Measurements were performed every 30 minutes over 48 hours at 25 °C. Plates were shaken double orbitrap with 200 rpm before each measurement. Bacteria were inoculated in replicates with an $OD_{600\ nm}$= 0.1 in 200 µl of media.

Table 4. List of ingredients and their concentrations tested for growth experiments of bacteria. The growth of *B. thermosphacta*, *C. divergens*, *C. maltaromaticum*, *L. gelidum* subsp. *gelidum*, *L. gelidum* subsp. *gasicomitatum* and *P. lundensis* was tested by addition of different ingredients harboring different concentrations.

Ingredient	Concentration(s)	Unit	Source
Meat extract with and without 0.5% glycerol	0.78, 1.56, 3.13, 6.25, 12.5, 25, 50, 100	g/l	(Macaskie *et al.*, 1984)
Hemin chloride	0.2	µg/ml	(Brooijmans *et al.*, 2009)
Menaquinone-4	20	ng/ml	(Brooijmans *et al.*, 2009)
Tween80	0, 0.05, 0.5, 0.7, 1, 5, 10	mM	----------
Glucose monohydrate	0.5	%	(Macaskie *et al.*, 1984; Reitermayer *et al.*, 2018)
Hydrogen peroxide	0.008, 0.001, 0.02, 0.03, 0.04, 0.05, 0.06, 0.07, 0.08, 0.09, 0.1, 0.2, 0.3, 0.4, 0.5	%	----------

3.1.6. Oxic and anaoxic cultivation in MS-media for strain selection

Oxic cultivation of strains was performed in 100 ml narrow-neck Erlenmeyer flasks filled with 45 ml of the previous developed species-specific MS-media. Cultures were inoculated with $OD_{600\ nm}$= 0.1 and shaken at 180 rpm at 25 °C. The cultivation time was depending on the growth rate of bacteria. *Carnobacterium* and *Brochothrix* species were cultivated for one day, *Leuconostoc* species for two days. Growth was monitored manually every two hours using one-way cuvettes and a Novaspec Plus spectrophotometer (GE Healthcare Europe, Freiburg, Germany).

For anoxic cultivation, diH_2O was cooked in a water boiler to remove residual O_2 prior to dissolving of ingredients for MS-media preparation. After autoclaving, MS-media was aerated one hour with nitrogen to further remove residual O_2 within the media and to replace air in the headspace of the bottles. An anaerobic chamber was used to aliquot 45 ml of the anoxic media

into 100 ml gas tight Schott flasks locked with rubber discs and protection caps. Inoculation ($OD_{600\,nm}$= 0.1) and sample taking was performed under the anaerobic chamber. Samples were taken every 2 hours and measured as described above. Cultivation was performed with horizontal lying gas tight locked flasks outside the anaerobic chamber with 180 rpm at 25 °C.

3.1.7. Anaerobic growth with sodium nitrate *in vitro* in minimal medium

Anaerobe dissimilatory nitrate reduction was tested for the six *Pseudomonas* strains *P. lundensis* TMW2.1732, *P. lundensis* TMW2.2076, *P. weihenstephanensis* TMW2.2077, *P. weihenstephanensis* TMW2.1728, *P. fragi* TMW2.2081, *P. fragi* TMW2.2082 and the positive control *P. aeruginosa* DSM 1117 in a 96-well microtiter plate. Therefore, a minimal medium containing 4.75 $g*l^{-1}$ K_2HPO_4 (Merck, Darmstadt, Germany), 4.55 $g*l^{-1}$ KH_2PO_4 and 2 $g*l^{-1}$ yeast extract (Roth, Karlsruhe, Germany) was prepared. Media was either supplemented with or without 20 mM $NaNO_3$ and pH was adjusted to 6.69. Both media were autoclaved and subsequent aliquoted within the anaerobic chamber into a microtiter plate. In order to ensure anoxic media, the microtiter plate was kept in the anaerobic chamber for 48 hours prior to inoculation. Plates were inoculated with an $OD_{600\,nm}$= 0.1 of a fresh prepared (chapter 3.1.2) and washed aerobe preculture and measured by a microtiter plate reader after 3 days of incubation at 25 °C within the anaerobic chamber. Significant differences between growth with or without $NaNO_3$ were determined by a Welch T-test with $p < 0.05$.

3.1.8. Anaerobic growth with arginine and glucose *in vitro* on minimal medium

Anaerobic growth based on arginine or glucose monohydrate was tested for the strains *P. lundensis* TMW2.1732, *P. lundensis* TMW2.2076, *P. weihenstephanensis* TMW2.2077, *P. weihenstephanensis* TMW2.1728, *P. fragi* TMW2.2081, *P. fragi* TMW2.2082 and *P. aeruginosa* DSM 1117. Therefore, agar plates containing 5 $g*l^{-1}$ NaCl (Roth, Karlsruhe, Germany), 2 $g*l^{-1}$ KH_2PO_4 (Merck, Darmstadt, Germany) and 1 $g*l^{-1}$ peptone from soy (Roth, Karlsruhe, Germany) were prepared. To detect arginine metabolism, 12 $mg*l^{-1}$ of the pH dye phenol red (Thermo Fisher Scientific, Waltham, MA) was added to the minimal medium changing from yellow to purple in case of alkalisation. Media were either supplemented with 20 mM arginine (Sigma-Aldrich GmbH, Darmstadt, Germany), 20 mM glucose monohydrate (Merck, Darmstadt, Germany) or without any additional ingredient. The pH of each medium was adjusted to 6.0 using inorganic acids and bases. All ingrediencies were sterile filtered into pre-autoclaved water/agar-agar due to their heat instability using a sterile filter with 0.02-mm pore size.

Plates were incubated with a freshly prepared (chapter 3.1.2) and washed preculture, exhibiting an $OD_{600\,nm}$= 0.5 adjusted in quarter-strength ringer solution. For incubation, 20 µl of each preculture were dripped on plates containing arginine, glucose or non-additional ingredient. The experiment was performed twice, as plates were incubated once under oxic

and once under anoxic conditions at 25 °C. Anoxic incubation of the plates was performed in PP-EVOH trays containing 100% N_2 atmosphere and an oxygen scavenger to ensure strict anoxic conditions. After four days, standardized pictures were taken by a colony doc-it imaging station (VWR, Darmstadt, Germany). *P. aeruginosa* DSM 1117 was used as a positive control.

3.1.9. API 20 NE test for *Pseudomonas* strains

To check for dissimilatory nitrate reduction as well as arginine fermentation, an API 20 NE test (BioMérieux, Nürtingen, Germany) was performed for the strains *P. lundensis* TMW2.1732, *P. lundensis* TMW2.2076, *P. weihenstephanensis* TMW2.2077, *P. weihenstephanensis* TMW2.1728, *P. fragi* TMW2.2081 and *P. fragi* TMW2.2082 following the manufacturer instructions. After 24 hours, results from the NO_3, TRP and GLU tests were recorded, while results from other tests were recorded after 48 hours.

3.1.10. Measurements of gases

Three measurement devices were applied for monitoring of dynamic gas changes in liquid media as well as atmospheric headspace. All measurement devices and their principles are explained in detail in the following:

I) Fluorescence based O_2 measurement by an oxygen sensor spot

A SP-PSt3 oxygen sensor spot provided by PreSens precision sensing GmbH (Regensburg, Germany) was applied, enabling a non-invasive, fast and easy monitoring of the oxygen content in the headspace of MAP trays as well as in liquid solutions. The oxygen sensor spot consists of a thin polymer film, containing an indicator and a reference dye, which are immobilized on a permeable polymer matrix layer. The principle concept of O_2 measurement is based on fluorescence quenching (Kautsky, 1939). Whereas the emitted fluorescence signal of the indicator dye is depending on the O_2 content, the fluorescence intensity of the reference dye does not. By calculating the ratio of both signals given as

$$I_R = \frac{I_{indicator}}{I_{reference}}$$

Equation 1. Calculating the fluorescence signal of SP-PSt3 sensor spots.

internal referencing can be done. Signals of the reference and indicator dye were measured by either a portable and easy to handle Fibox 3 LCD trace oxygen meter or an OXY-1-SMA fiber optic oxygen meter, which had to be connected to an external computer running the software PreSens measurement Studio (PMS2). Latter contains a polymer optic fiber cable (LED wavelength 505 nm) as well as a Pt100 temperature sensor (0-50 °C, ±1 °C) and considers the following parameters: Humidity, temperature, salinity and atmospheric pressure.

Prior to the start of a new experiment, a two-point calibration was done. Depending on the experimental setup, calibration was performed with gas or liquid references.

First calibration was done at 0% O_2 according to the manufacturer instructions. Therefore, oxygen-free water (**cal0**) was prepared, adding one gram of sodium sulfite (Na_2SO_3) and 50 µl cobalt nitrate ($Co(NO_3)_2$) standard solution (p(Co) = 1000 mg/l; in nitric acid 0.5 mol/l) to 100 ml of di$H_2$0. The vessel was closed and shaken for one minute. For calibration with gases, nitrogen gas (Westfalen AG, Münster, Germany) was used.

The second calibration was done at 20.1% O_2 (**cal100**) with air-saturated water. Therefore, air was bubbled into 100 ml di$H_2$0 for approx. 30 minutes. For calibration with gases, vessel or MAP trays filled with water-vapor-saturated air were used.

II) Fluorescence based oxygen measurement by a coated 96-well microtiter plate

High throughput oxygen measurement was performed, using 96-well OxoPlates provided by PreSens precision sensing GmbH. The round bottom part of each well of the OxoPlate was coated with the same fluorescence dye as described for the oxygen sensor spots. Thus, the principal method for oxygen measurement was the same as described above. The indicator and reference signal were read out by the fluorescence reader FLUOstar Omega (BMG Labtech, Ortenberg, Germany) in a dual kinetic mode with the extinction filter 544 nm and emission filter 650 nm (indicator signal) and 590 nm (reference signal). The integration start was set to 0 µs and the integration time to 500 µs. A two-point calibration was performed for each medium, preparing a **Cal0** solution with sodium sulfite and **Cal100** solution with air saturated medium according to the manufacturer instructions. Gain adjustment was done prior to first measurement and the oxygen content of each medium was calculated applying the following equation:

$$pO_2 = 100x(\frac{k_0}{I_R} - 1)/(\frac{k_0}{k_{100}} - 1)$$

Equation 2. Calculating the oxygen partial pressure in % air saturation for each well.

with I_R being defined as described in Equation 1 and k_0 and k_{100} representing both calibration points.

III) CO_2 and O_2 measurement of gaseous headspace by a gas analyzer

A gas analyzer PA7.0 (Witt-Gastechnik GmbH & Co KG, Witten, Germany) was used for measuring headspaces of glass bottles and controlling the defined gas mixtures of the packaging machine. The device is able to analyze O_2 (0-100% ± 0.2%) and CO_2 (0-100% ±

0.5%) contents of gas mixtures. Residual gas is given as N_2. According to the producer, CO_2 is monitored using an infrared measuring cell, whereas O_2 is measured chemically. For monitoring headspaces in glass bottles, the measuring mode was set to “tiny mode” as this consumes less than one milliliter of gas. Control measurements of gas mixtures in MAP trays were performed with “normal mode” consuming seven milliliters of gas. Furthermore, the gas analyzer PA7.0 was used to monitor the total gas pressure within glass bottles.

A two-point calibration of each gas was done prior to the start of a new experiment. For calibration of O_2, 100% N_2 gas was used as **cal0** whereas normal air (21% O_2) was used for **cal100**. CO_2 was calibrated using 100% N_2 gas as **cal0** and 100% CO_2 (Westfalen AG, Münster, Germany) as **cal100**.

3.1.11. Measuring oxygen consumption in 96-well OxoPlates

The effect of CO_2 on bacterial oxygen consumption was monitored in 96-well OxoPlates as described in chapter 3.1.10. Therefore, species-specific MS-media were prepared and bubbled either with **30% N_2** / 70% O_2 or **30% CO_2** / 70% O_2 for 1.5 hours until oxygen saturation. Media were aliquoted in triplicates by transferring 180 µl to each well. Inoculation was done with a freshly prepared (chapter 3.1.2) and washed preculture to a final $OD_{600\ nm}$ of 0.3 and oxygen diffusion to the environment was reduced adding 100 µl of paraffin oil to each well. Furthermore, inoculated wells were closed by a lid foil. In order to record oxygen diffusion from the media into the surrounding atmosphere, two non-inoculated wells per medium and gas were measured. The oxygen content of the media was monitored every 10 minutes for 14 hours in a FLUOstar Omega fluorescence reader. Bacterial growth was monitored simultaneously to oxygen consumption in a SPECTROstar Nano BMG Labtech microtiter plate reader. Therefore, a BMG 96-well plate was pipetted the same way and the OD was measured every 10 minutes at 600 nm.

3.2. Experiments in MS-media using glass bottles with a gassing system

3.2.1. Quantifying bacterial O_2 consumption

Bacteria were cultivated in one liter gas-tight locked Schott flasks using a butyl rubber plug and protection caps. A cannula was run through the rubber plug, enabling gas supply, inoculation and sample taking of the media. A second cannula enabled measurements of the gas composition and total gas pressure of the headspace using the PA 7.0 gas analyzer. Furthermore, for non-invasive measurement of the O_2 content within the media, the bottle was equipped with an autoclavable SP-PSt3 oxygen sensor spot. The spot was read-out using a Fibox 3 LCD trace oxygen meter. The bottle was filled half with the species-specific MS-medium, autoclaved and bubbled prior to inoculation with a gas mixture of 30% CO_2 and 70% O_2, until constant starting conditions of 70% O_2 saturation of the media and headspace were achieved. Afterwards, bottles were kept gas tight locking the cannulas with a protection cap. The described experimental setup can be seen in Figure 2.

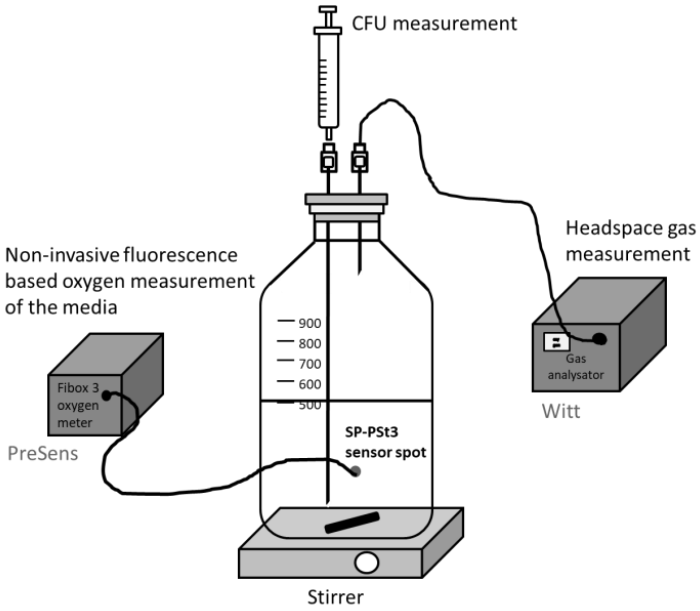

Figure 2. Experimental setup for determining the O_2 uptake rate of bacteria. Bacteria were cultivated in sterile glass bottles filled with 30% CO_2 / 70% O_2 saturated MS-media and a 30% CO_2 / 70% O_2 headspace atmosphere. O_2 consumption in the MS-media was measured by an integrated oxygen sensor spot, and O_2 as well as CO_2 headspace development was monitored by a gas analyzer.

Bacteria were inoculated with an $OD_{600\ nm}$ = 0.1 using a sterile syringe fitting to the cannula. Media was stirred at 160 rpm at 25 °C ± 2 °C. Bacterial growth (CFU), temperature, pH-value, the O_2 content of the media, changes of the headspace gas composition and total pressure of the headspace gases were monitored for 60 hours. All experiments were carried out in triplicates (3 inoculated bottles) for each of the species *B. thermosphacta* TMW2.2101,

C. divergens TMW2.1577, *C. maltaromaticum* TMW2.1581, *L. gelidum* subsp. *gelidum* TMW2.1618 and *L. gelidum* subsp. *gasicomitatum* TMW2.1619.

The amount of dissolved oxygen (DO) of the media was calculated using the O_2 unit calculator provided by PreSens precision sensing GmbH. This considers the following measure parameters: % of O_2 saturation of the media (readout of the O_2 sensor spot), temperature (reference bottle) and atmospheric pressure (PA7.0 gas analyzer). The amount of DO was then used to calculate the oxygen uptake rate (OUR) defined as

$$OUR = k_L a * ([O_2]^* - [O_2]) - d[O_2]/dt$$

Equation 3. Formula for calculating the oxygen uptake rate.

with $[O_2^*]$ representing the DO concentration of saturated media (starting conditions) and $[O_2]$ the DO of media measured at time points of sample taking. K_La is a constant value, defined as the volumetric mass transfer coefficient. This value has to be determined for each media separately, as it considers the O_2-diffusion rate from headspace into the media. Therefore, the gassing-out method was applied (Gupta and Rao, 2003) filling one liter glass bottles with 500 ml of the respective media. Media was gassed with 100% N_2 until O_2 expulsion. Afterwards, the headspace was replaced with 30% CO_2 / 70% O_2 and stirring was turned on (160 rpm). The O_2 entry into the media was monitored over time. K_La was calculated by the equation

$$-k_L a = \Delta ln([O_2]^* - [O_2])/\Delta t$$

Equation 4. Formula for calculating the volumetric mass transfer coefficient.

For comparing the oxygen uptake rate between species, the OUR has to be calculated per single bacteria of each species (OUR/CFU). Therefore, a mathematical model was applied representing dynamic cell growth over time. First, measured CFU values were fitted by a sigmoidal cell growth curve based on the Boltzmann function using OriginPro Version b9.5.0.193 (Northampton, MA, United States). Second, the antiderivative *F(x)* was calculated from the Boltzmann equation *f(x)* and the integral between two sampling time points t_1 and t_2 was calculated, defined as

$$\int_{t1}^{t2} \left(A_2 + \frac{A_1 - A_2}{1 + e^{x - x_0/dx}} \right) dx$$

Equation 5. General equation for calculating the integral between two time points of the Boltzmann function f(x).

with A_2, A_1, x, x_0 and dx representing the specified parameters of the Boltzmann function. Third, the calculated integral was divided by two and $(\int_{t1}^{t2} dx)/2$ was added to the integral of t_1 $\int_0^{t1}$. The resulting integral (y) was used to calculate x from the following equation

$$y = \left(\frac{A * \ln\left(e\frac{B}{D} - \frac{C * x}{E} + 1\right)}{F} + E * x \right)$$

Equation 6. Formula for calculating the time point (x) of average CFU between t_1 and t_2.

applying the Newton-Raphson method. A-F represent constants of the equation. Finally, (x) was inserted into the Boltzmann function to determine the fitted CFU value of the time point t_2. The fitted CFU was then used for calculating the OUR/CFU. For statistical data analyzation, the OUR/CFU was determined separately for each replicate and averaged afterwards.

For determining the amount of O_2 in the headspace in milligram per milliliter, the partial pressure of O_2 in the headspace of the bottles had to be calculated first. This was done using the equation

$$p_{O_2} = p_{total} * x_{O_2}$$

Equation 7. Equation for calculating the partial pressure of O_2 in the headspace of the bottles.

with x_{O2} representing the percentage of O_2 and p_{total} the total pressure of the headspace of the bottles measured by the gas analyzer. The amount of O_2 in the headspace was calculated by applying the ideal gas equation given as

$$p * V = n * R * T$$

Equation 8. Ideal gas equation used for calculating the amount of O_2 in the headspace.

with *p*= partial pressure, *V*= volume of the headspace, *n*= amount of oxygen, *R*= ideal gas constant and *T*= temperature. For comparing the total oxygen consumption in the headspace between different species, the total amount of O_2 consumed within 60 hours was divided by the integral of the CFU curve given as

$$\int_{t_1}^{t_{60}} \left(A_2 + \frac{A_1 - A_2}{1 + e^{x - x_0/dx}} \right) dx$$

Equation 9. Antiderivative *F(x)* of the Boltzmann function for calculating the total CFU within 60 hours.

For statistical data analysis, the total O_2 consumption / CFU in 60 hours was calculated for each replicate and averaged afterwards.

3.2.2. Analyzing bacterial metabolism at different gas atmospheres

In order to identify metabolic adaptation mechanisms to the protective gases O_2 and CO_2, bacteria were cultivated under the gas atmospheres air, N_2, 30% CO_2 / 70% O_2 and 30% CO_2 / 70% N_2, commonly used for MAP of red and white meat. Therefore, selected species (*B. thermosphacta* TMW2.2101, *C. divergens* TMW2.1577, *C. maltaromaticum* TMW2.1581,

L. gelidum subsp. *gelidum* TMW2.1618 and *L. gelidum* subsp. *gasicomitatum* TMW2.1619) were cultivated in 0.5-liter gas tight locked glass bottles filled with 0.4 ml of the corresponding MS-media (Figure 3). Two cannulas enabled constant gassing of the media and sample taking during the whole experiment. Gas used for aeration of the media, was filtered prior to entrance by passing sterile cotton. Bottles were inoculated with $OD_{600\ nm}$ = 0.1 of previously prepared aerobe and anaerobe glycerol stock cultures of bacteria (chapter 3.1.3 / chapter 3.1.6). Aerobe precultures were used for inoculation of experiments with air and 30% CO_2 / 70% O_2 whereas anaerobe precultures were used for experiments aerated with N_2 and 30% CO_2 / 70% N_2. Each species was cultivated under the four gas atmospheres in three independently inoculated gas bottles (total of 12 bottles per species). Cultivation was performed for 48 hours at 25 °C ± 2 °C at 120 rpm.

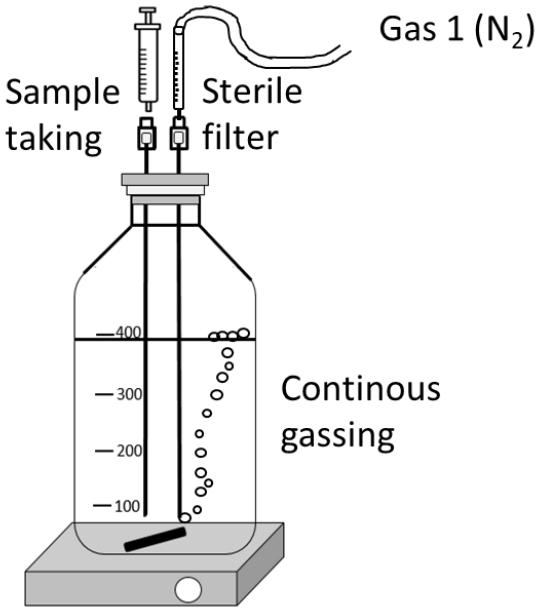

Figure 3. Experimental setup for metabolic analysis of meat bacteria. Bacteria were cultivated in glass bottles containing the developed corresponding MS-medium, which was constantly gassed with one of the four gas atmospheres air, N_2, 30% CO_2 / 70% O_2 and 30% CO_2 / 70% N_2 and stirred at 120 rpm at 25 °C. Samples for metabolic analysis were taken by a sterile syringe.

Bacterial growth was monitored every two hours taking samples by a sterile syringe. At exponential growth phase (log_{10}(CFU/ml) >7), samples for full proteomic analysis by HPLC-MS/MS and transcript analysis of selected target genes by qRT-PCR were taken. Samples were analyzed as described in chapter 3.4.7 (proteomic) and chapter 3.4.2 (qRT-PCR). Furthermore, growth analyses of bacteria cultivated under the different gas atmospheres were conducted.

Different pairwise comparisons of cultivation atmospheres were conducted and applied on proteomic and single transcript data, revealing the effect of CO_2 or O_2 on the metabolism of bacteria. Those pairwise comparisons are shown in Table 5.

Table 5. Conducted comparisons of cultivation atmospheres, which were applied on proteomic and single transcript data in order to uncover the effects of O_2 and CO_2 on bacterial metabolism.

Approach	Comparison	Read out
1	Air *vs*. N_2 Air *vs*. CO_2/N_2 CO_2/O_2 *vs*. CO_2/N_2	Effect of O_2 (oxic to anoxic conditions)
2	(air *vs*. N_2) *vs*. (CO_2/O_2 *vs*. CO_2/N_2) Air *vs*. CO_2/O_2	Effect of high O_2 concentration (70%) compared to low O_2 concentration (21%)
3	Air *vs*. CO_2/O_2	Effect of CO_2 under oxic conditions
4	N_2 *vs*. CO_2/N_2	Effect of CO_2 under anoxic conditions
5	(air *vs*. N_2) *vs*. (CO_2/O_2 *vs*. CO_2/N_2)	Effect of CO_2 under oxic compared to anoxic conditions

The same experimental setup was also applied, analyzing the aerobe and anaerobe metabolism of the six *Pseudomonas* strains *P. lundensis* TMW2.1732 and TMW2.2076, *P. weihenstephanensis* TMW2.1728 and TMW2.2077 and *P. fragi* TMW2.2081 and TMW2.2082. Therefore, the gas atmospheres air (21% O_2 / 79% N_2) and 100% N_2 were chosen and bottles were filled with the corresponding adapted MS-medium as described in chapter 3.1.4. Bacteria were inoculated with freshly prepared (chapter 3.1.2) and washed aerobe precultures, as anaerobe cultivation does not reveal sufficient cells for inoculation with an $OD_{600\ nm}$= 0.1. Cultivation was performed with constant aeration for 48 hours, 120 rpm at 25 °C. Growth of the strains was monitored during the whole cultivation period and samples for proteomic analysis (chapter 3.4.7) were taken at exponential growth phase. For statistical analysis a cut-off value of $p < 0.01$ and $\log_2$(fold-change) >2 was chosen. Furthermore, the pH value of MS-media was monitored over time.

3.2.3. Analyzing cell membrane changes at different gas atmospheres

Same experimental setup as descried in Figure 3 was applied for cultivating the selected species *B. thermosphacta* TMW2.2101, *C. divergens* TMW2.1577, *C. maltaromaticum* TMW2.1581, *L. gelidum* subsp. *gelidum* TMW2.1618 and *L. gelidum* subsp. *gasicomitatum* TMW2.1619 under the three gas atmospheres: 21% O_2 / 0% CO_2 / 79% N_2, 20% O_2 / 30% CO_2 / 50% N_2 and 70% O_2 / 30% CO_2 / 0% N_2. Bacteria were inoculated with an $OD_{600\ nm}$= 0.1 from freshly prepared (chapter 3.1.2) and washed precultures. Bacteria were cultivated at each gas atmosphere in three independently inoculated glass bottles (total of 9 bottles per species). Cultivation was performed at 120 rpm, at 25 °C ± 2 °C by a constant gas flow for 48 hours. Samples for physiological tests, analyzing cell membrane fluidity and permeability as well as fatty acid analysis and cell microscopy were taken at exponential cell growth phase ($\log_{10}$(CFU/ml) > 7). Samples were analyzed as described in chapter 3.4.8 (fatty acid analysis), chapter 3.4.9 (membrane fluidity), chapter 3.4.10 (membrane permeability) and chapter 3.4.11 (cell microscopy).

Effects of O_2 and CO_2 on the measured parameters, fatty acid composition, membrane fluidity, membrane permeability and cell size, were derived by performing pairwise comparisons of measured values under different gas atmospheres. Those comparisons are shown in Table 6.

Table 6. Gas comparisons for revealing the effect of O_2 and CO_2 on biological membranes.

Approach	Comparison	Read out
1	20% O_2 / 30% CO_2 / 50% N_2 *vs* 70% O_2 / 30% CO_2 / 0% N_2	Effect of 70% O_2
2	21% O_2 / 0% CO_2 / 79% N_2 *vs* 20% O_2 / 30% CO_2 / 50% N_2	Effect of 30% CO_2

3.3. Experiments with meat using a packaging machine

For modified atmosphere packaging of meat samples PP trays coated with EVOH were ordered (ES Plastic, Hutthurm, Germany). Those MAP trays (227 x 178 x 40mm) were transparent and exhibited a very high barrier property to O_2 (volumetric permeation rate 0.25 cc.20 µ/m^2.day.atm). For sealing, a corresponding PP-foil with EVOH coating on the outer side was ordered (VarioVAC, Zarrentin, Germany). Packaging was performed using a Rotarius packaging machine (VarioVAC, Zarrentin, Germany) combined with a KM20-100_3ME gas mixer (Witt-Gastechnik GmbH & Co KG, Witten, Germany). Oxygen (BIOGON O) was ordered from Linde (München, Germany), whereas carbon dioxide and nitrogen were obtained from Westfalen (Münster, Germany).

Prior to all MAP experiments, the accuracy of the gas mixer from the packaging machine was evaluated. Therefore, trays containing different gas mixtures of O_2, CO_2 and N_2 were packaged and measured directly afterwards using a PA7.0 gas analyzer. Gas mixtures measured exhibit an accuracy of ±1.2% to the set values. Furthermore, the gas tightness of sealed PP-EVOH trays was checked. Therefore, empty trays were packaged under high oxygen atmosphere (30% CO_2 / 70% O_2) and storage over 21 days. After 3 weeks, gas composition was checked using a gas analyzer. Packages were declared as gas tight with <±1% gas deviation after 21 days.

3.3.1. Inhibitory effect of CO_2 on bacteria inoculated on meat

Beef steaks packaged under high oxygen atmosphere (30% CO_2 / 70% O_2), exhibiting an use-by date >4 days were obtained from a local discounter. Each package contained five slices of beef resulting in a total weight of 320 gram. Packages were opened and beef slices were cut into equal sized round pieces (surface= 62.09 cm^2, volume= 10.94 cm^3). Furthermore, turkey samples stored under high oxygen atmosphere with an use-by date of >4 days were obtained from same discounter. Each package contained one big piece of turkey (600 gram), which was cut into homogenous thick and square pieces (surface= 36 cm^2, volume= 14.4 cm^3).

Cut meat pieces were inoculated with either one of the five species *B. thermosphacta* TMW2.2101, *C. divergens* TMW2.1577, *C. maltaromaticum* TMW2.1581, *L. gelidum* subsp. *gelidum* TMW2.1618 and *L. gelidum* subsp. *gasicomitatum* TMW2.1619. Therefore, cultures were prepared as described in chapter 3.1.2 and washed twice in sterile quarter-strength ringer solution. Cultures were cold adapted prior to inoculation at 4 °C for four hours. Each meat piece was inoculated on both sides with 100 µl of an $OD_{600\ nm}$= 10 adjusted in quarter-strength ringer solution Figure 4a. Cells were homogeneously spread on the cell surface using a sterile spatula. Afterwards meat pieces were packaged in empty PP-EVOH trays at increasing concentrations of CO_2 and constant concentrations of O_2, applying the

following modified atmospheres **15% CO_2** / 20% O_2 / 65% N_2, **30% CO_2** / 20% O_2 / 50% N_2, **50% CO_2** / 20% O_2 / 30% N_2, **70% CO_2** / 20% O_2 / 10% N_2. Nitrogen was used as filler gas to prevent collapsing of meat packages. In total, 48 trays with inoculated meat were packaged (3 replicates x 4 gases x 4 sampling days). MAP meat was stored at 4 °C in the cooling room until sampling. Meat sampling was performed after 0, 3, 7, 9 and 11 days for both *Carnobacterium* species as well as both *L. gelidum* subspecies. Due to its fast growth, *B. thermosphacta* TMW2.2101 was sampled after 0, 2, 4, 7 and 9 days. Therefore, three meat packages per gas atmosphere (12 packages) were opened, cut into quarters and placed in a sterile sampling bags with a lateral filter (VWR, Darmstadt, Germany) Figure 4b. Ten milliliters of quarter-strength ringer solution were added and bags were homogenized for two minutes using a bag mixer (Interscience, Saint Nom La Bretèche, France). Afterwards the homogenate was serial diluted and plated on BHI plates for determining the CFU. At day 0, meat was inoculated and sampled directly without packaging.

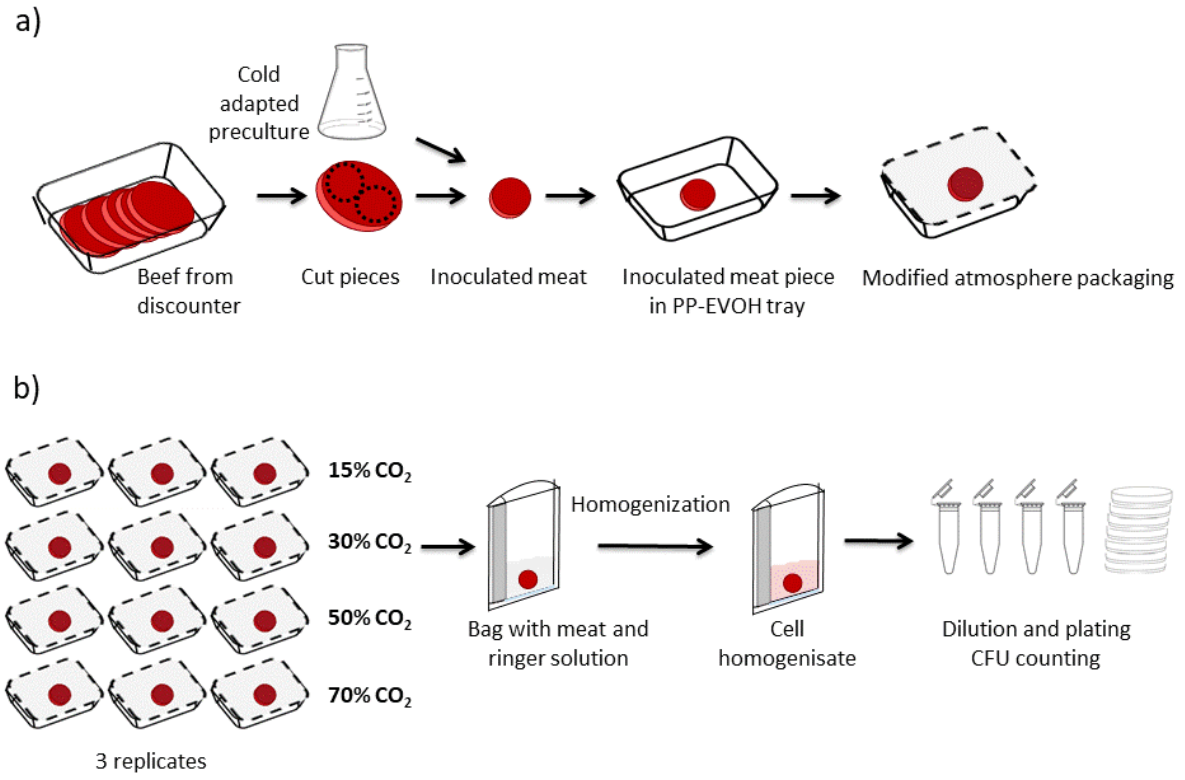

Figure 4. Sampling procedure of inoculated meat samples packaged with increasing CO_2 concentrations. a) Meat was cut into defined pieces, inoculated with one of the five meat-spoiling species using a cold adapted culture and packaged under one of the modified atmospheres: 15% CO_2 / 20% O_2 / 65% N_2, 30% CO_2 / 20% O_2 / 50% N_2, 50% CO_2 / 20% O_2 / 30% N_2 or 70% CO_2 / 20% O_2 / 10% N_2. b) Sampling procedure of MAP inoculated meat performed after 0, 3, 7, 9 and 11 days for both *Carnobacterium* species as well as both *L. gelidum* subspecies and after 0, 2, 4, 7 and 9 days for *B. thermosphacta* TMW2.2101. Meat was homogenized in bags and cell homogenate was plated on BHI plates for colony counting.

In order to prove the predominance of the inoculated strain, 12 colonies of each gas atmosphere (48 colonies) were randomly picked at the last sampling time point and checked

by RAPD-PCR analysis (chapter 3.4.4). Analysis of growth was performed as described in chapter 3.4.13. Significant differences in growth were evaluated as described in chapter 3.4.14, comparing the growth parameters obtained from growth analysis as well as comparing cell counts at different gas atmospheres after day 7.

3.3.2. Headspace O_2 consumption and spoilage of meat bacteria on MAP meat

In order to monitor the dynamic development of headspace gases in MA packages, the volume meat to volume headspace ratio of the experimental setup had to be reduced. Therefore, the inner volume of trays was displaced by inserting a self-made PVC insert, which was shaped with a PVC-laser cutter Figure 5. For the meat samples, a square pocket was incorporated on top of the mold. Furthermore, one corner of the mold was flattened, to enable the insertion of a sensor spot onto the inner part of the corner of the PP-EVOH tray. This way, the volume of the PP-EVOH trays could be reduced from 1250 ml to 350 ml (72%). The calculated volume meat to volume headspace ratio was 1:8 for beef and poultry samples. The surface meat to volume headspace ratio was 1:1.4 and 1:1.6 for beef and poultry.

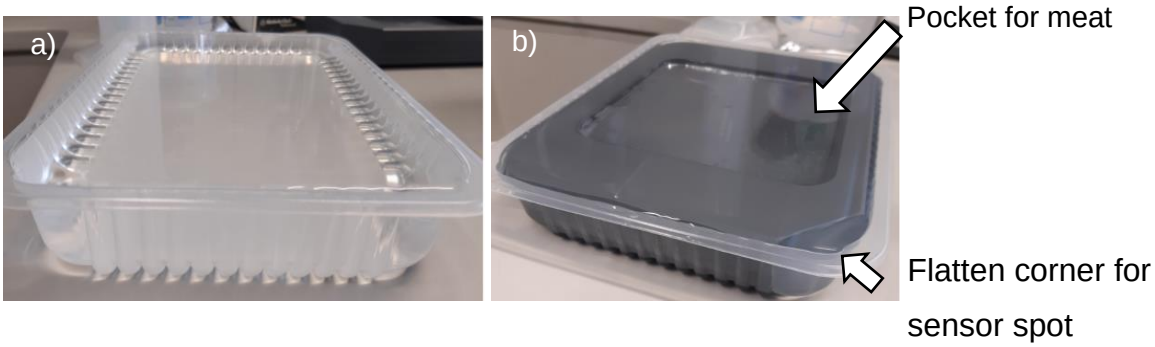

Figure 5. Developed inserts for reducing the headspace volume of PP-EVOH trays. a) empty PP-EVOH tray b) PP-EVOH tray with insert.

Beef steaks and chicken breast filet, packaged under 30% CO_2 / 70% O_2 atmosphere with an used-by date of >4 days, were bought from a local discounter and cut into round and square pieces (beef 52.8 cm^2, poultry 45.08 cm^2) exhibiting equal thickness. The cut beef pieces were inoculated with either *B. thermosphacta* TMW2.2101, *L. gelidum* subsp. *gelidum* TMW2.1618 or *L. gelidum* subsp. *gasicomitatum* TMW2.1619. Cut chicken pieces were inoculated with *C. divergens* TMW2.1577 or *C. maltaromaticum* TMW2.1581, based on their source of isolation. All meat pieces were inoculated both sides with 100 µl of a freshly prepared (chapter 3.1.2) cold adapted and washed cell culture adjusted to $OD_{600\ nm}$= 10 in sterile quarter-strength ringer solution. Cells were homogeneously distributed over the meat surface using a sterile spatula. The starting CFU was approx. 10^5-10^6 CFU/cm^2, which accelerates the process of meat spoilage and O_2 consumption. Each tray was equipped with a sensor spot and packaged under high oxygen atmosphere containing 30% CO_2 / 70% O_2. Trays were stored at 4 °C for 18 days. The oxygen content within each package was monitored daily by applying the sensor

spot technology (chapter 3.1.10). At the days 3/4, 7, 10, 14 and 18, three packages were opened (replicates) and used for determining the bacterial cell count (two meat pieces per package), bacterial metabolism (one meat piece per package) and the sensorial quality of meat (one meat piece per package) (Figure 6).

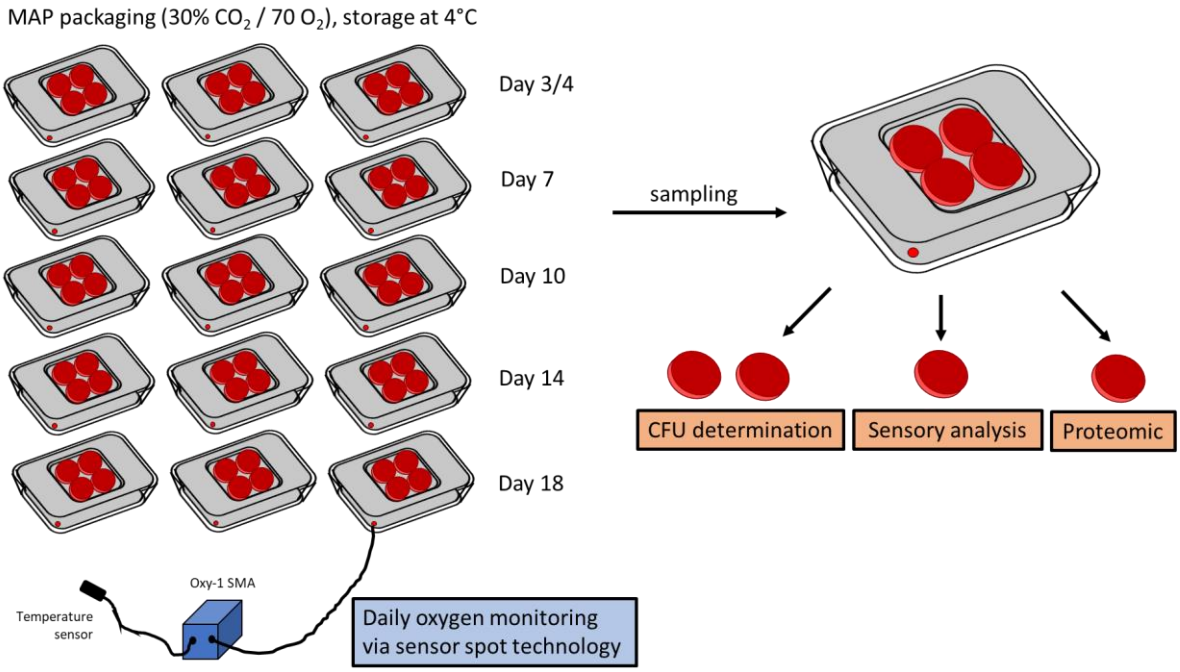

Figure 6. Sampling procedure of inoculated high oxygen MAP meat. Inoculated meat was packaged under 30% CO_2 / 70% O_2 atmosphere and stored in the cooling chamber at 4 °C for 18 days. The O_2 content of each tray was monitored daily by an oxygen sensor spot integrated in each package, which was read-out by an Oxy-1 SMA oximeter. At day 3/4, 7, 10, 14 and 18, three packages were opened and used for sample taking. Two meat pieces of each package were used for determining the CFU, one meat for determining the sensorial quality of meat and the last meat piece for a proteomic study of the metabolism of bacteria.

Sensorial analyses were done with an untrained panel of 10 persons, validating the olfactory and visual appearance of meat, attributing one of the following options: “Fresh”, “distinguishable from fresh, but still edible” and “spoiled”. Based on this analysis, the time point of spoilage was determined for each experiment described in Figure 6, by a rejection of meat of more than 50% of the sensory panel. Rejection was defined by a validation of “spoiled” for one of the organoleptic criteria olfactory or visual appearance. Furthermore, standardized pictures (72 dpi) were taken from each meat piece to support the sensory analysis. Therefore, a 16-megapixel camera was used with constant settings and pictures were taken in a non-sun lighted room. Each picture was dissected into its red, green and blue (RGB) values using the software Gimp (version 2.8). RGB values of three replicates were averaged for each time point and mean values were visualized by a synthetic color.

Growth was monitored by determining the CFU values as described in chapter 3.3.1. At day 0, three inoculated but unpackaged meat pieces were sampled for determining the CFU and

other three meat pieces were used for sensory analyses. No samples for proteomic analyses were taken at day 0. After 18 days, the recovery/identity of the inoculated strain on meat was checked by a RAPD-PCR analysis as described in chapter 3.4.4.

Proteomic samples were taken by collecting cells from the meat surface. Therefore, each meat piece was dipped into sterile quarter-strength ringer solution for several times. To obtain sufficient proteins for mass spectrometry measurement, cells of all three replicates (three meat pieces) had to be pooled. Thus, no biological replicates could be obtained. Harvested cell pellets were frozen with liquid nitrogen and stored at -80 °C until measurement. For mass spectrometric analysis only one sample of each species, which was taken at exponential growth phase, was measured (day 6 for *B. thermosphacta* TMW2.2101, day 3 for *L. gelidum* species and day 4 for *Carnobacterium* species). Proteomic sample preparation, sample measurement by LC-MS/MS as well as protein identification and quantification by MaxQuant (Tyanova *et al.*, 2016a) was performed as described in chapter 3.4.7. A statistical analyzation of label-free quantification (LFQ) values as describe in chapter 3.4.7 could not be performed due to missing replicates. Nevertheless, as the only aim of this proteomic experiment was to get an evidence for the comparability of significantly regulated proteins identified in MS-media (chapter 3.2.2) with those of real meat, a statistical analysis was not considered as obligate.

3.3.3. Monitoring anaerobic growth of *Pseudomonas* strains on chicken breast

High oxygen packaged chicken breast filet (use-by date >4 days) was bought from a local discounter and cut into equally thick, square pieces exhibiting a surface of 36 cm^2. Cut meat pieces were inoculated with a freshly prepared preculture (chapter 3.1.2) of one of the six *Pseudomonas* strains *P. lundensis* (TMW2.1732 / TMW2.2076), *P. weihenstephanensis* (TMW2.2077 / TMW2.1728) and *P. fragi* (TMW2.2081 / TMW2.2082). Cultures were precooled for 4 hours at 4 °C and washed twice in quarter-strength ringer solution. Each meat piece was inoculated on both sides with 100 µl of a culture exhibiting an $OD_{600\ nm}$= 10. Cells were distributed homogeneous on the meat surface using a sterile spatula. Afterwards meat pieces were packaged in PP-EVOH trays containing 100% N_2 atmosphere and an oxygen scavenger AnaeroGen 2.5 liter (Thermo Fisher Scientific, Waltham, MA). CO_2 in the MAP tray (as mostly used in industrial packages) was omitted to avoid any additional effects of this gas and strictly focus on the effect of anoxic conditions. In total three trays were packaged per species each contained three replicates. Packages were stored at 4 °C in the cooling room until sampling. At the days 0, 3, 5 and 7, meat sampling was performed in the anaerobic chamber. Therefore, meat was cut into pieces and put into a sterile Falcone tube containing 10 ml of quarter-strength ringer solution. After shaking for 2 minutes, supernatant was taken, serial diluted and plated on BHI agar plates. Plates were incubated aerobic for 48 hours at 25 °C. A summary of the packaging and sampling process is given in Figure 7.

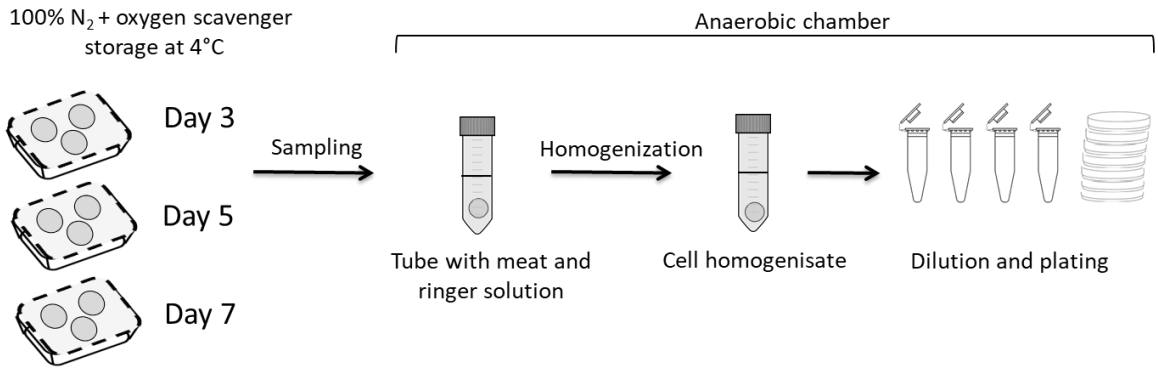

Figure 7. Sample taking procedure of anoxic packaged meat inoculated with *Pseudomonas* strains. MAP PP-EVOH trays containing three chicken pieces (replicates) inoculated with either *P. lundensis* (TMW2.1732 / TMW2.2076), *P. weihenstephanensis* (TMW2.2077 / TMW2.1728) or *P. fragi* (TMW2.2081 / TMW2.2082) were packaged under 100% N_2 atmosphere. Furthermore, an oxygen scavenger was added to each package to remove residual O_2. At day 3, 5 and 7 the CFU on each meat piece was determined performing a serial dilution, which was plated on BHI agar.

Significant growth was statistically analyzed by performing a Welch T-test between the $\log_{10}(CFU/cm^2)$ values obtained at day 0 with CFU values of the other days (day0-3, day0-5 and day0-7). Significant growth was claimed, if the increase in CFU from day 0 to day X was significant within the replicates with a p-value of <0.05. The recovery/identity of inoculated strains on meat was checked by a RAPD-PCR (chapter 3.4.4), picking 12 colonies of each replicate after 7 days.

3.4. Molecular and analytical methods

3.4.1. RNA extraction, DNA digestion and cDNA synthesis

Samples were taken by centrifuging three times one milliliter of exponential growing cells. Cell pellets were supplemented with one milliliter RNAlater stabilization solution (Thermo Fisher Scientific, Waltham, MA, USA) and incubated for 20 minutes at 4 °C. Afterwards cells were harvested by centrifuging and frozen at -80 °C. Ribonucleic acid (RNA) isolation and DNAse digestion was performed according to the user manual provided by the PureLink RNA Mini Kit Invitrogen and the corresponding PureLink DNAse Kit Invitrogen (Thermo Fisher Scientific, Waltham, MA, USA) with minor modifications. For cell lysis, three samples were pooled and mixed with 100 µl TE-buffer, a spatula-tip of lysozyme powder and 0.5 µl of SDS-solution (10%). Cells were incubated at 37 °C for 40 minutes. Afterwards, 350 µl of lysis buffer containing 1% β-mercaptoethanol was added. Cell lysis was enhanced using mechanical disruption. Therefore, samples were transferred to Matrix B tubes (MP Biomedicals EMEA, Illkirch Cedex, France) containing glass beats and homogenized 5x 1 min at 4 m/s with a FastPrep-24 homogenisator (MP Biomedicals EMEA, Illkirch Cedex, France). Extracted RNA was checked for purity and quantity with a NanoDrop. Purity was further confirmed by agarose gel electrophoreses (chapter 3.4.3) applying pure isolated RNA into the pockets.

Immediately after extraction, single stranded RNA was transcribed into double stranded cDNA according to the user manual of the iScript reverse transcription supermix kit (Biorad, Hercules, California, USA). The amount of template RNA was 1 µg. Transcription was performed in a thermal cycler (Eppendorf AG, Hamburg, Germany) following the reaction protocol provided by the kit. Obtained cDNA was frozen at -20 °C until usage.

3.4.2. Polymerase chain reaction

A polymerase chain reaction (PCR) (Saiki *et al.*, 1988) was performed to determine optimal annealing temperature of primers (temperature gradient PCR), quantify the amount of target genes (quantitative real-time-PCR (qRT-PCR)), amplifying a specific sequence part of the genome (normal PCR) or to amplify a random sequence part of the genome (random-amplified polymorphic DNA ((RAPD)) (Ehrmann *et al.*, 2003). The different primers used are given in Table 7.

Table 7. Designed primer sequences used in this study. F: Forward primer 3´-5´, R: Reverse primer 5´-3´, G3PD= Glycerin-3-phosphate dehydrogenase, MQ= 2-succinyl-5-enolpyruvyl-6-hydroxy-3-cyclohexene-1-carboxylic-acid synthase, NOX= NADH oxidase, SOD= Superoxide dismutase and POX= Pyruvate oxidase.

Species	Gene	Locus-Tag	Sequence
All species	RAPD	------	F/R: GTTTTCCCAGTCACGAC
C. divergens TMW2.1577	G3PD	EH150_04895	F: AGTTGTGCAGGAAGTTGGAC R: GGAGCCAAATGTTCCACCT
	Gyrase	EH150_11900	F: GTGTTCGTGAATTGGCGTTC R: CCTTGTTGTTCGCCTTCAATG
	MQ	EH150_11300	F: GGACCGACCTCACGAACTAC R: GCTCCCTTGCCATTTTGCAT
	NOX	EH150_00705	F: GCACGCAAGCAACTTCTG R: CTACTGAACGAACCTCTACGC
	SOD	EH150_04005	F: CCAAACGCTGGTGGTGTTC R: GCCCAGCCAGAACCAAAAC
B. thermosphacta TMW2.2101	G3PD	EHX26_08435	F: GATTTGGGAAGGCGAGAGTG R: CGAAGTCACCACCAGAAATTG
	Gyrase	EHX26_07610	F: TTATATGCGCCCACTCATCG R: GTTGCTCGGCATTCATCTCTC
	MQ	EHX26_11985	F: CGTCCCGTTGTATTGCTTTG R: CAATTCGTGTGGGCGATCTG
	NOX	EHX26_09890	F: AAAGCGACTGATGCTGCTAC R: GTTTTGCCGCTTCTGCGTAT
	POX	EHX26_03750	F: GTGGTGGAAATGGATGGAAG R: GCGTGTGCTCCATACAGTTG
	SOD	EHX26_06805	F: TTCTGGTTGGGCATGGTTAG R: CAGGACGACGGTTTTGGTAG
Leuconostoc gelidum subsp. *gasicomitatum* TMW2.1619	G3PD	BHS03_05720	F: TTCAGAGTTGTTTGCGGCTC R: GCTCCCAAGTCACGCATTTC
	Gyrase	BHS03_09160	F: TTAACCGGAGAAGATGTGCG R: CGCGCATCTGAGTTCCCT
	MQ	BHS03_04585	F: GCCGGGTTCTTTGCGTTAG R: CTTCAGCAACAGCCGAGGTA
	NOX	BHS03_04520	F: AGGTTTGACTGCGTTTCACG R: GCTGTATTAGCGGATTGCGA
	POX	BHS03_04365	F: ACGGTTCAGCAGTCCAAGAG R: GGCTTCCAACCAACTCGGAA

Reaction mixes differed depending on the PCR type. A list of all detergents and their amounts is given in Table 8. Isolated genomic deoxyribonucleic acids (DNA) was used as template for temperature gradient PCR and normal PCR, synthesized cDNA was used for qRT-PCR and supernatant of ultrasonic treated cells was used for RAPD-PCR.

Table 8. Reaction mixes of different PCR types.

	Temperature gradient PCR	qRT-PCR	RAPD	Normal PCR
Reagent	Amounts [µl]			
Water	42.25	8	31.2	24.7
10x $MgCl_2$	--	--	10	10
10x Taq-buffer without $MgCl_2$	--	--	5	5
10x Taq-buffer with $MgCl_2$	5	--	--	--
Primer (10mM)	2x 0.25	2x 0.5	0.5	2x 2.5
dNTPs (10mM)	1	--	2	4
Taq Polymerase (5 U/µL)	0.25	--	1	0.3
Sybr Green Mastermix	--	10	--	--
Template	1	1	1	1

Temperature gradient PCR, normal PCR and RAPD-PCR were performed in a thermal cycler (Eppendorf AG, Hamburg, Germany) and qRT-PCR was performed in a StepOnePlus Real-Time PCR cycler (Thermo Fisher Scientific, Waltham, MA, USA). The corresponding thermo-protocols are given in Table 9.

Table 9. Thermo-protocols of different PCR types. Temperature [°C] / time in seconds ["] and in minutes ['] / number of cycles [c].

	Temperature gradient PCR	**qRT-PCR**	**RAPD**	**Normal PCR**
Initializing	94 °C / 2" / 1c	95 °C / 60" / 1c	94 °C / 3' / 3c 40 °C / 5' / 3c 72 °C / 5' / 3c	
Denaturation	94 °C / 45" / 32c	95 °C / 15" / 45c	94 °C / 1' / 32c	94 °C / 1' / 35c
Annealing	56 °C/ R=3 °C/sec, G=5 °C / 32c	X °C / 30" / 45c	60 °C / 2' / 32c	57 °C / 1' / 35c
Elongation	72 °C / 45" / 32c	70 °C / 30" / 45c	72 °C / 3' / 32c	72 °C / 90" / 35c
Final extinction	72 °C / 5' / 1c		72 °C / 5' / 1c	72 °C / 10' / 1c
Melting curve		50-95 °C / 0.1" / 1c		

For qRT-PCR, the efficiency of each primer was determined. Therefore, different cDNAs isolated from the same species, were mixed (100 ng/µl) and diluted accordingly: 1:1, 1:5, 1:25, 1:125 und 1:625. A qRT-PCR was performed for each primer in replicates using the different cDNA dilutions as template. The cycle threshold (C_T) was set automatically by the StepOnePlus software of the thermal cycler. A linear relationship should be given, comparing the obtained C_T values and the amount of template. The slope of the linear equation was used for calculating the primer efficiency (E) defined as:

$$E = 10^{\frac{-1}{m}} - 1$$

Equation 10. Calculating the efficiency of primers used for qRT-PCR.

A relative quantification method was chosen, to compare the transcription of selected genes in different samples. Therefore, the beta subunit of the gyrase gene was selected as housekeeping gene. Relative gene transcription (RT) was calculated as followed for each cDNA:

$$RT = 2^{(C_T(reference\ gene) - C_T(test\ gene))}$$

Equation 11. Calculating the relative transcription of genes in each sample.

Control of the resulting qRT-PCR products and formation of primer dimers was done recording a melting curve at the end of each qRT-PCR run.

3.4.3. Agarose gel electrophorese

DNA obtained from RAPD-PCR, normal PCR, temperature gradient PCR and extracted RNA was separated and visualized by analytical agarose gel electrophoresis. Therefore, a 1.0% (w/w) (temperature gradient PCR) or 1.4% (w/w) (RAPD-PCR) agarose gel was prepared mixing agarose with 0.5% TBE buffer (45 mM TrisHCl, 45 mM boric acid, 1 mM Ethylenediaminetetraacetic acid (EDTA)). PCR samples were supplemented with loading dye (Thermo Fisher Scientific, Waltham, MA, USA) and filled into the pockets of the gel. For temperature gradient PCR, a 100-base pair (bp), 50 bp or 1 kB plus DNA ladder (Thermo Fisher Scientific, Waltham, MA, USA) and for RAPD-PCR a Lambda/EcoRI+HindIII marker (Thermo Fisher Scientific, Waltham, MA, USA) was used in order to identify products sizes. An electric current of 100 volt (V) and 200 milliampere (mA) (temperature gradient PCR) or 150 V and 400 mA (RAPD-PCR) was applied until separation of products was achieved. Therefore, an electrophoresis power supply (EPS 300, Pharmacica Biotech, Uppsala, Sweden) was used. Afterwards, gels were stained in dimidium bromide and DNA bands were visualized with an UVT-28M transilluminator (Herolab, Wiesloch, Germany).

3.4.4. RAPD-PCR clustering

Pictures of DNA bands obtained from RAPD-PCR agarose gel electrophoresis were processed and intraspecific strain clustering was performed using the software Bionumerics V7.6.2 (Applied Maths, Sint-Martens-Latem, Belgium). DNA band-patterns were normalized using the DNA ladder. Similarities between bands of different strains were identified using UPGMA (unweighted pair group method with arithmetic mean) and a 5% Dice similarity coefficient was applied for hierarchical cluster analysis.

3.4.5. MALDI-TOF MS analysis and clustering

Matrix assisted laser desorption/ionization time of flight mass spectrometry (MALDI-TOF MS) was applied routinely for species identification in order to exclude contaminations. Furthermore, it was used to compare the low molecular weight subproteome of different strains. Thus, a fingerprint cluster analysis was performed with obtained MALDI spectra for all strains of a species.

Samples were prepared as followed: Single colonies were picked and transferred on a MSP 96 polished steel target (Bruker Corporation, Billerica, MA, USA) using a sterile toothpick. Each sample was covered by 1 µl of 70% (v/v). After drying, 1 µl of matrix solution, consisting of α-4-hydroxy-cinnamic acid (HCCA, 10 mg/ml) dissolved in acetonitrile, diH_2O and trifluoroacetic acid (ratio 50:47.5:2.5%, v/v) was applied on each sample. MALDI-TOF MS measurements of the prepared target were performed using a Microflex LT spectrometer (Bruker Corporation, Billerica, MA, USA). Data were recorded and analyzed by the programs Biotyper Automation Flex Control 3.4 and Real Time Classification 3.1 (Bruker Corporation, Billerica, MA, USA).

Recorded spectra were matched against an internal Bruker database and an in-house database, containing spectra of specific selected food bacteria. Single mass spectrometry profiles (MSPs), obtained for each species, were exported by FlexAnalysis 3.4 (Bruker Corporation, Billerica, MA, USA) and used for hierarchical cluster analysis (HCA). Data were processed with an in-house software pipeline (Kern *et al.*, 2014) based on MASCARP (Mantini *et al.*, 2010). MALDI spectra clustering of strains was done based on Euclidean distance matrices and RStudio Version 3.5.0 (RStudio, Boston, MA, USA).

3.4.6. HPLC analysis of meat extract

Ingredients of meat extract (100 g/l; adjusted to pH5.8 with lactic acid) were analyzed by HPLC. Therefore, 1 ml of media was diluted appropriate with HPLC water, filtered by Minisart SRP Syringe polytetrafluorethylene filter 0.2 µM (Sartorius Stedim Biotech, Göttingen, Germany) and used for analysis of different ingredients. For analysis of organic acids and alcohols, proteins were precipitated adding 50 µl of 70% perchloric acid prior to dilution. Different systems were used for analysis of different ingredients.

Amino acids and biogenic amines were analyzed using an Ultimate 3000 HPLC with corresponding UV/Vis wavelength detector (Thermo Fisher Scientific, Waltham, MA, USA). A C18 Gemini column 150x3 mm (Phenomenex, Aschaffenburg, Germany) was used for separation (flow rate 0.8 ml/min). Pre-column derivatization of amino acids and biogenic amines was performed according to Bartóak *et al.* (1994). Therefore, 5 µl of each sample was mixed with 5 µl of bicine, 2 µl of o-phthalaldehyde-3-mer-captopropionic, 1 µl of 9-fluorenylmethyl chloroformate and 10 µl mobile phase A (2 mM NaH_2PO_4, 20 mM Na_2HPO_4, 0.8% Tetrahydrofuran adjusted to pH7.8). A gradient of mobile phase A and mobile phase B (300 ml acetonitrile, 500 ml methanol, 200 ml HPLC H_2O) was used for separation, as described by Schurr *et al.* (2013). Detection of derivative amino acids was done at 338 nm wavelength, whereas biogenic amines were detected at 269 nm wavelength.

Organic acids, alcohols and sugars were separated using an Ultimate 3000 HPLC (Thermo Fisher Scientific, Waltham, MA, USA) with RI 71 refraktometer (Gynkotek, Sollten, Germany). A Rezex ROA-column (Phenomenex, Aschaffenburg, Germany) was used for separation (flow rate 0.7 ml/min) of organic acids and alcohols. Furthermore, a mobile phase A (2.5 mM H_2SO_4 in HPLC water) was run. For separation of sugars, a Carbopac PA20 column (Thermo Fisher Scientific, Waltham, MA, USA) was used (flow rate 0.6 ml/min). Filtrated HPLC water served as mobile phase A.

Quantification and identification of substances was executed employing calibration adjustment by external HPLC grade standards using the software Chromeleon version 6.80 (Dionex,

Idstein, Germany). For amino acid analysis, the amino acid standard AAS18 (Sigma-Aldrich, St. Louis, MO, United States) was used.

3.4.7. Proteomic sample preparation and data analysis

Proteomic analyses were performed for the four LAB bacteria and *B. thermosphacta* cultivated in MS-media under the four gas atmospheres air, 100% N_2, 30% CO_2 / 70% O_2 and 30% CO_2 / 70% N_2 (chapter 3.2.2) as well as on same species inoculated on beef and poultry with 30% CO_2 / 70% O_2 atmosphere (chapter 3.3.2). Furthermore, proteomic analysis was done for *Pseudomonas* strains cultivated under air and 100% N_2 atmosphere (chapter 3.2.2). A brief summary of steps performed on proteomic samples is given in Figure 8 and explained in detail in the following.

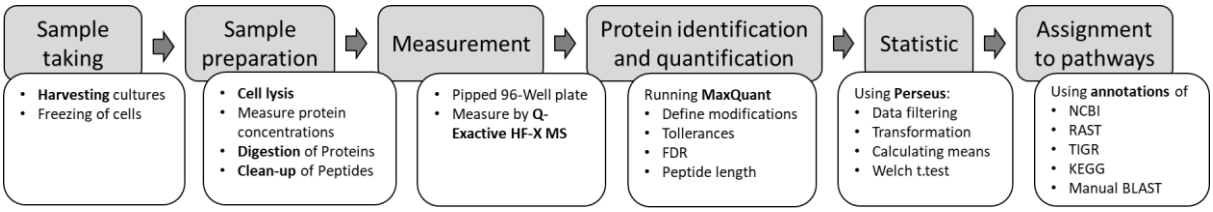

Figure 8. Proteomic sample preparation pipeline.

Sample taking. Exponential growing cells were harvested by centrifugation and washed two-times with quarter-strength ringer solution (Merck, Darmstadt, Germany). Harvesting was performed on ice, to slow down metabolic activity. Washed cell pellets were frozen immediately by liquid nitrogen and stored at -80 °C until sample preparation.

Sample preparation. Cell lysis was done with 900 µl of a high molecular urea buffer (8 M urea, 5 mM EDTA, 100 mM ammonium hydrogen carbonate, 1 mM dithiothreitol, 1 M protease inhibitor cocktail) and mechanical disruption using 400 mg of acid washed glass beats (10 minutes shaking at 4 °C). Supernatant of lysed cells was collected and protein concentrations were determined using a bicinchoninic acid (BCA) assay. Therefore, a standard curve (signal / BCA concentration) was recorded. Samples were measured in replicates using a 96-well plate measured by a spectrophotometer (Tecan, Männedorf, Switzerland) at 562 nm.

Further on, 100 µg of proteins were used for protein digestion. Therefore, 10 mM dithiothreitol was added and proteins were incubated for 30 minutes at 32 °C, 400 rpm. Afterwards, 55 mM chloroacetamide were added and incubation was continued for another hour at 25 °C in the dark. Samples were diluted 1:5 with freshly prepared 0.05 M ammonium bicarbonate buffer and protein digestion was started adding 1/100 (w/w) trypsin. After 5 hours of incubation at 32 °C, trypsin was added a second time and protein digestion was last until next morning. By adding 1% of formic acid, digestion was stopped and pH was adjusted to <3.

Peptide mixtures were cleaned up using Sep-Pak Vac tC18 1cc columns with 0.1-0.5 mg protein lading capacity (Waters Corporation, Milford, USA). Columns were activated adding one-time 100% methanol. Afterwards, filter cleaning was done adding one-time equilibrium buffer (80% acetonitrile, 20% H_2O, 0.1% formic acid) and five-times washing solution (2% acetonitrile, 98% H_2O, 0.1% formic acid). Samples were loaded and flow-through was applied a second time on the column. After repeated washing (five-times with washing solution), peptides were eluted two-times with elution buffer (40% acetonitrile, 60% H_2O, 0.1% formic acid). Cleaned up peptides were dried in a speed vacuum centrifuge and frozen at -80 °C.

Measurement. For mass spectrometric analysis, peptides were suspended adding 50 µl washing solution. Peptide concentrations were determined using a NanoDrop2000 spectrophotometer (Thermo Fisher Scientific, Waltham, MA, USA). Samples were diluted to a final concentration of 0.1 µg/µl with washing solution and randomized for measurement.

0.5 µg of peptides were measured per sample using an Ultimate 3000 RSLCnano system, which was coupled to a Q-Exactive HF-X mass spectrometer (Thermo Fisher Scientific, Waltham, MA, USA). Analysis was performed running HPLC grade water with 0.1% formic acid at a flow rate of 5 µl/min on a trap column (ReproSil-pur C18-AQ, 5 µm, Dr. Maisch, 20 mm × 75 µm, self-packed). 10 minutes after loading, peptides were separated on an analytical column (ReproSil Gold C18AQ, 3 µm, Dr. Maisch, 450 mm × 75 µm, self-packed) using a 50 min gradient from 4 to 32% of solvent B (0.1% formic acid in acetonitrile and 5% (v/v) DMSO) applying a flow rate of 300 nl/min. Solvent A contained 0.1% formic acid in HPLC grade water and 5% (v/v) DMSO. The mass spectrometer was operated in positive ionization and data dependent acquisition mode. An automatic gain control target value of 3e6 and maximum injection time of 45 ms was used for recording MS1 spectra (360.1300 m/z) at a resolution of 60000. For fragmentation, up to 18 peptides were selected. Precursors exhibiting charge states 2 to 6 were selected and dynamic exclusion of 25 sec was enabled. A normalized collision energy of 26% and higher energy collision induced dissociation was used for peptide fragmentation. Window width for precursor isolation was set to 1.3 m/z. The maximum injection time of MS2 was set to 25 ms by a resolution of 25000 with an automatic gain control target value of 1e5. Full proteomic was performed.

Protein identification and quantification. MaxQuant (version 1.5.3.30) with its built-in search engine Andromeda (Cox *et al.*, 2011; Tyanova *et al.*, 2016a) was used for protein identification and quantification. Fragment ion tolerance was set to 20 ppm, precursor tolerance to 4.5 ppm and false discovery rate to 1%. Peptide spectrum match and protein level were adjusted using reversed protein sequences. A minimal peptide length of 7 amino acids was defined and the function “match between-run” was disabled. The settings “carbamidomethylated cysteine”,

“oxidation of methionine” and “N-terminal protein acetylation” were activated as variable modifications.

Statistical analysis. Perseus was used for data processing and statistical analysis (Tyanova *et al.*, 2016b). Therefore, LFQ values were used for analysis of differentially regulated proteins between two sampling conditions. Intensity based absolute quantification (iBAQ) values were used to compare expression profiles of different proteins within one sample. Both, LFQ and iBAQ values were processed identically. First, data were clean-up by removing proteins identified as “contaminants”, “only by site” or “reverse”. Second, data were log_2-transformed and normalized, followed by a further clean-up step, removing proteins only found in one replicate. Replicates were averaged and a Welch T-test of two sampling conditions was performed (only with LFQ values). Proteins were filtered for significance based on q-values <0.05 (LAB and *B. thermosphacta*) or <0.01 (*Pseudomonas*) and a log_2 (fold-change) >= 2.

Protein assignment to pathways. For data interpretation, proteins were assigned to specific metabolic pathways using functional annotations provided by the databases “national center for biotechnology information” (NCBI), “rapid annotations using subsystems technology” (RAST), SEED, “the institute for genomic research” (TIGR) and “Kyoto encyclopedia of genes and genomes” (KEGG). A manual “Basic local alignment search tool” (BLAST) was employed to further assign proteins to pathways.

The effect of O_2 and CO_2 on single proteins as well as whole pathways was identified by performing pairwise comparisons of the detected protein amounts at different gas atmospheres as described in chapter 3.2.2.

3.4.8. Fatty acid sample preparation and analysis

Analyses of the fatty acid composition were done of samples taken from the experimental setup described in chapter 3.2.3. After harvesting, cells were frozen at -80 °C, freeze dried and the dry-weight of each sample was determined. Glyceryl trinonanoate was added as internal standard, in order to detect losses during sample preparation. Fatty acid extraction was performed adding 14 ml of 1:1 methanol/chloroform to each sample. Cell lysis was enhanced by two times ultrasonic treatment (1 min, 60% amplitude). Fat, dissolved in the supernatant of lysed cells was extracted and separated in a separating funnel adding 14 ml of sodium chloride (0.58% in diH_20). Afterwards, samples were evaporated using a rotary evaporator (Heidolph, Kelheim, Germany). For fatty acid methylation, extracted fat was dissolved adding 200 µl of tetrahydrofuran and 400 µl of 0.5 mol l^{-1} natriummethylat (dissolved in 100% methanol). Samples were incubated for 15 minutes at 80 °C and 200 µl water and 200 µl hexane was added. Finally, the hexane layer containing the methylated fatty acids was transferred into a HPLC vial.

Samples were measured on a GCMS-TQ8040 (Shimadzu, Kyoto, Japan) injecting 1 µl of each sample. A split of 10 was set and helium was chosen as carrier gas. Samples were separated using a Zebron ZB-5MSplus column (30 m x 0.25 mm x 0.25 µm) (Phenomenex, Aschaffenburg, Germany) running the gradient: 35 °C for 2 minutes, a rise of 10 °C min^{-1} until 140 °C, 140 °C for 10 minutes, a rise of 2 °C min^{-1} until 240 °C and finally 240 °C for 10.5 minutes. LabSolution – GCMS solution Version 4.30 (Shimadzu, Kyoto, Japan) was used for data analyzation. Two standards were used for fatty acid identification and quantification. A bacterial acid methyl ester standard (BAME Mix) (Sigma-Aldrich, St. Louis, Missouri) and a mixture of fatty acid methyl esters (Supelco 37 FAME mix) (Supelco, Bellefonte, PA, USA). Peak identification was further confirmed by matching mass spectra against the Nist11 database.

For fatty acid (FA) quantification, the peak area was correlated to those of the internal standard (C9:0, 20.95 µg) to obtain µg values for each fatty acid. Second the amounts of each single fatty acid was calculated per gram freeze dried cell pellet. Calculated µg FA/ gram cells were finally relativized to the total amount of fatty acids identified within each sample (% (µg FA/ g cells)) and grouped according to similar physiological properties e.g. *iso*/*anteiso* methyl group branching, long (>C16) and short chain length (<C16) (LCFAs and SCFAs), saturated and unsaturated fatty acids (SFAs and UFAs) as well as branched and unbranched chain fatty acids (BCFA and UBFA) calculating the ∑ % (µg FA/g cells) for each sample. The effect of O_2 and CO_2 on single fatty acids as well as on grouped fatty acids was identified by calculating the ratio of % (µg FA/g cells) values obtained from samples (replicates) at different gas atmospheres as described in chapter 3.2.3, Table 6.

3.4.9. Measuring membrane fluidity

Membrane fluidity was measured by the fluorescence dye 6-dodecanoyl-2-dimethylaminonaphthalene (Laurdan), as previously described by Behr *et al.* (2006). The fluorescence spectrum of this dye is known to be highly sensitive to the polarity of the environment such as fluctuations in phospholipid vesicles and membrane phase transitions (Parasassi *et al.*, 1986). Thus, an altered membrane fluidity due to CO_2 exposure is expected to also affect the fluorescence signal of Laurdan, shifting the emission wavelength from 440 nm to 490 nm. In detail, samples taken from the experiment described in chapter 3.2.3 were centrifuged and washed in 10 ml of phosphate-buffer (50 mM phosphate [pH6.5], 10 mM glucose). $OD_{600\ nm}$ was adjusted to 1. 0 in the same buffer and the fluorescence dye Laurdan (stock 2 mM in 100% ethanol) was added to a final concentration of 40 µM. Staining of cells was performed for 30 minutes at 30 °C in the dark. Cells were washed once using phosphate buffer and resuspended again in the same buffer. Dyed samples were measured using a LS 50B luminescence spectrometer (Perkin-Elmer, Rodgau-Jügesheim, Germany). The excitation

wavelength was set to 360 nm and the emission wavelength was varied from 380 to 550 nm using 5 nm steps. The general polarization (GP) was calculated for each sample by the following equation:

$$GP = \frac{I_{440nm} - I_{490nm}}{I_{440nm} + I_{490nm}}$$

Equation 12. General polarization representing membrane fluidity of cells.

$I_{440\ nm}$ is defined as the relative fluorescence at 440 nm and $I_{490\ nm}$ as the relative fluorescence at 490 nm (Parasassi, 1990). Furthermore, the CFU of each sample was determined after fluorescence measurement. By calculating the GP value per single cell (GP/CFU) samples taken from different gas atmospheres can be compared.

3.4.10. Measuring membrane permeability

Cell membrane permeability was measured using the fluorescence dye propidium iodide. When propidium iodide penetrates cell membranes, it is known to intercalate into bacterial DNA shifting its absorbance / emission spectrum from 493 nm / 636 nm to 535 nm / 617 nm (Klotz *et al.*, 2010). Thus, diffusion of propidium iodide through membranes, which exhibit an altered permeability due to CO_2 exposure, should consequently be also altered and the absorbance maxima should be shifted. Sample preparation was done as described by Klotz *et al.* (2010), with slight modifications. In detail, samples taken from the experiment described in chapter 3.2.3 were harvested and washed using 10 ml of phosphate-buffered-saline (PBS) (137 mM NaCl, 2.7 mM KCl, 1.44 g/l Na_2HPO_4, 0.2 g/l KH_2PO_4). Afterwards, an $OD_{600\ nm}$ of 1.0 was adjusted in PBS and cells were stained for 10 minutes in the dark adding 2.9 µM of propidium iodide. Cells were repeatedly washed with PBS and fluorescence was measured at 544 nm excitation wavelength / 620 nm emission wavelength using a FLUOstar Omega microplate reader (BMG Labtech, Ortenberg, Germany). The CFU of each sample was determined after fluorescence measurement and finally correlated to the intensity signal (fluorescence intensity/CFU). Thus, comparisons between samples obtained from different gas atmospheres can be done.

3.4.11. Measuring cell surfaces

The cell surface of bacteria, taken from samples of the experiment described in chapter 3.2.3 were analyzed using an Axiostar plus microscope (Zeiss, Jena, Germany). Therefore, cell sizes of 50 cells grown under the same gas atmosphere were measured. The cell surface was calculated according to Sun and Liu (2003).

The following model was applied for calculating the surface of the spherical-shaped *Leuconostoc gelidum* bacteria (shape code 1-H):

$$Surface\ (A_{sphere}) = \pi\ x\ a^2$$

Equation 13. Equation used for calculating the surface of a spherical bacterium.

The corresponding diameter of the sphere is defined as a. For calculation of the surface of a rod-shaped bacterium (*B. thermosphacta, C. divergens and C. maltaromaticum*) the following model was applied (shape code 5-H):

$$Surface\ (A_{rod}) = \pi\ x\ a\ x\ b$$

Equation 14. Equation used for the calculation of the surface of a rod-shaped bacterium.

A represents the length and b the wide of a rod-shaped bacterium.

3.4.12. Genomic sample preparation and analysis

Genomic DNA was isolated for *C. divergens* TMW2.1577, *B. thermosphacta* TMW2.2101 and *P. lundensis* TMW2.1732. Genomes of *C. maltaromaticum* TMW2.1581, both *L. gelidum* subspecies as well as the other *Pseudomonas* strains (TMW2.2076, TMW2.1728, TMW2.2077, TMW2.2081 and TMW2.2082) were isolated and annotated in previous studies (Höll *et al.*, 2016; Hilgarth *et al.*, 2018a; Hilgarth *et al.*, 2019). Cell lysis of *C. divergens* TMW2.1577, *B. thermosphacta* TMW2.2101 and *P. lundensis* TMW2.1732 was performed incubating cells in TE-Buffer (10 mM Tris-HCl, 1 mM EDTA, pH= 8) added with two grams of fresh lysozyme powder and 3.3 µl lysostaphin overnight at 4 °C. The next day, cells were incubated for one hour at 37 °C in a water bath and DNA isolation was done following the instructions given by the E.Z.N.A. Bacterial DNA Kit (Omega Bio-Tek, Norcross, GA, USA). The extracted DNA was quantified and checked for purity using a NanoDrop 1000 spectrophotometer (NanoDrop Technologies, Wilmington, NC, USA). Genomes were sent for sequencing to the ZIEL institute (Freising, Germany). Illumina sequencing was performed using a MiSeq sequencing platform (Illumina, Inc., San Diego, CA, USA). Data were processed and assembled using SPAdes V3.9.0 (Bankevich *et al.*, 2012) as described by Huptas *et al.* (2016). Consensus .fasta files obtained from sequencing were used for gene annotation. Therefore, the NCBI Prokaryotic Genome Annotation Pipeline (PGAP) (Angiuoli *et al.*, 2008) and RAST (Aziz *et al.*, 2008; Overbeek *et al.*, 2014) was used.

NCBI accession numbers of the species/strains used in this study are CP017196 (*L. gelidum* subsp. *gelidum* TMW2.1618), CP017197 (*L. gelidum* subsp. *gasicomitatum* TMW2.1619), RSDV00000000.1 (*C. divergens* TMW2.1577), CP016844 (*C. maltaromaticum* TMW2.1581), RSDU00000000.1 (*B. thermosphacta* TMW2.2101), JAAEBS000000000 (*P. lundensis* TMW2.2076), JACJCQ000000000 (*P. lundensis* TMW2.1732), JAAEBV000000000 (*P. weihenstephanensis* TMW2.1728), JAAEBW000000000 (*P. weihenstephanensis*

TMW2.2077), JAAEBQ000000000 (*P. fragi* TMW2.2081) and JAAEBR000000000 (*P. fragi* TMW2.2082).

Annotated genomic data were used to predict the potential of bacteria to perform basic energy providing metabolic pathways as well as specific metabolic pathways, which are related to O_2 or CO_2 adaptation.

3.4.13. Growth analysis

Growth curves recorded by measuring the OD or CFU were analyzed using the open source software RStudio ver. 3.5.0 (RStudio, Inc., Boston, USA) running the CRAN package grofit ver. 1.1.1.-1 with default settings (Zwietering *et al.*, 1990). This package performs fitting of growth curves based on the gompertz model. By applying different parametric functions (e.g. gcFitModel, gcFitSpline) the growth characterizing parameters lag-phase, maximal growth rate (μ_{max}) and maximal OD / maximal CFU are calculated for each growth curve. Those parameters can be compared and statistically validated to uncover the effects of O_2 and CO_2 on bacterial growth.

3.4.14. Statistical analysis

Data obtained from each experiment were analyzed for statistical relevance. The methods applied depended on the number of comparisons of matrixes.

Comparing two matrixes – Welch T-test in Excel. First, comparing only two data matrixes, a variance test was performed using the F-test function in Excel. Significant differences in the variances of both matrixes were defined as probability value (p) <0.05 (two-side confidence interval). Based on this, a Welch T-test was conducted analyzing significant differences between the means of the two matrixes. Significant differences were defined as p <0.05 (two-side confidence interval).

Pairwise comparisons of matrixes – ANOVA and Tukey post-hoc test. In case of multiple comparisons of matrixes, an one-way analysis of variance (ANOVA) was performed to identify if the group of means of the matrixes differs significantly (p <0.05). In case of significance, pairwise comparisons of the means were performed by applying a post-hoc analysis based on the Tukey´s test (significant differences between comparisons p <0.05). All analyses were done using the open-source software RStudio ver. 3.5.0 (RStudio, Inc., Boston, USA).

4. Results

4.1. Metabolic adaptation of meat organisms to MAP gases

4.1.1. Development of a species-specific MS-medium

In order to develop a species-specific MS-medium, growth of selected meat bacteria was monitored at different concentrations of meat extract (3.125, 6.25, 12.5, 25, 50 and 100 g/l) with and without supplementation of 0.5% glycerol. Concentration of meat extract were chosen as low as possible, to reduce the amount of meat proteins, which interfere in the proteomic experiments but concomitantly enable growth of sufficient cells for harvesting for proteomic analysis ($OD_{600\ nm}$> 0.2). Furthermore, a significantly enhanced growth with glycerol was considered for the selection of meat extract concentrations, as this is obligate to substitute missing fat in the meat extract and has been demonstrated to be used for gluconeogenesis by LAB under conditions of sugar limitation (Höll *et al.*, 2020) (Figure 9).

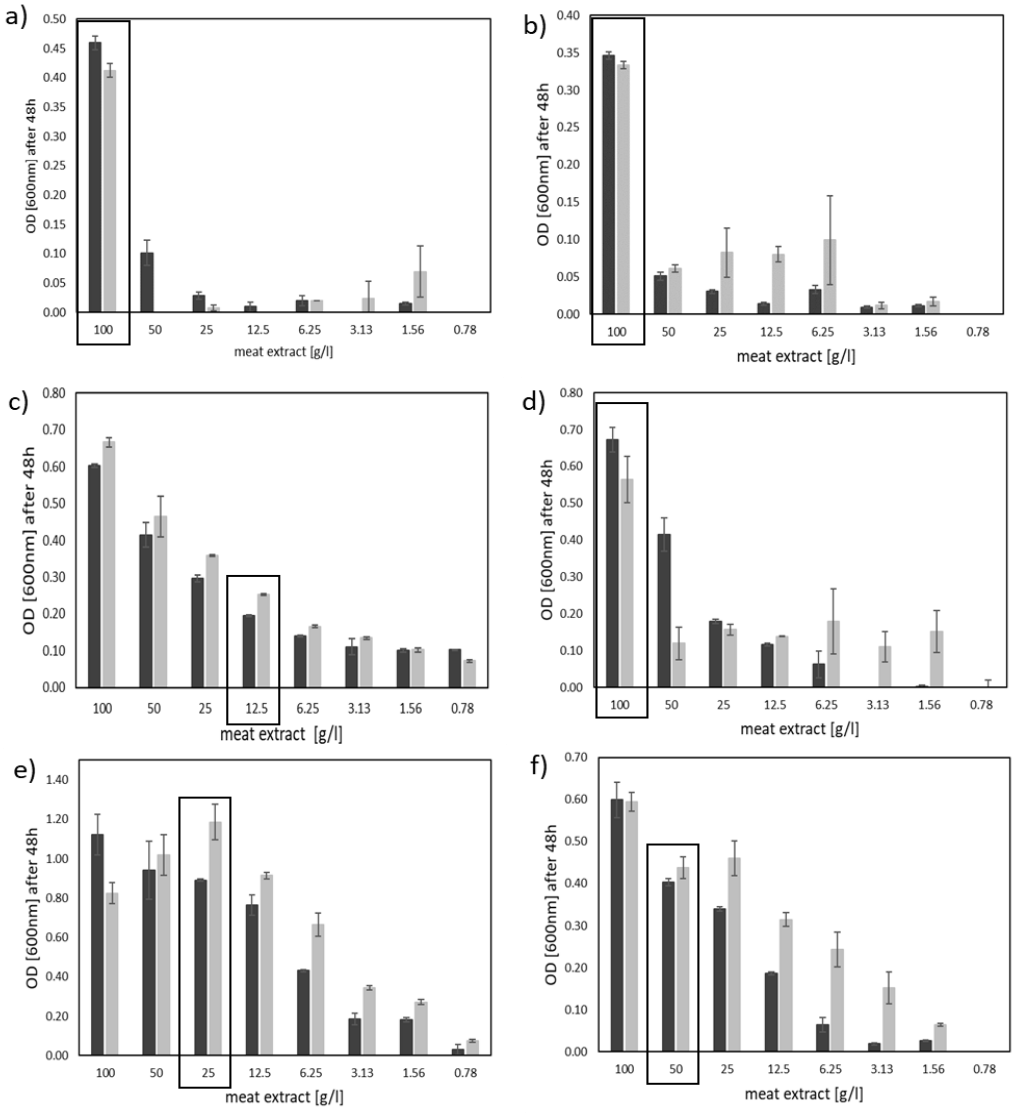

Figure 9. Growth of representative strains of each species by varying meat extract concentrations with and without glycerol. Growth of selected strains for each species with decreasing meat extract concentrations, supplemented with (■) and without (■) 0.5% glycerol was monitored. Concentrations used for further experiments are marked in boxes. a) *L. gelidum* subsp. *gelidum* TMW2.1618 b*) L. gelidum* subsp. *gasicomitatum* TMW2.1507 c) *C. divergens* TMW2.1577 d) *C. maltaromaticum* TMW2.1583 e) *P. lundensis* TMW2.1732 and f) *B. thermosphacta* TMW2.2331. All values are based on three independent replicates. Error bars represent calculated standard deviations.

Enhanced growth with glycerol could be detected for *B. thermosphacta* TMW2.2331, *P. lundensis* TMW2.1732 and *C. divergens* TMW2.1577. The other species exhibited slightly reduced growth by addition of 0.5% glycerol. However, as glycerol is needed to supplement the missing fat in meat extract, it was used as an additive in further experiments. Both *L. gelidum* subspecies grew worse in meat extract concentrations lower than 100 g/l. Lowest concentration of meat extract, which significantly measurable induced growth by addition of glycerol was 12.5 g/l for *C. divergens* TMW2.1577 whereas *B. thermosphacta* TMW2.2331, *P. lundensis* TMW2.1732 and *C. maltaromaticum* TMW2.1583 did not exhibit growth below the meat extract concentrations of 50, 25 and 100 g/l under conditions of complete oxygen exclusion as tested in further experiments (data not shown). Thus, meat extract concentration chosen for each species comprise *C. divergens* 12.5 g/l, *P. lundensis* 25 g/l, *B. thermosphacta* 50 g/l, C*. maltaromaticum* and both *L. gelidum* subspecies 100 g/l.

As addition of glucose is obligate for *B. thermosphacta* to enable anaerobic growth and both *L. gelidum* subspecies exhibited poor growth independently of the cultivation conditions, 0.5% glucose monohydrate was supplemented to the media of all three species to enhance their growth. Secondly, growth curves for all species were recorded with different concentrations of tween80. Results are shown in Figure 10.

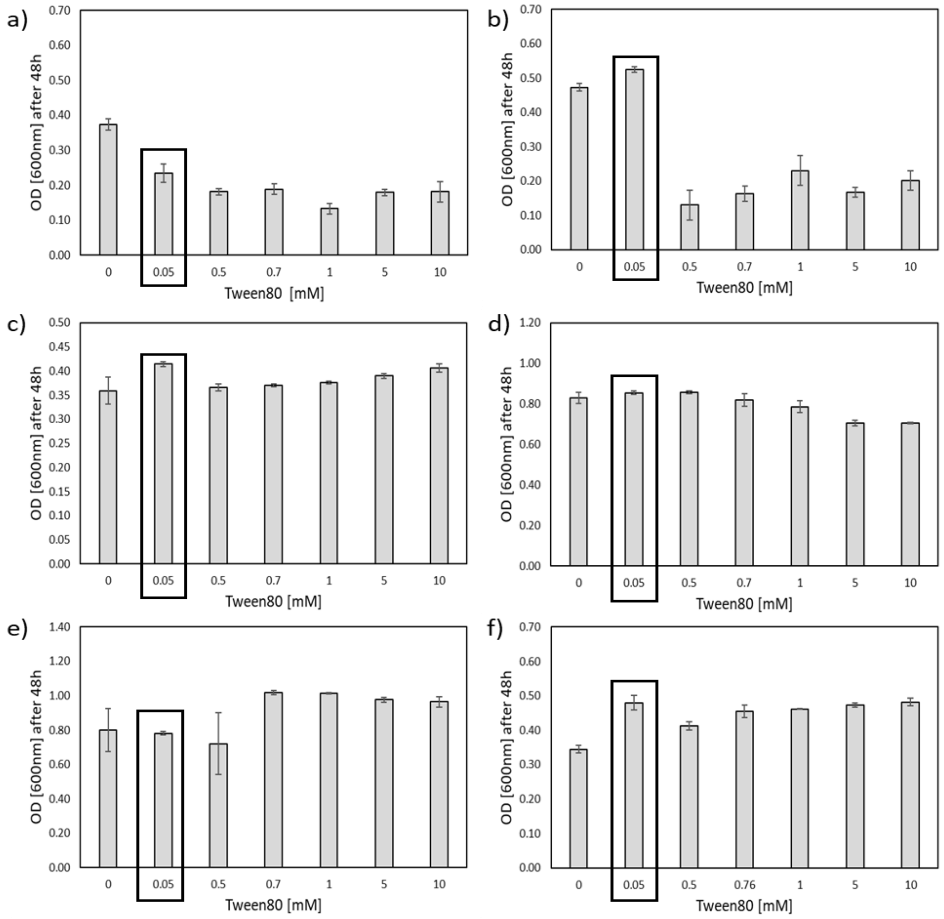

Figure 10. Growth of representative strains for each species with selected meat extract concentration and 0.5% glycerol varying tween80 concentrations. Growth of representative strains in selected concentrations of meat extract supplemented with 0.5% glycerol and 0.5% glucose monohydrate was monitored for decreasing tween80 concentrations. Concentrations used for further experiments are marked in boxes. a) *L. gelidum* subsp. *gelidum* TMW2.1618 b) *L. gelidum* subsp. *gasicomitatum* TMW2.1507 c) *C. divergens* TMW2.1577 d) *C. maltaromaticum* TMW2.1583 e) *P. lundensis* TMW2.1732 and f) *B. thermosphacta* TMW2.2331. All values are based on three independent replicates. Error bars represent calculated standard deviations.

Growth of *P. lundensis* TMW2.1732 and *C. maltaromaticum* TMW2.1583 was almost unaffected by addition of tween80, whereas *C. divergens* TMW2.1580, *L. gelidum* subsp. *gasicomitatum* TMW2.1507 and *B. thermosphacta* TMW2.2331 exhibited enhanced growth. Thus, 0.05% tween80 was added to the media of each species. Next, growth was monitored with and without addition of 0.2 µg/ml hemin chloride or with and without addition of 20 ng/ml menaquinone-4 (Figure 11).

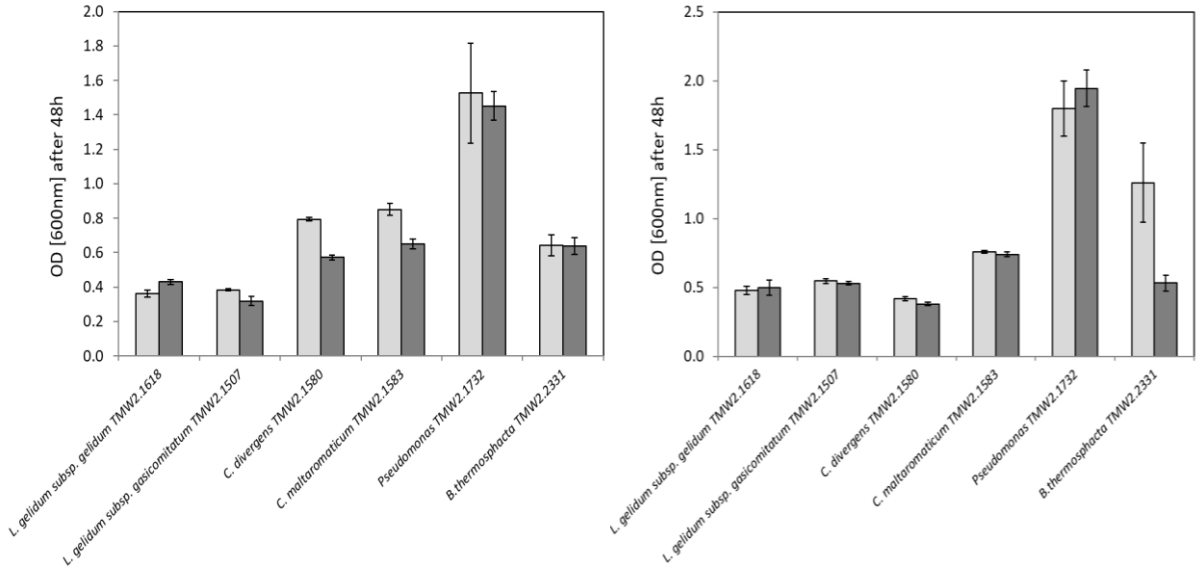

Figure 11. Growth of representative strains for each species in selected concentrations of meat extract, glycerol and tween80 with and without addition of hemin chloride and menaquinone. Growth of representative strains in selected concentrations of meat extract, 0.5% glycerol, 0.5% glucose monohydrate, 0.05 mM tween80 with (■) and without (■) addition of 2 µg/ml hemin chloride (left graph) or 20 ng/ml menaquinone-4 (right graph) was monitored. All values are based on independent replicates. Error bars are based on calculated standard deviations.

L. gelidum subsp. *gasicomitatum* TMW2.1507, both *Carnobacterium* species and *P. lundensis* TMW2.1732 exhibited significant enhanced growth by addition of heme. The other species were almost unaffected. Therefore, 0.2 µg/ml hemin chloride was added to the media of each species. Contrary, menaquinone-4 did not enhance the growth of any species except for *B. thermosphacta* TMW2.2331. Thus, menaquinone was not added as additional ingredient to the MS-media of each species. The final composition of the developed species-specific MS-media for each species is given in Table 10.

Table 10. Species-specific composition of the developed MS-media.

	C. divergens	***Pseudomonas***	***B. thermosphacta***	***C. maltaromaticum***	***L. gelidum* subspecies**
Meat extract	12.5 g/l	25 g/l	50 g/l	100 g/l	100 g/l
Glycerol	0.5%	0.5%	0.5%	0.5%	0.5%
Tween80	0.05 mM	0.05 mM	0.05 mM	0.05 mM	0.05 mM
Hemin chloride	2 µg/ml	2 µg/ml	2 µg/ml	2 µg/ml	2 µg/ml
Glucose	--	--	0.5%	--	0.5%

The pH of the media was adjusted to 5.8 with lactic acid prior to autoclaving. Glucose monohydrate was dissolved in 10% of final volume, autoclaved separately, and added to the media after cooling down to less than 50 °C. Hemin chloride was added directly before starting the experiments due to its light, oxygen and temperature sensitivity.

In order to evaluate other components of MS-media present in meat extract, HPLC and BCA analysis of 100 g/l meat extract were performed. BCA analysis revealed a protein content of 32.49 gram in one liter meat extract. The only carbon sources, which could be detected by HPLC were glucose (6.67 mM), citrate (0.03 mM) and malate (0.05 mM). Furthermore, small amounts (0.12-0.99 mM) of several free amino acids were measured by HPLC analysis. Most abundant amino acids comprised arginine, alanine, serine, glycine and leucine. Traces of 2.3-butanedion (0.04 mM) and the biogenic amines agmatine (0.4 mM) and tyramine (0.24 mM) could also be detected (Supplementary Table1).

4.1.2. Selection of one representative strain per species

For conducting further experiments, one strain per species best representing the physiological, genetic and proteomic properties of all isolates obtained from meat had to be selected. Therefore, the three analyses I) Aerobic and anaerobic growth II) RAPD-clustering III) MALDI-TOF MS clustering were performed. Results are shown in detail in the following.

Notice: Strain selection of meat-spoiling *Pseudomonas* species was based on other criteria (chapter 4.3.1). Thus, the following experiments were not performed for *Pseudomonas* species.

I. Growth under oxic and anoxic conditions

Growth experiments were conducted in the prior developed species-specific MS-media. Bacteria were cultivated as described in chapter 3.1.6 under oxic (Erlenmeyer flasks with diffusible cotton plugs) or strict anoxic (gas tight locked Schott flasks within the anaerobic chamber) conditions. Recorded growth curves of aerobically and anaerobically growing strains for each species can be seen in Figure 12.

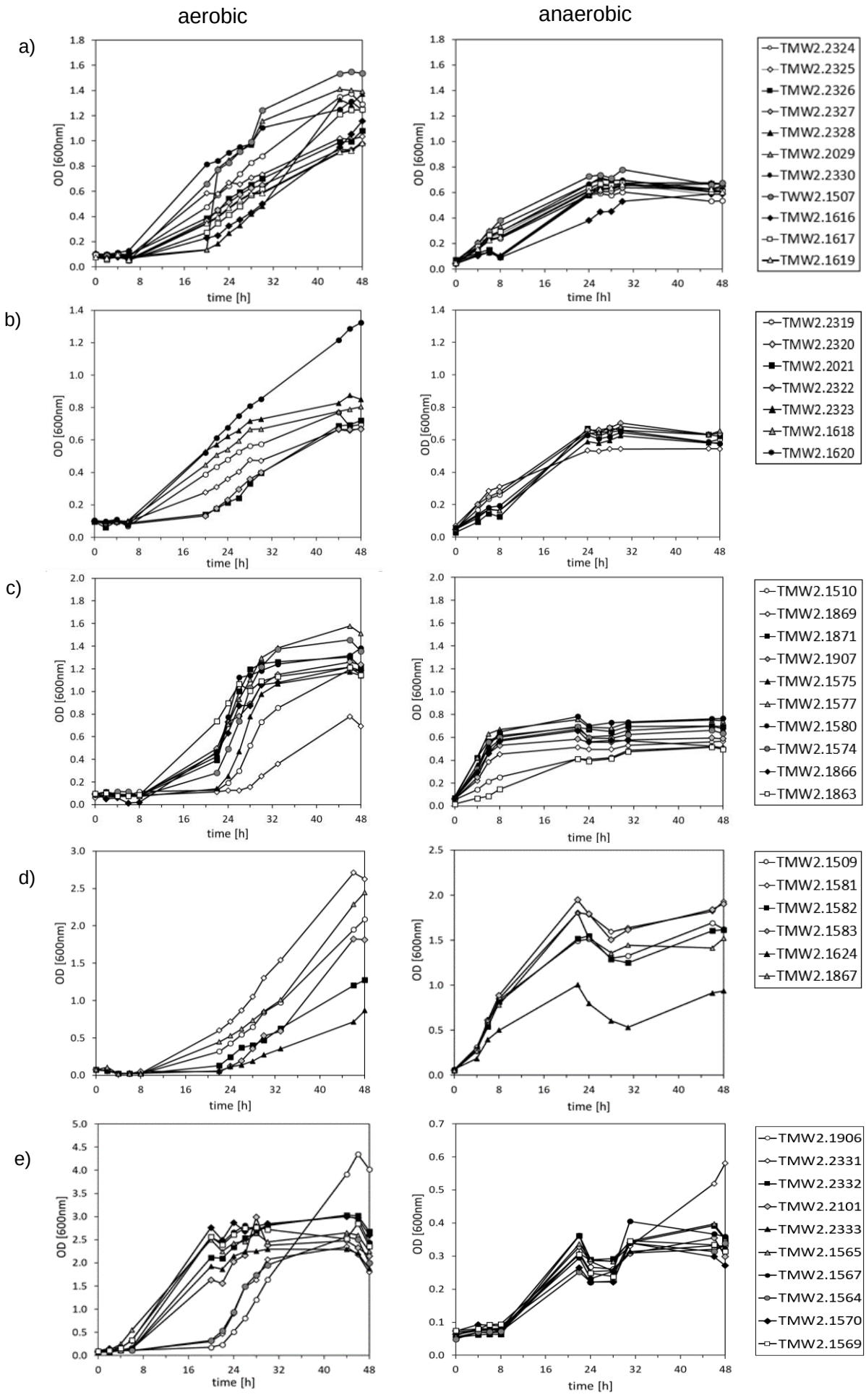
aerobic
anaerobic
a)
b)
c)
d)
e)
OD [600nm]
time [h]
TMW2.2324
TMW2.2325
TMW2.2326
TMW2.2327
TMW2.2328
TMW2.2029
TMW2.2330
TWW2.1507
TMW2.1616
TMW2.1617
TMW2.1619
TMW2.2319
TMW2.2320
TMW2.2021
TMW2.2322
TMW2.2323
TMW2.1618
TMW2.1620
TMW2.1510
TMW2.1869
TMW2.1871
TMW2.1907
TMW2.1575
TMW2.1577
TMW2.1580
TMW2.1574
TMW2.1866
TMW2.1863
TMW2.1509
TMW2.1581
TMW2.1582
TMW2.1583
TMW2.1624
TMW2.1867
TMW2.1906
TMW2.2331
TMW2.2332
TMW2.2101
TMW2.2333
TMW2.1565
TMW2.1567
TMW2.1564
TMW2.1570
TMW2.1569

Figure 12. Selection of representative strains of the five meat-spoiling bacteria due to their aerobic and anaerobic growth. Aerobic and anaerobic growth of different strains of the species a) *L. gelidum* subsp. *gasicomitatum* (n=11), b) *L. gelidum* subsp. *gelidum* (n=7), c) *C. divergens* (n=10), d) *C. maltaromaticum* (n=6) and e) *B. thermosphacta* (n=10).

All strains exhibited measurable growth in the developed MS-media, except for *L. gelidum* subsp. *gelidum* TMW2.1998, which was consequently excluded from this analysis. Strains, exhibiting noticeable different growth compared to other strains of the same species were not considered for further experiments and marked by a cross in Table 11. Those strains comprise *B. thermosphacta* TMW2.1906, TMW2.1564 and TMW2.2331, *C. divergens* TMW1869 and TMW2.1863, *L. gelidum* subsp. *gelidum* TMW2.1620, *L. gelidum* subsp. *gasicomitatum* TMW2.1507, TMW2.1616, TMW2.2324 and TMW2.2328 and *C. maltaromaticum* TMW2.1624.

II. Randomly amplified polymorphic DNA (RAPD) clustering

Strain selection was further supported on genetic basis, by performing a RAPD-PCR analysis, which randomly amplifies genomic sequences from each strain. Thus, based on the genomic diversity, each strain has its unique band pattern. These patterns were clustered on their similarity as described in chapter 3.4.4. Results of the RAPD-PCR band clustering of different strains can be seen in Figure 13.

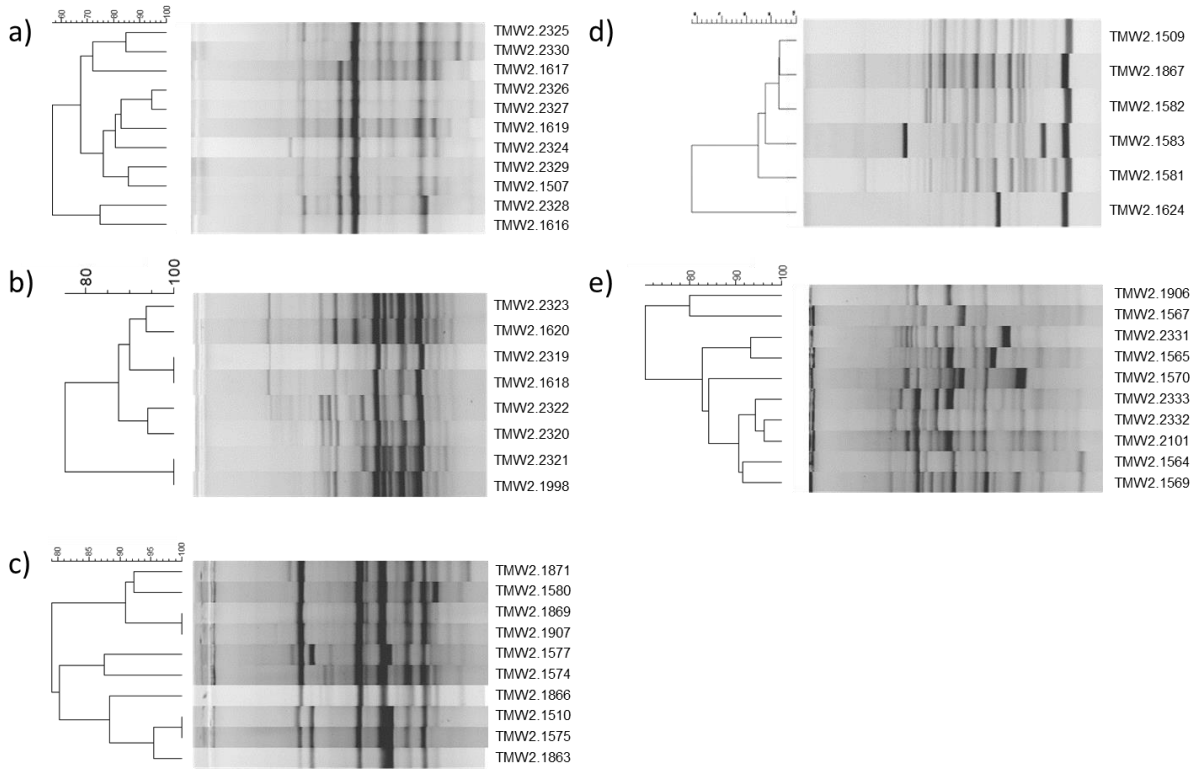

Figure 13. Selection of representative strains of the five meat-spoiling bacteria due to their genomic fingerprint. RAPD-PCR band clustering of different strains for the five species a) *L. gelidum* subsp. *gasicomitatum* (n=11), b) *L. gelidum* subsp. *gelidum* (n=8), c) *C. divergens* (n=10), d) *C. maltaromaticum* (n=6) and e) *B. thermosphacta* (n=10). The dendrogram is based on the method UPGMA, with a Dice´s similarity coefficient and 5% tolerance. Scale bars refer to the Pearson correlation coefficient.

All strains of the species *L. gelidum* subsp. *gasicomitatum*, *C. maltaromaticum* and *B. thermosphacta* exhibited an unique band pattern based on their genetic diversity, whereas some strains of the species *L. gelidum* subsp. *gelidum* exhibited similar band patterns and were clustered as same strains by the given method parameters (TMW2.1618 and TMW2.2319, TMW2.1998 and TMW2.2321). Furthermore, the strains TMW2.1869 and TMW2.1907 as well as TMW2.1510 and TMW2.1575 of *C. divergens* could not be differentiated by their band pattern and were identified as same strains. However, strains outlying the main RAPD-PCR clusters were marked by a cross in Table 11 and were not considered for strain selection. Those comprise *B. thermosphacta* TMW2.1906, TMW2.1567 and TMW2.1570, *L. gelidum* subsp. *gasicomitatum* TMW2.1616, TMW2.1617, TMW2.2330, TMW2.2328 and TMW2.2325, *L. gelidum* subsp. *gelidum* TMW2.1998 and TMW2.2321, *C. divergens* TMW2.1863 and TMW2.1866 and *C. maltaromaticum* TMW2.1624.

III. MALDI-TOF MS clustering

Third, strains were differentiated based on their proteomic diversity. Therefore, a mass spectrometric approach (MALDI-TOF MS) was chosen. This method analyzes low molecular weight peptides of strains. Thus, the higher the diversity in peptide composition, the more different patterns can be seen for each strain. Hierarchical clustering of strains was done calculating Euclidean distance matrices by RStudio (chapter 3.4.5). Results are shown in Figure 14.

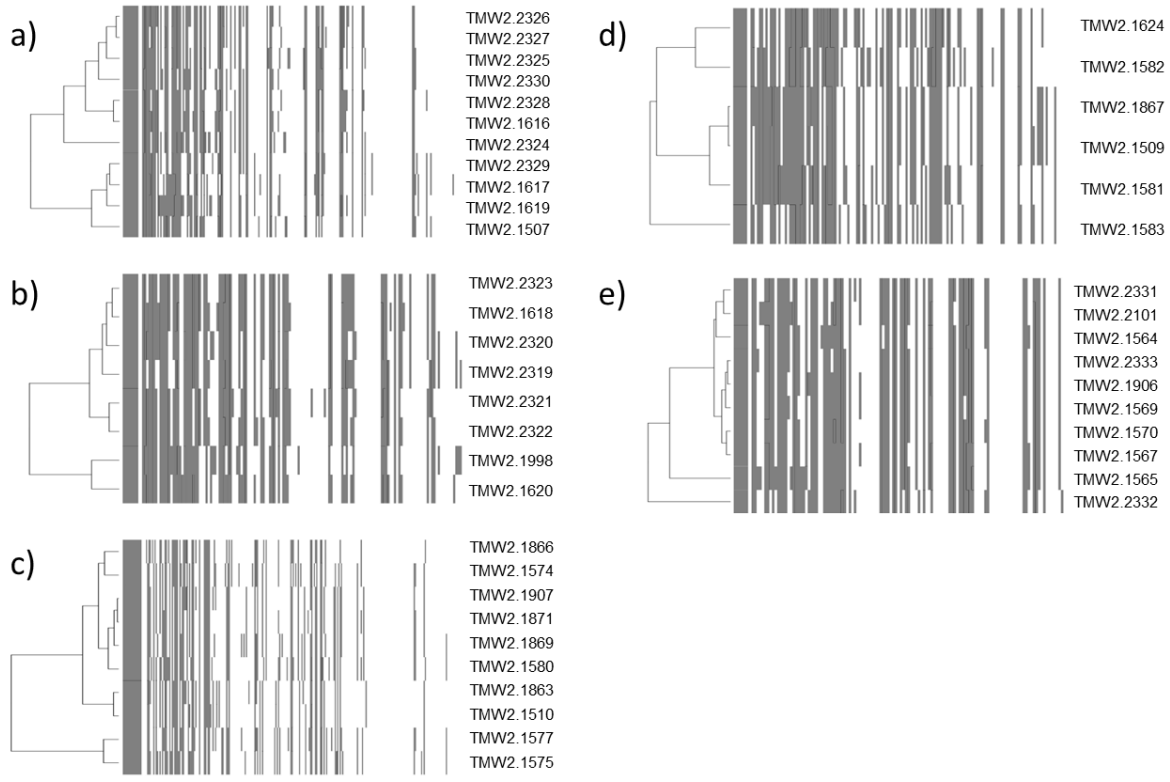

Figure 14. Selection of representative strains of the meat-spoiling bacteria due to their proteomic fingerprint. Hierarchical clustering analyzes of different strains of the species a) *L. gelidum* subsp. *gasicomitatum* (n=11), b) *L. gelidum* subsp. *gelidum* (n=8), c) *C. divergens* (n=10), d) *C. maltaromaticum* (n=6) and e) *B. thermosphacta* (n=10). Clustering is based on Euclidean distance matrices calculated by RStudio.

High strain differentiation was obtained using MALDI-TOF MS hierarchical clustering. All strains of all species could be differentiated. Even strains exhibiting same band patterns by RAPD-PCR, were identified as unique strains using mass spectrometry. Strains outlying the main cluster of proteomic related strains comprise *B. thermosphacta* TMW2.1565 and TMW2.2332, *L. gelidum* subsp. *gelidum* TMW2.1998 and TMW2.1620, *L. gelidum* subsp. *gasicomitatum* TMW2.1507 and TMW2.2324, *C. divergens* TMW2.1574 and TMW2.1866 and *C. maltaromaticum* TMW2.1583. Those strains were excluded from the strain selection and marked by a cross in Table 11.

The final strain selection was done as illustrated in Table 11. Strains marked by a cross for one of the three categories “Growth”, “RAPD-PCR” or “MALDI-TOF MS” were excluded for selection. The remaining strains were marked by grey shadow within Table 11 as they best represent the physiological, genetical and proteomic properties of all other strains isolated from meat.

Table 11. Selection of representative strains for further experiments. Strains analyzed by RAPD, MALDI-TOF MS and aerobic/anaerobic growth for each species are listed. Those strains, exhibiting noticeable differences or distanced clustering in one of the three analyses were marked by a cross. Strains with closely related physiological, genomic and protein chemical properties were highlighted by a grey shadow. Selected strains, representing most other strains of the same species were highlighted.

L. gelidum* subsp. *gelidum

Strain	Growth	RAPD-PCR	MALDI-TOF MS
TMW2.2319			
TMW2.2320			
TMW2.2321		x	
TMW2.2322			
TMW2.2323			
TMW2.1998	x	x	x
TMW2.1618			
TMW2.1620	x		x

B. thermosphacta

Strain	Growth	RAPD-PCR	MALDI-TOF MS
TMW2.1906	x	x	
TMW2.2331	x		
TMW2.2332			x
TMW2.2101			
TMW2.2333			
TMW2.1565			x
TMW2.1567		x	
TMW2.1564	x		
TMW2.1570		x	
TMW2.1569			

C. maltaromaticum

Strain	Growth	RAPD-PCR	MALDI-TOF MS
TMW2.1509			
TMW2.1581			
TMW2.1582			
TMW2.1583			x
TMW2.1624	x	x	
TMW2.1867			

L. gelidum* subsp. *gasicomitatum

Strain	Growth	RAPD-PCR	MALDI-TOF MS
TMW2.2324	x		x
TMW2.2325		x	
TMW2.2326			
TMW2.2327			
TMW2.2328	x	x	
TMW2.2329			
TMW2.2330		x	
TMW2.1507	x		x
TMW2.1616	x	x	
TMW2.1617		x	
TMW2.1619			

C. divergens

Strain	Growth	RAPD-PCR	MALDI-TOF MS
TMW2.1510			
TMW2.1869	x		
TMW2.1871			
TMW2.1907			
TMW2.1575			
TMW2.1577			
TMW2.1580			
TMW2.1574			x
TMW2.1863	x	x	
TMW2.1866		x	x

The finally selected strains for further experiments were highlighted by black boxes in Table 11 and comprise: *B. thermosphacta* TMW2.2101, *C. divergens* TMW2.1577, *C. maltaromaticum* TMW2.1581, *L. gelidum* subsp. *gelidum* TMW2.1618 and *L. gelidum* subsp. *gasicomitatum* TMW2.1619.

4.1.3. Influence of O_2 and CO_2 on growth of bacteria in MS-media

Growth of bacteria cultivated under different gas atmospheres was monitored in two experiments (chapter 3.2.2 and chapter 3.2.3) applying the same experimental setup but different gas atmospheres. However, both experiments enable to uncover the effect of O_2 and CO_2 on the metabolism of the five meat-spoiling bacteria applying different gas atmosphere comparisons. Growth curves, sampling time points and statistical analysis of growth parameters (lag-phase, OD_{max} and μ_{max}) of the experiment describe in chapter 3.2.2 are shown in Supplementary Figure 1 and Supplementary Table 2. Same data, obtained from the experiment described in chapter 3.2.3 are shown in Supplementary Figure 2 and Supplementary Table 3. Table 12 summarizes the effect of O_2 and CO_2 on bacterial growth based on data analysis from both experiments.

Table 12. Summary of the effects of O_2 and CO_2 on growth of bacteria in MS-media. The effect of O_2 and CO_2 on the five meat-spoiling bacteria was highlighted, based on the calculated growth parameter growth rate (μ_{max}), maximal optical density (OD_{max}) and lag-phase by the R package grofit. Arrows indicate if the parameter was increased (⇧) or decreased (⇩) due to the corresponding gas. Numbers of arrows represent the strength of the effect measured based on the p-value of significance tests (0.05> p >0.01 one arrow, 0.01> p >0.001 two arrows, p <0.001 three arrows). "–" = not effect detected, * manually performed t-test, ** Controversial results obtained from both experiments

	Effect of CO_2			Effect of O_2		
	μ_{max}	OD_{max}	Lag-phase	μ_{max}	OD_{max}	Lag-phase
B. thermosphacta TMW2.2101	--	--	⇧⇧⇧	⇧	⇧*	**
C. divergens TMW2.1577	--	--	⇧⇧	⇧	⇧⇧	⇧⇧⇧
C. maltaromaticum TMW2.1581	⇧⇧	--	**	⇧⇧⇧	⇧⇧⇧	⇧⇧⇧
L. gelidum subsp. *gelidum* TMW2.1618	⇧	--	**	⇧⇧⇧	⇧⇧⇧	--
L. gelidum subsp. *gasicomitatum* TMW2.1619	⇧⇧⇧	**	--	**	⇩⇩⇩	--

The species *B. thermosphacta* TMW2.2101 exhibited an increased lag-phase when exposed to CO_2. Exposure to O_2 resulted in an increase of the maximal OD and growth rate of *B. thermosphacta* TMW2.2101. *C. divergens* TMW2.1577 exhibited delayed growth due to CO_2, which is indicated by a strong increase of the lag-phase. O_2 also delayed the growth of *C. divergens* as the lag-phase significantly increased. Nevertheless, this species reached a higher OD and growth rate when exposed to O_2. *C. maltaromaticum* TMW2.1581 exhibited an increase in its growth rate due to CO_2. Controversial results were obtained in both experiments regarding the influence of CO_2 on the lag-phase of *C. maltaromaticum* TMW2.1581 enabling no clear statement. Contrary, O_2 strongly affected growth of *C. maltaromaticum* TMW2.1581

as the growth rate and maximal OD increased. Nevertheless, the lag-phase was prolonged when *C. maltaromaticum* TMW2.1581 was exposed to O_2. The species *L. gelidum* subsp. *gelidum* TMW2.1618 slightly increased its growth rate due to CO_2. However, controversial results were obtained from both experiments when analyzing the influence of CO_2 on the lag-phase of *L. gelidum* subsp. *gelidum* TMW2.1618. O_2 promoted the growth of this species, as an increase in growth rate and maximal OD could be detected due to high O_2 exposure (70%). *L. gelidum* subsp. *gasicomitatum* TMW2.1619 also exhibited an increased growth rate due to CO_2. This species was more sensitive to O_2, as it exhibited a markedly lower maximal OD due to exposure to 70% O_2.

4.1.4. Influence of CO_2 on growth of bacteria on meat

Growth of the bacteria *B. thermosphacta* TMW2.2101, *C. divergens* TMW2.1577, *C. maltaromaticum* TMW2.1581, *L. gelidum* subsp. *gelidum* TMW2.1618 and *L. gelidum* subsp. *gasicomitatum* TMW2.1619 on inoculated beef and turkey samples was monitored under application of rising CO_2 (15, 30, 50 and 70%) and constant O_2 (21%) concentrations (chapter 3.3.1). Growth curves were recorded, determining the CFU at specific time points and can be seen in Figure 15.

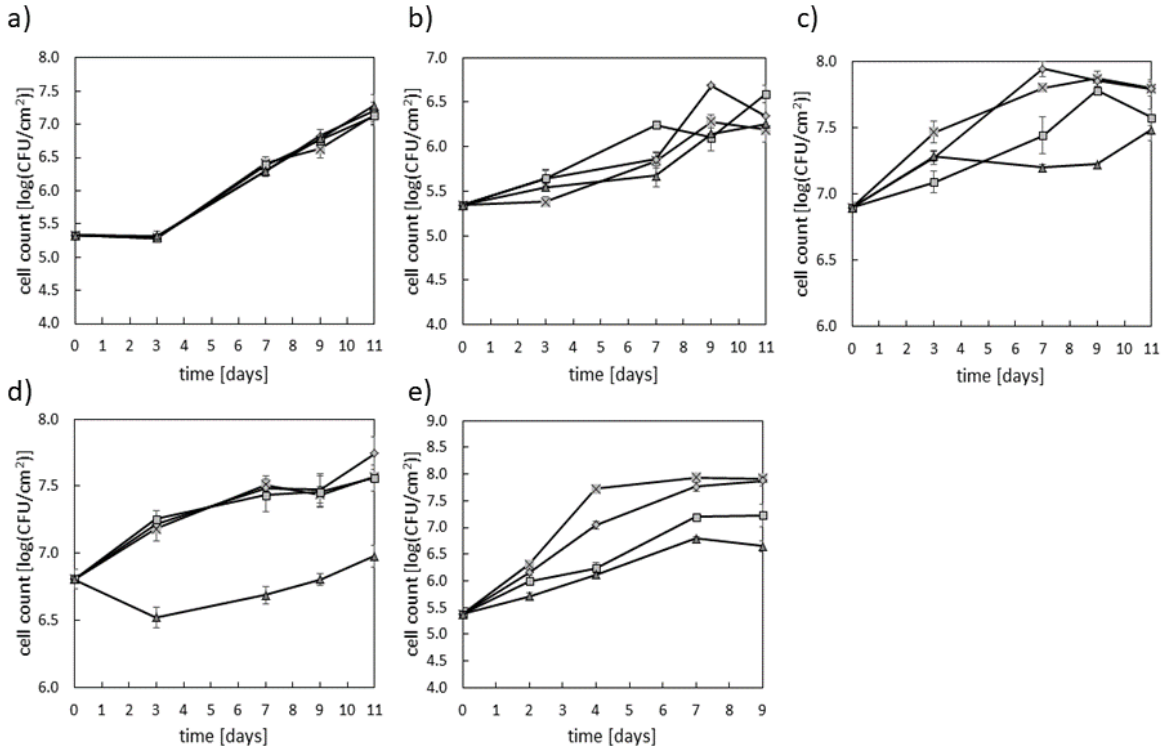

Figure 15. Growth of the five meat-spoiling bacteria with increasing CO_2 concentrations on meat. Growth curves were recorded for the five meat-spoiling bacteria (a) *L. gelidum* subsp. *gelidum* TMW2.1618 (b) *L. gelidum* subsp. *gasicomitatum* TMW2.1619 (c) *C. divergens* TMW2.1577 (d) *C. maltaromaticum* TMW2.1581 and (e) *B. thermosphacta* TMW2.2101 cultivated under the gas atmospheres (x) 15% CO_2 / 20% O_2 / 65% N_2, (◇) 30% CO_2 / 20% O_2 / 50% N_2, (□) 50% CO_2 / 20% O_2 / 30% N_2, (△) 70% CO_2 / 20% O_2 / 10% N_2. All values given are means of three independent replicates. Error bars represent calculated standard errors.

Growth curves were analyzed using two methods. First, growth parameters were calculated using grofit (chapter 3.4.13) and analyzed by R (chapter 3.4.14). Results are shown in Supplementary Table 4. Second, a comparative statistical analysis of the determined $log_{10}(CFU/cm^2)$ values after 7 days was performed (Supplementary Table 5). A summary of both analysis methods as well as an overall conclusion about the inhibitory effect of CO_2 on the analyzed bacteria is given in Table 13.

Table 13. Effect of CO_2 on the growth of the five meat-spoiling bacteria when cultivated on meat. Summary of the effects of CO_2 on growth of bacteria on inoculated meat, based on the calculated growth parameter growth rate (μ_{max}), maximal CFU (CFU_{max}) and lag-phase as well as the determined $log_{10}(CFU/cm^2)$ after 7 days. Arrows indicate if the parameter was increased (⇧) or decreased (⇩) comparing two CO_2 concentrations. Numbers of arrows indicate the strength of the effect measured based on the regulation (one arrow = 0-2-fold regulation, two arrows= 2-4-fold regulation). All data given have been validated as significant ($p < 0.05\%$).

	Effect of CO_2				Overall Inhibition by CO_2 / MIC CO_2
	μ_{max}	CFU_{max}	Lag-phase	$Log_{10}(CFU/cm^2)$ after 7 days	
B. thermosphacta TMW2.2101	⇩15-70%	⇩15-70%	⇧15-70% ⇧30-70%	⇩15-50% ⇩15-70% ⇩30-50% ⇩30-70% ⇩50-70%	**Yes / >30%**
C. divergens TMW2.1577	---	⇩30-70%	---	⇩15-50% ⇩15-70% ⇩30-50% ⇩30-70%	**Yes / >30%**
C. maltaromaticum TMW2.1581	⇩⇩30-70%	⇩30-70% ⇩15-70% ⇩50-70%	---	⇩15-70% ⇩30-70% ⇩50-70%	**Yes / >70%**
L. gelidum subsp. *gelidum* TMW2.1618	---	----	---	---	**No**
L. gelidum subsp. *gasicomitatum* TMW2.1619	---	---	---	⇩50-70%	**No**

A measurable inhibition of *B. thermosphacta* TMW2.2101 by CO_2 was detected, as this species exhibited a lower growth rate, maximal CFU and an increased lag-phase due to CO_2 exposure >30%. Furthermore, the determined $log_{10}(CFU/cm^2)$ values after 7 days decreased with increasing CO_2 concentrations. *C. divergens* TMW2.1577 exhibited similar correlations compared to *B. thermosphacta* TMW2.2101. A decrease in maximal CFU due to CO_2 exposure was detected. The determined $log_{10}(CFU/cm^2)$ values after 7 days were also decreasing with increasing CO_2 concentrations. Growth of *C. maltaromaticum* TMW2.1581 was inhibited above concentrations of 70%. This was concluded by a significant decrease of the growth rate and maximal CFU due to CO_2 exposure as well as a significantly reduced growth after 7 days

comparing 70% CO_2 exposure and other CO_2 concentrations. Both *L. gelidum* subspecies exhibited no measurable inhibition of their growth due to CO_2 exposure.

After 11 days of cultivation, the predominance of the inoculated strains was checked on meat. RAPD-PCR analysis proved the appearance of the inoculated strain, as well as the absence of any other strain or species of the natural microbiota on meat at the end of fermentation (data not shown).

4.1.5. Proteomic studies of meat-spoiling bacteria

In order to explain the different sensitivities of the meat-spoiling bacteria to the gases O_2 and CO_2, two proteomic studies with the five selected meat-spoiling bacteria were performed. Firstly, species were cultivated in MS-media under different gas atmospheres (chapter 3.2.2) and secondly species were inoculated on beef steaks packaged under 30% CO_2 / 70% O_2 atmosphere (chapter 3.3.2). The latter proteomic experiment was only performed to provide evidence for the transferability of data obtained in MS-media to real meat. Thus, this experiment was not done in replicates.

Comparative proteomics of meat-spoiling bacteria in MS-media

Pairwise comparisons of identified proteins of each bacterium cultivated at different gas atmospheres were done and enhanced or reduced expression of proteins regarding exposure to O_2 and CO_2 were defined based on $p < 0.05$ and a $\log_2$ fold change $>= 2$. Supplementary Table 6 provides a list of all differentially expressed proteins identified by this analysis. Those proteins were sorted to metabolic pathways based on KEGG, RAST, SEED and NCBI annotation as well as manual research. A summary of metabolic pathways differentially regulated due to O_2 or CO_2 exposure for each species is provided in Table 14.

Table 14. Summary of metabolic pathways exhibiting significantly enhanced or reduced expression of proteins due to O_2 and CO_2 exposure. A list of all identified metabolic pathways containing differentially expressed proteins for the analyzed meat-spoiling bacteria is provided. Significantly enhanced expression of proteins due to the corresponding gas was marked by a green arrow (⇧), whereas significant reduced expression was marked by a red arrow (⇩).

	O_2 (21%) (Approach 1)		O_2 (70%) (Approach 2)		CO_2 (oxic) (Approach 3, 5)		CO_2 (anoxic) (Approach 4, 5)	
B. thermosphacta TMW2.2101	NADH oxidase	⇧	Oxidative stress	⇧			Ethanolamine degradation	⇧
	Oxidative stress	⇧	Pyruvate formate-lyase	⇩				
	Amino acid degradation	⇧						
	Acetoin and Acetate production	⇧						
	Pentose phosphate pathway	⇧						
	Glycerol metabolism	⇧						
	Myo-Inositol metabolism	⇧						
	Ethanolamine degradation	⇩						
C. divergens TMW2.1577	Oxidative and osmotic stress	⇧	Oxidative stress	⇧	Osmotic stress	⇧	ADI pathway	⇧
	Heme degradation	⇧	Pyruvate formate-lyase	⇩			Tyrosine and alanine catabolism	⇧
	Amino acid degradation	⇧					Purine and pyrimidine metabolism	⇧
	Pyruvate dehydrogenase	⇧						
	L-lactate dehydrogenase	⇧						
	Purine and pyrimidine metabolism	⇩						
	Fatty acid degradation	⇩						
C. maltaromaticum TMW2.1581	Oxidative stress	⇧	Heme uptake	⇧	Fatty acid biosynthesis	⇧	Fatty acid biosynthesis	⇧
	Amino acid transporter	⇧	Oxidative stress	⇧	Folate metabolism	⇧	Ethanolamine degradation	⇧
	Sugar uptake transporter	⇧	Pyruvate formate-lyase	⇩	Fatty acid degradation	⇧	Sugar uptake transporter	⇧
	Glycerol metabolism	⇧			Glycerophospholipid metabolism	⇧	Glycerol metabolism	⇧
	Allantoin degradation	⇧			Pentose phosphate pathway	⇧	Ribose degradation	⇧
	Ribose degradation	⇧			Ethanol amine degradation	⇩	ADI pathway	⇧
					ADI pathway	⇩	Alanine catabolism	⇧
					Sugar uptake transporter	⇩	Glycolysis	⇧
					Glycerol metabolism	⇩	Fatty acid degradation	⇧
					Ribose degradation	⇩	Pentose phosphate pathway	⇧
L. gelidum subsp. *gelidum* TMW2.1618	Oxidative stress	⇧	Oxidative stress	⇧	Ion transporter	⇩		
	Acetolactate synthase	⇧						
L. gelidum subsp. *gasicomitatum* TMW2.1619	Oxidative stress	⇧	Oxidative stress	⇧	Citrate utilization	⇧	Pentose phosphate pathway	⇩
	Acetolactate synthase	⇧			Ion transporter	⇩		
	Lactate dehydrogenase	⇧						
	Citrate utilization	⇧						
	Pentose phosphate pathway	⇩						

B. thermosphacta TMW2.2101 exhibited the highest metabolic response to 21% O_2 compared to the other species. An enhanced expression of several enzymes and metabolic pathways was detected for this species comprising the NADH oxidase, enzymes for oxidative stress reduction, amino acid, pentose, glycerol and myoinositol degradation as well as acetoin and acetate production. Contrary, enzymes for ethanolamine degradation exhibited a reduced expression under these conditions. When exposed to high O_2 concentrations, *B. thermosphacta* TMW2.2101 expressed higher amounts of oxidative stress enzymes whereas it reduced the expression of the pyruvate-formate lyase. The expression of the ethanolamine degradation cluster was further increased for this species when exposed to CO_2 under anoxic conditions.

C. divergens TMW2.1577 exhibited an increased expression of oxidative and osmotic stress proteins, the lactate dehydrogenase and pyruvate dehydrogenase as well as proteins involved in amino acid and heme degradation under oxic conditions (21% O_2). Enzymes for fatty acid, purine and pyrimidine degradation exhibited a reduced expression under the same cultivation condition. Similar to *B. thermosphacta* TMW2.2101, exposure of *C. divergens* TMW2.1577 to high O_2 concentrations induced an enhanced expression of oxidative stress enzymes and a reduced expression of the pyruvate-formate lyase. An enhanced expression of osmotic stress proteins was detected for this species under CO_2 exposure in the presence of O_2. Furthermore, CO_2 in combination with the absence of O_2, increased the expression of enzymes involved in arginine, tyrosine, alanine, purine and pyrimidine degradation for *C. divergens* TMW2.1577.

The species *C. maltaromaticum* TMW2.1581 exhibited an enhanced expression of enzymes involved in oxidative stress reduction, amino acid and sugar uptake as well as glycerol, allantoin and ribose degradation when exposed to 21% O_2. Enzymes for the uptake of exogenous heme as well as oxidative stress enzymes were induced in their expression, whereas the expression of the pyruvate-formate lyase was reduced under high O_2 conditions. When exposed to CO_2 under oxic conditions, *C. maltaromaticum* TMW2.1581 exhibited an enhanced expression of enzymes involved in fatty acid biosynthesis as well as degradation of folate, fatty acids, glycerophospholipids and pentoses. Contrary, enzymes for ethanolamine, arginine, glycerol and ribose degradation as well as sugar uptake exhibited a reduced expression under those conditions. Exposure of CO_2 under anoxic conditions increased the expression of proteins involved in fatty acid biosynthesis, sugar uptake and degradation of ethanolamine, glycerol, ribose, glucose, fatty acids, arginine and alanine for *C. maltaromaticum* TMW2.1581.

The expression of the acetolactate synthase as well as oxidative stress enzymes were enhanced for *L. gelidum* subsp. *gelidum* TMW2.1618 when exposed to 21% O_2. Expression of oxidative stress enzymes was further induced under high O_2 conditions. The exposure to CO_2

under oxic conditions reduced the expression of ion transporters for this species. CO_2 under anoxic conditions did not affect the expression of enzymes for *L. gelidum* subsp. *gelidum* TMW2.1618.

L. gelidum subsp. *gasicomitatum* TMW2.1619 exhibited an enhanced expression of the acetolactate synthase, lactate dehydrogenase as well as enzymes involved in oxidative stress and citrate utilization under 21% O_2 exposure. Furthermore, enzymes of the pentose phosphate pathway exhibited reduced expression under the same conditions. Similar to *L. gelidum* subsp. *gelidum* TMW2.1618, an enhanced expression of oxidative stress enzymes could be observed for *L. gelidum* subsp. *gasicomitatum* TMW2.1619 under high O_2 conditions. CO_2 exposure under oxic conditions resulted in an enhanced expression of citrate utilizing enzymes as well as a reduced expression of ion transporters. Enzymes for pentose phosphate metabolism exhibited a reduced expression under CO_2 exposure in the absence of O_2.

The expression profile of respiratory chain enzymes was further examined, focusing on LFQ and iBAQ values. None of the analyzed meat-spoiling bacteria exhibited a significantly differential regulation of respiration chain enzymes, except for some enzymes involved in heme uptake or menaquinone biosynthesis. However, a constitutive expression of corresponding enzymes for all species could be detected independent of the gas atmospheres.

Proteomics of meat-spoiling bacteria on inoculated beef steak

A second proteomic experiment was performed, cultivating the five meat-spoiling bacteria on inoculated beef and chicken under high oxygen atmosphere (70% O_2 / 30% CO_2). The number of identified proteins of this experiment was comparable low. 506 proteins were identified for *B. thermosphacta* TMW2.2101, 257 for *C. divergens* TMW2.1577, 57 for *C. maltaromaticum* TMW2.1581, 118 for *L. gelidum* subsp. *gelidum* TMW2.1618 and 88 for *L. gelidum* subsp. *gasicomitatum* TMW2.1619. The obtained data were compared to the results obtained from the proteomic experiment done in MS-media, which are summarized in Table 14**.** In detail, significantly differential regulated proteins and pathways referred to 70% O_2 and CO_2 in Table 14 were compared to those proteins identified on inoculated meat. Identified matching proteins are listed in Table 15.

Table 15. List of matching enzymes of the five meat-spoiling bacteria when growing on beef or chicken compared to real meat under high oxygen atmosphere. A comparison of enzymes measured in the proteomic study on real meat was done with significantly differentially regulated enzymes obtained from the proteomic study under 70% O_2 or 30% CO_2 exposure in MS-media (see Table 14). Matching enzymes identified for each of the five meat-spoiling species are displayed.

Enzyme	Locus tag
***B. thermosphacta* TMW2.2101**	
Alanine dehydrogenase	**EHX26_02725**
Glycine betaine/L-proline ABC transporter ATP-binding protein	**EHX26_10880**
Glycine/betaine ABC transporter	**EHX26_10870**
Catalase	**EHX26_11130**
Superoxide dismutase	**EHX26_06805**

Organic hydroperoxide resistance protein	**EHX26_08890**
Thiol peroxidase	**EHX26_10115**
Thioredoxin	**EHX26_01515**
Thioredoxin-disulfide reductase	**EHX26_08380**
OsmC family peroxiredoxin	**EHX26_10775**
Acetolactate synthase	**EHX26_01770**
***C. divergens* TMW2.1577**	
Arginine deiminase	**EH150_00245**
Carbamate kinase	**EH150_00260**
Ornithine carbamoyltransferase	**EH150_00250**
Thioredoxin	**EH150_04700**
Catalase	**EH150_10970**
Superoxide dismutase	**EH150_04005**
Peroxiredoxin	**EH150_11315**
Organic hydroperoxide resistance protein	**EH150_12635**
NADH oxidase	**EH150_00705**
Acetolactate synthase	**EH150_03770**
***C. maltaromaticum* TMW2.1581**	
Tyrosine decarboxylase	**BFC23_10455**
Glycine/betaine ABC transporter ATP-binding protein	**BFC23_04715**
Superoxide dismutase	**BFC23_07340**
***L. gelidum* subsp. *gelidum* TMW2.1618**	
Potassium transporter Kup	**BHS02_00505**
Acetolactate synthase	**BHS02_06300**
***L. gelidum* subsp. *gasicomitatum* TMW2.1619**	
Potassium transporter Kup	**BHS03_00445**
Thioredoxin	**BHS03_02850**
Peroxiredoxin	**BHS03_02400**

Several antioxidant and osmo-protectant proteins as well as the acetolactate synthase and alanine dehydrogenase could be measured for *B. thermosphacta* TMW2.2101 under high oxygen atmosphere on inoculated beef steak. Expressed proteins identified for *C. divergens* TMW2.1577 comprised the NADH oxidase, acetolactate synthase, several antioxidant enzymes as well as enzymes of the ADI pathway. The number of proteins identified for *C. maltaromaticum* TMW2.1581 was quite low, including the tyrosine decarboxylase, superoxide dismutase and a glycine/betaine transporter. Identified proteins of *L. gelidum* subsp. *gelidum* TMW2.1618 matching to those in Table 14 comprised the acetolactate synthase and a potassium ion transporter. Latter protein could also be identified for *L. gelidum* subsp. *gasicomitatum* TMW2.1619. Additionally, the thioredoxin and peroxiredoxin enzyme was identified for this species.

4.1.6. Analysis of differential transcription data of genes due to O_2 and CO_2

The transcription profile of O_2-consuming enzymes of three meat-spoiling species was examined, when cultivated under different gas atmospheres. Samples analyzed by qRT-PCR were obtained from the experiment described in chapter 3.2.2. Results are listed in Table 16 and in detail in Supplementary Figure 3.

Table 16. Single transcription analysis of selected target genes for three meat spoilers cultivated under different gas atmospheres. The effect of high O_2 on the relative transcription of selected marker genes involved in O_2 consumption of bacteria was analyzed by qRT-PCR. G3PD= Glycerin-3-phosphate dehydrogenase, MQ= 2-succinyl-5-enolpyruvyl-6-hydroxy-3-cyclohexene-1-carboxylic-acid synthase, NOX= NADH oxidase, SOD= Superoxide dismutase, POX= Pyruvate oxidase. Arrows indicate if the transcription of a gene was enhanced (⇧) or reduced (⇩) due to the corresponding gas. Numbers of arrows indicate the strength of regulation (one arrow = 0-2 fold regulation, two arrows= 2-4 fold regulation, three arrows= >4 fold regulation).

	O_2 (21%) (Approach 1)	**O_2 (70%)** (Approach 2)	**CO_2 (oxic)** (Approach 3)	**CO_2 (anoxic)** (Approach 4)
B. thermosphacta TMW2.2101	⇩⇩ MQ	⇧⇧ POX ⇧⇧ NOX ⇧⇧ G3PDH ⇧⇧ MQ	⇧⇧ POX ⇧⇧ NOX ⇧⇧ G3PDH ⇧⇧ MQ	
C. divergens TMW2.1577	⇩⇩⇩ NOX ⇧ SOD	⇩⇩ G3PDH ⇩⇩ SOD	⇩⇩ G3PDH ⇩⇩ SOD	⇧⇧⇧ G3PDH ⇧⇧⇧ NOX
L. gelidum subsp. *gasicomitatum* TMW2.1619	⇩⇩ G3PDH ⇩⇩ MQ ⇩⇩⇩ NOX ⇩⇩ POX	⇧ G3PDH ⇧⇧ MQ ⇧⇧ NOX ⇧⇧ POX	⇧ G3PDH ⇧⇧ MQ ⇧⇧ NOX ⇧⇧ POX	⇧ G3PDH

An overall enhanced transcription of enzymes was observed for bacteria when exposed to high oxic conditions (70% O_2) compared to normal oxic conditions (21% O_2). Those comprise the O_2 consuming pyruvate oxidase, NADH oxidase and glycerin-3-phosphate dehydrogenase for *B. thermosphacta* TMW2.2101 and *L. gelidum* subsp. *gasicomitatum* TMW2.1619. Furthermore, the enzyme 2-succinyl-5-enolpyruvyl-6-hydroxy-3-cyclohexene-1-carboxylic-acid synthase, involved in menaquinone biosynthesis exhibited an increased transcription under high O_2 conditions for both species. Contrary, a reduced transcription of the glycerin-3-phosphate dehydrogenase and superoxide dismutase was observed for *C. divergens* TMW2.1577 under high O_2 conditions.

When CO_2 was exposed under oxic conditions, same regulation of enzymes of all species could be observed compared to exposure to high oxic conditions, whereas exposure of CO_2 under anoxic conditions resulted in an enhanced transcription of the glycerin-3-phosphate dehydrogenase for *L. gelidum* subsp. *gasicomitatum* TMW2.1619 and *C. divergens* TMW2.1577. Latter species also upregulated the transcription of the NADH oxidase under this condition.

4.1.7. Cell membrane changes due to O_2 and CO_2

Changes of the membrane fluidity and permeability of the meat-spoiling bacteria due to O_2 and CO_2 exposure were analyzed as described in chapter 3.2.3. Therefore, bacteria were cultivated under different gas atmospheres. Samples were taken during the exponential growth phase and analyzed by two approaches. Firstly, a targeted approach was applied, which directly measures membrane fluidity and permeability by the fluorescence dyes Laurdan and propidium iodide. Secondly, an untargeted approach analyzing the fatty acid profile of bacteria was conducted, enabling conclusions about changes of membrane fluidity and permeability.

Results obtained from membrane fluidity and permeability measurement (approach 1) with the fluorescence dye Laurdan and propidium iodide (chapter 3.4.9 and chapter 3.4.10) are shown in Figure 16.

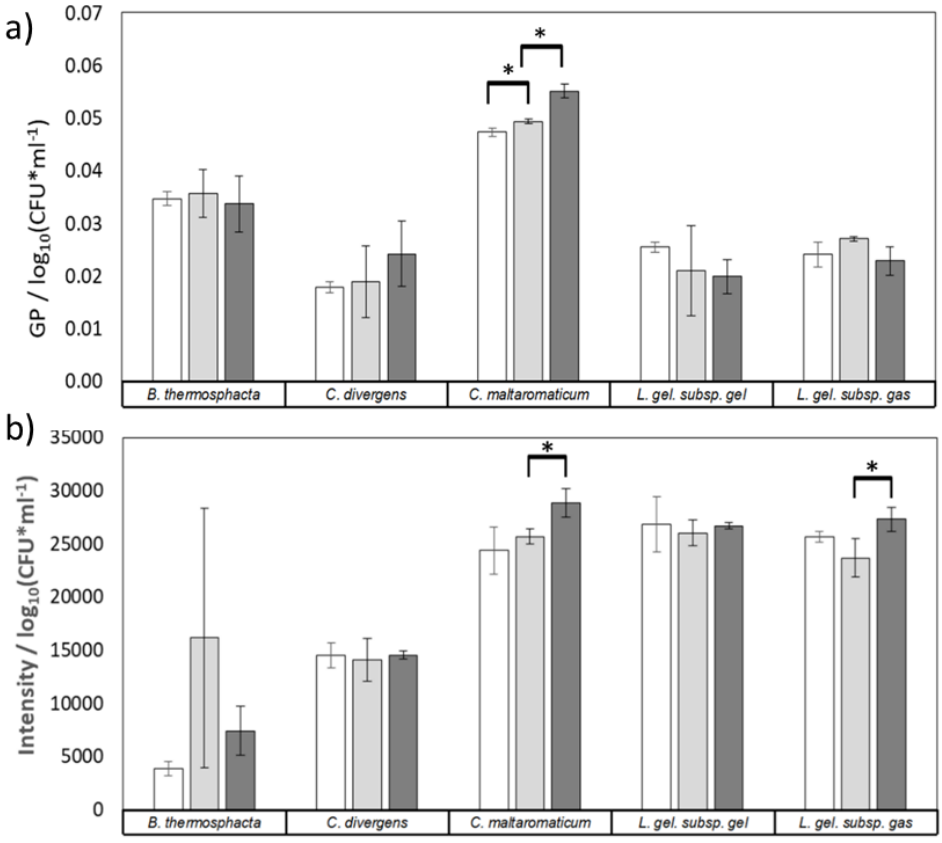

Figure 16. Changes in the membrane fluidity and permeability of the five meat-spoiling bacteria in response to O_2 and CO_2. Cell membrane fluidity a) and permeability b) were analyzed for the five meat-spoiling bacteria cultivated under the atmospheres (■) 21% O_2 / 0% CO_2 / 79% N_2 (air) (■) 20% O_2 / 30% CO_2 / 50% N_2 and (■) 70% O_2 / 30% CO_2 / 0% N_2 by a physiological assay using Laurdan and propidium iodide. Bars represent mean values of three independent experiments and error bars represent standard deviations. * indicate significant differences between gas atmospheres identified by a Welch T-test with $p < 0.05$.

The only species exhibiting a measurable and significant decrease in membrane fluidity due to O_2 and CO_2 exposure was *C. maltaromaticum* TMW2.1581. This species also significantly increased its membrane permeability in response to O_2 exposure. Furthermore, an increase in membrane permeability could be detected for *L. gelidum* subsp. *gasicomitatum* TMW2.1619 in response to O_2 exposure.

Furthermore, cell surfaces of bacteria from the same experiment were analyzed by microscopy (chapter 3.4.11). Results are shown in Supplementary Figure 4. In brief, an increase in cell surface due to CO_2 could be detected for *B. thermosphacta* TMW2.2101, *C. maltaromaticum* TMW2.1581 and *L. gelidum* subsp. *gasicomitatum* TMW2.1619. Contrary, *C. divergens* TMW2.1577 decreased its cell surface due to CO_2 exposure. Oxygen decreased the cell

surface of *B. thermosphacta* TMW2.2101 and *C. maltaromaticum* TMW2.1581 and increased the cell surface of *C. divergens* TMW2.1577 and *L. gelidum* subsp. *gelidum* TMW2.1618.

Additionally, a non-targeted approach was applied, analyzing the detailed fatty acid composition of bacteria by GC-MS analysis. A list of all detected single fatty acids for each species as well as their differential regulation due to O_2 and CO_2 is given in the Supplementary Table 7. Single fatty acids, exhibiting same physiological structure (double bonds, methyl side chains, chain length) were grouped. Changes of those physiological groups in response to O_2 and CO_2 can be seen in Table 17.

Table 17. Changes of the fatty acid profile of five meat-spoiling bacteria in response to O_2 and CO_2. Effect of O_2 and CO_2 on the fatty acid profile of the five meat-spoiling bacteria cultivated under different gas atmospheres. Values are based on biological replicates. "X-fold upregulated by CO_2": Ratio of ∑ % (µg FA/g cells) identified for the gas atmosphere 21% O_2 / 0% CO_2 / 79% N_2 and 20% O_2 / 30% CO_2 / 50% N_2. "X-fold upregulated by O_2": Ratio of ∑ % (µg FA/gam cells) identified for the gas atmosphere 20% O_2 / 30% CO_2 / 50% N_2 and 70% O_2 / 30% CO_2 / 0% N_2. Significantly different ($p < 0.05$) regulated fatty acids are highlighted in dark gray and bold letters.

	***B. thermosphacta* TMW2.2101**	***C. divergens* TMW2.1577**	***C. maltaromaticum* TMW2.1581**	***L. gelidum* subsp. *gelidum* TMW2.1618**	***L. gelidum* subsp. *gasicomitatum* TMW2.1619**	***B. thermosphacta* TMW2.2101**	***C. divergens* TMW2.1577**	***C. maltaromaticum* TMW2.1581**	***L. gelidum* subsp. *gelidum* TMW2.1618**	***L. gelidum* subsp. *gasicomitatum* TMW2.1619**
	x-fold upregulation by CO_2					**x-fold upregulation by O_2**				
Iso	**1.18**	0.24	1.07	1.09	**0.45**	**1.20**	3.25	1.51	0.72	**0.67**
Anteiso	0.96	0.16	1.10	1.18	1.23	**0.83**	4.93	1.27	0.61	0.70
Long chain	**0.63**	0.90	1.00	1.00	**0.81**	0.96	1.03	1.03	**1.03**	1.02
Short chain (<C16)	**1.13**	1.14	1.01	0.99	**1.74**	1.01	0.96	0.91	**0.93**	0.97
Saturated	1.02	**1.28**	0.97	**1.11**	**2.08**	0.98	**0.78**	0.99	1.05	0.98
Unsaturated	0.85	**0.87**	1.01	**0.89**	**0.67**	1.16	**1.15**	1.00	0.94	1.02
Branched	1.02	0.93	1.06	0.97	1.56	**0.95**	**1.23**	1.09	1.01	0.96
Unbranched	0.92	1.02	0.99	1.00	0.95	**1.19**	**0.95**	1.00	1.00	1.01
Total Fatty acid content [µg FA / g cell]	0.77	1.23	0.83	0.75	**1.31**	1.13	**1.29**	**1.42**	1.16	0.98

B. thermosphacta TMW2.2101 increased its content in *iso*- and SCFA and decreased its content in LCFA in response to CO_2. Oxygen exposure resulted in an increase of *iso* and UBFA and a decrease in *anteiso* and BCFA for this species. A shift from UFA to SFA could be detected for *C. divergens* TMW2.1577 in response to CO_2. Exposure to O_2 resulted in an increase of UFA and BCFA and a decrease in SFA and UBFA for *C. divergens* TMW2.1577. Furthermore, the total amount of fatty acid increased significantly for this species in response to O_2 exposure. No effect of CO_2 or O_2 on the fatty acid profile of *C. maltaromaticum* TMW2.1581 could be detected. Nevertheless, a significant regulation of single fatty acids due

to O_2 was detected, as can be seen in Supplementary Table 7. In detail, this species exhibited an enhance production of long-chain unsaturated fatty acids (conjugated linoleic acid (18:2 conj.), arachidonic (C20:4 Δ5,8,11,14) and eicosapentaenoic acid (C20:5 Δ5,8,11,14,17) in response to high oxygen conditions. Similar, to *C. divergens* TMW2.1577, the total amount of fatty acids significantly increased due to O_2 exposure for *C. maltaromaticum* TMW2.1581. *L. gelidum* subsp. *gelidum* TMW2.1618 exhibited a shift from UFA to SFA in response to CO_2 whereas a shift from SCFA to LCFA was detected in response to O_2 exposure. *L. gelidum* subsp. *gasicomitatum* TMW2.1619 increased its content of SCFA, SFA and total fatty acids and decreased its content in *iso*, LCFA and UFA in response to CO_2. The only response to O_2 exposure was a decrease in the content of *iso* fatty acids for this species.

A summary of results of both approaches (measurement of membrane fluidity and permeability (approach 1) and single fatty acid measuring (approach 2)) is given in Table 18. Therefore, fatty acid derived changes on the membrane properties fluidity and permeability were listed, although those are explained later in the discussion part.

Table 18. Summary of the identified impact of O_2 and CO_2 on the membrane properties fluidity and permeability. Fatty acid derived and directly measured changes of the membrane fluidity and membrane permeability due to O_2 and CO_2 exposure are listed for all species. Arrows indicate, if the measured parameter is increasing (⇧) or decreasing (⇩) due to the corresponding gas. "M" = directly measured changes based on physiological assays (approach 1) and "FA" = fatty acid derived changes (approach 2).

	Membrane Fluidity	Membrane Permeability	Membrane Fluidity	Membrane Permeability
	Effect of CO_2		Effect of O_2	
B. thermosphacta TMW2.2101	⇩ FA		⇩ FA	
C. divergens TMW2.1577	⇩ FA	⇩ FA	⇧ FA	⇧ FA
C. maltaromaticum TMW2.1581	⇩ M		⇩ FA / M	⇧ M
L. gelidum subsp. *gelidum* TMW2.1618	⇩ FA	⇩ FA		
L. gelidum subsp. *gasicomitatum* TMW2.1619	⇩ FA	⇩ FA	⇧ FA	⇧ M

4.1.8. Genomic analysis of metabolic pathways

A genomic analysis for all species was conducted in order to predict the presence or absence of specific metabolic pathways (Table 19). Beside pathways involved in the basic energy metabolism of bacteria, reactions, which could be related to O_2 or CO_2 adaptation or consumption, were also highlighted. A detailed list of all genes involved in this metabolic pathway and their presence or absence for the five analyzed species is provided in the Supplementary Table 8.

Table 19. Genomically predicted metabolic pathways of the five meat-spoiling bacteria. The main metabolic pathways of the five meat-spoiling bacteria were predicted based on their genomic setting. "✓" = genes for the whole metabolic pathway were found in the genome, "(✓)" = single genes of the pathway are missing, nevertheless the pathway is expected to be completely functional. "-- = no genes for this pathway are present in the genome, "(--)" some genes of the pathway are present but the pathway is not expected to be completely functional.

	Genes / Gen cluster	*B. thermosphacta* TMW2.2101	*L. gelidum* subsp. *gelidum* TMW2.1618	*L. gelidum* subsp. *gasicomitatum* TMW2.1619	*C. divergens* TMW2.1577	*C. maltaromaticum* TMW2.1581
Basic energy metabolism						
Glycolysis	*pgi, pfkA, fbaA, gapdh, pkg, pgam, pk*	✓	✓	✓	✓	✓
Gluconeogenesis	*pyc, pckA, ppsA, fdp, ldh*	✓	(--)	(--)	(--)	✓
Oxidative pentose phosphate pathway	*zwf, devB, gntZ, rpe, rpiA*	✓	✓	✓	✓	✓
Citrate cycle	*icdA, sdhABCD, FumA, mdh, ppc, ncgl, aceB / suc, cit*	(--)	--	--	(--)	(--)
Amino acid metabolism	*Arg, speB, hdcA, icdC, hdcA, icdC, tdcA, gadB, aspB, mdh, gdh, sdaAB, tyrB, ilvE, ald, aspA, nadB /spe, arc*	✓	✓	✓	✓	✓
Pyruvate metabolism	*pta, poxB, ackA, adhE, pflB, focA, aldC, budC /pdh*	✓	✓	✓	✓	✓
Heterolactic fermentation	*xpkA, zwf*	--	✓	✓	--	--
Homolactic fermentation	*pfkA, fbaA*	✓	✓	✓	✓	✓
Allantoin metabolism	*hpxB, allc, ylba*	--	--	--	✓	✓
Nucleoside and ribose metabolism	*nubA, kunH, rihC/ rbs, deo, nrd*	✓	✓	✓	✓	✓
Respiration						
NADH dehydrogenase	*ndh*	✓	✓	✓	✓	✓
Menaquinone biosynthesis	*ubi E / men*	✓	✓	✓	(✓)	✓
Cytochrome bd ubiquinol oxidase	*cyb / cyd*	✓	✓	✓	✓	✓
Cytochrome O ubiquinol oxidase	*/ cyo*	--	(--)	(--)	--	(--)
Cytochrome ba_3 quinol oxidase	*cyb / qox*	✓	--	--	--	--
Cytochrome aa_3 quinol oxidase	*/ qox*	✓	--	--	--	--
Heme biosynthesis	*/ hem*	✓	--	--	(--)	(--)
Heme uptake	*/ isd*	✓	(--)	(--)	(✓)	(✓)
F0F1-ATP synthase	*/ atp*	✓	✓	✓	✓	✓
Oxidative stress						
Catalase	*cat*	✓	--	--	✓	✓
Superoxide dismutase	*sod*	✓	--	--	✓	✓
2-Cys Peroxiredoxin	*/ prdx2*	--	✓	✓	--	✓
Glutathione peroxidase	*/ gpx*	✓	✓	✓	✓	✓
Other peroxidases	--	✓	✓	✓	✓	--
Single oxygen consuming enzymes						
Pyruvate oxidase	*poxB*	✓	--	✓	--	--

Glycerol-3-phosphate oxidase	*gps*	✓	✓	✓	✓	✓
NADH oxidase	*nox*	✓	✓	✓	✓	✓
Acetolactate synthase	*alsS*	✓	✓	✓	✓	✓
Pyridoxine 5´-phosphate oxidase	*pdxH*	--	✓	✓	--	--
Fatty acid de-novo biosynthesis and regulation						
SFA and UFA biosynthesis by FASII	*acc / fab*	✓	(✓)	(✓)	✓	✓
Branched chain fatty acid biosynthesis	*BCKDC / Ilv, Leu*	✓	(✓)	(✓)	✓	✓
Exogenous fatty acid incorporation	*fadL / fak*	✓	✓	✓	✓	✓
Fatty acid incorporation into membrane	*/ pls*	✓	✓	✓	✓	✓
Regulation of fatty acid biosynthesis	*spoT, fabR, fadR*	✓	✓	✓	✓	✓
Conversion of existing fatty acids						
Cyclisation of fatty acids	*cfas*	--	✓	✓	✓	--
Cis/Trans isomerization of fatty acids	*cti*	--	--	--	--	--
Conjugation of fatty acids	*/ cla*	--	--	--	--	--
Desaturation of fatty acids	*/ des*	--	--	--	--	--
Fatty acid degradation						
Saturated medium and long chain fatty acid degradation (beta-oxidation)	*/ fad*	(✓)	--	--	✓	✓
Saturated short chain fatty acid degradation	*/ ato*	✓	✓	(✓)	✓	✓
Polyunsaturated fatty acid degradation	*fadH, fadB*	--	--	--	✓	✓
Glycerophospholipid metabolism						
Glycerol degradation	*/ glp*	✓	✓	✓	✓	✓
Biosynthesis of phosphatic acid (PA)	*plsB, plsC*	✓	✓	✓	✓	✓
Biosynthesis of phosphatidylserine (PS)	*cdsA, pssA*	✓	--	--	--	✓
Degradation of phosphatidylserine	*psp*	✓	--	--	--	✓
Biosynthesis of phosphatidylethanolamine (PE)	*psd*	✓	--	--	--	✓
Degradation of ethanolamine	*/ eut*	✓	--	--	--	✓
Biosynthesis of phosphatidylcholine (PC)	*plpp, cpt1*	--	✓	--	--	--
Biosynthesis of Phosphatidylglycerol (PG)	*cdsA, pgsA, pgpP*	--	✓	✓	✓	✓
Biosynthesis of phosphatidylinositol (PI)	*pis*	--	--	--	--	--
Degradation of phosphatidylinositol	*plc, impa1, tpiA / Iol*	✓	--	--	(--)	✓
Biosynthesis of Cardiolipin (CL)	*cls*	✓	✓	✓	✓	✓
Degradation of Cardiolipin	*ltaS, dgkB*	✓	✓	✓	✓	✓

B. thermosphacta TMW2.2101 possesses all genes to perform glycolysis, gluconeogenesis, oxidative pentose pathway and homolactic fermentation. It is predictively able to utilize nucleosides, ribose and pyruvate as well as specific amino acids such as ornithine, glutamate, aspartate, alanine, leucine, isoleucine and valine. It is predictively unable to utilize allantoin or perform a complete citric acid cycle, due to missing succinyl-CoA-synthase, phosphoenolpyruvate carboxylase and malate synthase genes. Furthermore, *B. thermosphacta* TMW2.2101 misses the phosphoketolase gene needed for heterolactic fermentation. All genes needed to build up a functional respiratory chain including several cytochromes such as cytochrome aa_3, ba_3 and bd were detected. Furthermore, *B. thermosphacta* TMW2.2101 is the only species predictively able to biosynthesize heme. It

is also predictively able to take up heme from the environment. Regarding oxidative stress, this species is equipped with a lot of antioxidant enzymes e.g. a catalase or superoxide dismutase. Beside respiration, a set of other enzymes consuming O_2 were found. Such enzymes comprise a pyruvate oxidase, glycerol-3-phosphate oxidase, NADH oxidase and an acetolactate synthase. The ability of *B. thermosphacta* TMW2.2101 to biosynthesize and take up fatty acids and incorporate them into the membrane was predicted from the genome. Nevertheless, specific genes for fatty acid conjugation, isomerization, desaturation or cyclisation could not be found in the genome. Although *B. thermosphacta* TMW2.2101 misses some single enzymes, this species is expected to be able to perform beta-oxidation and degrade saturated fatty acids. *B. thermosphacta* TMW2.2101 is predictively unable to degrade polyunsaturated fatty acids. Regarding glycerophospholipid metabolism, all genes needed for the biosynthesis of the following glycerophospholipid head groups could be found: Phosphatic acid (PA), phosphatidylserine (PS), phosphatidylethanolamine (PE), phosphatidylinositol (PI), Cardiolipin (CL). Furthermore, it is predictively able to degrade glycerol, ethanolamine, PI and CL.

The predicted basic energy metabolism of *C. divergens* TMW2.1577 comprises glycolysis, oxidative pentose phosphate pathway, homolactic fermentation as well as utilization of pyruvate, external nucleoside and ribose, allantoin and the amino acids arginine, ornithine, tyrosine, glutamate, alanine, leucine, isoleucine and valine. It is predictively unable to perform gluconeogenesis, heterolactic fermentation and a complete citric acid cycle. Despite some genes missing for menaquinone biosynthesis and heme uptake, *C. divergens* TMW2.1577 is predicted to establish a complete respiratory chain. Gens for heme biosynthesis are missing in the genome. Further O_2-related enzymes found in the genome of *C. divergens* comprise a catalase, superoxide dismutase, glutathione peroxidase as well as a glycerol-3-phosphate oxidase, NADH oxidase and an acetolactate synthase. All genes needed to biosynthesize and incorporate fatty acids could be found. Similar to *L. gelidum*, *C. divergens* TMW2.1577 is predictively able to cyclize fatty acids. It is further equipped with all genes needed to degrade saturated fatty acids by beta-oxidation as well as polyunsaturated fatty acids. Genomic analysis reveals the potential to synthesize PA, PG and CL. Furthermore, glycerol and CL can predictively be degraded by this species.

C. maltaromaticum TMW2.1581 can predictively perform glycolysis, gluconeogenesis, oxidative pentose phosphate pathway and homolactic fermentation. Additionally, it is predicted to be able to utilize pyruvate, allantoin, external nucleosides and ribose as well as the amino acids arginine, ornithine, lysine, tyrosine, glutamate, aspartate, malate, serine, alanine, leucine, isoleucine and valine. It is expected to be unable to perform a functional citric acid cycle and heterolactic fermentation. Genomic analyses reveal the ability to build up a functional

respiratory chain including a cytochrome bd ubiquinol oxidase. Nevertheless, genes for heme biosynthesis are missing while genes for heme uptake are present in the genome of *C. maltaromaticum* TMW2.1581. Further genes encoded by this species comprise a catalase, superoxide dismutase, 2-Cys peroxiredoxin and a glutathione peroxidase as well as the O_2-consuming enzymes glycerol-3-phosphate oxidase, NADH oxidase and acetolactate synthase. *C. maltaromaticum* TMW2.1581 is predictively able to synthesize and incorporate fatty acids whereas no genes for the cyclisation, isomerization, conjugation or desaturation of those fatty acids could be found in the genome. It is further predictively able to perform beta-oxidation and degrade polyunsaturated fatty acids. The genomic potential to synthesize PA, PS, PE, PG and CL was predicted from the genome. Furthermore, this species is predictively able to degrade glycerol, ethanolamine, PS, PI and CL.

L. gelidum subsp. *gelidum* TMW2.1618 and *L. gelidum* subsp. *gasicomitatum* TMW2.1619 are both predictively able to perform glycolysis, oxidative pentose pathway and hetero- and homolactic fermentation but no gluconeogenesis or citrate cycle. Furthermore, they can predictively utilize and convert pyruvate, external nucleotides and ribose as well as the amino acids ornithine, aspartate, malate, valine, leucine and isoleucine. No genes needed for the degradation of allantoin could be found for both subspecies. Except the fact that some genes for heme uptake are missing, the potential to establish a fully active respiratory chain, including a cytochrome bd ubiquinol oxidase, is predicted for *L. gelidum*. Regarding oxidative stress tolerance, major enzymes such as the superoxide dismutase or catalase are not present in both genomes. Nevertheless, *L. gelidum* is equipped with other antioxidant enzymes such as peroxiredoxin or peroxidases. Furthermore, a set of O_2-consuming enzymes could be found in the genome of both species comprising a glycerol-3-phosphate oxidase, NADH oxidase, acetolactate synthase and a pyridoxine 5´-phosphate oxidase. Genes encoding a pyruvate oxidase are missing for *L. gelidum* subsp. *gelidum* TMW2.1618. The predicted lipid metabolism for both species comprises the biosynthesis und uptake of fatty acids, cyclisation of fatty acids and degradation of glycerol and saturated short chain fatty acids. Essential genes needed for beta-oxidation are missing for both subspecies. According to the genome, *L. gelidum* is predictively able to biosynthesis the phospholipid head groups PA, CL and phosphatidylglycerol (PG). *L. gelidum* subsp. *gelidum* TMW2.1618 is the only species predictively able to biosynthesize phosphatidylcholine (PC). Furthermore, both subspecies are predictively able to degrade CL and glycerol.

4.2. Headspace changes due to microbial metabolism

4.2.1. Quantification of the oxygen uptake rate / CFU of bacteria

Oxygen consumption of each selected strain of the five species *B. thermosphacta* TMW2.2101, *C. divergens* TMW2.1577, *C. maltaromaticum* TMW2.1581, *L. gelidum* subsp.

gelidum TMW2.1618 and *L. gelidum* subsp. *gasicomitatum* TMW2.1619 was monitored in gas tight locked glass bottles filled with MS-media and a headspace of 30% CO_2 / 70% O_2 (chapter 3.2.1). The recorded dissolved oxygen, growth curves as well as the calculated oxygen uptake rate of *L. gelidum* subsp. *gelidum* TMW2.1618 for replicate one over a time period of 20 hours can be seen in Figure 17a. The correlations shown in Figure 17a are representative for all species and replicates. A detailed summary of DO, OUR and CFU changes over time for all specie and replicates is given in Supplementary Figure 5. Figure 17b shows the calculated average and maximum OURs/CFU for each species, which is based on data from Figure 17a / Supplementary Figure 5.

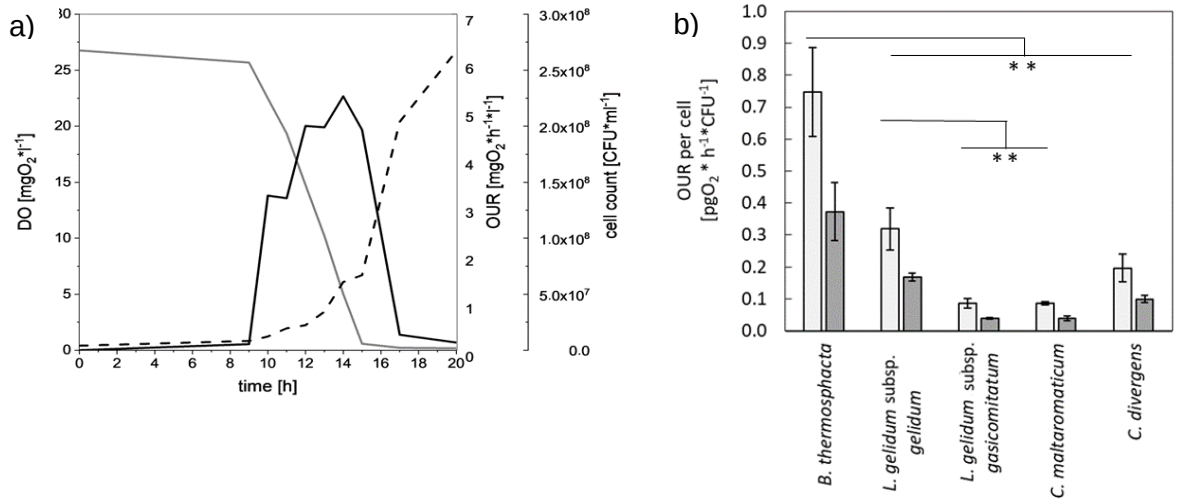

Figure 17. Oxygen consumption in liquid MS-media for each of the analyzed bacteria. a) Development of dissolved oxygen (gray solid line), oxygen uptake rate (black, solid line) and cell count (black dotted line) over 20 hours in liquid media inoculated with *L. gelidum* subsp. *gelidum* TMW2.1618. Displayed is replicate one of this species, which is representative for all other species. b) Calculated maximum (□) and average (■) oxygen uptake rate for a single cell of each species. Bars represent standard errors based on three independent replicates. ** significant differences between means with $p < 0.05$.

A clear correlation between DO, CFU and OUR could be observed for *L. gelidum* subsp. *gelidum* TMW2.1618. The amount of DO in the media decreased as soon as bacteria started growing. Concomitantly, the OUR of bacteria increased and reached a maximum after 14 hours. As soon as media run out of O_2, the OUR began to decrease. Even after O_2 depletion, a rise in cell count could be observed.

Comparing the calculated maximum and average OUR / CFU for all species, *B. thermosphacta* TMW2.2101 exhibited significant higher values. In detail, the maximum OUR / CFU was two-times higher compared to *L. gelidum* subsp. *gelidum* TMW2.1618, four-time higher compared to *C. divergens* TMW2.1577 and eight-times higher compared to *L. gelidum* subsp. *gasicomitatum* TMW2.1619 and *C. maltaromaticum* TMW2.1581. All differences were classified as significant ($p < 0.05$). Within the LABs, *L. gelidum* subsp. *gelidum* TMW2.1618

exhibited a significant higher maximum OUR / CFU compared to *L. gelidum* subsp. *gasicomitatum* TMW2.1619 and *C. maltaromaticum* TMW2.1581.

Furthermore, the atmospheric development of O_2 and CO_2 in the headspace of the glass bottles was monitored over 60 hours Figure 18a. Quantitative analysis of the O_2 consumption in 60 hours for all cells or one single cell of each species can be seen in Figure 18b.

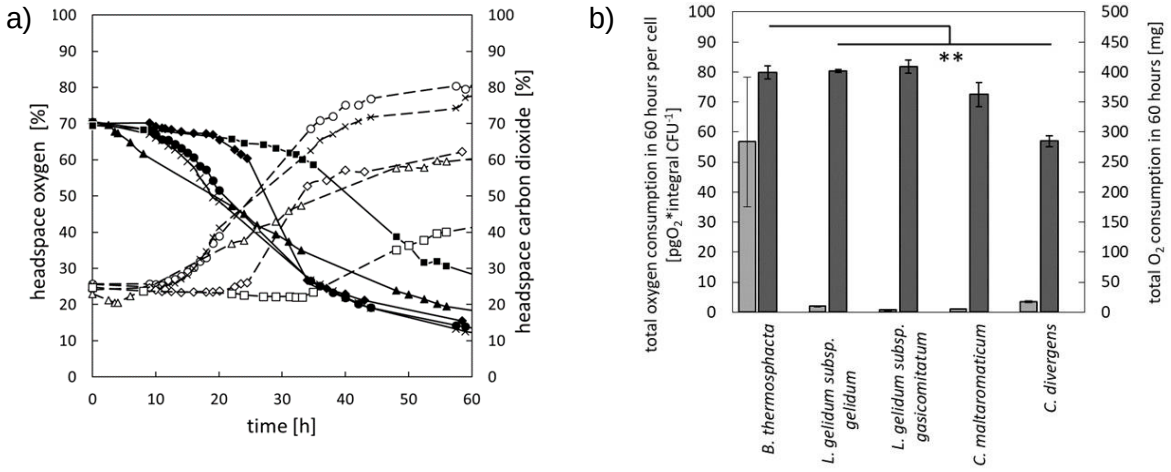

Figure 18. Oxygen uptake rate of the analyzed bacteria in the headspace of the meat model system. The atmospheric headspace development in a model system was monitored and quantified. a) Changes of the headspace gas composition of the species *B. thermosphacta* TMW2.2101 (◆), *C. divergens* TMW2.1577 (■), *C. maltaromaticum* TMW2.1581 (▲), *L. gelidum* subsp. *gelidum* TMW2.1618 (●) and *L. gelidum* subsp. *gasicomitatum* TMW2.1619 (x). Solid line, black symbols: O_2 concentration, dotted line, white symbol: CO_2 concentrations. b) Calculated total O_2 consumption in 60 hours for all cells (■) (secondary y-axis) or a single cell (■) (primary y-axis). ** significant differences between means with $p < 0.05$.

A decrease of the O_2 content in the headspace could be observed for all species. Starting from initial 70% O_2, the values decreased to almost 30% over 60 hours. *C. divergens* TMW2.1577 was the only species exhibiting higher concentrations of residual O_2 after 60 hours of fermentation. Reciprocally to changes of the O_2 concentration, CO_2 levels increased from initial 25% to values >60% for all species, except for *C. divergens* TMW2.1577. This is rather unexpected, as the media of *C. divergens* TMW2.1577 exhibited the highest diffusion coefficient (12.5 g/l K_La =0.0653; 50 g/l K_La=0.0172; 100 g/l K_La=0.0054) (Supplementary Figure S6).

Upon quantification of the O_2 consumption in the headspace similar total amounts of O_2 were consumed by all bacteria during 60 hours of fermentation. Nevertheless, *B. thermosphacta* TMW2.2101 consumed 31-times more headspace O_2 per single cell in 60 hours compare to the other species (p-values <0.019).

Growth curves during whole fermentation (60 hours) of this experiment can be seen in Supplementary Figure 7. Growth of *B. thermosphacta* TMW2.2101 differed from the others, as its CFU strongly decreased as soon as the dissolved oxygen of the media was consumed (after

25 hours). Furthermore, a long lag-phase with initially decreasing CFU could be observed for *C. divergens* TMW2.1577 until bacteria started growing and consuming O_2.

4.2.2. Growth with hemin chloride and menaquinone-4

The selected strains *B. thermosphacta* TMW2.2101, *C. divergens* TMW2.1577, *C. maltaromaticum* TMW2.1581, *L. gelidum* subsp. *gelidum* TMW2.1618 and *L. gelidum* subsp. *gasicomitatum* TMW2.1619 were tested for enhanced growth with and without addition of hemin chloride and menaquinone-4. Results are shown in Table 20.

Table 20. Growth of selected strains with (+) and without (-) addition of hemin chloride and menaquinone-4.

	Hemin chloride		Menaquinone-4	
	+	-	+	-
B. thermosphacta TMW2.2101	1.364	0.990	0.992	1.014
L. gelidum subsp. *gelidum* TMW2.1618	1.250	1.031	1.088	1.024
L. gelidum subsp. *gasicomitatum* TMW2.1619	1.412	0.872	0.950	0.936
C. maltaromaticum TMW2.1581	1.845	1.317	1.399	1.376
C. divergens TMW2.1577	0.855	0.610	0.634	0.615

All tested species exhibited significant enhanced growth when hemin chloride was added to the medium (p-values range from 0.01-2.4x10^{-6}). Addition of menaquinone-4 did not enhance the growth of any species.

4.2.3. Minimal inhibitory concentration of hydrogen peroxide

Growth of the selected strains was tested by addition of different concentrations (0.008, 0.001, 0.02, 0.03, 0.04, 0.05, 0.06, 0.07, 0.08, 0.09, 0.1, 0.2, 0.3, 0.4 and 0.5%) of hydrogen peroxide to the MS-media. The lowest concentration, exhibiting no inhibitory effect on growth was chosen for each species and defined as minimal inhibitory concentration. Results of the identified MIC values are shown in Table 21.

Table 21. Minimal inhibitory concentrations (MIC) of hydrogen peroxide for each species.

	MIC [%]
B. thermosphacta TMW2.2101	0.090
L. gelidum subsp. *gelidum* TMW2.1618	0.016
L. gelidum subsp. *gasicomitatum* TMW2.1619	0.020
C. maltaromaticum TMW2.1581	0.024
C. divergens TMW2.1577	0.012

The highest MIC could be detected for *B. thermosphacta* TMW2.2101 tolerating 0.09% of hydrogen peroxide. The MIC of this species was 4-7 times higher compared to the LAB. Within the LAB, determined MIC values were similar, with *C. maltaromaticum* TMW2.1581 exhibiting highest and *C. divergens* TMW2.1577 lowest resistance to hydrogen peroxide.

4.2.4. Influence of CO_2 on bacterial oxygen consumption

The effect of CO_2 on bacterial oxygen consumption was studied in fluorescence coated 96-well OxoPlates (chapter 3.1.10 and 3.1.11). Therefore, media was gassed either with 30% N_2 / 70% O_2 or 30% CO_2 / 70% O_2 until oxygen saturation occurred, and was subsequent pipetted and inoculated in 96-well plates. The determined oxygen content of the media during incubation of the plate can be seen in Figure 19.

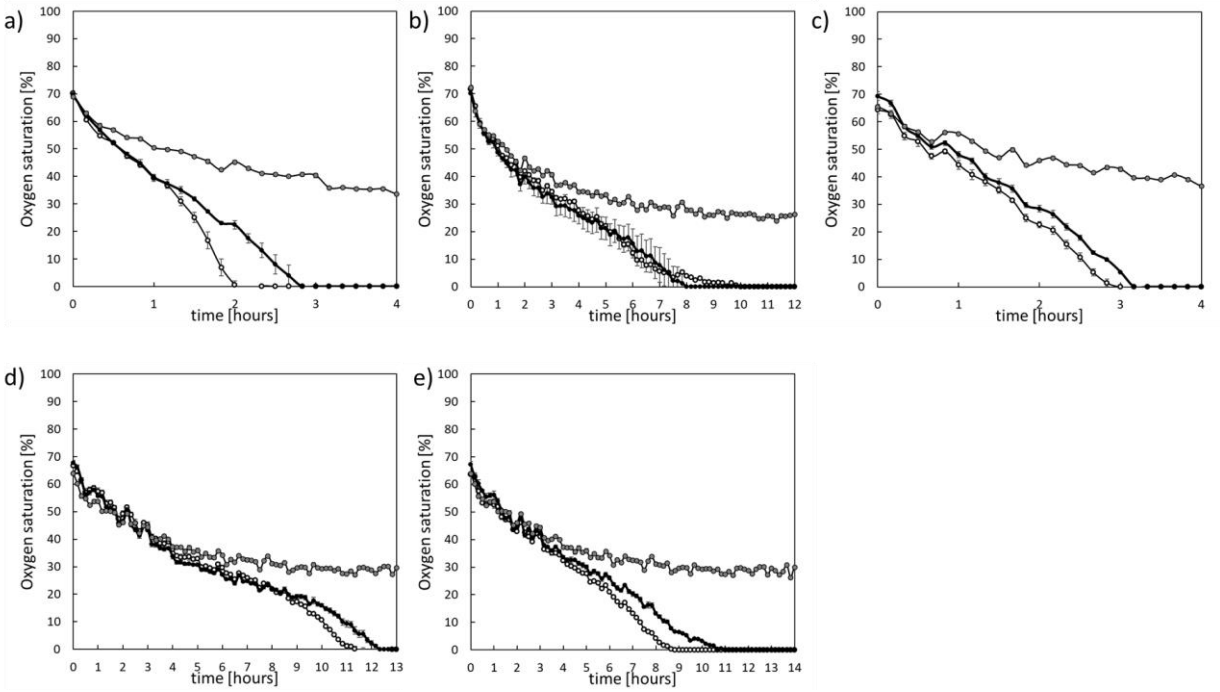

Figure 19. Influence of CO_2 on bacterial oxygen consumption in liquid media. The change in the oxygen content of inoculated media during cultivation time is displayed for each of the five species a) *B. thermosphacta* TMW2.2101 b) *C. divergens* TMW2.1577 c) *C. maltaromaticum* TMW2.1581 d) *L. gelidum* subsp. *gelidum* TMW2.1618 and e) *L. gelidum* subsp. *gasicomitatum* TMW2.1619. Bacteria were inoculated with $OD_{600\ nm}$= 0.3 in media, which was previously gassed with (○) 30% N_2 / 70% O_2 or (●) 30% CO_2 / 70% O_2. Spontaneous oxygen diffusion into the surrounding atmosphere is displayed with grey dots (●).

Oxygen diffusion from the 70% O_2-saturated media to the surrounding atmosphere (21% O_2) could be detected in each sample. Diffusion of oxygen stopped after approximately five hours reaching an equilibrium of ~30% O_2. However, active oxygen consumption could be monitored in each well inoculated with one of the five species. *B. thermosphacta* TMW2.2101 and *C. maltaromaticum* TMW2.1581 exhibited fastest oxygen consumption comparing all species (within 2-3 hours). Oxygen consumption in media gassed with 30% CO_2 was less rapid for *B. thermosphacta* TMW2.2101 and both *L. gelidum* subspecies compared to media gassed with 30% N_2. Both *Carnobacterium* species did not exhibit a reduced oxygen consumption due to exposure to 30% CO_2.

In order to compare the oxygen consumption rate of each bacterium in the presence and absence of oxygen, bacterial growth was monitored simultaneously to the reduction of O_2 in

the media (Supplementary Figure 8). Growth of both *Carnobacterium* and both *L. gelidum* subspecies was quite low, with only minor increase of the cell density within the time period of oxygen consumption. *B. thermosphacta* was the only species exhibiting a strong increase in cell density during oxygen consumption. Furthermore, each species exhibited similar growth curves for both applied atmospheres, thus enabling to neglect the correlation of O_2 consumption to cell density.

4.2.5. Headspace oxygen consumption and spoilage of bacteria on MAP meat

Sensory perceptible meat spoilage, growth and oxygen consumption was monitored of high oxygen MAP beef inoculated with *B. thermosphacta* TMW2.2101 and both *L. gelidum* subspecies as well as on high oxygen MAP chicken breast inoculated with *C. divergens* TMW2.1577 and *C. maltaromaticum* TMW2.1581 (chapter 3.3.2). Sensory analyses of inoculated meat pieces were done at defined time points validating olfactory and visual appearance (Supplementary Figure 9). The time point of perceptible meat spoilage was determined based on a rejection of meat due to either olfactory or visual appearance from more than 50% of the sensory panel. Results are shown in Figure 20.

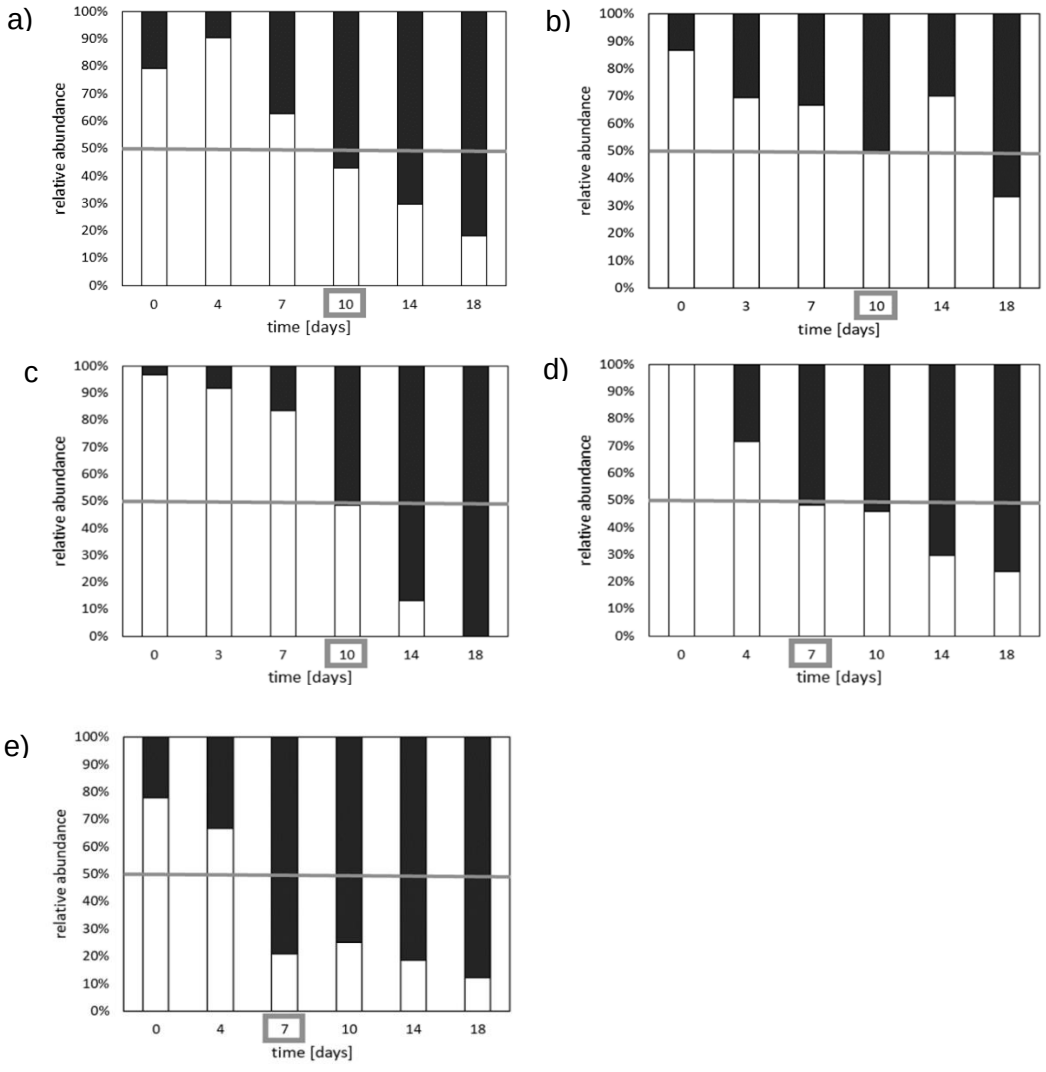

Figure 20. Summary of the visual and olfactory validation of inoculated meat pieces. Sensorial validation of meat pieces inoculated with a) *B. thermosphacta* TMW2.2101, b) *L. gelidum* subsp. *gasicomitatum* TMW2.1619, c) *L. gelidum* subsp. *gelidum* TMW2.1618, d) *C. divergens* TMW2.1577 and (e) *C. maltaromaticum* TMW2.1581 and stored over 18 days at 4 °C. Bares represent the percentage of persons, which validated either olfactory or visual appearance of the meat as “spoiled” (■) or “fresh” / “not-fresh-but edible” (□). Grey lines indicate the time point of meat spoilage, based on sensorial rejection of more than 50% of the panel.

Beef inoculated with either *B. thermosphacta* TMW2.2101 or one of the two *L. gelidum* subspecies was considered as spoiled after 10 days, whereas chicken inoculated with one of the two *Carnobacterium* species was considered as spoiled after 7 days of storage at 4 °C. Additionally to the sensory analysis, the color development of each meat piece was monitored during storage period. Results are shown in Supplementary Figure 10. Recorded growth curves, headspace O_2 consumption and determined time points of meat spoilage for each of the five meat-spoiling bacteria are displayed in Figure 21.

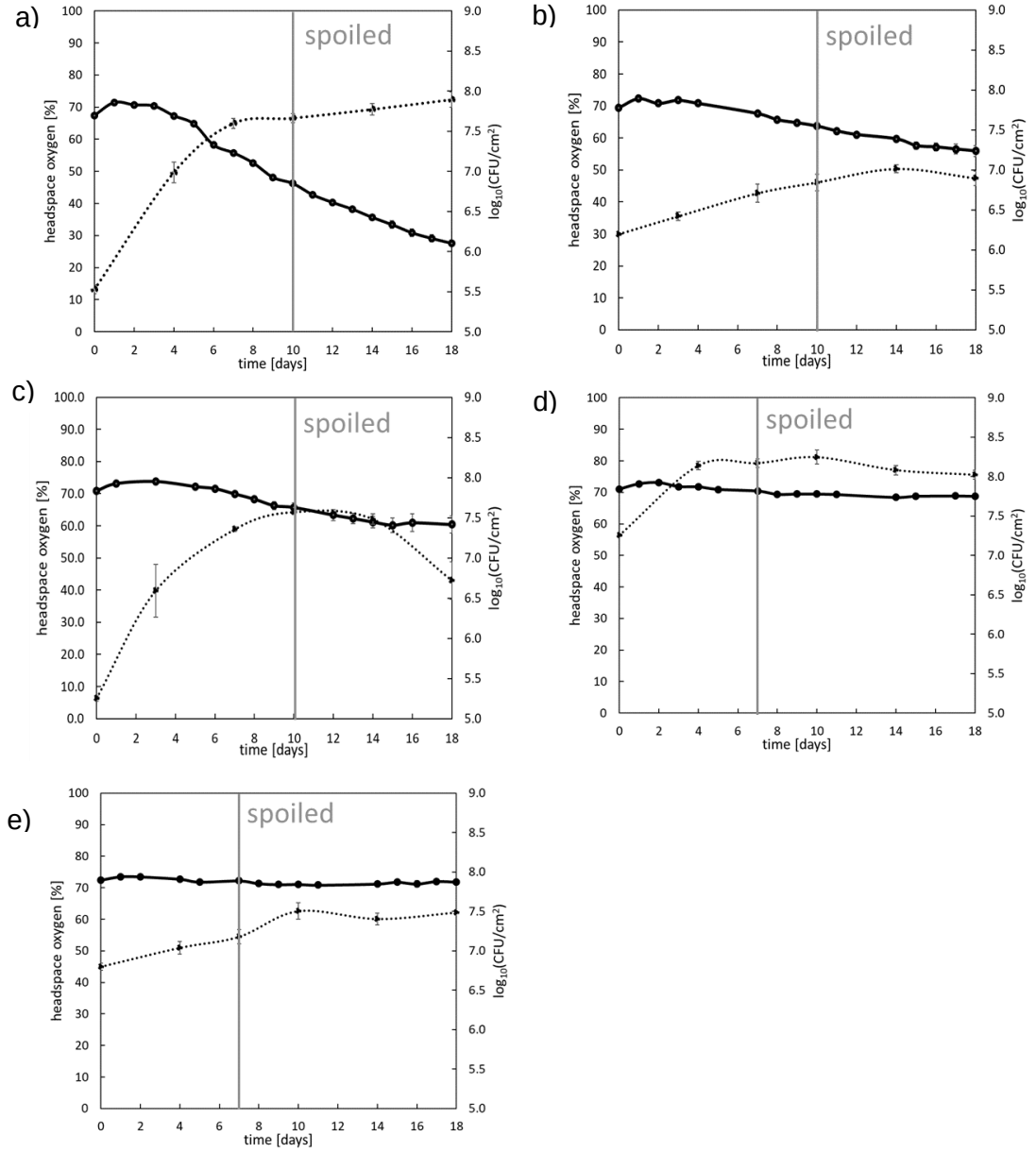

Figure 21. Headspace O_2 consumption and growth of meat-spoiling bacteria on beef and chicken. Growth (dotted lines) and headspace O_2 consumption (solid lines) of high oxygen MAP meat inoculated with a) *B. thermosphacta* TMW2.2101 b) *L. gelidum* subsp. *gasicomitatum* TMW2.1619 c) *L. gelidum* subsp. *gelidum* TMW2.1618 d) *C. divergens* TMW2.1577 and e) *C. maltaromaticum* TMW2.1581 was monitored over 18 days. Grey lines indicate the time point of spoilage, which is based on a 50% rejection of the inoculated meat by the sensory panel. All values are based on three independent replicates with error bars representing standard errors.

A first decrement in headspace O_2 could be observed for MA packages containing meat inoculated with *B. thermosphacta* TMW2.2101 after exceeding a $log_{10}(CFU/cm^2)$ of 7.0. The headspace O_2 decreased linearly from 70% to 28% within 18 days. Beef inoculated with *B. thermosphacta* TMW2.2101 was considered as spoiled after 10 days when O_2 was 46% and the $log_{10}(CFU/cm^2)$ was 7.7. MA packages containing meat inoculated with *L. gelidum* subsp. *gasicomitatum* TMW2.1619 exhibited a first decrease in headspace O_2 after a $log_{10}(CFU/cm^2)$ of 6.4 was exceeded. The O_2 content in the headspace decreased linearly reaching a value of 56% after 18 days. Beef was considered as spoiled after 10 days, when the O_2 content was 64% and the $log_{10}(CFU/cm^2)$ was 6.8. A first decrease in headspace O_2 was observed for MA packages containing meat inoculated with *L. gelidum* subsp. *gelidum* TMW2.1618 after exceeding a $log_{10}(CFU/cm^2)$ of 7.4. The O_2 content in the headspace decreased linearly to a value of 60% within 18 days. Beef inoculated with *L. gelidum* subsp. *gelidum* TMW2.1618 was considered as spoiled after 10 days, when the O_2 content was 66% and the $log_{10}(CFU/cm^2)$ was 7.6. The headspace O_2 content remained constant over 18 days for MA packages inoculated with *C. divergens* TMW2.1577. Chicken meat inoculated with *C. divergens* TMW2.1577 was considered as spoiled after 7 days, when $log_{10}(CFU/cm^2)$ was 8.2 and the headspace O_2 was 70%. Similar to MA packages with *C. divergens* TMW2.1577, the O_2 content in the headspace of MAP meat inoculated with *C. maltaromaticum* TMW2.1581 did not exhibit a significant change within 18 days. Chicken meat inoculated with *C. maltaromaticum* TMW2.1581 was considered as spoiled after 7 days, when $log_{10}(CFU/cm^2)$ was 7.2 and the headspace O_2 was 72%. A summary of the determined CFU values at the time point of first O_2 decrement and perceptible meat spoilage, as well as the headspace O_2 content at the time point of perceptible meat spoilage is given in Table 22.

Table 22. Correlation of the microbial O_2 consumption and meat spoilage. The CFU at the time point of first O_2 decrease and perceptible meat spoilage is given for all species inoculated on the corresponding meat type. Furthermore, the headspace O_2 content at the time point of perceptible meat spoilage was determined.

		$log_{10}(CFU/cm^2)$		**O_2 content**
	TMW	O_2 decrease	Meat spoilage	Meat spoilage
B. thermosphacta	2.2101	7.0 ±0.13	7.7 ± 0.06	46%
L. gelidum subsp. *gasicomitatum*	2.1619	6.4 ±0.05	6.8 ± 0.10	63.7%
L. gelidum subsp. *gelidum*	2.1618	7.4 ±0.03	7.6 ± 0.03	65.7%
C. divergens	2.1577	-	8.2 ± 0.05	70.4%
C. maltaromaticum	2.1581	-	7.2 ± 0.09	72.2%

After 18 days of cultivation, the predominance of the inoculated strains was checked on meat. RAPD-PCR analysis proved the appearance of the inoculated strain, as well as the absence of any other strain or species of the natural microbiota on meat at the end of fermentation (data not shown).

4.3. Role and lifestyle of *Pseudomonas* strains on anoxic MAP meat

4.3.1. Strain verification

Two strains of the species *P. lundensis* (TMW2.1732 / TMW2.2076), *P. weihenstephanensis* (TMW2.1728 / TMW2.2077) and *P. fragi* (TMW2.2081 / TMW2.2082) were selected from the TMW strain collection based on a previous study done by Hilgarth *et al.* (2019). In this study, corresponding strains were isolated *in situ* from minced beef stored under high oxygen modified atmosphere at a time point where O_2 was limited within the package, and the anaerobic growth of corresponding strains was proven *in vitro* on agar plates (Hilgarth *et al.*, 2019).

To ensure selection of different strains of the three *Pseudomonas* species, all isolates were differentiated on strain level applying a RAPD-PCR. Obtained strain specific band patterns were used for genomic similarity clustering as described in chapter 3.4.4. The resulting dendrogram is shown in Figure 22.

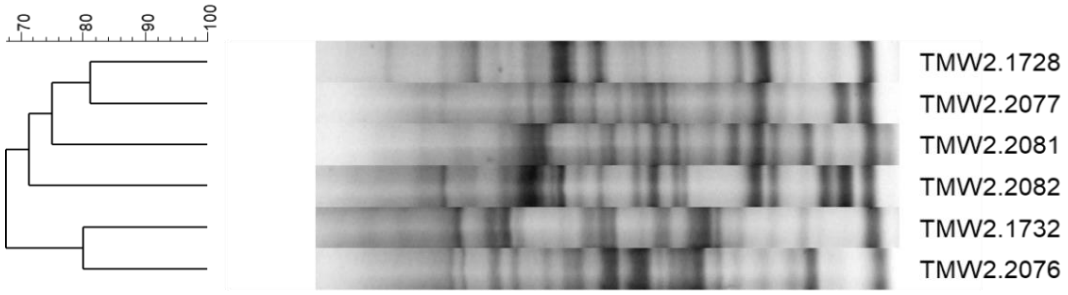

Figure 22. Identification of *Pseudomonas* organisms on strain level by RAPD-PCR fingerprinting. A RAPD-PCR cluster analysis of the selected *Pseudomonas* strains based on UPGMA and a 1% Dice similarity coefficient was performed, to differentiate all organisms on strain level.

A differentiation of all organisms was possible on strain level using RAPD-PCR fingerprinting. All *Pseudomonas* isolates exhibit different band patterns dedicating different strains. Furthermore, strains, which clustered closely together in the dendrogram also belong to the same species.

4.3.2. Anaerobic growth on chicken breast filet and in MS-media

Growth of all *Pseudomonas* strains on inoculated chicken breast samples was monitored under strict anoxic conditions in MA packages containing 100% N_2 and an oxygen scavenger. Results can be seen in Table 23.

Table 23. Anaerobic growth of *Pseudomonas* strains on chicken breast filet. Growth of the six *Pseudomonas* strains on anoxic packaged chicken breast filet over 7 days at 4 °C was monitored. *significant (0.05 > p > 0.01) or **highly significant (p =<0.01) CFU/cm^2 compared to the CFU/cm^2 on day 0 were marked by grey color. SE= standard error based one three independent replicates

		log$_{10}$(CFU/cm^2)							
		day 0		day 3		day 5		day 7	
	TMW	mean	SE	mean	SE	mean	SE	mean	SE
P. lundensis	2.1732	6.3	0.11	6.8*	0.40	7.1	0.27	7.4**	0.05
P. lundensis	2.2076	7.2	0.04	7.3	0.40	7.4*	0.01	7.6**	0.03
P. weihenstephanensis	2.2077	6.8	0.13	7.0	0.04	7.1	0.18	7.1*	0.06
P. weihenstephanensis	2.1728	6.8	0.04	7.0*	0.03	7.2**	0.02	7.2	0.16
P. fragi	2.2081	7.0	0.13	7.1	0.03	7.4*	0.01	6.8	0.15
P. fragi	2.2082	7.1	0.07	7.2	0.02	7.4*	0.03	6.9	0.07

After three days, the strains *P. lundensis* TMW2.1732 and *P. weihenstephanensis* TMW2.1728 exhibited significant growth on chicken meat stored at 4 °C. *P. lundensis* TMW2.2076 and both *P. fragi* strains exhibited significant growth after 5 days and *P. weihenstephanensis* TMW2.2077 after 7 days. 2-3 cell divisions within 7 days could be calculated for all *Pseudomonas* strains except for *P. lundensis* TMW2.1732, which exhibited a cell division rate of 5-6 within 7 days.

After 7 days of cultivation, the predominance of the inoculated strains was checked on chicken breast. RAPD-PCR analysis proved the appearance of the inoculated strain, as well as the absence of any other strain or species on chicken at the end of fermentation (data not shown).

Growth under strictly anoxic conditions was further checked for all strains in MS-medium by monitoring the $OD_{600\ nm}$ (Supplementary Figure 11). Similar to growth on meat, the anoxically growth in MS-medium was limited for all strains, reaching a maximal $OD_{600\ nm}$ of 0.25. The pH development during fermentation in MS-media can be seen in Supplementary Figure 12. An increase of the pH-values of the MS-media of approximately 0.65 was detected for all strains over time.

4.3.3. Proteomic analysis of the anaerobic metabolism of *Pseudomonas* strains

About 53-57% of all encoded proteins were detected for each strain by mass spectrometry. Approximately twice as much significantly differential regulated proteins were detected for both *P. weihenstephanensis* strains as well as *P. fragi* TMW2.2082 compared to the other strains. *P. fragi* TMW2.2081 exhibited the lowest amounts of significantly regulated proteins (Supplementary Table 9). A detailed list of single significantly differential regulated proteins of all species is given in Supplementary Table 10. Single regulated proteins were grouped into functional pathways, which were subsequent grouped into functional categories listed in Table 24. Sorting was performed by different annotation programs e.g. KEGG, RAST, NCBI, SEED and on own research.

Table 24. Main differentially regulated metabolic pathways of the analyzed *Pseudomonas* strains. "⇧": The metabolic pathway was upregulated under anoxic conditions, "⇩": The metabolic pathway was downregulated under anoxic conditions.

	P. lundensis TMW2.1732	*P. lundensis* TMW2.2076	*P. weihenstephanensis* TMW2.2077	*P. weihenstephanensis* TMW2.1728	*P. fragi* TMW2.2081	*P. fragi* TMW2.2082
Enzyme / pathway						
Aerobic and anaerobic respiration						
Enzymes of the respiratory chain						
Cytochrome c	⇩	⇩	⇩	⇩	⇩	⇩
Riboflavin synthesis		⇩				
Cytochrome b of bc complex			⇧			
Copper proteins / cupredoxin	⇧	⇧	⇧	⇧		
Enzymes for usage of different electron donors						
Sulphite:quinone oxidoreductase					⇧	⇧
Sulphite oxidoreductase	⇧		⇧	⇧		⇧
Sorbosone dehydrogenase			⇧	⇧		⇧
Pyrroloquinoline quinone-dependent dehydrogenase			⇧	⇧		⇧
Ubiquinone-dependent pyruvate dehydrogenase			⇧	⇧		
NADP-dependent oxidoreductase (quinone)			⇧	⇧		
Cyanide-forming glycine dehydrogenase			⇩			⇩
Malate dehydrogenase (quinone)				⇩		⇩
Glucose membrane-bound PQQ-dependent dehydrogenase			⇩	⇩		
Enzymes for usage of different electron acceptors						
Nitrite / Sulphite reductase						⇩
Pseudoazurin						⇩
Sulphate / Nitrate transporter / nitrogen regulator			⇧	⇧		
Ferrous metabolism						
$Fe3^+$ uptake			⇧ ⇩	⇧ ⇩		
Fe-S cluster			⇩	⇩		
Iron-chelate complexes	⇩	⇩		⇩	⇩	⇩
Carbohydrate and Pyruvate metabolism						
Glucose metabolism						
Glucose oxidation	⇩	⇩	⇩	⇩	⇩	⇩
Maltose –> D-Glucose + Amylose			⇧	⇧	⇧	⇧
Sucrose –> D-Glucose + D-Fructose			⇧	⇧		⇧
Amylose / Starch / Glycogen –> Glucose-1-phosphate			⇧	⇧		⇧
Polyhydroxyalkanoate metabolism			⇧	⇧		⇧
Cellobiose –> 2x D-Glucose		⇩				⇩
Trehalose6Phosphate -> 2x D-Glucose					⇩	⇩
Pyruvate fermentation						
Pyruvate -> Acetyl-CoA -> Acetaldehyde -> Acetate			⇧	⇧	⇧	⇧
Pyruvate <-> Lactate		⇩	⇩	⇩	⇩	
Pyruvate -> Acetyl-CoA -> Acetaldehyde		⇩				
TCA cycle						
Ful TCA cycle					⇩	⇩
Shortened TCA cycle (Isocitrate lyase)		⇧	⇧	⇧	⇧	⇧
Amino acid metabolism						
Amino acid transporter	⇧		⇩	⇧	⇧	
Asparagine -> Aspartate –> Fumarate / Oxaloacetate	⇩	⇩	⇩	⇩	⇩	⇩
Glutamine –> Glutamate –> Gabba / 2-oxoglutarate			⇧	⇧		⇧
Alanine –> Pyruvate		⇧		⇧		
B-Alanine –> Uracil						⇧
Arginine deiminase pathway			⇧	⇧		⇧
Glycine cleavage system	⇧	⇧	⇧	⇧		⇧
Val / Leu / Ile degradation via BCKDHC complex			⇧	⇧		⇧

Serine –> Cysteine			⇧	⇧		
Cell division						
Proteins / DNA / RNA						
Protein biosynthesis	⇩		⇩	⇩	⇩	⇩
Cell division			⇩	⇩	⇩	⇩
Flagellar assembly			⇩		⇩	⇩
Chemotaxis				⇩	⇩	
Purine and Pyrimidine metabolism			⇩			
DNA replication and methylation	⇩	⇩	⇩	⇩	⇩	⇩
RNA translation	⇩		⇩	⇩		⇩
RNA degradation	⇧	⇧	⇧		⇧	⇧
Cell wall						
Lipopolysaccharide Biosynthesis		⇩	⇩	⇩		⇩
Peptidoglycan synthesis	⇩	⇩	⇩	⇩	⇩	⇩
ADP-glyceromanno-heptose 6-epimerase	⇧	⇧	⇧	⇧	⇧	⇧
Murein degradation		⇧	⇧	⇧		
Cell membrane						
FASII complex	⇧		⇧	⇧		⇧
Beta oxidation			⇧	⇧		⇧
Biosynthesis of unsaturated fatty acids			⇩	⇩		
Stress resistance						
General stress proteins						
Chaperones	⇧		⇧ ⇩	⇧ ⇩	⇧	⇧ ⇩
DNA repair		⇩	⇩			⇩
Antibiotics			⇧	⇧		⇧
Toxin-Antitoxin system			⇧	⇧ ⇩	⇧	⇧
Virulence factors	⇩	⇧	⇩	⇩		⇧
Sensor histidine kinase			⇧	⇧ ⇩	⇩	
Protein folding / Cystein bond formation						
Others		⇧	⇧	⇧		⇧
Peroxiredoxin	⇧		⇧	⇧		⇧
Thioredoxin				⇧		⇧
Oxidative stress						
Catalase		⇩	⇧	⇧	⇧	
Starvation inducible proteins		⇧	⇧	⇧		⇧
Other pathways / enzymes						
Benzoate degradation	⇧		⇧	⇧		⇧
Biotin synthesis			⇩	⇧	⇩	⇩
Urease		⇩	⇧			⇧
Oxidoreductases		⇧	⇧	⇧	⇧	⇧

Several of the listed pathways in Table 24 exhibited the same differential proteomic expression patterns for strains of all three *Pseudomonas* species, indicating genus specific metabolic reactions upon exposure to anoxic conditions. For a better overview, the effects of anoxic cultivation on the most important energy providing metabolic pathways for the analyzed *Pseudomonas* stains were illustrated. The genomically predicted respiratory chain of the meat-spoiling *Pseudomonas* strains is illustrated in Figure 23. Genus specific metabolic regulations in response to anoxic cultivation were highlighted by a green color (enhanced expression of enzymes) or red color (reduced expression of enzymes), according to the proteomic data.

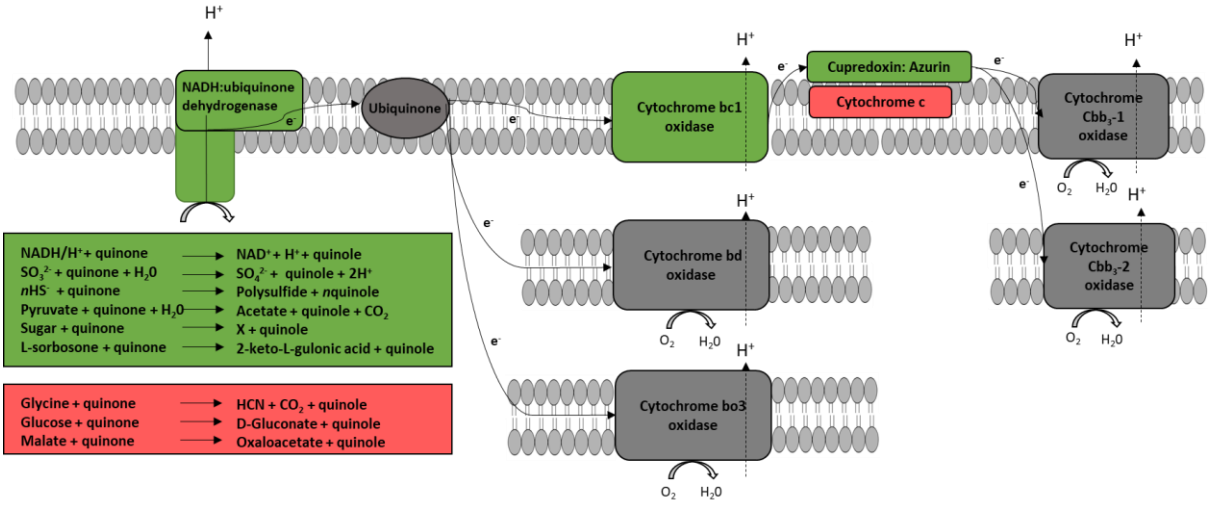

Figure 23. Predicted respiratory chain of *Pseudomonas* strains based on their genomic settings. The respiratory chain of the *Pseudomonas* strains was predicted based on their genomes and differentially expressed enzymes identified by the proteomic study were highlighted. Enzymes marked in green exhibit enhanced expression under anoxic conditions, while enzymes marked in red exhibit reduced expression under anoxic conditions for at least one strain.

All components of a functional aerobic respiratory chain could be found in the genome of the *Pseudomonas* strains comprising several dehydrogenase enzymes, ubiquinone, cytochrome bd oxidase, cytochrome bo_3 oxidase, cytochrome bc_1 oxidase, cytochrome c, cytochrome Cbb_3-1 oxidase and the cytochrome Cbb_3-2 oxidase. No enzymes for denitrification (NarGHIJ, NirS, NorCB, NosZ) or dissimilatory nitrate reduction (NarG, NIR) could be found in the genome of the strains, except for *P. fragi* TMW2.2082, which encodes (but not expresses) an assimilatory nitrate reductase, a small subunit of the nitrite reductase (NirD) as well as the enzyme NirE. Enzymes with an enhanced expression under anoxic conditions for at least one strain comprise several alternative electron donors, the cytochrome bc_1 oxidase and cupredoxin, while cytochrome c and some other enzymes for alternative electron donors exhibited a reduced expression under anoxic conditions.

Figure 24 illustrates the genomically predicted glucose and pyruvate metabolism of the analyzed *Pseudomonas* strains.

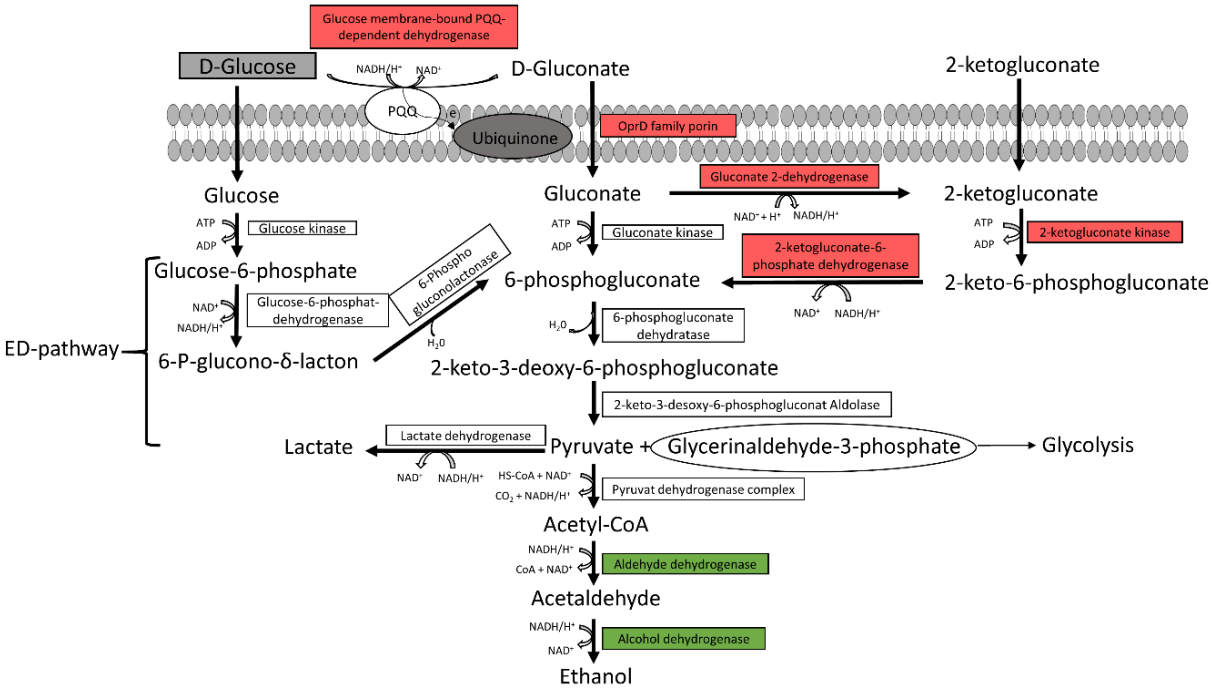

Figure 24. Predicted glucose and pyruvate metabolism of *Pseudomonas* strains based on their genomic settings. The glucose and pyruvate metabolism were predicted from the genome of the analyzed *Pseudomonas* strains and differentially expressed enzymes identified by the proteomic study were highlighted. ED= Entner-Doudoroff pathway. Enzymes marked in green exhibit enhanced expression under anoxic conditions, while enzymes marked in red exhibit reduced expression under anoxic conditions for at least one strain.

A reduced expression of several proteins involved in gluconate and 2-ketogluconate uptake and degradation was measured under anoxic conditions. However, a constitutive expression of enzymes involved in glucose uptake and degradation to pyruvate under oxic and anoxic conditions could be observed. Additionally, the aldehyde dehydrogenase and alcohol dehydrogenase enzymes exhibited an enhanced expression under anoxic conditions.

Figure 25 illustrates the genomically predicted tricarboxylic acid (TCA) cycle of the analyzed *Pseudomonas* strains.

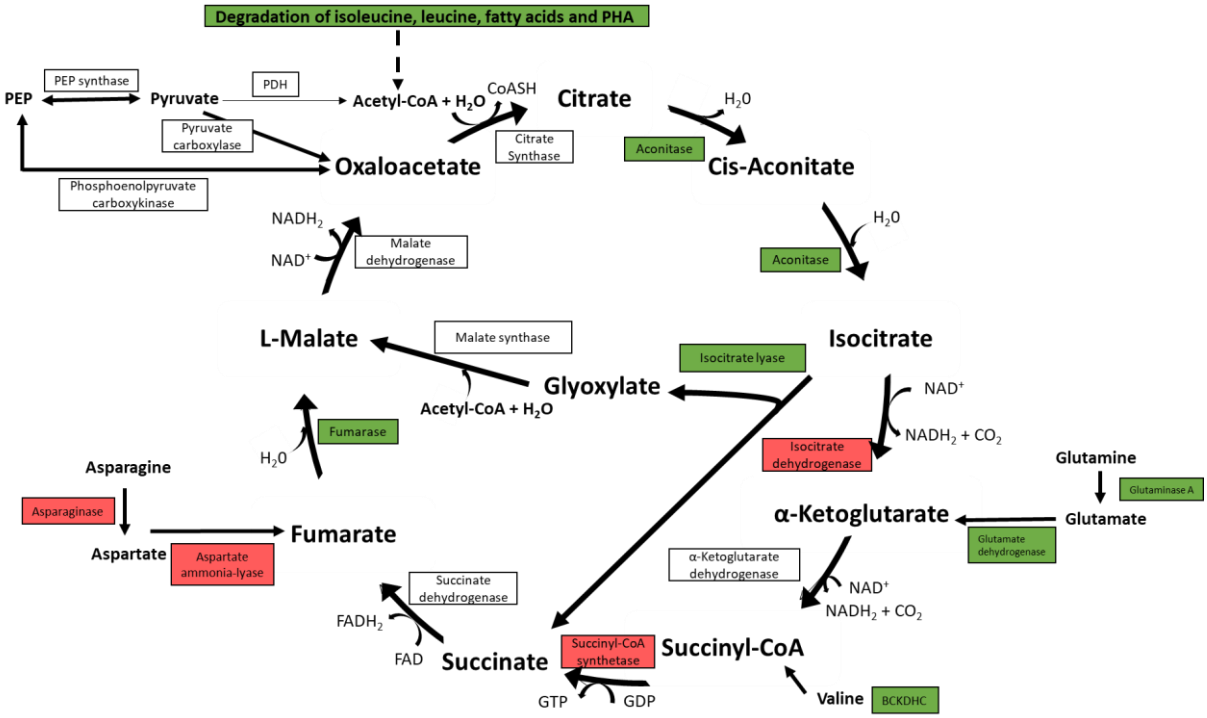

Figure 25. Predicted TCA cycle of *Pseudomonas* strains based on their genomic settings. The TCA cycle and reactions of anaplerotic metabolism were predicted from the genome of the *Pseudomonas* strains and differentially expressed enzymes identified by the proteomic study were marked. PHA= poly-3-hydroxyalkanoate, PEP= phosphoenolpyruvate, PDH= pyruvate dehydrogenase. Enzymes marked in green exhibit enhanced expression under anoxic conditions, while enzymes marked in red exhibit reduced expression under anoxic conditions for at least one strain.

An enhanced expression of several enzymes of the TCA cycle as well as anaplerotic reactions could be detected under anoxic conditions for almost all strains comprising an aconitase, isocitrate lyase, fumarase, glutaminase A and glutamate dehydrogenase as well as enzymes of the BCKDH complex, poly-3-hydroxyalkanoate degradation and fatty acid beta-oxidation. Contrary, a reduced expression of the isocitrate dehydrogenase, succinyl-CoA synthase, aspartate ammonia-lyase and asparaginase was detected under anoxic conditions for several strains.

At least, the arginine metabolism was predicted from the genome of the *Pseudomonas* strains and illustrated in Figure 26.

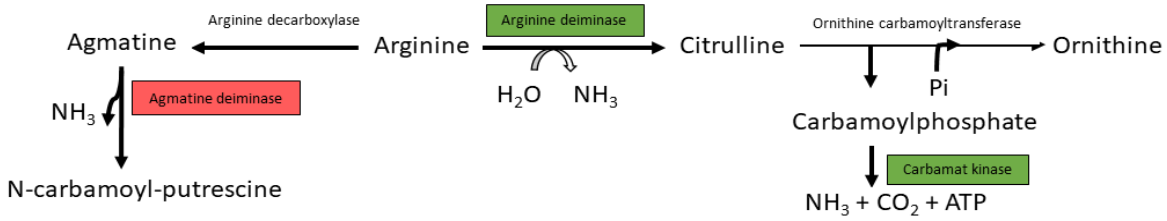

Figure 26. Predicted arginine metabolism of *Pseudomonas* strains based on their genomic settings. The arginine metabolism was predicted from the genome of the *Pseudomonas* strains and differentially expressed enzymes identified by the proteomic study were marked. Enzymes marked in green exhibit enhanced expression under anoxic conditions, while enzymes marked in red exhibit reduced expression under anoxic conditions for at least one strain.

Regarding enzymes of the ADI pathway, a reduced expression of the agmatine deiminase was identified under anoxic conditions, while an enhanced expression of the arginine deiminase, ornithine carbamoyltransferase (0.05> p >0.01) and carbamate kinase was observed for almost all strains under anoxic conditions.

Beside the proteomic regulated enzymes and metabolic pathways shown in Figure 23-26, several other differentially expressed enzymes listed in Table 24 were identified by the proteomic study. Those comprise enzymes involved in degradation of maltose, sucrose, amylose, benzoate, RNA and murein as well as the glycine cleavage system, fatty acid biosynthesis, urease and oxidative stress proteins, which exhibit an enhanced expression under anoxic conditions and enzymes involved in the ferrous metabolism, cellobiose and trehalose degradation, lipopolysaccharide and peptidoglycan synthesis and cell division, which exhibit a reduced expression under anoxic conditions for almost all strains.

4.3.4. Anaerobic growth with sodium nitrate, arginine and glucose

Growth of *Pseudomonas* strains was monitored in the anaerobic chamber *in vitro* in minimal medium containing glucose as electron donor, with or without the addition of $NaNO_3$ (chapter 3.1.7). Results are to be seen in Table 25.

Table 25. Anaerobic growth of *Pseudomonas* strains with or without addition of $NaNO_3$. Growth of the six *Pseudomonas* strains was determined under strict anoxic conditions in minimal media supplemented with or without $NaNO_3$. *P. aeruginosa* DSM 1117 was included as a positive control, able to perform nitrate respiration. Significant differences between mean $OD_{600\ nm}$ values were calculated for each strain based on a Welch T-test (p <0.01) and were marked in grey.

		with $NaNO_3$		without $NaNO_3$		p-value
	TMW	mean	SE	mean	SE	
P. lundensis	2.1732	0.01	0.00	0.03	0.01	0.346
P. lundensis	2.2076	0.00	0.00	0.00	0.00	0.856
P. weihenstephanensis	2.2077	0.01	0.00	0.01	0.00	0.848
P. weihenstephanensis	2.1728	0.00	0.00	0.00	0.00	0.783
P. fragi	2.2081	0.01	0.00	0.00	0.00	0.026
P. fragi	2.2082	0.00	0.00	0.01	0.01	0.345
P. aeruginosa	DSM 1117	0.12	0.02	0.02	0.00	0.008

None of the six *Pseudomonas* strains exhibited significant growth under anoxic conditions in minimal medium supplemented with $NaNO_3$ or without $NaNO_3$. *P. aeruginosa* DSM 1117 was the only species exhibiting significant growth under anoxic conditions due to the addition of $NaNO_3$.

Furthermore, all strains were cultivated oxically and anoxically on agar plates, containing minimal media supplemented with either 20 mM arginine or 20 mM glucose or none of the two ingredients (chapter 3.1.8). The pH dye phenol red was added to the media, visualizing growth by a color change from yellow to purple in case of alkalization (Figure 27).

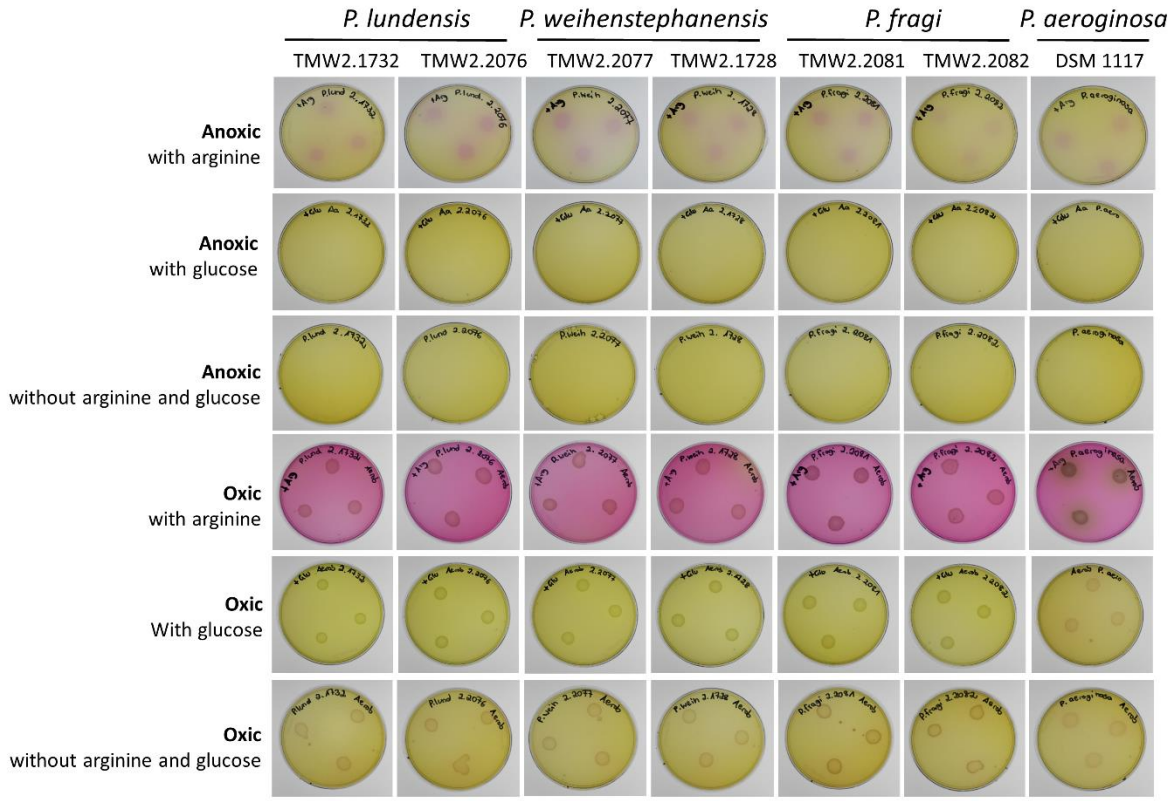

Figure 27. Arginine and glucose utilization of *Pseudomonas* strains under anoxic conditions. Growth of the six *Pseudomonas* strains on agar plates containing minimal medium supplemented with either 20 mM arginine or 20 mM glucose or without any additional ingredient was monitored under oxic or anoxic conditions. A color change from yellow to purple indicates alkalization by microbial arginine utilization based on the supplemented pH indicator phenol red.

All strains were able to grow under oxic conditions with or without supplementation of arginine or glucose. Nevertheless, a visible color change under oxic conditions could only be observed for plates containing arginine. Under anoxic conditions, no growth and color change could be observed on plates without ingredients or with glucose. Contrary, all strains exhibit a visible growth and color change under anoxic conditions on agar plates containing arginine.

An API 20 NE test was conducted for all strains, to support the physiological performed experiments regarding $NaNO_3$ and arginine utilization. Results are shown in Supplementary Table 11. Briefly, reduction of nitrate to nitrite and nitrite to nitrogen was negative for all strains, whereas the arginine deiminase (ADI) test was positive for all strains.

5. Discussion

This study investigates the interaction between meat-spoiling bacteria and commercially applied modified atmospheres, following the aim to provide a deeper understanding of the lifestyle, adaptation and formation of a microbial consortium to/on MAP meat. Thus, this study complements the knowledge about meat-spoiling bacteria, which was hitherto focused on their abundance on MAP meat as well as production of putrid metabolites, by applying an advanced mass spectrometric method providing detailed insights into bacterial metabolism. Furthermore, this work evaluates and proves a novel strategy, which can be followed to reduce the amount of meat wasted in supermarkets based on an early detection of meat-spoilage.

Main aspects of the interaction of meat-spoilers with modified atmospheres, which were addressed in this thesis are highlighted in Figure 28.

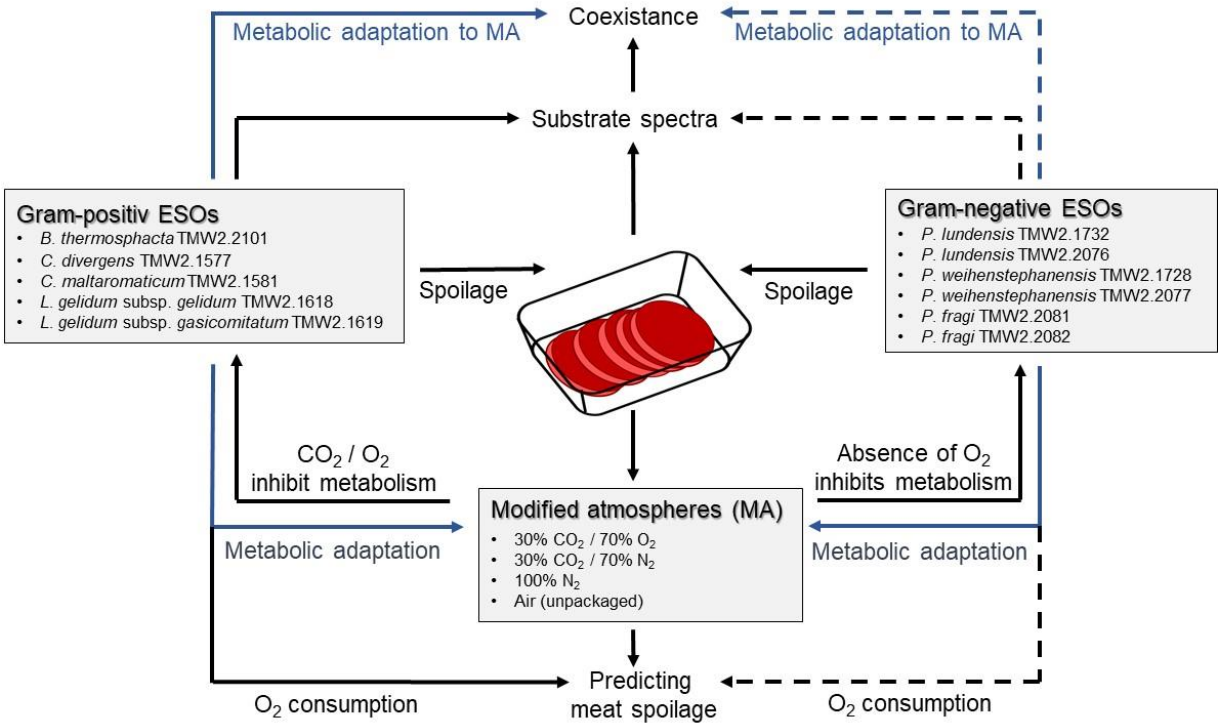

Figure 28. Investigated interactions of meat-spoiling bacteria with commercially applied modified atmospheres. All interactions of Gram-positive and Gram-negative ephemeral spoilage organisms (ESOs) with commercially applied modified atmospheres, which were investigated in this thesis are highlighted. Dotted lines indicate putative interactions, which were not analyzed in this study but still shown, to provide a complete overview of the interconnections taking place on/in MAP meat.

Regarding the analyzed interactions in Figure 28, the following theses could be derived, which are further discussed along the three sections of this study:

I) Metabolic adaptation of meat organisms to MAP gases

- The sensitivity of ESOs regarding CO_2 varies between species. *B. thermosphacta* TMW2.2101 and *C. divergens* TMW2.1577 exhibit a growth reduction at 30% CO_2, *C. maltaromaticum* TMW2.1581 at 70% CO_2 and both *L. gelidum* subspecies exhibit an intrinsic resistance to CO_2
- Mechanisms counteracting the detrimental effects of CO_2 and O_2 are frequently shared between ESOs
- Tolerance to CO_2 is provided by increasing the intracellular pH, reducing membrane fluidity and permeability and maintaining osmotic balance
- High amounts of O_2 induce oxidative stress within cells, which is counteracted by increasing the expression of antioxidant enzymes, catabolic O_2 consumption, decreasing membrane permeability and regulating the expression of oxygen sensitive enzymes
- Mechanisms identified in the meat simulation system can also be applied to real meat
- Anoxic meat packaging (30% CO_2 / 70% N_2) inhibits the growth of *B. thermosphacta* TMW2.2101 and *C. divergens* TMW2.1577 whilst high oxygen meat packaging (30% CO_2 / 70% O_2) does not inhibit any of the five analyzed Gram-positive species
- *B. thermosphacta* TMW2.2101 is highly sensitive towards the absence of O_2, showing a markedly reduction in growth under O_2 limiting conditions
- Meat organisms share a basic substrate spectrum, with some ESOs exhibit also the ability to utilize unique substrates
- Depending on the applied gas atmosphere, each species selects for the usage of specific substrates within its spectrum, thus avoiding substrate concurrence with other species

II) Change of the headspace atmosphere by microbial metabolism

- Oxygen consumption of bacteria is induced by respiratory chain activity and single oxygen consuming enzymes
- Enzymes of the respiratory chain are constitutively expressed within bacteria, whereas single oxygen consuming enzymes exhibit differential expression in response to different gas atmospheres

- *B. thermosphacta* TMW2.2101 exhibits a 31-time higher oxygen uptake rate compared to the other four LAB
- The higher oxygen uptake rate of *B. thermosphacta* TMW2.2101 can be explained by additional encoded genes for a cytochrome ca_3 and heme biosynthesis cluster as well as its higher resistance to oxidative stress compared to the other LAB
- The content of O_2 within the headspace of MA packages is decreasing due to microbial metabolism
- High oxygen MA packages with a high initial microbial load of *B. thermosphacta* exhibit a faster decrement in headspace O_2
- The decrease in headspace O_2 can be correlated to meat spoilage by the cell count of bacteria and occurs prior to spoilage of meat. Thus, a prediction of meat spoilage based on the headspace O_2 content of MAP meat is possible
- 30% CO_2 as applied in MAP inhibits O_2 consumption of *B. thermosphacta* TMW2.2101, *L. gelidum* subsp. *gelidum* TMW2.1618 and *L. gelidum* subsp. *gasicomitatum* TMW2.1619
- An inhibition of the O_2 consumption is not the main inhibitory effect of CO_2 on the metabolism of LAB, but might contribute to the prolonged lag-phase of *B. thermosphacta* TMW2.2101 under high oxygen atmospheres containing 30% CO_2

III) Role and lifestyle of *Pseudomonas* species on anoxic MAP meat

- Meat-spoiling *Pseudomonas* species exhibit restricted growth on anoxic packaged chicken meat
- Anaerobic growth of meat-spoiling *Pseudomonas* species on MAP meat resides in arginine metabolism as predicted from proteomic and physiological data
- The ED and EMP pathway coupled to ethanol fermentation predictively provide long-term survival of the analyzed *Pseudomonas* species, while anaerobic nitrate respiration and glucose fermentation to acetate cannot be performed due to missing genes
- A disabled respiratory chain is suggested to induce redox stress within the cell as NAD^+ cannot be regenerated. This impairs protein folding processes and restricts the TCA cycle as well as the glucose metabolism.

5.1. Metabolic adaptation to MAP gases and differential substrate utilization are drivers for the coexistence of bacteria in a meat consortium

A microbial consortium is considered as a mixture of organisms that coexists (synergistically) in a defined habitat such as soil, water, human bodies or on meat (Padmaperuma *et al.*, 2018; Khoo *et al.*, 2020). The initial microbial meat microbiota is given in the process of slaughtering by the endogenous animal microbiota, but further microbial load of carcasses can take place during transport and subsequent handling (Nychas *et al.*, 2007; De Filippis *et al.*, 2013). Further on, the microbiota is formed by several intrinsic and extrinsic ecological factors such as packaging conditions, storage temperature, pH, meat surface morphology, a_w-value, substrate diversity as well as by the presence of bacteria (Koutsoumanis *et al.*, 2006; Nychas *et al.*, 2008; Ercolini *et al.*, 2009; Hilgarth *et al.*, 2018c). Thus, a metabolic adaptation to those parameters is essential for survival and coexistence as a member of the meat consortium. Less adapted bacteria will be displaced rapidly by those, which possess unique substrate specificity or survival strategies to environmental stress. Until yet, those adaptation mechanisms are almost unknown, while the dynamic development of a microbial consortium on meat is explored in more detail (Ercolini *et al.*, 2006; Pennacchia *et al.*, 2011; Doulgeraki *et al.*, 2012; Höll *et al.*, 2016; Hilgarth *et al.*, 2018a). This study aimed to complement the hitherto limited knowledge about the lifestyle and adaptation of bacteria on MAP meat as well as their coexistence in a meat consortium by applying proteomics as an advanced comparative mass spectrometric method.

5.1.1. Bacteria exhibit resistance to MAP gases by different metabolic adaptation

Meat packaging under a defined modified atmosphere is commonly used to suppress the growth of spoilage microorganisms found as initial contamination on packaged meat thus shaping the microbial consortium (McMillin, 2008). Commercially applied gas atmospheres comprise 100% N_2, 30% CO_2 / 70% O_2 and 30% CO_2 / 70% N_2 (Kakouri and Nychas, 1994; Değirmencioğlu *et al.*, 2012; Rossaint *et al.*, 2015). Even though it is known that these gas atmospheres suppress the growth of specific microorganisms, the detailed mechanistic way of action is not known yet (Molin, 1983; Daniels *et al.*, 1985; Blombach and Takors, 2015). Furthermore, it is unclear how and to which degree spoilers of the meat consortium (ESOs) are able to adapt to those gas atmospheres. To answer these questions, this study investigates the proteomic response of specific ESOs to the MAP gases O_2 and CO_2. In the following, the metabolic adaptation of single ESOs and their sensitivity to MAP gases are discussed.

***B. thermosphacta* TMW2.2101.** Based on measured prolonged lag-phases and reduced maximal ODs, the meat-spoiling organism *B. thermosphacta* TMW2.2101 is considered to be

highly sensitive to CO_2 concentrations >30%. At 15% CO_2 concentrations, this species exhibited less sensitivity and reached similar maximal cell counts after seven days compared to 30% CO_2. This confirms previous studies demonstrating an inhibition of *B. thermosphacta* by MAP gases containing 30% CO_2 (Molin, 1983; Eklund, 1984; Stanbridge and Davies, 1998; Esmer *et al.*, 2011). The high sensitivity of *B. thermosphacta* TMW2.2101 to CO_2, could be explained by its inability to properly adapt its metabolism compared to the other ESOs. Only two metabolic adaptations could be detected for this species in response to CO_2, comprising firstly an enhanced expression of the ethanolamine degradation cluster. Ethanolamine is a part of the headgroup of phospholipids in mammalian cells (Garsin, 2010). When degraded by bacteria, ammonia is gained, which is known to contribute to intracellular pH homeostasis by binding of a free proton (Marquis *et al.*, 1987). Thus, the CO_2-induced effect of intracellular pH decrease, based on dissociation of CO_2 into carbonate and free protons (Becker, 1936; Daniels *et al.*, 1985; Smith *et al.*, 1990; Farber, 1991), can be compensated by degrading meat-derived ethanolamine. A second physiological adaptation to CO_2 of *B. thermosphacta* TMW2.101 could be identified by membrane fatty acid analysis. Similar to the other species, *B. thermosphacta* TMW2.2101 exhibited an increase in iso fatty acids in response to CO_2. According to Zhang and Rock (2008), a shift from *anteiso* to *iso*-fatty acids results in a reduction of the membrane fluidity. There are several studies dealing with the penetration of CO_2 through biological membranes. Even though some membrane bound proteins acting as gas channels have been identified for eukaryotes (Uehlein *et al.*, 2003; Endeward *et al.*, 2006), passive diffusion of CO_2 through membranes is still the most accepted way of penetration into prokaryotic cells (Missner *et al.*, 2008). While a cell membrane exhibiting low permeability is expected to also have a reduced permeability for gases such as CO_2 and O_2, no analogical prove for membrane fluidity is known yet. However, an increase in membrane fluidity due to CO_2 exposure on *Bacillus cereus* spores has been suggested previously (Enfors and Molin, 1980), fitting to the observed increase in membrane fluidity of the analyzed species in response to CO_2 of this study. Thus, it can be suspected that diffusion of CO_2 through membranes is also impaired by reduced membrane fluidity.

Contrary to CO_2, presence of O_2 or even high amounts of O_2 (70%) favored the growth of *B. thermosphacta* TMW2.2101. This was demonstrated by an increased growth rate and maximal OD when *B. thermosphacta* TMW2.2101 was cultivated in the presence of O_2. Several proteomic adaptations of this species were identified comprising an enhanced expression of oxidative stress enzymes such as thioredoxin and catalase enzymes in response to 21% and 70% O_2, which are known to enhance the resistance to O_2-derived oxidative stress (Feng and Wang, 2020). The expression of the O_2 sensitive pyruvate formate-lyase was reduced under high oxygen conditions while the expression of the O_2-consuming enzyme NADH oxidase was enhanced due to 21% O_2. Thus, regulation of O_2-sensitive enzymes as

well as catabolic O_2 consumption can be seen as another adaptation mechanism of this species to high O_2 concentrations. Furthermore, fatty acid analysis revealed a shift from *anteiso* to *iso* and branched to unbranched chain fatty acids in response to 70% O_2 what results in a decrease in membrane fluidity according to (Zhang and Rock, 2008).

Summing up, the enhanced growth of *B. thermosphacta* TMW2.2101 under high oxygen MA, detected in this and other studies (Höll *et al.*, 2016; Hilgarth *et al.*, 2018a), can be explained by its well adaptation to high oxygen concentrations as well as its ability, to efficiently use oxygen for respiratory activity (chapter 5.2.1). Even though a strong sensitivity to 30% CO_2 could be observed, *B. thermosphacta* TMW2.2101 was able to grow in MAs containing 30% CO_2 / 70% O_2, as the benefits from 70% O_2 outcompeted the negative effects of CO_2. Complementing the knowledge about this species, this study further demonstrated that *B. thermosphacta* TMW2.2101 is highly sensitive to the absence of O_2, as anoxic atmospheres such as 30% CO_2 / 70% N_2 or 100% N_2 resulted in a significant reduction of growth of this species.

***C. divergens* TMW2.1577**. Similar to *B. thermosphacta* TMW2.2101, CO_2 concentrations of >30% markedly prolonged the lag-phase of *C. divergens* TMW2.1577 when applied in combination with 70% N_2 but also with 70% O_2. Lower concentrations of CO_2 did not inhibit *C. divergens* TMW2.1577. Nevertheless, this species exhibited well metabolic adaptation to CO_2, which enabled fast growth after the adaptation period, resulting in similar maximal OD compared to growth without CO_2 exposure. In detail, the identified metabolic adaptations comprised an enhanced expression of glycine betaine transporters under CO_2 conditions without oxygen. A functional glycine betaine transport system is known to be relevant for maintaining intracellular osmolarity homeostasis (Csonka, 1989). CO_2 is known to destroying the cell membrane permeability to ionic species, thus impairing the osmolarity homeostasis (Sears and Eisenberg, 1961). As glycine betaine is present on chicken (Jung *et al.*, 2015) and beef (Zeisel *et al.*, 2003), a functional glycine betaine transport system appears to be one major adaptation mechanisms of *C. divergens* TMW2.1577 to the detrimental effects of CO_2. Furthermore, similar to *B. thermosphacta* TMW2.2101, *C. divergens* TMW2.1577 also exhibited adaptation mechanism to counteract the CO_2 induced low intracellular pH-value. Therefore, *C. divergens* TMW2.1577 enhanced the expression of specific enzymes such as alanine dehydrogenase, tyrosine decarboxylase and enzymes of the ADI pathway all leading to the production of basic components such as ammonia and biogenic amines increasing the intracellular pH (Lindgren *et al.*, 2014). Fatty acid analysis also revealed reduced membrane fluidity and permeability as an adaptation mechanism to CO_2, which was uncovered by a shift of unsaturated to saturated fatty acids. A decrease of membrane ion permeability due to CO_2 was also detected by Sears and Eisenberg (1961), which further claimed cis-unsaturated fatty

acids to increase and saturated fatty acids to decrease membrane permeability. Additionally, an acid stress induced decrease in membrane permeability could also be demonstrated for other Gram-positive bacteria e.g. *Listeria monocytogenes* (Datta and Benjamin, 1997) or *Streptococcus mutans* (Boyd *et al.*, 2000). Interestingly, *C. divergens* TMW2.1577 also produced higher amounts of lactobacillic acid (C19:0 delta) in response to CO_2. This cyclopropane fatty acid has been described to reduce cell membrane permeability and further enhance the resistance to acid stress (Guerzoni *et al.*, 2001; Shabala and Ross, 2008; Zhang and Rock, 2008)

This study demonstrates that aerobic conditions containing 21% or 70% O_2 promote the growth of *C. divergens* TMW2.1577 compared to anaerobic growth. Nevertheless, this species also needs some time to change its basic metabolism from hetero-fermentation to respiration (Holzapfel and Gerber, 1983), what explains its observed prolonged lag-phase comparing oxic and anoxic cultivation. Once adapted, growth with O_2 was significant better as without O_2, which was indicated by higher OD_{max} and growth rate. This can be explained by its respiratory activity (chapter 5.2.1), but also by its well metabolic adaptation to high O_2 conditions uncovered by proteomic and fatty acid analysis. Similar to *B. thermosphacta* TMW2.2101, this species adapted its pyruvate metabolism in response to O_2 by decreasing the expression of O_2 sensitive enzymes such as the pyruvate-formate lyse, while enhancing the expression of the pyruvate dehydrogenase. Furthermore, an enhanced expression of oxidative stress enzymes comprising peroxiredoxin, catalase and hydroperoxide resistance proteins was observed for this species, providing resistance to oxidative stress. Regarding fatty acid analysis, *C. divergens* TMW2.1577 was less adapted to high O_2 concentrations exhibiting increased membrane fluidity and permeability by an increased unsaturation of fatty acids and a shift from unbranched to branched chain fatty acids. The measured increased amounts of total fatty acids per gram cell did predictively not affect membrane properties, as the overall cell surface also increased under high O_2 conditions.

Summing up, a sensitivity of *C. divergens* TMW2.1577 to 30% CO_2 could be observed, mainly resulting in a delayed onset of growth on meat. However, due its metabolic capacity to adapt to CO_2 exposure as well as its ability to gain energy from respiratory chain activity (chapter 5.2.1), *C. divergens* TMW2.1577 is expected to be well adapted to the commercially applied MAP gas 30% CO_2 / 70% O_2. This is in accordance to other studies, describing *C. divergens* to be part of the dominating microbiota on high oxygen packaged meat (Nieminen *et al.*, 2011; Doulgeraki *et al.*, 2012; Höll *et al.*, 2016). As demonstrated in this study, *C. divergens* TMW2.1577 exhibits a higher sensitivity to anoxic conditions (30% CO_2 / 70% N_2) compared to high oxic atmospheres, which can be traced back to an inhibition by CO_2 with concomitant absence of O_2 needed for respiration.

***C. maltaromaticum* TMW2.1581.** The meat-spoiling species *C. maltaromaticum* TMW2.1581 exhibited a high resistance to CO_2 concentrations. This was demonstrated by the meat inoculation experiment, where no significant inhibition of *C. maltaromaticum* TMW2.1581 could be detected below CO_2 concentrations of 70%. This could be explained by a high metabolic adaptation capacity of *C. maltaromaticum* TMW2.1581 to CO_2. An antidromic regulation of enzymatic pathways comparing CO_2 adaptation under oxic and anoxic conditions was observed for this species. In detail, *C. maltaromaticum* TMW2.1581 exhibited the same adaptation mechanism described for *B. thermosphacta* TMW2.2101 and *C. divergens* TMW2.1577, comprising maintenance of the intracellular pH homeostasis by enhanced ethanolamine degradation, arginine degradation via the ADI pathway and alanine degradation via the alanine dehydrogenase enzyme under anoxic CO_2 exposure. Additionally, *C. maltaromaticum* TMW2.1581 enhanced the expression of several enzymes involved in fatty acid biosynthesis under CO_2 exposure with and without oxygen, assuming a denser packaged cell membrane under those conditions. Although, no changes in the fatty acid profile for *C. maltaromaticum* TMW2.1581 could be observed, the physiological assay indicated a decrease in membrane fluidity for this species when exposed to CO_2.

Similar to *C. divergens* TMW2.1577, exposure to O_2 prolonged the lag-phase of *C. maltaromaticum* TMW2.1581 compared to anoxic cultivation. However, after adaption of its metabolism, growth was significantly enhanced under oxic compared to anoxic conditions, indicating well metabolic adaptation to the detrimental effects of O_2. Beside the already named reduced expression of the pyruvate formate-lyase as well as the enhanced expression of oxidative stress enzymes, an increased expression of the heme uptake system was identified under high oxygen conditions for *C. maltaromaticum* TMW2.1581. This indicates enhanced respiratory activity leading to increased oxygen consumption and thus reduction of oxidative stress as described in chapter 5.2.1. Thus, enhanced respiration can be considered as another adaptation mechanism to high oxygen conditions as demonstrated for this species. Regarding fatty acid analysis, a decrease of the membrane fluidity under high oxygen conditions was observed, which was traced back to an increase in total amounts of fatty acids concomitant with a decrease in cell surface. Thus, the cell membrane of *C. maltaromaticum* TMW2.1581 is expected to be tighter packaged and consequently less fluid. Furthermore, a strong increase of long-chain unsaturated fatty acids such as conjugated linoleic acid (18:2 conj.), arachidonic (C20:4 Δ5,8,11,14) and eicosatetraenoic acid (C20:5 Δ5,8,11,14,17) were observed for this species exposed to high oxygen conditions, resulting in an increase in membrane permeability. Assuming an O_2 dependent desaturase system being responsible for this long-chain fatty acid unsaturation (Erwin and Bloch, 1964; Bajpai and Bajpai, 1993; Guerzoni *et al.*, 1997; Guerzoni *et al.*, 2001), catabolic O_2 consumption by fatty acid unsaturation can be seen as an additional adaptation mechanism to high oxygen conditions.

Taken together, the species *C. maltaromaticum* TMW2.1581 exhibited no inhibition to 30% CO_2 concentrations and showed only slight prolonged lag-phases by high O_2 concentrations. Thus, *C. maltaromaticum* TMW2.1581 is well adapted to the commercially applied gas atmospheres 30% CO_2 / 70% O_2 and 30% CO_2 / 70% N_2. This can be traced back to an extensive metabolic adaptation capacity identified for this species when exposed to O_2 and CO_2.

***L. gelidum* subsp. *gelidum* TMW2.1618.** Growth experiments on meat revealed no inhibition of the species *L. gelidum* subsp. *gelidum* TMW2.1618 by CO_2 in the range of 15-70%. Furthermore, this species exhibited lowest proteomic regulation due to CO_2 exposure compared to the other tested species. The only proteomic regulation found for this species in response to CO_2 was a decreased expression of four ion transporters. It can be speculated that this is due to the increased ion permeability of the membrane caused by CO_2. Fatty acid analysis exhibited a shift from unsaturated to saturated fatty acids in response to CO_2, resulting in a decrease in membrane permeability and fluidity. Similar to *C. divergens* TMW2.1577, this species also enhanced the production of lactobacillic acid (C19:0 delta) in response to CO_2, which is expected to be a protective mechanism against CO_2 induced acid stress.

Growth of *L. gelidum* subsp. *gelidum* TMW2.1618 under high oxygen packaging conditions (70% O_2) was strongly promoted compared to normal air conditions (21% O_2). Similar to the other analyzed species, this can be explained by a tolerance to oxidative stress as well as an energy gain due to respiratory activity. Indeed, an enhanced expression of thioredoxin reductase and peroxiredoxin under high oxic conditions was identified, providing oxidative stress tolerance. Furthermore, an enhanced expression of the acetolactate dehydrogenase was detected, indicating increased O_2 consumption under oxic conditions. Fatty acid analysis revealed no significant adaptation of the cell membrane in response to high oxygen for *L. gelidum* subsp. *gelidum* TMW2.1618.

Based on the missing inhibition of *L. gelidum* subsp. *gelidum* TMW2.1618 by CO_2 and its enhanced growth with high O_2 concentrations, it can be concluded that this species even benefits from high oxygen MA packaging with 30% CO_2 / 70% O_2. This is in accordance to findings of other studies, demonstrating *L. gelidum* subsp. *gelidum* to dominate preferably on high oxygen packaged meat (Hilgarth *et al.*, 2018a; Hilgarth *et al.*, 2019). However, this study also demonstrates a resistance of *L. gelidum* subsp. *gelidum* TMW2.1618 to anoxic atmospheres such as 30% CO_2 / 70% N_2 or 100% N_2. Furthermore, as almost no proteomic responses could be observed for *L. gelidum* subsp. *gelidum* TMW2.1618 to O_2 and CO_2 exposures, an intrinsic resistance to both gases can be assumed for this species.

***L. gelidum* subsp. *gasicomitatum* TMW2.1619.** Similar to *L. gelidum* subsp. *gelidum* TMW21618, growth experiments revealed no inhibition of *L. gelidum* subsp. *gasicomitatum* TMW2.1619 by CO_2 concentrations ranging from 15-70%. The metabolic adaptation was the same as for *L. gelidum* subsp. *gelidum* TMW2.1618, with only some ion transporters being downregulated due to CO_2 exposure. Furthermore, reduced membrane fluidity and permeability due to a shift from unsaturated to saturated fatty acids was detected for this species under CO_2 exposure. The amount of the cyclopropane fatty acid lactobacillic acid (C19:0 delta) was also increased due to CO_2. The measured increase in the total fatty acid content was concomitant with an increase in cell surface, thus predictively not affecting membrane properties.

High oxygen concentrations do inhibit the growth of *L. gelidum* subsp. *gasicomitatum* TMW2.1619 as demonstrated by the experiments. The maximal OD was strongly reduced due to 70% O_2 compared to normal air conditions. Interestingly, this subspecies exhibited same metabolic adaptation mechanism as described for *L. gelidum* subsp. *gelidum* TMW2.1618 but appears to be less tolerant to high oxygen. Those mechanism comprised an enhanced oxidative stress tolerance by upregulating antioxidant enzymes such as thioredoxin reductase and peroxiredoxin as well as increased O_2 consumption by the acetolactate synthase enzyme. However, the reduced tolerance to oxidative stress might be explained by its membrane properties. An increase in membrane permeability as well as a fatty acid derived increase in membrane fluidity was detected for this species in response to high O_2, which is both expected to be unbeneficial regarding O_2 penetration into the cell.

Due to its insensitivity to CO_2, *L. gelidum* subsp. *gasicomitatum* TMW2.1619 appears to be well adapted to the gas atmosphere 30% CO_2 / 70% N_2. The gas atmosphere 30% CO_2 / 70% O_2 inhibited the growth of *L. gelidum* subsp. *gasicomitatum*, which could be traced back to its sensitivity to high O_2 concentrations. Similar to *L. gelidum* subsp. *gelidum* TMW2.1618, *L. gelidum* subsp. *gasicomitatum* TMW2.1619 is expected to exhibit an intrinsic resistance to both gases O_2 and CO_2, due to missing proteomic regulations.

Summary. This study demonstrates that all of the analyzed five meat-spoiling bacteria are able to cope with their environmental atmosphere by a multifactorial adaptation of their metabolism, thus providing their existence on MAP meat. Even though, different enzymes, pathways and fatty acids were regulated for each species in response to O_2 and CO_2, the overall physiological mechanisms against the harmful effects of both gases were often shared between the species. To illustrate this, a summary of the species-specific different proteomic regulations and their underlying mechanistic way of action is given in Table 26.

Table 26. Identified mechanisms and enzymatic regulations of the meat-spoiling bacteria in response to O_2 and CO_2. A summary of all identified proteomic regulations in MS-media and on beef

steak as well as their underlying mechanistic way of action against the harmful effects of the gases O_2 and CO_2 is given. Colors represent species, which exhibited the corresponding proteomic regulation with (■) *B. thermosphacta* TMW2.2101, (■) *C. divergens* TMW2.1577, (■) *C. maltaromaticum* TMW2.1581, (■) *L. gelidum* subsp. *gelidum* TMW2.1618 and (■) *L. gelidum* subsp. *gasicomitatum* TMW2.1619. *packaged under 30% CO_2 / 70% O_2 atmosphere, data are not based on replicates. "n.d." = not detected, as fatty acid measurements have not been performed from cells grown on meat.

Bacterial metabolic adaptation to CO_2			
Proteomic regulation and fatty acid changes	**MS-media**	**Beef steak***	**Mechanism**
Ethanolamine degradation	■ ■		**pH maintenance**
Alanine dehydrogenase	■ ■	■	
Tyrosine decarboxylase	■	■	
ADI pathway	■ ■	■	
Glycine-betaine	■	■ ■	**Osmolarity maintenance**
Ion transporters	■ ■	■ ■	
Shift *anteiso* to *iso* fatty acids	■	n.d.	**Reduction of membrane fluidity and permeability**
Shift unsaturated to saturated fatty acids	■ ■ ■		
Bacterial metabolic adaptation to O_2			
Proteomic regulation and fatty acid changes	**MS-media**	**Beef steak***	**Mechanism**
Thioredoxin	■	■ ■ ■	**Oxidative stress reduction**
Catalase	■ ■ ■	■ ■	
Superoxide dismutase		■ ■ ■	
Peroxiredoxin	■ ■ ■	■ ■ ■	
Hydroperoxide resistance protein	■	■ ■	
Thioredoxin reductase	■ ■ ■	■	
Peroxidase	■ ■	■	
NADH oxidase	■	■	**Catabolic oxygen consumption**
Enhanced respiration	■		
Acetolactate synthase	■ ■	■ ■ ■	
Pyruvate-format lyase	■ ■ ■		**Reduced expression of O_2 sensitive enzymes**
Shift *anteiso* to *iso* fatty acids	■	n.d.	**Reduction of membrane fluidity**
Shift branched to unbranched chain fatty acids	■		
Increase total fatty acids	■		

Actually, several of the observed proteomic regulations and almost all predicted mechanisms obtained from the experiment performed in MS-media could also be identified by the proteomic study on beef steak packaged under 30% CO_2 / 70% O_2 atmosphere. This comparison proves that results obtained in MS-media can be transferred to real meat system. Interestingly, even equal amounts of proteins were used for mass spectrometric analysis of both experiments, the number of detected meat proteins was significant higher for the meat experiment compared to the experiment performed in meat extract. Thus, it can be concluded that non-microbial proteins in meat extract (approx. 33 g/l according to BCA analysis) can be more efficiently removed compared to those proteins in cell suspensions obtained from real meat. This might be due to fat and microparticles, which cannot be accurately separated from bacteria by centrifugation or filtering, but are missing in meat extract.

However, based on these results, as well as growth experiments with different gas atmospheres, the resistance of the meat-spoiling bacteria to the protective gas atmospheres used for red and white meat was evaluated, which is essential for their existence on MAP meat (Table 27).

Table 27. Overall conclusions about the predicted resistance of the meat-spoiling bacteria to the gas atmospheres used in MAP of white and red meat.

		Resistance to gas atmospheres of	
	TMW	**White meat (30% CO_2 / 70% N_2)**	**Red meat (30% CO_2 / 70% O_2)**
B. thermosphacta	**2.2101**	No	Yes
C. divergens	**2.1577**	No	Yes
C. maltaromaticum	**2.1581**	Yes	Yes
L. gelidum* subsp*. gelidum	**2.1618**	Yes	Yes
L. gelidum* subsp*. gasicomitatum	**2.1619**	Yes	Yes

B. thermosphacta TMW2.2101 and *C. divergens* TMW2.1577 are predictively less adapted to the gas atmosphere applied in white meat packaging (30% CO_2 / 70% N_2), which is thought to be due to the absence of O_2 needed for respiration and an inhibition by CO_2. Contrary, both species appear to be well adapted to high oxygen atmospheres. *C. maltaromaticum* TMW2.1581 was expected to be resistant to both modified atmospheres, as it exhibited distinct proteomic adaptation mechanism to the detrimental effects of O_2 and CO_2. Contrary, *L. gelidum* subsp. *gelidum* TMW2.1618 and *L. gelidum* subsp. *gasicomitatum* TMW2.1619 are predictively intrinsically resistant to both MAP gases, without the need to conduct extensive proteomic regulation.

5.1.2. Preferential and unique substrate usage avoids nutrient competition of bacteria and enables their coexistence on meat

Meat is a highly perishable food product, containing proteins, fat, DNA and some carbohydrates such as glycogen, ribose and glucose, making it conductive to the growth of a wide range of spoilage bacteria (Ellis and Goodacre, 2001; Cobos *et al.*, 2015; Çelen *et al.*, 2016; Oblakova *et al.*, 2016; Chmiel *et al.*, 2019). However, as growth of bacteria occurs only on the meat surface (Ingram and Dainty, 1971; Chung *et al.*, 1989), free and easily accessible substrates such as glucose and amino acids are readily consumed (Gill, 1976; Ellis and Goodacre, 2001; Nychas *et al.*, 2007). Therefore, bacteria are equipped with proteolytic and lipolytic enzymes, degrading extracellular meat-bound proteins and fat, in order to gain amino acid, glycerol and phospholipids for their metabolism (Signorini *et al.*, 2003). Furthermore, DNA released from dead meat cells exhibits a precious source of nutrients for bacteria. In the process of evolution, meat-colonizing bacteria have adapted and optimized their metabolism to the utilization of those substrates. This was demonstrated by the performed genomic and proteomic experiments of this study, uncovering a similar basic substrate spectrum for all of

the species as well as a constitutive expression of corresponding enzymes. These basic substrates comprised degradation of glucose, ribose, purines and pyrimidines, glycerol, amino acids and other pentoses (Table 28)**.** However, an equal substrate spectrum of coexisting species does not automatically imply substrate competition, as the obtained proteomic expression profiles also revealed species-specific substrate preferences, which additionally differ regarding the applied modified atmosphere. Thus, bacteria appear to avoid substrate competition by differential preferent substrate usage on MAP meat. Furthermore, some species are able to utilize unique substrates, which cannot be used by others, providing them a competitive advantage on MAP meat.

Table 28. Identified preferred substrate usage of the meat-spoiling bacteria. Summary of the proteomic predicted preferred substrate usage of the meat-spoiling bacteria *B. thermosphacta* TMW2.2101 (■), *C. divergens* TMW2.1577 (■), *C. maltaromaticum* TMW2.1581 (■), *L. gelidum* subsp. *gelidum* TMW2.1618 (■) and *L. gelidum* subsp. *gasicomitatum* TMW2.1619 (■) when cultivated under 30% CO_2 / 70% N_2 or 30% CO_2 / 70% O_2 atmosphere. Data are based on expression profiles of iBAQ values of the proteomic experiment. Underlined boxes indicate an enhanced expression of enzymes for the usage of the corresponding substrate for this species under that specific gas atmosphere, which is based on LFQ values of the proteomic data.

Substrates	Derived from	Pathway	White meat (30% CO_2/ 70% N_2)	Red meat (30% CO_2/ 70% O_2)
Glucose		EMP pathway		
Ribose	DNA	Nucleoside / ribose metabolism		
Purine/ Pyrimidine	DNA	Nucleoside / ribose metabolism		
Glycerol	Fat	Fatty acid degradation		
Amino acids	Proteins	Amino acid degradation		
Pentoses		Pentose phosphate pathway		
Myo-inositol	Fat	Myo-inositol degradation		
Ethanolamine	Fat	Ethanolamine degradation		
Citrate		Citrate fermentation		
Allantoin	DNA	Allantoin degradation		
Fatty acids	Fat	Beta-oxidation		

In detail, *B. thermosphacta* TMW2.2101 preferred ethanolamine utilization under anoxic atmospheres, which is derived from glycerophospholipids of meat cells. Degradation of ethanolamine results in the production of acetyl-CoA, which can be shuttled into the TCA cycle (Fogerty *et al.*, 1991). Beside *C. maltaromaticum* TMW2.1581, this species is the only one able to utilize this substrate. Under aerobe conditions, *B. thermosphacta* TMW2.2101 preferred the utilization of myo-inositol and glycerol, which both derive from microbial degradation of meat cell membranes as described by Love and Pearson (1971). Thus, findings of this study are in accordance to previous studies, describing B*. thermosphacta* as a highly lipolytic bacterium dominating fatty meat products such as minced beef (Grau, 1983; Talon *et al.*, 1992). Based on the proteomic study, *C. divergens* TMW2.1577 predictively prefers degradation of nucleosides resulting in ribose, purine and pyrimidine production as well as fatty acids under atmospheres lacking O_2. Contrary, under high oxic atmospheres, *C. divergens* TMW2.1577 is

expected to prefer utilization of amino acids, which can be shuttled into the TCA cycle via anaplerotic reactions. *C. maltaromaticum* TMW2.1581 is expected to utilize glycerol, allantoin and amino acids as preferred substrates under high oxic conditions, whereas it preferred utilization of ethanolamine under O_2 limiting conditions. The utilization of allantoin is limited to C*. divergens* TMW2.1577 and *C. maltaromaticum* TMW2.1581, what provides an assertiveness advantage to those species. However, only *C. maltaromaticum* TMW2.1581 exhibited an expression of corresponding genes. No preferred substrate usage of the species *L. gelidum* subsp. *gelidum* TMW2.1618 under different atmospheres could be identified, whereas *L. gelidum* subsp. *gasicomitatum* TMW2.1619 appear to preferentially utilize pentoses under anoxic atmospheres.

Concluding, the conducted proteomic study demonstrates that meat-spoiling bacteria can counteract substrate competition by preferential and unique substrate utilization and further adapt their metabolism to the detrimental effects of the applied atmosphere gases, which are both two main factors enabling these bacteria to coexist on and synergistically spoil MAP meat.

5.2. Change of the headspace atmospheres by microbial metabolism

Several previous studies demonstrated that the initially gas atmosphere of MA meat packages is not static but rather changing significantly within the storage period (Ercolini *et al.*, 2006; Esmer *et al.*, 2011; Höll *et al.*, 2016; Hilgarth *et al.*, 2018a; Hilgarth *et al.*, 2019). All of those studies reported an O_2 decrement with a concomitant CO_2 evolution during 14 days of storage at 4 °C under high oxygen (70-80% O_2 / 20-30% CO_2) atmosphere. In detail, an increase of 5% CO_2 and decrease of 5% O_2 could be observed for MAP minced beef in the study of Esmer *et al.* (2011). Similar to this, Hilgarth *et al.* (2019) also reported an increase of 2% CO_2 and decrease of 7% O_2 for cold stored MAP minced beef. Contrary, headspace changes were higher in MAP beef steaks with approx. 13% CO_2 increase and 15% O_2 decrease reported by Hilgarth *et al.* (2019). Whereas on chicken breast filet, CO_2 levels increased approx. 2% and O_2 levels decreased approx. 7% within same time span and storage condition (Höll *et al.*, 2016).

5.2.1. ESOs exhibit different potentials to consume headspace oxygen, which depend on their genomic setting

Several factors have been considered to be responsible for the observed headspace changes in MA packages. Beside permeability of MAP trays and respiration of meat, microbial metabolism is expected to be the main source for headspace changes. Whereas the increase in CO_2 is thought to be due to heterofermentative lactic acid metabolism performed by several LAB (Mebrouk *et al.*, 2008), the observed O_2 decrease is supposed to result from respiratory activity of members of the meat microbiota (Brooijmans *et al.*, 2009; Lechardeur *et al.*, 2011). During respiration, electrons are shuttled via membrane bound enzymes to molecular O_2, resulting in the production of water and synthesis of ATP via a proton gradient (Brooijmans *et al.*, 2009). Thus, a microbial respiratory metabolism provides energy by concomitant consumption of molecular O_2. Beside respiratory chain activity, microbial O_2 consumption can also be performed by the activity of single oxygen consuming enzymes. However, a direct evidence for the linkage of microbial metabolism and headspace O_2 consumption has not been provided yet. Thus, the potential of the five meat-spoiling bacteria to consume O_2 as well as to concomitant perform a respiratory metabolism was analyzed. Therefore, the oxygen uptake rate for each species was calculated and correlated to their genomic settings, enabling to perform a functional respiratory chain, heme and menaquinone biosynthesis and uptake, a functional TCA cycle, efficient oxidative stress tolerance and single oxygen consuming reactions.

Calculated OUR/CFU for each species. The potential of meat-spoiling bacteria to consume dissolved and headspace oxygen in glass bottles filled half with O_2 saturated MS-media and half with a 70% O_2 / 30% CO_2 atmosphere was analyzed. Indeed, a decrease in headspace

O_2 as well as an increase in headspace CO_2 during cultivation of each single species was observed, fitting the headspace development observed in MA packages. Thus, all bacteria were able to consume molecular O_2 as well as to produce CO_2 during their growth. To enable a direct comparison between species, production of atmospheric CO_2 as well as consumption of atmospheric and dissolved O_2 per single cell was calculated for each species. The determined OURs for the analyzed species was comparable to those previously determined for *E. coli* (0.32 pg O_2 /cell *h) (Riedel *et al.*, 2013). However, strong differences between the five meat-spoiling bacteria were detected, with *B. thermosphacta* TMW2.2101 consuming 32-time more atmospheric O_2 as well as two-time more dissolved O_2 and producing 34-time more atmospheric CO_2 compared to the LAB. Thus, all bacteria studied in this work will likely contribute to headspace changes in MA packages, with packages dominated by *B. thermosphacta* predictively exhibiting a faster O_2 decrement compared to MAP dominated by LAB at similar CFU. Interestingly, a strong decrease in the CFU of *B. thermosphacta* TMW2.2101 was observed, as soon as dissolved O_2 in the media was consumed, indicating that an efficient growth of this species is obligate to the presence of O_2. This fits to the previous study performed by Hilgarth *et al.* (2018a), who detected a strong decrease in the abundance of this species on high oxygen MAP beef steaks after depletion of headspace O_2 in the package.

Respiratory chain enzymes. In order to explain the significant higher OUR of *B. thermosphacta* TMW2.2101 compared to the other species, investigations about the ability of the five meat-spoiling bacteria to set up and perform a functional respiratory chain were done. Indeed, all analyzed bacteria encode for the corresponding genes needed to establish a functional minimal respiratory chain as described for LAB (Brooijmans *et al.*, 2009; Lechardeur *et al.*, 2011). This respiratory machinery consists of an electron donor (NADH dehydrogenase), an electron shuttle (menaquinone), a terminal electron acceptor (cytochrome quinol oxidase), and a proton gradient-driven F_0F_1-ATP synthase. Interestingly, compared to LAB, *B. thermosphacta* TMW2.2101 additionally encodes for a cytochrome a_3 quinol oxidase as well as an a-type cytochrome oxidase. Thus, this species can predictively build up two additional cytochrome oxidases (aa_3 and ba_3) compared to the other LAB. A similar cytochrome composition of *B. thermosphacta* has previously also been described by Gil *et al.* (1992), who further shows that the abundance of different cytochromes of this species is dependent on extracellular O_2 concentrations. Thus, varying the cytochrome composition for an efficient usage of variable O_2 concentrations might be an explanation for the high OUR of *B. thermosphacta*.

Heme biosynthesis and uptake. Furthermore, Lechardeur *et al.* (2011) and Brooijmans *et al.* (2009) describes LAB bacteria to be auxotrophic to exogenous heme, as they are unable to

biosynthesize heme *in vitro*. Heme is required as an important cofactor for cytochrome oxidase activity and is thus obligate for respiratory activity. Indeed, the analyzed LAB do not encode the genes needed for heme biosynthesis. However, supplementation of exogenous hemin chloride boosted the growth of LABs in MS-media, indicating that the analyzed LAB are able to take up and use exogenous heme for respiration. Indeed, corresponding genes for a heme-uptake system could be found in the genome of the LAB. Actually, heme can be found in meat, where it is bound within the muscle pigments hemoglobin and myoglobin. Whereas beef contains moderate amounts of hemoglobin (0.64mg/g) and myoglobin (2.66 mg/g), the amount of both pigments in chicken muscle is not detectable (Babji *et al.*, 1989; Han *et al.*, 2006). Thus, it can be assumed that on MAP beef, LAB take up exogenous heme from meat and perform a respiratory metabolism consuming headspace O_2, whereas on MAP chicken headspace O_2 consumption is limited for LAB bacteria due to missing heme. Contrary to the LAB, the performed genomic analysis predicted *B. thermosphacta* TMW2.2101 to be able to biosynthesize heme A, B and O themselves. Furthermore, it is also expected to be able to take up heme from the environment. When offered free heme, *B. thermosphacta* TMW2.2101 showed enhanced growth, indicating uptake of extracellular heme instead of biosynthesis to safe energy. This genomic difference between the analyzed meat-spoiling species also explains the higher OUR of *B. thermosphacta* TMW2.2101 compared to the other species.

Menaquinone biosynthesis and uptake. Complementary to the study of Brooijmans *et al.* (2009) the potential of the five meat-spoiling species to biosynthesize menaquinone was analyzed. Menaquinone is considered as an important electron carrier for respiratory chain. According to the genomic study, all analyzed species were predictively able to biosynthesize menaquinone themselves. This confirms to the performed physiological experiments, where addition of exogenous menaquinone did not enhance growth of any of the five analyzed species. Furthermore, single transcription data demonstrated an upregulation of the transcription of one gene for menaquinone biosynthesis under high oxygen conditions for *B. thermosphacta* TMW2.2101 and *L. gelidum* subsp. *gasicomitatum* TMW2.1619. Thus, it can be concluded that all analyzed LAB as well as *B. thermosphacta* TMW2.2101 are able to biosynthesize menaquinone themselves and thus are not obligate to exogenous menaquinone from meat.

Tricarboxylic acid (TCA) cycle. Furthermore, none of the five analyzed species is predicatively able to perform a full TCA cycle, as corresponding genes are missing. A TCA cycle is known to be coupled to respiration via NADH/NAD^+ interconversion. However, respiration can also be coupled to a fermentative metabolism, generating NADH, which is *vice versa* oxidized by respiration. Thus, a missing TCA cycle for the five meat-spoiling species does not impair respiratory activity.

Oxidative stress tolerance. At least, oxidative stress tolerance was analyzed for each of the five meat-spoiling bacteria. Oxidative stress is induced by reactive oxygen species such as H_2O_2, OH^- and O_2^-, which are generated by high amounts of O_2 but also during respiratory chain activity, where H_2O_2 can be produced with a prevalence of 0.1-2% by incomplete reduction of molecular O_2 to H_2O (Madamanchi and Runge, 2007; Li *et al.*, 2013). This study demonstrates all analyzed species to tolerate exposure of H_2O_2 to a certain degree (0.01-0.09% H_2O_2) and further shows all species to be equipped with corresponding antioxidant enzymes such as superoxide dismutase or catalase, which are needed to detoxify ROS (Feng and Wang, 2020). However, in a direct comparison, *B. thermosphacta* TMW2.2101 tolerated 4-7 times higher concentrations of H_2O_2 and further exhibits higher amounts of antioxidant enzymes compared to the other species. Consequently, it can be assumed that *B. thermosphacta* TMW2.2101 tolerates higher respiratory rates compared to LAB bacteria, what further explains the calculated higher OUR compared to the other species.

Single oxygen consuming reactions. Beside respiratory chain activity, headspace O_2 can also be consumed by single oxygen consuming enzymes. Indeed, the performed proteomic study revealed an enhanced expression of several of those enzymes under high oxygen conditions comprising a NADH oxidase, dioxygenase and a heme oxygenase for *B. thermosphacta* TMW2.2101, a NADH oxidase, heme oxygenase and glycerin-3-phosphat dehydrogenase for *C. maltaromaticum* TMW2.1581 and a heme oxidase for *C. divergens* TMW2.1577. The heme oxidase, is known to degrade heme by using O_2 and NADPH. Thus, it remains unclear whether bacteria degrade heme to consume molecular O_2 in order to reduce oxidative stress or if heme is degraded as it becomes toxic within the cell. However, an enhanced transcription of those and other oxygen consuming enzymes was also determined by the performed single gene-transcription study in response to high oxygen conditions. Those enzymes comprise a pyruvate oxidase, NADH oxidase and glycerin-3-phosphate oxidase for *B. thermosphacta* TMW2.2101 and *C. maltaromaticum* TMW2.1581 as well as the glycerin-3-phosphate dehydrogenase for *C. divergens* TMW2.1577. Thus, based on results obtained from the proteomic and single gene-transcription study, O_2 consumption of single enzymes predictively also contributes to the determined OURs for each of the five meat-spoiling species.

Taken together, this study proves metabolic O_2 consumption and CO_2 production for certain ESOs in a meat model system and establishes the missing linkage to certain metabolic pathways. In detail, the recorded headspace development in artificial environment (glass bottles) matches accurately to the observed headspace development of MAP meat. Furthermore, the potential of all species to perform aerobic respiratory activity was uncovered, what partially explains the headspace O_2 decrement of MA packages. Thus, findings of this study are in accordance to other studies, which also demonstrated a respiratory metabolism

for LAB (Brooijmans *et al.*, 2009; Johansson *et al.*, 2011; Lechardeur *et al.*, 2011; Jaaskelainen *et al.*, 2013). However, a heme-based respiration has not yet been described for the species *L. gelidum* subsp. *gelidum*. Furthermore, this study quantifies the oxygen uptake rate of the five meat-spoiling bacteria, enabling to trace back the contribution of certain species in headspace O_2 decrement. A faster O_2 consumption in MA packages dominated by *B. thermosphacta* compared to MA packages dominated by LAB was predicted due to the determined higher OUR. The high OUR of *B. thermosphacta* TMW2.2101 could be explained by some unique genomic settings, comprising a heme biosynthesis cluster enabling enhanced respiration, additional cytochromes for adapting to varying O_2 concentrations and a comparative higher tolerance to H_2O_2 enabling higher respiratory rates. Beside respiration, other O_2 consuming reactions are also predicted to contribute to headspace O_2 consumption, as corresponding enzymes were upregulated under high O_2 conditions in the proteomic and single gene-transcription study. Thus, it can be concluded that atmospheric changes in MA packages are induced by a broad consortium of bacteria, who's species-specific potential for O_2 consumption is differing and depending on the presence or absence of certain genes.

5.2.2. Carbon dioxide reduces microbial O_2 consumption by inhibiting respiratory chain and single oxygen consuming enzymes

Increased concentrations of CO_2, as commercially applied in high oxygen MA packaging, are thought to reduce O_2 consumption of bacteria (King Jr and Nagel, 1975; Gill and Tan, 1979). This was demonstrated in a previous study by Gill and Tan (1980), who measured a reduction in cell respiration due to CO_2 exposure for the meat-spoiling species *Pseudomonas*, *Shewanella* (*Alteromonas*) *putrefaciens* and *Yersinia enterocolitica*. In accordance to this, a reduced O_2 consumption due to 30% CO_2 exposure could also be detected in this study for the species *B. thermosphacta* TMW2.2101, *L. gelidum* subsp. *gelidum* TMW2.1618 and *L. gelidum* subsp. *gasicomitatum* TMW2.1619.

Although the detailed mechanistic way of inhibition of CO_2 on the oxidative metabolism of bacteria has not been uncovered yet, several possible explanations are discussed in science. First it has been expected that CO_2 is competitive to molecular O_2 within cells, partially or fully displacing O_2 for enzymatic reactions consequently slowing down metabolic processes (Daniels *et al.*, 1985). According to this, one major target of CO_2 was thought to be the heme molecule binding O_2 within cytochromes during respiratory chain activity. However, previous studies demonstrated that the molecular binding site of CO_2 is not targeted on heme, rather than to the four α-amino groups at the end of the α and β chains of the hemoglobin molecule (Perrella *et al.*, 1975). King Jr and Nagel (1975) further supported this assumption, as they detected no inhibition of the cytochrome c oxidase activity in the presence of CO_2 for *P. aeruginosa*. Thus, competitive displacement of O_2 by CO_2 within the respiratory chain can

be rejected as explanation for the observed impaired O_2 consumption of the analyzed species. However, a passive inhibition of the respiratory chain by CO_2 was also suspected, which is due to an inhibition of decarboxylase and dehydrogenase reactions of the TCA cycle, needed to reduce redox equivalents for respiration (Daniels *et al.*, 1985). It has been demonstrated that increased amounts of CO_2 and H^+ especially inhibit these enzymes by shifting the equilibrium of the reactions to the non-decarboxylated /-protonated side. In detail, King Jr and Nagel (1975) measured a decrease in the isocitrate dehydrogenase and malate dehydrogenase activity in response to 50% CO_2 exposure. No inhibition of the oxaloacetate decarboxylase was detected in the same study, which was traced back to its high equilibrium constant for decarboxylation. However, as none of the five analyzed meat-spoiling species of this study encodes for a full TCA cycle and redox equivalents are rather reduced by a fermentative metabolism, this attempt to explain the impaired respiration rate due to CO_2 exposure remains questionable. Another passive way of inhibiting the respiratory chain was thought to be the membrane proton gradient, which is disturbed by CO_2 in two different ways. Firstly, CO_2 entering cells is known to dissociate with H_2O to HCO_3 and free H^+, thus increasing the intracellular proton concentrations (Becker, 1936; Daniels *et al.*, 1985). Secondly, CO_2 is thought to increase the membrane permeability for small molecules, thus destroying the membrane barrier function of the cell (Sears and Eisenberg, 1961; Hon and Pyun, 2001). Indeed, metabolic response mechanisms to a decreased pH as well as membrane permeability could be observed in the conducted proteomic study of this thesis (chapter 5.1.1). Thus, considering all discussed direct and passive ways of how CO_2 can inhibit respiratory chain activity, latter seems to be the most likely explanation.

In addition to the expected reduction of respiratory chain activity, an inhibition of single O_2 consuming reactions might also contribute to the observed reduction in O_2 consumption by the analyzed species. Corresponding targeted enzymes comprise the pyruvate and NADH oxidase, both consuming O_2 by a concomitant production of CO_2 or free H^+. Consequently, those enzymatic reactions are also a target of the mass transfer action of increased CO_2 / H^+ concentrations within the cell. Indeed, an enhanced expression of the pyruvate and NADH oxidase enzyme due to CO_2 exposure could be measured for *B. thermosphacta* TMW2.2101 and *L. gelidum* subsp. *gasicomitatum* TMW2.1619 in the single transcript and proteomic study. Interestingly, both *Carnobacterium* species do not encode for a pyruvate oxidase enzyme, thus explaining their insensitivity to CO_2 regarding O_2 consumption.

Taken together, the observed reduction in O_2 consumption due to CO_2 exposure to the five analyzed species is thought to be due to a passive inhibition of the respiratory chain by a disturbed proton gradient as well as single oxygen consuming enzymes. Nevertheless, as an inhibition of cell growth by CO_2 was also proven for some species under anoxic conditions in

this thesis, reduced O_2 consumption is expected to be not the main inhibitory mechanism of action of CO_2 on meat-spoiling bacteria. However, et least for the highly respiratory active species *B. thermosphacta* TMW2.2101, this effect of CO_2 might contribute to the observed prolonged lag-phase and reduced growth under 30% CO_2 / 70% O_2 conditions compared to air.

5.2.3. Monitoring headspace oxygen consumption by sensor spot technology enables to predict the onset of meat spoilage

As headspace O_2 consumption and meat spoilage is both considered to be linked by bacterial cell counts on meat, a study was conducted investigating the question, whether O_2 consumption in the headspace of MA packages can be used to predict the onset of meat spoilage prior to human perception. Therefore, an O_2 sensor spot was integrated into the PP-EVOH tray, enabling an easy, fast and non-invasive measurement of the headspace O_2 content in MA packages. This technology would provide a powerful tool for retails to detect individual spoilage of single packages before the actual onset, thus enabling early individual sorting of MA packages, which consequently reduces meat disposal.

To prove the applicability and principle of this method, beef and chicken was inoculated with single meat-spoiling bacteria, corresponding to their isolation source, and packaged under a high oxygen atmosphere (30% CO_2 / 70% O_2) in trays containing an integrated sensor spot. Inoculation was performed with high cell counts, to accelerate the onset of meat spoilage and headspace O_2 consumption. According to literature, meat is considered as spoiled after the cell count exceeds a threshold-level of $\log_{10}(CFU/cm^2)$ >7 (Prieto *et al.*, 1991; Ayres, 2007; Nychas *et al.*, 2008). Similar to this, but depending on the species, perceptible spoilage was determined to occur at a bacterial count of $\log_{10}(CFU/cm^2)$ >6.8 - 8.2. Interestingly, microbial headspace O_2 consumption on MAP beef steaks was recorded earlier at a $\log_{10}(CFU/cm^2)$ = 6.4-7.4. In detail, meat inoculated with *B. thermosphacta* TMW2.2101 was considered as spoiled at a $\log_{10}(CFU/cm^2)$ =7.7 whereas oxygen started to decrease at a $\log_{10}(CFU/cm^2)$ =7.0. Similar correlations could also be observed for *L. gelidum* subsp. *gelidum* TMW2.1618 and *L. gelidum* subsp. *gasicomitatum* TMW2.1619 (Table 22)**.** Thus, the applied sensor spot technology in this study enabled to detect microbial O_2 consumption in the headspace of inoculated MAP beef, before critical cell numbers for spoilage were reached and before meat was perceived as spoiled, proving the principal concept of this method. Considering that the ratio of headspace volume to meat volume was increased compared to industrial standards in this study, (1:8 for this study, 1:2 for industry) (Gill and Gill, 2005), the relative headspace O_2 decrement should be even faster in an industrial MAP system compared to this study.

Furthermore, the headspace O_2 decrement in MA packages containing beef inoculated with *B. thermosphacta* TMW2.2101 was significant higher compared to those packages containing beef inoculated with one of the two *L. gelidum* subspecies. This is in accordance to the previous determined significant higher (31-times) OUR calculated for *B. thermosphacta* TMW2.2101 in the headspace of glass bottle compared to the other species. However, in the previous experiment, an OUR of both *Carnobacterium* species was determined, which was comparable to those calculated for both *L. gelidum* subspecies, whereas in this experiment, no decrease in the headspace O_2 content of MA packages containing inoculated chicken with both *Carnobacterium* was measured. This might be explained by the absence of heme on chicken meat (Han *et al.*, 2006), whereas hemin chloride was added to MS-media after autoclaving in the previous experiment. As mentioned above, both *Carnobacterium* species are auxotroph to exogenous heme, which is taken up and used for reparation (Lechardeur *et al.*, 2011). Thus, a prediction of meat spoilage in high oxygen MA packages containing chicken meat is limited to those spoilage-cases, where bacteria able to biosynthesize heme dominate the microbiota, consequently reducing measurable amounts of headspace O_2. *C. divergens* TMW2.1577 and *C. maltaromaticum* TMW2.1581 were also cultivated on beef steak, which are expected to contain higher amounts of exogenous heme (Han *et al.*, 2006), but no significant growth could be measured for both species (data not shown). This might be due to their adaptation to a chicken environment, as both species have been isolated from chicken breast (Höll *et al.*, 2016).

Concluding, this study demonstrates the applicability of an integrated O_2 sensor spot for an easy and fast monitoring of the headspace oxygen content in individual MA packages. Furthermore, an onset of headspace O_2 consumption prior to perceptible meat spoilage was determined for inoculated MAP beef steaks. This correlation can be used to predict meat spoilage in individual MA packages prior to its onset and thus enables an individual package evaluation and sorting within retail, consequently reducing meat disposal as waste. Based on data obtained for *Carnobacterium*, this method can predictively also be applied on chicken meat products, as long as bacteria able to biosynthesize heme themselves dominate the initial microbiota.

Regarding the color analysis of inoculated meat pieces (Supplementary Figure S10), it should be mentioned that chicken meat inoculated with both *Carnobacterium* species did not exhibit a visible discoloration during the storage period. Nevertheless, it was considered as spoiled quite early (after 7 days), which can be explained by the sensory analysis revealing an enhanced rejection of inoculated chicken meat due to olfactory compared to visual appearance. Indeed, *Carnobacterium* species are known to produce high amounts of VOCs (Laursen *et al.*, 2006; Casaburi *et al.*, 2011), thus fitting to observations of this study. Contrary,

beef inoculated with *L. gelidum* subspecies showed a moderate discoloration from dark red to brown during storage, which results in a higher rejection of those meat pieces due to visual appearance compared to olfactory. This brown discoloration might be explained by a mixture of the bright red oxymyoglobin and green sulfmyoglobin pigments of beef. Especially latter origins from the metabolism of *Leuconostoc* species, as those are known to produce undesired H_2S and H_2O_2 components (Borch *et al.*, 1996; Vihavainen and Björkroth, 2007). Interestingly, meat inoculated with *B. thermosphacta* TMW2.2101 exhibited no visible discoloration after 18 days of storage. Actually, this species is known to contribute to meat spoilage by production of high amounts of VOC such as acetoin, 2-methylbutyric and isovaleric acid under oxic and high oxic conditions (Dainty and Hibbard, 1980; Dainty and Hibbard, 1983; Pin *et al.*, 2002). Considering that the freshness of gas tight packaged meat can only be validated by visual appearance, rather to olfactory, results of this study indicate that beef spoiled by *B. thermosphacta* would be considered as fresh by consumers even after exceeding the critical cell count for meat spoilage. The same holds true for chicken meat, which exhibits generally less discoloration due to missing color pigments such as haemoglobin or myoglobin (Han *et al.*, 2006). However, as demonstrated in this study, the O_2 sensor method would identify those non-obvious but actually spoiled MA packages even prior to the onset of spoilage, thus again highlighting the benefits of this method.

5.3. Growth and lifestyle of *Pseudomonas* strains on anoxic MAP meat

The majority of *Pseudomonas* species, comprising currently more than 240 valid published species, are generally considered as obligately aerobic organisms, unable to grow without oxygen (Garrity *et al.*, 2005; Özen and Ussery, 2012; Parte, 2018; Parte *et al.*, 2020). Still, certain species such as *P. aeruginosa, P. denitrificans, P. stutzeri* and strains of *P. fluorescens* have been described to grow under conditions of complete oxygen depletion (O_2 < 1ppm). However, the habitats of those species are not related to meat, rather to human, marine or soil environments as well as other food products such as tofu (Carlson and Ingraham, 1983; Yoon *et al.*, 2002; Wu *et al.*, 2005; Lalucat *et al.*, 2006; Stoops *et al.*, 2012). Thus, storage of meat under anoxic conditions by vacuum packaging or MA packaging effectively inhibits spoilage by supressing the growth of the most common meat-spoiling *Pseudomonas* species *P. fragi*, *P. putida, P. weihenstephanensis* and *P. lundensis* (Wang *et al.*, 2018b). Nevertheless, within those species, certain strains of *P. fragi* and *P. putida* have been found to also persist under anoxic conditions in a model system and/or on vacuum packaged beef (Ercolini *et al.*, 2011; Jääskeläinen *et al.*, 2016; Lai *et al.*, 2016; Wang *et al.*, 2017; De Filippis *et al.*, 2019). However, until yet no investigations have been done revealing the potential of strains of those species to actually grow on anoxic packaged meat and the underlying anaerobic metabolism still remains unknown.

5.3.1. Certain strains of meat-spoiling *Pseudomonas* species are able to grow on anoxic MAP meat

In a previous study, Hilgarth *et al.* (2019) identified and isolated strains of the species *P. lundensis*, *P. weihenstephanensis* and *P. fragi* from long-time stored MAP minced beef packages. Even though meat was initially packaged under high oxygen atmosphere, isolates were highly abundant at a late storage time point, where the headspace oxygen was already depleted within the packages. Furthermore, Hilgarth *et al.* (2019) proved the anaerobic growth of some of those isolates *in vitro* on BHI agar plates, thus suspecting also anaerobic growth *in situ* on minced beef (Hilgarth *et al.*, 2019). To prove this assumption, a follow-up study was conducted, monitoring the growth of those *Pseudomonas* strains on strictly anoxic packaged meat.

Therefore, an inoculation experiment on chicken meat packaged under 100% N_2 atmosphere was performed with two strains of each of the three isolated anaerobe *Pseudomonas* species from Hilgarth *et al.* (2019). Chicken meat was deliberately used instead of minced beef, as the latter is always packaged under a high oxygen atmosphere in food industry, due to reasons of color stability (Değirmencioğlu *et al.*, 2012). Furthermore, as *Pseudomonas* species are

considered as highly sensitive to CO_2 (Gill and Tan, 1979; Hendricks and Hotchkiss, 1997; Devlieghere and Debevere, 2000), 100% N_2 atmosphere was used for anoxic packaging, to prevent any inhibitory effects of CO_2 on the anaerobic growth of the strains. Indeed, a restricted but significant growth of all six *Pseudomonas* strains under anoxic conditions was detected, comprising cell division rates of approximately 0.4-0.8 /day. In accordance to this, restricted anaerobic growth *in vitro* in meat extract could also be observed for all strains. Thus, this is the first study, proving restricted growth of certain strains of *P. lundensis*, *P. weihenstephanensis* and *P. fragi* under anoxic conditions *in situ* on chicken meat and *in vitro* in MS-media. Nevertheless, the contribution of these strains to spoilage of anoxic packaged meat products remains open, as determined cell division rates were quite low, thus suspecting a low assertiveness of those strains compared to other anaerobic food-spoiling bacteria. However, the metabolism of existing cells might still contribute to a minor extent to meat spoilage of anoxically packaged products.

5.3.2. Anaerobic growth of certain *Pseudomonas* strains is based on arginine fermentation while glucose fermentation enables long-term survival

P. aeruginosa has functioned as model organism for exploring anaerobic energy metabolism of *Pseudomonas* species. Several studies demonstrated the ability of this species to persist and grow under anoxic conditions by performing either anaerobic nitrate respiration, arginine fermentation or pyruvate fermentation (Fewson and Nicholas, 1961; Vander Wauven *et al.*, 1984; Eschbach *et al.*, 2004; Schreiber *et al.*, 2006; Line *et al.*, 2014). In the following, corresponding and other metabolic pathways are discussed for the analyzed *Pseudomonas* strains of this study based on physiological assays and a comparative proteomic study under air and 100% N_2 atmosphere.

Anaerobic respiration. In order to validate, whether denitrification and dissimilatory nitrate reduction as described for *P. aeruginosa* (Fewson and Nicholas, 1961; Line *et al.*, 2014) explains the observed anaerobic growth of the analyzed meat-spoiling *Pseudomonas* strains on chicken meat, their respiratory chain was reconstructed based on genomic data. Indeed, almost all enzymes described for the respiratory chain of *P. aeruginosa* by Liang *et al.* (2020) could be found in the genome of the six analyzed *Pseudomonas* strains, except of those, needed for denitrification or dissimilatory nitrate reduction. Thus, it can be predicted that anaerobic respiration based on nitrate reduction is dysfunctional for the analyzed *Pseudomonas* strains, due to missing enzymes for nitrate reduction. The performed physiological experiments further supported this assumption, as addition of nitrate did not enable the growth of any of the six *Pseudomonas* strains *in vitro* under anoxic conditions and nitrate reduction was negative for all strains in the API 20 NE test. Furthermore, the amount of nitrate on white and red meat is quite limited (max. 0.2 $mmol*kg^{-1}$ on red meat) (Lammarino

and Di Taranto, 2012), thus making it unlikely that even anaerobic NO_3 respiring *Pseudomonas* species such as *P. aeruginosa* or *P. denitrificans* are able to grow to high amounts on meat. Nevertheless, the proteomic analysis of this study revealed an enhanced expression of several alternative electron donor enzymes under anoxic conditions, which might be explained by an attempt of the cell, to make the anaerobic respiratory chain running somehow, regardless if substrates and cofactors for their functionality are provided.

Arginine fermentation. Another well-studied pathway of *P. aeruginosa,* enabling weak biomass increase under anoxic conditions in the absence of a terminal electron acceptor, is degradation of arginine (Vander Wauven *et al.*, 1984; Lu *et al.*, 1999). Conversion of arginine via the ADI pathway does result in an alkalisation of the environment and further provides generation of one molecule ATP per molecule arginine. Therefore, only three enzymes are needed, comprising an arginine deiminase, ornithine carbamoyl transferase and carbamate kinase (Mercenier *et al.*, 1980). Proteomic analysis revealed an enhanced expression of all three enzymes under anoxic conditions for almost all analyzed *Pseudomonas* strains, indicating increased arginine fermentation under conditions of O_2 limitation. Furthermore, the *in vitro* plate assay with and without addition of 20 mM arginine demonstrated that arginine fermentation does provide sufficient energy to enable significant growth of the six *Pseudomonas* strains under anoxic conditions. Indeed, arginine was one of the most abundant amino acids in MS-media identified by HPLC analysis and is also highly abundant on red and white meat (440 $mmol*kg^{-1}$ protein on beef and 344 mmol/kg protein on chicken) (Wladyka and Dawson, 1968; Ahmad *et al.*, 2018). Furthermore, an increase in pH of the MS-media during the proteomic experiment was observed and the arginine deiminase test was positive for all strains in the API 20 NE test. Thus, arginine fermentation is expected to be a main metabolic pathway enabling anaerobic growth of the six meat-spoiling *Pseudomonas* species *in vitro* in MS-media but also *in situ* on anoxic packaged chicken meat.

Pyruvate fermentation to acetate. The third metabolic pathway described for *P. aeruginosa*, enabling long-term survival but no significant growth under anoxic conditions, is thought to be conversion of pyruvate to acetate providing one molecule of ATP (Eschbach *et al.*, 2004; Schreiber *et al.*, 2006). Therefore, the two enzymes phosphotransacetylase and acetate kinase are needed. However, none of these two enzymes could be identified in the genomes of the six meat-spoiling *Pseudomonas* strains, thus rejecting the hypothesis of acetate fermentation for long-term survival of *Pseudomonas* strains on chicken meat.

Glucose fermentation. However, besides the previously described anaerobic energy providing metabolic pathways of *P. aeruginosa*, the basic glucose metabolism of the six meat-spoiling *Pseudomonas* strains was investigated. According to Chavarría *et al.* (2013), *Pseudomonas* species either directly import glucose into the cell or convert glucose via a

membrane bound PQQ-dependent dehydrogenase enzyme to D-gluconate. Within the cell, D-gluconate can either be directly metabolized or converted to 2-ketogluconate. All of these three central metabolic intermediates, glucose, gluconate and 2-ketogluconate are ultimately shunted into the Entner-Doudoroff (ED) pathway, which further yields one molecule of ATP per glucose via the production of glycerinaldehyde-3-phosphate entering the Embden Meyerhof Parnas (EMP) pathway. Interestingly, a reduced expression of several enzymes under anoxic conditions was observed for the analyzed *Pseudomonas* species, which are involved in the interconversion of glucose to gluconate and 2-ketogluconate as well as degradation of those two metabolites to the precursor 6-phosphogluconate of the ED pathway. One major enzyme responsible for these observed protein regulations is expected to be the membrane bound PQQ-dependent dehydrogenase, converting glucose to gluconate by shuttling electrons into the respiratory chain (Umezawa *et al.*, 2015). As the respiratory chain is predictively dysfunctional for the analyzed strains under anoxic conditions, gluconate cannot be generated from glucose, explaining the reduced expression of downstream enzymes.

However, a constitutive expression of enzymes for glucose conversion to 6-phosphogluconate as well as enzymes of the ED pathway was measured for all *Pseudomonas* strains independent of the gas atmosphere. Thus, it can be supposed that glucose is directly converted by the analyzed *Pseudomonas* strains under anoxic conditions yielding ATP via the ED pathway coupled to the EMP pathway. This assumption is further supported by the observed enhanced expression of enzymes utilizing maltose, sucrose and amylose, yielding high amounts of D-glucose, under anoxic conditions. As glucose is mainly bound as di-, tri- and polysaccharides in meat (Komiyama *et al.*, 2008; Koutsidis *et al.*, 2008), this might explain the anaerobic growth of the strains on chicken meat. However, the physiological experiment with and without addition of glucose demonstrated that sole fermentation of glucose does not provide significant anaerobic growth of the meat-spoiling *Pseudomonas* strains under anoxic conditions. Furthermore, contrary to arginine fermentation, glucose fermentation depends on redox equivalents such as $NADH/H^+$, which have to be reoxidized to NAD^+ to maintain redox balance within the cell. Reoxidation of redox equivalents cannot be performed by anaerobic respiratory activity for the analyzed *Pseudomonas* strains and is thus predictively performed by pyruvate fermentation to ethanol, indicated by an enhanced expression of corresponding enzymes (aldehyde and alcohol dehydrogenases) under anoxic conditions. Thus, glucose metabolism via the Entner-Doudoroff pathway and NAD+ recycling by ethanolic formation can be assumed to enable long-term survival, but no growth, of the analyzed six *Pseudomonas* strains on chicken meat.

Glyoxylate shunt. The proteomic analysis of this study further revealed an enhanced expression of several enzymes of the glyoxylate shunt as well as a concomitant reduced

expression of bypassed enzymes of the TCA cycle for the analyzed *Pseudomonas* strains under anoxic conditions. Contrary to other pathways, the TCA cycle does not produce energy, but is important for the regeneration of redox equivalents needed for aerobe and anaerobe respiratory activity. Thus, a bypass of $NADH/H^+$ generating enzymes of the TCA cycle under anoxic conditions, where the respiratory chain is disabled, can be seen as a logical feedback reaction of the cell to maintain redox balance. However, this does not explain the enhanced expression of enzymes of the glyoxylate shunt, which is commonly known to be activated under carbon source limitation. In more detail, some bacteria are able to gain C5 or C6 compounds under conditions of carbon source limitations, by degradation of acetate and fatty acids to acetyl-CoA, which is shuttled into the glyoxylate shunt to obtain C4 compounds, which are further channelled into gluconeogenesis (Maloy *et al.*, 1980; Son *et al.*, 2007). Interestingly, an enhanced production of acetyl-CoA from fatty acid beta-oxidation as well as amino acid and poly-3-hydroxyalcanoate degradation under anoxic condition can be assumed for the analyzed *Pseudomonas* strains due to our proteomic study, as several corresponding enzymes showed an enhanced expression under this condition. This might be due to the relative low amounts of glucose (1.7 mM) in MS-media, forcing *Pseudomonas* species to also utilize the added tween80. However, no differential regulation of gluconeogenetic enzymes was observed for the analyzed *Pseudomonas* strains comparing oxic and anoxic conditions. Even though, other studies also observed an enhanced activation of the glyoxylate shunt under conditions of reduced or disabled respiration, concomitant with a bypass of $NADH/H^+$ generating enzymes (Tielen *et al.*, 2013; Ahn *et al.*, 2016; Meylan *et al.*, 2017), the actual function of the glyoxylate shunt under anoxic conditions still remains open.

Protein folding. Another metabolism exhibiting differential proteomic regulation under anoxic conditions comprised correct disulphide bond formation of polypeptide chains. In detail, an enhanced expression of the DsbA protein under anoxic conditions was observed for some of the six analyzed *Pseudomonas* strains. According to Collet and Bardwell (2002), DsbA is needed to shuttle the electrons released from disulphide bond formation to a terminal electron acceptor of the respiratory chain, thus reoxidizing DsbA. As enzymes for the usage of terminal electron acceptors (except for O_2) are missing for the six *Pseudomonas* strains, DsbA is predominantly kept in a reduced status, unable to performed correct disulphide bond formation. Thus, incorrect protein folding is supposed to occur for the analyzed *Pseudomonas* strains under anoxic conditions, which is induced by an imbalance of redox stress due to a dysfunction of respiratory chain. As a consequence, cells try to repair those incorrect folded proteins by isomerization of existing S-S bonds, what could be observed by an enhanced expression of thioredoxin, peroxiredoxin, cysteine hydrolases and S-S-oxide reductases for several of the analyzed *Pseudomonas* strains under anoxic conditions. Interestingly, the transcription factor OxyR, regulating thioredoxin and peroxiredoxin, also controls the transcription level of catalase

enzymes (Wei *et al.*, 2012), which might explain the observed enhanced expression of the catalase PHII for some of the *Pseudomonas* strains under anoxic conditions.

Concluding, based on physiological experiments as well as proteomic and genomic data, the observed anaerobic growth of the six *Pseudomonas* strains under strict anoxic conditions on chicken breast can be explained. Arginine fermentation was predicted to gain sufficient energy for significant anaerobic growth on chicken meat and glucose fermentation to ethanol via the ED and EMP pathway is assumed to enable long-term survival of the six *Pseudomonas* strains under conditions of O_2 exclusion. Anaerobic nitrate respiration and fermentation of glucose to acetate, as described for *P. aeruginosa*, could be excluded for the strains due to the absence of respective genes. Furthermore, this study highlights the problem of redox stress, triggered by an imbalance of redox equivalents such as NADH/NAD^+ due to missing respiratory activity, on important metabolic pathways of the analyzed *Pseudomonas* strains. A truncated TCA cycle, bypassing NADH/H+ generating enzymes as well as a restricted glucose metabolism was uncovered to be a consequence of intracellular redox stress. Furthermore, incorrect protein folding was predicted to occur under anoxic conditions, which is counteracted by an enhanced expression of refolding enzymes for the analyzed *Pseudomonas* strains. Thus, this study also complements the hitherto limited research on the general anaerobic metabolism of different *Pseudomonas* species.

6. Summary

This study analyzes the mutual interaction of modified atmosphere packaging gases and meat-spoiling bacteria, following the overall aim to complement the hitherto limited knowledge about the basic lifestyle and coexistence of spoilage bacteria on MAP meat as well as to validate a novel method, which enables to reduce the amount of discarded meat in industry. Firstly, a comparative proteomic study was employed, uncovering a set of metabolic adaptation mechanisms of five analyzed meat-spoiling bacteria to the industrial MAP gases O_2 and CO_2. Whereas the identified mechanisms were the same for all species, the implementation of those mechanisms was species-specific, comprising enhanced or reduced expression of different enzymes and metabolic pathways. Furthermore, it appears that bacteria differ regarding their resistance to MAP gases, exhibiting either intrinsic adaptation providing basic resistance (e.g. *L. gelidum* subspecies), resistance due to metabolic adaptation (e.g. *C. maltaromaticum*) or increased sensitivity, especially to CO_2, even though metabolic adaptation was conducted (e.g. *B. thermosphacta*, *C. divergens*). Based on these results, the inhibition of specific bacteria by industrially applied atmospheres could be derived. Whereas both *L. gelidum* subspecies and *C. maltaromaticum* TMW2.1581 appear to be resistant to the atmospheres 30% CO_2 / 70% O_2 and 30% CO_2 / 70% N_2, *B. thermosphacta* TMW2.2101 and *C. divergens* TMW2.1577 are predictively inhibited by latter atmosphere due to the presence of CO_2 and the absence of O_2. Furthermore, the coexistence of a complex spoilage community on MAP meat could be explained by uncovering the preferential (dependent on the atmosphere) and individual usage of different substrates for each species.

As a *vice versa* interaction, this study proves the metabolic activity of bacteria to be mainly responsible for observed headspace changes of MA packages during storage period. Therefore, the potential of single meat spoilers to consume oxygen was analyzed, and their contribution to headspace oxygen consumption of MA packages was validated. All bacteria consumed measurable amounts of atmospheric and dissolved oxygen, which was traced back to respiratory activity as well as single oxygen consuming enzymes. Furthermore, *B. thermosphacta* TMW2.2101 consumes 31-time more atmospheric oxygen compared to the other species, which could be traced back to its respiratory setting and high oxidative stress tolerance. Thus, it is expected that MA packages containing meat with a high microbial load of *B. thermosphacta* exhibit a faster decrement in the headspace oxygen compared to MA packages dominated by other ESOs. In a follow up study, monitoring the headspace oxygen consumption in PP-EVOH MAP trays with inoculated meat samples and an integrated oxygen sensor spot, the usage of the headspace oxygen content as an indicator to predict spoilage of MAP meat prior to its actual onset could be demonstrated. In detail, a decrease in the headspace oxygen at microbial cell counts, which were occurring prior to those leading to perceptible meat spoilage were detected. Thus, the novel sensor spot technology

of this study provides a fast and easy method, to individually evaluate the freshness of single MA meat packages. This enables individual sorting within retail, consequently reducing the amount of discarded meat.

Furthermore, the ability of commonly considered obligate aerobic meat-spoiling *Pseudomonas* species to grow under anoxic atmospheres, as applied in white meat packaging, was analyzed. This project was based on a previous study, demonstrating that some strains of the species *P. lundensis, P. weihenstephanensis* and *P. fragi* also occur on anoxic packaged meat, which would make them a hitherto underestimated spoilage organism of vacuum packaged and low oxygen MAP meat. Indeed, restricted growth on anoxic packaged chicken meat could be proven for certain strains of the species *P. lundensis, P. weihenstephanensis* and *P. fragi*, and their anaerobic energy metabolism was uncovered by a proteomic study. It is predicted that arginine fermentation via the ADI pathway provides sufficient energy to enable true anaerobic growth of those *Pseudomonas* strains, whereas glucose utilization coupled to ethanol production only enables long-term survival under anoxic conditions. However, even though limited anaerobic growth of certain *Pseudomonas* strains was proven in this study, their contribution to meat spoilage of anoxic packaged meat needs to be further studied in the future.

Taken together, obtained findings of this study help to understand microbiological safety of meat products provided by the application of industrial MAP gases and further mechanistically explain the lifestyle and coexistence of specific spoilers on MAP meat. Furthermore, an application of the sensor spot technology in meat industry can save millions of tons of discarded meat on global scale.

7. Zusammenfassung

Diese Arbeit untersucht die Wechselwirkung zwischen Schutzgasatmosphären und fleischverderbenden Mikroorganismen, mit dem übergeordneten Ziel, das bisher begrenzte Wissen zum grundlegenden Lebensstil sowie die Koexistenz dieser Bakterien auf MAP Fleisch zu ergänzen. Weiterhin, sollte eine neue Methode zur Reduzierung der Menge von weggeworfenem Fleisch in der Industrie validiert werden. Im ersten Abschnitt dieser Arbeit wurde dafür eine Proteinstoffwechselanalyse durchgeführt, welche eine Reihe von metabolischen Anpassungsmechanismen der fünf untersuchten fleischverderbenden Mikroorgansimen an die beiden industriell verwendeten Schutzgase Sauerstoff und Kohlenstoffdioxide aufdeckte. Interessanterweise waren die identifizierten Mechanismen für alle Spezies gleich, wohingegen die jeweilige Umsetzung der Strategie sich durch die erhöhte oder erniedrigte Expression von verschiedenen Enzymen und Stoffwechselwegen zwischen den Spezies unterschied. Weiterhin unterschieden sich die Bakterien hinsichtlich ihrer Resistenz zu MAP Gasen und wiesen entweder eine durch intrinsische Anpassung grundlegende Resistenz (beide *L. gelidum* Subspezies), Resistenz auf Grund von Anpassung (*C. maltaromaticum*) oder erhöhte Sensitivität, speziell gegenüber CO_2, trotz metabolischer Anpassung (*B. thermosphacta*, *C. divergens*) auf. Anhand dieser Ergebnisse wurde auf die Hemmung von Bakterien durch industriell verwendeter Gasatmosphären zurückgeschlossen. Während beide *L. gelidum* Subspezies und *C. maltaromaticum* TMW2.1581 resistent gegenüber den Atmosphären 30% CO_2 / 70% O_2 und 30% CO_2 / 70% N_2 sind, wird eine Hemmwirkung von letzterer Atmosphäre auf *B. thermosphacta* TMW2.2101 und *C. divergens* TMW2.1577 durch die Anwesenheit von CO_2 sowie Abwesenheit von O_2 vorhergesagt. Weiterhin konnte das gemeinschaftliche Zusammenleben einer komplexen Verderbs-Mikrobiota auf schutzgasverpacktem Fleisch, durch die Aufdeckung von präferierter (abhängig von der Atmosphäre) und individueller Nutzung von unterschiedlichen Substraten für jede Spezies erklärt werden.

Neben den Einfluss von Schutzgasatmosphären auf den Stoffwechsel von Bakterien, wird andersherum auch eine Veränderung der Gaszusammensetzung im Kopfraum von MAP Fleisch durch mikrobiellen Stoffwechsel vermutet. Deshalb galt der zweite Teil dieser Arbeit dem Nachweis sowie der Quantifizierung des Sauerstoffverbrauchs der fünf Mikroorganismen *in vitro* sowie *in situ* in MAP Fleisch. Alle Bakterien verbrauchten messbare Mengen an atmosphärischen und gelösten Sauerstoff, was auf ihre Atmungsketten Aktivität sowie einzelne sauerstoffzehrende Enzyme zurückgeführt werden konnte. Insbesondere die Spezies *B. thermosphacta* TMW2.2101 wies dabei eine einzigartige genetische Ausstattung von atmungsrelevanten Enzymen sowie eine hohe Toleranz gegenüber Wasserstoffperoxid auf, was eine 31-fach erhöhte Sauerstoffverbrauchsrate pro Zelle gegenüber den anderen untersuchten Mikroorganismen zur Folge hatte. Daraus lässt sich eine schnellere Abnahme

des Sauerstoffgehalts im Kopfraum von MAP Fleisch vermuten, wenn dieses von der Spezies *B. thermosphacta* dominiert wird, gegenüber MA Verpackungen die von anderen ESOs dominiert werden. In einer darauf aufbauenden Folgestudie, sollte die Anwendbarkeit einer neuen Methode zur Bewertung der Qualität des verpackten Fleisches durch Monitoring des Sauerstoffgehalts in MAP Verpackungen bewertet werden. Dazu wurde der Sauerstoffgehalt im Kopfraum mithilfe eines integrierten Sauerstoff Sensor Spots erfasst sowie eine Bewertung der Qualität des verpackten Fleischs über die Lagerzeit durchgeführt. Es konnte eine Abnahme des Sauerstoffgehalts im Kopfraum von MA Verpackungen vor dem Einsetzten des sensorisch wahrnehmbaren Verderbs gemessen werden, was eine Vorhersage der Haltbarkeit von einzelnen atmosphärisch verpackten Fleischprodukten ermöglicht ohne diese zu öffnen. Dies ermöglich das Sortieren von individuellen Schutzgasverpackungen im Einzelhandel und reduziert somit die Menge an unnötig weggeworfenen Fleisch Produkten.

Basierend auf einer vorrangegangenen Studie zum Vorkommen von *Pseudomonas* Spezies auf MAP Fleisch unter Abwesenheit von Sauerstoff, sollte im letzten Abschnitt dieser Arbeit das Wachstum jener Spezies auf Hühnchen Fleisch untersucht und ein potentieller anaerober Energiestoffwechsel mittels Proteinstoffwechselanalyse untersucht werden. Ein anaerobes Wachstum von Vertretern der Gattung *Pseudomonas* wurde bisher noch nicht für Fleisch besiedelnde Spezies beschrieben, wodurch ihre Rolle als Verderbnis Bakterien auf vakuumverpackten oder anoxisch Verpackten MAP Fleisch bislang unterschätzt wurde. Tatsächlich konnte ein begrenztes Wachstum einzelner Stämme der Spezies *P. lundensis, P. weihenstephanensis* and *P. fragi* unter anoxischen Bedingungen auf Hühnchen Fleisch gemessen werden, welches sich vermutlich auf die energetisch wertvolle Umsetzung der Aminosäure Arginine über den ADI Stoffwechselweg zurückführen lässt. Weiterhin wird vermutet, dass die Umsetzung von Glucose mit gekoppelter Produktion von Ethanol genug Energie für das Überdauern der *Pseudomonas* Stämme auf anoxischen MAP Fleisch liefert. Abschließend wird darauf hingewiesen, dass weitere Studien notwendig wären um den Beitrag dieser *Pseudomonas* Spezies am Verderb von anoxisch Verpackten Fleisch zu bestimmen.

Zusammenfassend, ermöglichen die Ergebnisse dieser Arbeit ein tieferes Verständnis der durch Schutzgasverpackungen gewährleisteten mikrobiologischen Sicherheit von Fleischprodukten und erklären den Lebensstil sowie die Koexistenz von spezifischen Verderbnis Bakterien auf MAP Fleisch. Des Weiteren kann die Anwendung der beschriebenen Sensor Spot Technologie in der Lebensmittelindustrie massiv zu Reduzierung von weltweit weggeworfenen Fleischprodukten beitragen.

8. References

Ahmad, H., and Marchello, J. (2006). Effect of gas atmosphere packaging on psychrotrophic growth and succession on steak surfaces. *Journal of Food Science* 54**,** 274-276.

Ahmad, R., Imran, A., and Hussain, M. (2018). "Nutritional Composition of Meat", in: *Meat Science and Nutrition.* (ed.) M.S. Arshad. (Rijeka: IntechOpen).

Ahn, S., Jung, J., Jang, I.-A., Madsen, E.L., and Park, W. (2016). Role of glyoxylate shunt in oxidative stress response. *The Journal of Biological Chemistry* 291**,** 11928-11938.

Aljasass, F. (2013). Assessment of the microbial, growth and chemical change in beef and lamb meat samples collected from supermarket and shops during the summer and winter seasons. *Research Journal of Recent Science* 2**,** 20-27.

Amanatidou, A., Smid, E.J., and Gorris, L.G. (1999). Effect of elevated oxygen and carbon dioxide on the surface growth of vegetable-associated micro-organisms. *Journal of Applied Microbiology* 86**,** 429-438.

Ana Beatriz, A., Marcondes Viana Da, S., and Suzana Caetano Da Silva, L. (2018). Lipid oxidation in meat: mechanisms and protective factors a review. *Food Science and Technology* 38**,** 1-15.

Angiuoli, S.V., Gussman, A., Klimke, W., Cochrane, G., Field, D., Garrity, G., Kodira, C.D., Kyrpides, N., Madupu, R., Markowitz, V., Tatusova, T., Thomson, N., and White, O. (2008). Toward an online repository of standard operating procedures (SOPs) for (meta)genomic annotation. *Omics : A Journal of Integrative Biology* 12**,** 137-141.

Ayres, J. (2007). Temperature relationships and some other characteristics of the microbial flora developing on refrigerated beef. *Journal of Food Science* 25**,** 1-18.

Aziz, R.K., Bartels, D., Best, A.A., Dejongh, M., Disz, T., Edwards, R.A., Formsma, K., Gerdes, S., Glass, E.M., Kubal, M., Meyer, F., Olsen, G.J., Olson, R., Osterman, A.L., Overbeek, R.A., Mcneil, L.K., Paarmann, D., Paczian, T., Parrello, B., Pusch, G.D., Reich, C., Stevens, R., Vassieva, O., Vonstein, V., Wilke, A., and Zagnitko, O. (2008). The RAST Server: Rapid annotations using subsystems technology. *BMC Genomics* 9**,** 75.

Babji, A., Ooi, P., and Abdullah, A. (1989). Determination of meat content in processed meats using currently available methods. *Pertanika* 12**,** 33-41.

Bajpai, P., and Bajpai, P.K. (1993). Eicosapentaenoic acid (EPA) production from microorganisms: a review. *Journal of Biotechnology* 30**,** 161-183.

Bala, K., Marshall, R.T., Stringer, W.C., and Naumann, H.D. (1977). Effect of *Pseudomonas fragi* on the color of beef. *Journal of Food Science* 42**,** 1176-1179.

Balamatsia, C.C., Paleologos, E.K., Kontominas, M.G., and Savvaidis, I.N. (2006). Correlation between microbial flora, sensory changes and biogenic aminesformation in fresh chicken meat stored aerobically or under modified atmosphere packaging at 4 °C: possible role of biogenic amines as spoilage indicators. *Antonie van Leeuwenhoek* 89**,** 9-17.

Balasubramanian, D., Harper, L., Shopsin, B., and Torres, V.J. (2017). *Staphylococcus aureus* pathogenesis in diverse host environments. *Pathogens and Disease* 75**,** ftx005.

Bankevich, A., Nurk, S., Antipov, D., Gurevich, A.A., Dvorkin, M., Kulikov, A.S., Lesin, V.M., Nikolenko, S.I., Pham, S., Prjibelski, A.D., Pyshkin, A.V., Sirotkin, A.V., Vyahhi, N., Tesler, G., Alekseyev, M.A., and Pevzner, P.A. (2012). SPAdes: a new genome assembly algorithm and its applications to single-cell sequencing. *Journal of Computational Biology* 19**,** 455-477.

Bartóak, T., Szalai, G., Lőrincz, Z.S., Bőurcsök, G., and Sági, F. (1994). High-speed RP-HPLC/FL analysis of amino acids after automated two-step derivatization with o-phthaldialdehyde/3-mercaptopropionic acid and 9-fluorenylmethyl chloroformate. *Journal of Liquid Chromatography* 17**,** 4391-4403.

Becker, Z.E. (1936). A comparison between the action of carbonic acid and other acids upon the living cell. *Protoplasma* 25**,** 161-175.

Behr, J., Gänzle, M.G., and Vogel, R.F. (2006). Characterization of a highly hop-resistant *Lactobacillus brevis* strain lacking hop transport. *Applied and Environmental Microbiology* 72**,** 6483-6492.

Belcher, J.N. (2006). Industrial packaging developments for the global meat market. *Meat Science* 74**,** 143-148.

Bellassi, P., Cappa, F., Fontana, A., and Morelli, L. (2020). Phenotypic and genotypic investigation of two representative strains of microbacterium species isolated from micro-filtered milk: Growth capacity and spoilage-potential assessment. *Frontiers in Microbiology* 11.

Blickstad, E., and Molin, G. (1983). Carbon dioxide as a controller of the spoilage flora of pork, with special reference to temperature and sodium chloride. *Journal of Food Protection* 46**,** 756-763.

Blickstad, E., and Molin, G. (1984). Growth and end-product formation in fermenter cultures of *Brochothrix thermosphacta* ATCC 11509T and two psychrotrophic *Lactobacillus* spp. in different gaseous atmospheres. *Journal of Applied Bacteriology* 57**,** 213-220.

Blombach, B., and Takors, R. (2015). CO_2 – Intrinsic product, essential substrate, and regulatory trigger of microbial and mammalian production processes. *Frontiers in Bioengineering and Biotechnology* 3.

Board, R.J. (1998). *Microbiology of meat and poultry.* eds. A.R. Davies & R.J. Board. New York: Springer.

Borch, E., Kant-Muermans, M.-L., and Blixt, Y. (1996). Bacterial spoilage of meat and cured meat products. *International Journal of Food Microbiology* 33**,** 103-120.

Borges, S., García De Fernando, G., Lopez‐Galvez, D., Selgas, M.D., García, M., Cambero, I., and Ordónez, J. (2007). Growth/survival of natural flora and *Listeria monocytogenes* on refrigerated uncooked pork and turkey packaged under modified atmospheres. *Journal of Food Safety* 15**,** 305-319.

Boskou, G., and Debevere, J. (1997). Reduction of trimethylamine oxide by *Shewanella spp*. under modified atmospheresin vitro. *Food Microbiology* 14**,** 543-553.

Bowman, J.P. (2006). "The Genus *Psychrobacter*," in *The Prokaryotes,* eds. M. Dworkin, S. Falkow, E. Rosenberg, K.-H. Schleifer & E. Stackebrandt. New York: Springer, 920-930.

Boyd, D.A., Cvitkovitch, D.G., Bleiweis, A.S., Kiriukhin, M.Y., Debabov, D.V., Neuhaus, F.C., and Hamilton, I.R. (2000). Defects in D-alanyl-lipoteichoic acid synthesis in

Streptococcus mutans results in acid sensitivity. *Journal of Bacteriology* 182**,** 6055-6065.

Brenes, A., and Roura, E. (2010). Essential oils in poultry nutrition: Main effects and modes of action. *Animal Feed Science and Technology* 158**,** 1-14.

Brisse, S., Grimont, F., and Grimont, P.a.D. (2006). "The genus *Klebsiella*," in *The Prokaryotes,* eds. M. Dworkin, S. Falkow, E. Rosenberg, K.-H. Schleifer & E. Stackebrandt. New York: Springer, 159-196.

Broda, D.M., Delacy, K.M., Bell, R.G., and Penney, N. (1996). Association of psychrotrophic *Clostridium spp*. with deep tissue spoilage of chilled vacuum-packed lamb. *International Journal of Food Microbiology* 29**,** 371-378.

Brooijmans, R., Smit, B., Santos, F., Van Riel, J., De Vos, W.M., and Hugenholtz, J. (2009). Heme and menaquinone induced electron transport in lactic acid bacteria. *Microbial Cell Factories* 8**,** 28-28.

Carlson, C.A., and Ingraham, J.L. (1983). Comparison of denitrification by *Pseudomonas stutzeri*, *Pseudomonas aeruginosa*, and *Paracoccus denitrificans*. *Applied and Environmental Microbiology* 45**,** 1247.

Casaburi, A., Nasi, A., Ferrocino, I., Di Monaco, R., Mauriello, G., Villani, F., and Ercolini, D. (2011). Spoilage-related activity of *Carnobacterium maltaromaticum* strains in air-stored and vacuum-packed meat. *Applied and Environmental Microbiology* 77**,** 7382-7393.

Casaburi, A., Piombino, P., Nychas, G.-J., Villani, F., and Ercolini, D. (2015). Bacterial populations and the volatilome associated to meat spoilage. *Food Microbiology* 45**,** 83-102.

Cavett, J. (2008). A diagnostic key for identifying the lactic acid bacteria of vacuum packed bacon. *Journal of Applied Microbiology* 26**,** 453-470.

Çelen, M., Söğüt, B., Zorba, Ö., Demirulus, H., and Tekeli, A. (2016). Comparison of normal and PSE turkey breast meat for chemical composition, pH, color, myoglobin, and drip loss. *Revista Brasileira de Zootecnia* 45**,** 441-444.

Chaix, E., Guillaume, C., and Guillard, V. (2014). Oxygen and carbon dioxide solubility and diffusivity in solid food matrices: A review of past and current knowledge. *Comprehensive Reviews in Food Science and Food Safety* 13**,** 261-286.

Chan, K.F., Le Tran, H., Kanenaka, R.Y., and Kathariou, S. (2001). Survival of clinical and poultry-derived isolates of *Campylobacter jejuni* at a low temperature (4 °C). *Applied and Environmental Microbiology* 67**,** 4186-4191.

Chan, W.K.M., Joo, S.-T., Faustman, C., Sun, Q.U.N., and Vieth, R. (1998). Effect of *Pseudomonas fluorescens* on beef discoloration and oxymyoglobin oxidation in vitro†. *Journal of Food Protection* 61**,** 1341-1346.

Chang, C.L., Jeong, J., Shin, J.H., Lee, E.Y., and Son, H.C. (1999). *Rahnella aquatilis* sepsis in an immunocompetent adult. *Journal of Clinical Microbiology* 37**,** 4161-4162.

Chavarría, M., Nikel, P.I., Pérez-Pantoja, D., and De Lorenzo, V. (2013). The Entner–Doudoroff pathway empowers *Pseudomonas putida* KT2440 with a high tolerance to oxidative stress. *Environmental Microbiology* 15**,** 1772-1785.

Chaves, R.D., Silva, A.R., Sant'ana, A.S., Campana, F.B., and Massaguer, P.R. (2012). Gas-producing and spoilage potential of *Enterobacteriaceae* and lactic acid bacteria isolated

from chilled vacuum-packaged beef. *International Journal of Food Science & Technology* 47**,** 1750-1756.

Cheah, K.S., and Cheah, A.M. (1971). Post-mortem changes in structure and function of ox muscle mitochondria. 1. Electron microscopic and polarographic investigations. *Journal of Bioenergetics* 2**,** 85-92.

Cheah, K.S., and Cheah, A.M. (1974). Properties of mitochondria from ox neck muscle after storage in situ. *International Journal of Biochemistry* 5**,** 753-760.

Chenoll, E., Macián, M.C., Elizaquível, P., and Aznar, R. (2007). Lactic acid bacteria associated with vacuum-packed cooked meat product spoilage: population analysis by rDNA-based methods. *Journal of Applied Microbiology* 102**,** 498-508.

Chmiel, M., Roszko, M., Adamczak, L., Florowski, T., and Pietrzak, D. (2019). Influence of storage and packaging method on chicken breast meat chemical composition and fat oxidation. *Poultry Science* 98**,** 2679-2690.

Chun, H.-N., Kim, B., and Shin, H.-S. (2014). Evaluation of a freshness indicator for quality of fish products during storage. *Food Science and Biotechnology* 23**,** 1719-1725.

Chung, K.T., Dickson, J.S., and Grouse, J.D. (1989). Attachment and proliferation of bacteria on meat. *Journal of Food Protection* 52**,** 173-177.

Ćirić, J., Janjić, J., Boskovic, M., Baltic, M., Dokmanovic, M., Đorđević, V., and Glamoclija, N. (2014). Survival *Yersinia enterocolitica* in ground pork meat in different packages. *Journal of Pure and Applied Microbiology* 8**,** 4317-4323.

Clark, D.S., and Lentz, C.P. (1973). Use of mixtures of carbon dioxide and oxygen for extending shelf-life of prepackaged fresh beef. *Canadian Institute of Food Science and Technology Journal* 6**,** 194-196.

Cobos, Á., Díaz, O., and Cheung, P.C.K. (2015). "Chemical composition of meat and meat products," in *Handbook of Food Chemistry,* ed. B.M. Mehta. Berlin, Heidelberg: Springer, 1-32.

Collet, J.-F., and Bardwell, J.C.A. (2002). Oxidative protein folding in bacteria. *Molecular Microbiology* 44**,** 1-8.

Cornforth, D., and Hunt, M.C. (2008). Low-oxygen packaging of fresh meat with carbon monoxide: Meat quality, microbiology, and safety. *AMSA White Paper Series* 2.

Cox, J., Neuhauser, N., Michalski, A., Scheltema, R.A., Olsen, J.V., and Mann, M. (2011). Andromeda: a peptide search engine integrated into the MaxQuant environment. *Journal of Proteome Research* 10**,** 1794-1805.

Crowley, K.M., Prendergast, D.M., Sheridan, J.J., and Mcdowell, D.A. (2010). The influence of storing beef aerobically or in vacuum packs on the shelf life of mince. *Journal of Applied Microbiology* 109**,** 1319-1328.

Cruz, A.T., Cazacu, A.C., and Allen, C.H. (2007). *Pantoea agglomerans*, a plant pathogen causing human disease. *Journal of Clinical Microbiology* 45**,** 1989-1992.

Csonka, L.N. (1989). Physiological and genetic responses of bacteria to osmotic stress. *Microbiology Reviews* 53**,** 121-147.

D'amico, S., Collins, T., Marx, J.-C., Feller, G., Gerday, C., and Gerday, C. (2006). Psychrophilic microorganisms: challenges for life. *EMBO reports* 7**,** 385-389.

Dainty, R.H., Edwards, R.A., Hibbard, C.M., and Marnewick, J.J. (1989). Volatile compounds associated with microbial growth on normal and high pH beef stored at chill temperatures. *Journal of Applied Bacteriology* 66**,** 281-289.

Dainty, R.H., and Hibbard, C.M. (1980). Aerobic metabolism of *Brochothrix thermosphacta* growing on meat surfaces and in laboratory media. *Journal of Applied Bacteriology* 48**,** 387-396.

Dainty, R.H., and Hibbard, C.M. (1983). Precursors of the major end products of aerobic metabolism of *Brochothrix thermosphacta*. *Journal of Applied Bacteriology* 55**,** 127-133.

Dainty, R.H., and Mackey, B.M. (1992). The relationship between the phenotypic properties of bacteria from chill-stored meat and spoilage processes. *Journal of Applied Bacteriology* 73**,** 103s-114s.

Daniels, J.A., Krishnamurthi, R., and Rizvi, S.S.H. (1985). A review of effects of carbon dioxide on microbial growth and food quality. *Journal of Food Protection* 48**,** 532-537.

Datta, A.R., and Benjamin, M.M. (1997). Factors controlling acid tolerance of *Listeria monocytogenes*: effects of nisin and other ionophores. *Applied and Environmental Microbiology* 63**,** 4123-4126.

Davies, A.R. (2003). "Modified atmospheres and vacuum packaging," in *Food Preservatives,* eds. N.J. Russell & G.W. Gould. Boston: Springer, 218-239.

De Bruyn, I.N., Holzapfel, W.H., Visser, L., and Louw, A.I. (1988). Glucose metabolism by *Lactobacillus divergens*. *Microbiology* 134**,** 2103-2109.

De Fernando, G.D.G., Nychas, G.J.E., Peck, M.W., and Ordóñez, J.A. (1995). Growth/survival of psychrotrophic pathogens on meat packaged under modified atmospheres. *International Journal of Food Microbiology* 28**,** 221-231.

De Filippis, F., La Storia, A., Villani, F., and Ercolini, D. (2013). Exploring the sources of bacterial spoilers in beefsteaks by culture-independent high-throughput sequencing. *PLoS One* 8**,** e70222.

De Filippis, F., La Storia, A., Villani, F., and Ercolini, D. (2019). Strain-level diversity analysis of *Pseudomonas fragi* after in situ pangenome reconstruction shows distinctive spoilage-associated metabolic traits clearly selected by different storage conditions. *Applied and Environmental Microbiology* 85**,** e02212-02218.

Değirmencioğlu, Esmer, O., Irkin, R., and Değirmencioğlu, A. (2012). Effects of vacuum and modified atmosphere packaging on shelf life extention of minced meat chemical and microbiological changes. *Journal of Animal and Veterinary Advances* 11**,** 898-911.

Devlieghere, F., and Debevere, J. (2000). Influence of dissolved carbon dioxide on the growth of spoilage bacteria. *LWT - Food Science and Technology* 33**,** 531-537.

Devlieghere, F., Debevere, J., and Van Impe, J. (1998). Effect of dissolved carbon dioxide and temperature on the growth of *Lactobacillus sake* in modified atmospheres. *International Journal of Food Microbiology* 41**,** 231-238.

Dhananjayan, R., Han, I.Y., Acton, J.C., and Dawson, P.L. (2006). Growth depth effects of bacteria in ground turkey meat patties subjected to high carbon dioxide or high oxygen atmospheres. *Poultry Science* 85**,** 1821-1828.

Dichristina, T.J., Bates, D.J., Burns, J.L., Dale, J.R., and Payne, A.N. (Year). "Shewanella: Novel strategies for anaerobic respiration", in: *Past and Present Water Column Anoxia*, ed. L.N. Neretin: Springer), 443-469.

Djenane, D., and Roncalés, P. (2018). Carbon monoxide in meat and fish packaging: Advantages and limits. *Foods* 7**,** 12.

Djenane, D., Sánchez-Escalante, A., Beltrán, J.A., and Roncalés, P. (2003). Extension of the shelf life of beef steaks packaged in a modified atmosphere by treatment with rosemary and displayed under UV-free lighting. *Meat Science* 64**,** 417-426.

Doulgeraki, A.I., Ercolini, D., Villani, F., and Nychas, G.-J.E. (2012). Spoilage microbiota associated to the storage of raw meat in different conditions. *International Journal of Food Microbiology* 157**,** 130-141.

Doyle, E. (2002). "Survival and growth of *Clostridium perfringens* during the cooling step of thermal processing of meat products", (ed.) F.R. Institute. (Madison: https://fri.wisc.edu/files/Briefs_File/cperfsurvivgrow.pdf).

Doyle, M.P. (1983). Effect of carbon dioxide on toxin production by *Clostridium botulinum*. *European Journal of Applied Microbiology and Biotechnology* 17**,** 53-56.

Drosinos, E.H., and Board, R.G. (1995). Microbial and physicochemical attributes of minced lamb: Sources of contamination with *Pseudomonads*. *Food Microbiology* 12**,** 189-197.

Duffes, F., Corre, C., Leroi, F., Dousset, X., and Boyaval, P. (1999). Inhibition of *Listeria monocytogenes* by in situ produced and semipurified bacteriocins of *Carnobacterium* spp. on vacuum-packed, refrigerated cold-smoked salmon. *Journal of Food Protection* 62**,** 1394-1403.

Duffy, E., Hearty, A.P., Gilsenan, M., and Gibney, M. (2006). Estimation of exposure to food packaging materials. 1: Development of a food-packaging database. *Food Additives and Contaminants* 23**,** 623-633.

Duport, C., Jobin, M., and Schmitt, P. (2016). Adaptation in *Bacillus cereus*: From stress to disease. *Frontiers in Microbiology* 7.

Dušková, M., Kameník, J., and Karpiskova, R. (2013). *Weissella viridescens* in meat products - A review. *Acta Veterinaria Brno* 82**,** 237-241.

Edwards, R.A., Dainty, R.H., Hibbard, C.M., and Ramantanis, S.V. (1987). Amines in fresh beef of normal pH and the role of bacteria in changes in concentration observed during storage in vacuum packs at chill temperatures. *Journal of Applied Bacteriology* 63**,** 427-434.

Ehrmann, M.A., Müller, M.R.A., and Vogel, R.F. (2003). Molecular analysis of sourdough reveals *Lactobacillus mindensis* sp. nov. *International Journal of Systematic and Evolutionary Microbiology* 53**,** 7-13.

Eilert, S.J. (2005). New packaging technologies for the 21st century. *Meat Science* 71**,** 122-127.

Eklund, T. (1984). The effect of carbon dioxide on bacterial growth and on uptake processes in bacterial membrane vesicles. *International Journal of Food Microbiology* 1**,** 179-185.

Eklund, T., and Jarmund, T. (1983). Microculture model studies on the effect of various gas atmospheres on microbial growth at different temperatures. *Journal of Applied Bacteriology* 55**,** 119-125.

Ellis, D.I., and Goodacre, R. (2001). Rapid and quantitative detection of the microbial spoilage of muscle foods: current status and future trends. *Trends in Food Science & Technology* 12**,** 414-424.

Endeward, V., Musa-Aziz, R., Cooper, G.J., Chen, L.M., Pelletier, M.F., Virkki, L.V., Supuran, C.T., King, L.S., Boron, W.F., and Gros, G. (2006). Evidence that aquaporin 1 is a major pathway for CO_2 transport across the human erythrocyte membrane. *Federation of American Societies for Experimental Biology* 20**,** 1974-1981.

Enfors, S.O., and Molin, G. (1980). Effect of high concentrations of carbon dioxide on growth rate of *Pseudomonas fragi*, *Bacillus cereus* and *Streptococcus cremoris*. *Journal of Applied Bacteriology* 48**,** 409-416.

Enfors, S.O., and Molin, G. (1981). The influence of temperature on the growth inhibitory effect of carbon dioxide on *Pseudomonas fragi* and *Bacillus cereus*. *Canadian Journal of Microbiology* 27**,** 15-19.

Ercolini, D., Ferrocino, I., Nasi, A., Ndagijimana, M., Vernocchi, P., La Storia, A., Laghi, L., Mauriello, G., Guerzoni, M.E., and Villani, F. (2011). Monitoring of microbial metabolites and bacterial diversity in beef stored under different packaging conditions. *Applied and Environmental Microbiology* 77**,** 7372-7381.

Ercolini, D., Russo, F., Nasi, A., Ferranti, P., and Villani, F. (2009). Mesophilic and psychrotrophic bacteria from meat and their spoilage potential *in vitro* and in beef. *Applied and Environmental Microbiology* 75**,** 1990-2001.

Ercolini, D., Russo, F., Torrieri, E., Masi, P., and Villani, F. (2006). Changes in the spoilage-related microbiota of beef during refrigerated storage under different packaging conditions. *Applied and Environmental Microbiology* 72**,** 4663-4671.

Erwin, J., and Bloch, K. (1964). Biosynthesis of unsaturated fatty acids in microorganisms. *Science* 143**,** 1006.

Eschbach, M., Schreiber, K., Trunk, K., Buer, J., Jahn, D., and Schobert, M. (2004). Long-term anaerobic survival of the opportunistic pathogen *Pseudomonas aeruginosa* via pyruvate fermentation. *Journal of Bacteriology* 186**,** 4596-4604.

Esmer, O.K., Irkin, R., Degirmencioglu, N., and Degirmencioglu, A. (2011). The effects of modified atmosphere gas composition on microbiological criteria, color and oxidation values of minced beef meat. *Meat Science* 88**,** 221-226.

Evans, J.B., Braddord, W.L., and Niven, C.F. (1955). Comments concerning the taxonomy of the genera *Micrococcus* and *Staphylococcus*. *International Journal of Systematic and Evolutionary Microbiology* 5**,** 61-66.

Evtushenko, L.I., and Takeuchi, M. (2006). "The family *Microbacteriaceae*," in *The Prokaryotes,* eds. M. Dworkin, S. Falkow, E. Rosenberg, K.-H. Schleifer & E. Stackebrandt. New York: Springer, 1020-1098.

Fadda, S., Chambon, C., Champomier-Vergès, M., Talon, R., and Vignolo, G. (2008). *Lactobacillus* role during conditioning of refrigerated and vacuum-packaged Argentinean meat. *Meat Science* 79**,** 603-610.

Fall, P.A., Leroi, F., Cardinal, M., Chevalier, F., and Pilet, M.F. (2010). Inhibition of *Brochothrix thermosphacta* and sensory improvement of tropical peeled cooked shrimp by *Lactococcus piscium* CNCM I-4031. *Letters in Applied Microbiology* 50**,** 357-361.

Farber, J.M. (1991). Microbiological aspects of modified-atmosphere packaging technology - A review. *Journal of Food Protection* 54**,** 58-70.

Feiner, G. (2006). "The microbiology of specific bacteria," in *Meat Products Handbook*. Cambridge: Woodhead Publishing, 595-615.

Feng, T., and Wang, J. (2020). Oxidative stress tolerance and antioxidant capacity of lactic acid bacteria as probiotic: a systematic review. *Gut Microbes* 12**,** 1801944.

Fewson, C.A., and Nicholas, D.J.D. (1961). Nitrate reductase from *Pseudomonas aeruginosa*. *Biochimica et Biophysica Acta* 49**,** 335-349.

Finn, T.J., Shewaramani, S., Leahy, S.C., Janssen, P.H., and Moon, C.D. (2017). Dynamics and genetic diversification of *Escherichia coli* during experimental adaptation to an anaerobic environment. *PeerJ Life & Environment* 5**,** e3244-e3244.

Fitzgerald, M., Papkovsky, D.B., Smiddy, M., Kerry, J.P., O'sullivan, C.K., Buckley, D.J., and Guilbault, G.G. (2001). Nondestructive monitoring of oxygen profiles in packaged foods using phase-fluorimetric oxygen sensor. *Journal of Food Science* 66**,** 105-110.

Foa (2020). "Food Outlook: Biannual report on global food markets june 2020". http://www.fao.org/3/ca9509en/CA9509EN.pdf).

Foegeding, P.M., and Busta, F.F. (1983). Effect of carbon dioxide, nitrogen and hydrogen gases on germination of *Clostridium botulinum* spores. *Journal of Food Protection* 46**,** 987-989.

Fogerty, A.C., Whitfield, F.B., Svoronos, D., and Ford, G.L. (1991). The composition of the fatty acids and aldehydes of the ethanolamine and choline phospholipids of various meats. *International Journal of Food Science & Technology* 26**,** 363-371.

Foster, J.W., and Davis, J.B. (1949). Carbon dioxide inhibition of anaerobic fumarate formation in the mold *Rhizopus nigricans*. *Archives of Biochemistry* 21**,** 135-142.

Francis, C.A., Obraztsova, A.Y., and Tebo, B.M. (2000). Dissimilatory metal reduction by the facultative anaerobe *Pantoea agglomerans* SP1. *Applied and Environmental Microbiology* 66**,** 543-548.

Franzke, C., Grosch, W., and Schieberle, P. (2008). *Allgemeines Lehrbuch der Lebensmittelchemie.* Hamburg, Germany: Behr's Verlag.

Frayn, K.N. (1983). Calculation of substrate oxidation rates in vivo from gaseous exchange. *Journal of Applied Physiology* 55**,** 628-634.

Fu, Q., Liu, R., Zhang, W., Li, Y., Wang, J., and Zhou, G.H. (2014). Effects of different packaging systems on beef tenderness through protein modifications. *Food and Bioprocess Technology* 8.

Fuertes-Perez, S., Hauschild, P., Hilgarth, M., and Vogel, R.F. (2019). Biodiversity of *Photobacterium* spp. isolated from meats. *Frontiers in Microbiology* 10.

Fuertes, G., Soto, I., Carrasco, R., Vargas, M., Sabattin, J., and Lagos, C. (2016). Intelligent packaging systems: Sensors and nanosensors to monitor food quality and safety. *Journal of Sensors* 2016**,** 4046061.

Fusco, V., Quero, G.M., Cho, G.-S., Kabisch, J., Meske, D., Neve, H., Bockelmann, W., and Franz, C.M.a.P. (2015). The genus *Weissella*: taxonomy, ecology and biotechnological potential. *Frontiers in Microbiology* 6**,** 155-155.

Gao, X., Xie, L., Wang, Z., Li, X., Luo, H., Ma, C., and Dai, R. (2013). Effect of postmortem time on the metmyoglobin reductase activity, oxygen consumption, and colour stability of different lamb muscles. *European Food Research and Technology* 236**,** 579-587.

Garip, S., Bozoglu, F., and Severcan, F. (2007). Differentiation of mesophilic and thermophilic bacteria with fourier transform infrared spectroscopy. *Applied Spectroscopy* 61**,** 186-192.

Garrity, G.M., Bell, J.A., and Lilburn, T. (2005). "*Pseudomonadales* Orla-Jensen 1921, 270^{AL}," in *Bergey's manual of systematic bacteriology,* ed. B. D.J. Boston: Springer 323-397.

Garsin, D.A. (2010). Ethanolamine utilization in bacterial pathogens: roles and regulation. *Nature Reviews Microbiology* 8**,** 290-295.

Gerday, C., Aittaleb, M., Arpigny, J.L., Baise, E., Chessa, J.P., Garsoux, G., Petrescu, I., and Feller, G. (1997). Psychrophilic enzymes: a thermodynamic challenge. *Biochimica et Biophysica Acta* 1342**,** 119-131.

Gil, A., G. Kroll, R., and Poole, R. (1992). The cytochrome composition of the meat spoilage bacterium *Brochothrix thermosphacta*: identification of cytochrome a_3- and d-type terminal oxidases under various conditions. *Archives of Microbiology* 158**,** 226-233.

Gill, A.O., and Gill, C.O. (2005). "Preservative packaging for fresh meats, poultry, and fin fish," in *Innovations in Food Packaging,* ed. J.H. Han. London: Academic Press, 204-226.

Gill, C.O. (1976). Substrate limitation of bacterial growth at meat surfaces. *Journal of Applied Bacteriology* 41**,** 401-410.

Gill, C.O., and Reichel, M.P. (1989). Growth of the cold-tolerant pathogens *Yersinia enterocolitica*, *Aeromonas hydrophila* and *Listeria monocytogenes* on high-pH beef packaged under vacuum or carbon dioxide. *Food Microbiology* 6**,** 223-230.

Gill, C.O., and Tan, K.H. (1979). Effect of carbon dioxide on growth of *Pseudomonas fluorescens*. *Applied and Environmental Microbiology* 38**,** 237-240.

Gill, C.O., and Tan, K.H. (1980). Effect of carbon dioxide on growth of meat spoilage bacteria. *Applied and Environmental Microbiology* 39**,** 317-319.

Godziszewska, J., Guzek, D., Pogorzelska, E., Brodowska, M., Górska-Horczyczak, E., Sakowska, A., Wojtasik-Kalinowska, I., Gantner, M., and Wierzbicka, A. (2017). A simple method of the detection of pork spoilage caused by *Rahnella aquatilis*. *LWT - Food Science and Technology* 84**,** 248-255.

Gopal, P. (2020). "Lactic acid bacteria: An overview," in *Reference Module in Food Science*. Oxford: Elsevier.

Gram, L., and Dalgaard, P. (2002). Fish spoilage bacteria--problems and solutions. *Current Opinion in Biotechnology* 13**,** 262-266.

Grau, F.H. (1983). Microbial growth on fat and lean surfaces of vacuum-packaged chilled beef. *Journal of Food Science* 48**,** 326-328.

Graumann, P., and Marahiel, M.A. (1996). Some like it cold: response of microorganisms to cold shock. *Archives of Microbiology* 166**,** 293-300.

Gribble, A., Mills, J., and Brightwell, G. (2014). The spoilage characteristics of *Brochothrix thermosphacta* and two psychrotolerant *Enterobacteriacae* in vacuum packed lamb and the comparison between high and low pH cuts. *Meat Science* 97**,** 83-92.

Guerzoni, M.E., Ferruzzi, M., Sinigaglia, M., and Criscuoli, G.C. (1997). Increased cellular fatty acid desaturation as a possible key factor in thermotolerance in *Saccharomyces cerevisiae*. *Canadian Journal of Microbiology* 43**,** 569-576.

Guerzoni, M.E., Lanciotti, R., and Cocconcelli, P.S. (2001). Alteration in cellular fatty acid composition as a response to salt, acid, oxidative and thermal stresses in *Lactobacillus helveticus*. *Microbiology* 147**,** 2255-2264.

Gupta, A., and Rao, G. (2003). A study of oxygen transfer in shake flasks using a non-invasive oxygen sensor. *Biotechnology Bioengineering* 84**,** 351-358.

Gustavsson, J., Cederberg, C., Sonesson, U., Van Otterdijk, R., and Meybeck, A. (2011). "Global food losses and food waste – Extent, causes and prevention.", (ed.) Fao. (Rome: http://www.fao.org/3/i2697e/i2697e.pdf).

Hamasaki, Y., Ayaki, M., Fuchu, H., Sugiyama, M., and Morita, H. (2003). Behavior of psychrotrophic lactic acid bacteria isolated from spoiling cooked meat products. *Applied and Environmental Microbiology* 69**,** 3668-3671.

Han, D., Mcmillin, K., and Godber, J. (2006). Hemoglobin, myoglobin, and total pigments in beef and chicken muscles: Chromatographic determination. *Journal of Food Science* 59**,** 1279-1282.

Hendricks, M.T., and Hotchkiss, J.H. (1997). Effect of carbon dioxide on the growth of *Pseudomonas fluorescens* and *Listeria monocytogenes* in aerobic atmospheres. *Journal of Food Protection* 60**,** 1548-1552.

Hernández-Macedo, M.L., Contreras-Castillo, C.J., Tsai, S.M., Da Cruz, S.H., Sarantopoulos, C.I.G.L., Padula, M., and Dias, C.T.S. (2012). Gases and volatile compounds associated with micro-organisms in blown pack spoilage of Brazilian vacuum-packed beef. *Letters in Applied Microbiology* 55**,** 467-475.

Hilgarth, M., Behr, J., and Vogel, R.F. (2018a). Monitoring of spoilage-associated microbiota on modified atmosphere packaged beef and differentiation of psychrophilic and psychrotrophic strains. *Journal of Applied Microbiology* 124**,** 740-753.

Hilgarth, M., Fuertes, S., Ehrmann, M., and Vogel, R.F. (2018b). *Photobacterium carnosum* sp. nov., isolated from spoiled modified atmosphere packaged poultry meat. *Systematic and Applied Microbiology* 41**,** 44-50.

Hilgarth, M., Lehner, E.M., Behr, J., and Vogel, R.F. (2019). Diversity and anaerobic growth of *Pseudomonas* spp. isolated from modified atmosphere packaged minced beef. *Journal of Applied Microbiology* 127**,** 159-174.

Hilgarth, M., Nani, M., and Vogel, R.F. (2018c). Assertiveness of meat-borne *Lactococcus piscium* strains and their potential for competitive exclusion of spoilage bacteria in situ and in vitro. *Journal of Applied Microbiology* 124**,** 1243-1253.

Hitchener, B.J., Egan, A.F., and Rogers, P.J. (1979). Energetics of *Microbacterium thermosphactum* in glucose-limited continuous culture. *Applied and Environmental Microbiology* 37**,** 1047-1052.

Hoffman, P.S., and Goodman, T.G. (1982). Respiratory physiology and energy conservation efficiency of *Campylobacter jejuni*. *Journal of Bacteriology* 150**,** 319.

Hofmeister, A.E., Albracht, S.P., and Buckel, W. (1994). Iron-sulfur cluster-containing L-serine dehydratase from *Peptostreptococcus asaccharolyticus*: correlation of the cluster type with enzymatic activity. *FEBS Letters* 351**,** 416-418.

Höll, L., Behr, J., and Vogel, R.F. (2016). Identification and growth dynamics of meat spoilage microorganisms in modified atmosphere packaged poultry meat by MALDI-TOF MS. *Food Microbiology* 60**,** 84-91.

Höll, L., Hilgarth, M., Geissler, A.J., Behr, J., and Vogel, R.F. (2019). Prediction of in situ metabolism of *Photobacteria* in modified atmosphere packaged poultry meat using metatranscriptomic data. *Microbiological Research* 222**,** 52-59.

Höll, L., Hilgarth, M., Geissler, A.J., Behr, J., and Vogel, R.F. (2020). Metatranscriptomic analysis of modified atmosphere packaged poultry meat enables prediction of *Brochothrix thermosphacta* and *Carnobacterium divergens* in situ metabolism. *Archives of Microbiology* 202**,** 1945-1955.

Holzapfel, W.H., and Gerber, E.S. (1983). *Lactobacillus divergens* sp. nov., a New heterofermentative *Lactobacillus* species producing L(+)-lactate. *Systematic and Applied Microbiology* 4**,** 522-534.

Hon, S.I., and Pyun, Y.R. (2001). Membrane damage and enzyme inactivation of *Lactobacillus plantarum* by high pressure CO_2 treatment. *International Journal of Food Microbiology* 63**,** 19-28.

Huptas, C., Scherer, S., and Wenning, M. (2016). Optimized Illumina PCR-free library preparation for bacterial whole genome sequencing and analysis of factors influencing de novo assembly. *BMC Research Notes* 9**,** 269-269.

Hussong, R.V., Long, H.F., and Hammer, B. 1937. Classification of the organisms important in dairy products II. *Pseudomonas fragi*. 20.

Imran, M., Desmasures, N., Coton, M., Coton, E., Le Flèche-Matéos, A., Irlinger, F., Delbès-Paus, C., Stahl, V., Montel, M.C., and Vernoux, J.P. (2019). Safety assessment of Gram-negative bacteria associated with traditional French cheeses. *Food Microbiology* 79**,** 1-10.

Ingram, M., and Dainty, R.H. (1971). Changes caused by microbes in spoilage of meats. *Journal of Applied Bacteriology* 34**,** 21-39.

Jääskeläinen, E., Hultman, J., Parshintsev, J., Riekkola, M.-L., and Björkroth, J. (2016). Development of spoilage bacterial community and volatile compounds in chilled beef under vacuum or high oxygen atmospheres. *International Journal of Food Microbiology* 223**,** 25-32.

Jaaskelainen, E., Johansson, P., Kostiainen, O., Nieminen, T., Schmidt, G., Somervuo, P., Mohsina, M., Vanninen, P., Auvinen, P., and Björkroth, J. (2013). Significance of heme-based respiration in meat spoilage caused by *Leuconostoc gasicomitatum*. *Applied and Environmental Microbiology* 79**,** 1078-1085.

Jääskeläinen, E., Vesterinen, S., Parshintsev, J., Johansson, P., Riekkola, M.-L., and Björkroth, J. (2015). Production of buttery-odor compounds and transcriptome response in *Leuconostoc gelidum* subsp. *gasicomitatum* LMG18811T during growth on various carbon sources. *Applied and Environmental Microbiology* 81**,** 1902-1908.

Jakobsen, M., and Bertelsen, G. (2000). Colour stability and lipid oxidation of fresh beef. Development of a response surface model for predicting the effects of temperature, storage time, and modified atmosphere composition. *Meat Science* 54**,** 49-57.

Jayasingh, P., Cornforth, D.P., Brennand, C.P., Carpenter, C.E., and Whittier, D.R. (2002). Sensory evaluation of ground beef stored in high-oxygen modified atmosphere packaging. *Journal of Food Science* 67**,** 3493-3496.

Jiang, Y., Gao, F., Xu, X.-L., Su, Y., Ye, K., and Zhou, G.H. (2010). Changes in the bacterial communities of vacuum-packaged pork during chilled storage analyzed by PCR–DGGE. *Meat Science* 86**,** 889-895.

Jofré, A., Garriga, M., and Aymerich, T. (2008). Inhibition of *Salmonella sp*. *Listeria monocytogenes* and *Staphylococcus aureus* in cooked ham by combining antimicrobials, high hydrostatic pressure and refrigeration. *Meat Science* 78**,** 53-59.

Johansson, P., Paulin, L., Sade, E., Salovuori, N., Alatalo, E.R., Björkroth, K.J., and Auvinen, P. (2011). Genome sequence of a food spoilage lactic acid bacterium, *Leuconostoc gasicomitatum* LMG 18811T, in association with specific spoilage reactions. *Applied and Environmental Microbiology* 77**,** 4344-4351.

Jørgensen, L.V., Huss, H.H., and Dalgaard, P. (2000). The effect of biogenic amine production by single bacterial cultures and metabiosis on cold-smoked salmon. *Journal of Applied Microbiology* 89**,** 920-934.

Juneja, V.K., Mohr, T.B., Silverman, M., and Snyder, O.P., Jr. (2018). Influence of cooling rate on growth of Bacillus cereus from spore inocula in cooked rice, beans, pasta, and combination products containing meat or poultry. *Journal of Food Protection* 81**,** 430-436.

Jung, S., Bae, Y.S., Yong, H.I., Lee, H.J., Seo, D.W., Park, H.B., Lee, J.H., and Jo, C. (2015). Proximate composition, and l-carnitine and betaine contents in meat from korean indigenous chicken. *Asian-Australasian Journal of Animal Sciences* 28**,** 1760-1766.

Kakouri, A., and Nychas, G.J. (1994). Storage of poultry meat under modified atmospheres or vacuum packs: possible role of microbial metabolites as indicator of spoilage. *Journal of Applied Bacteriology* 76**,** 163-172.

Kang, S.M., Kang, G., Seong, P., Park, B., and Cho, S. (2014). Effect of packaging method on the lipid oxidation, protein oxidation, and color in aged top round from hanwoo (Korean native cattle) during refrigerated storage. *Korean Journal for Food Science of Animal Resources* 34**,** 273-279.

Karpinets, T.V., Obraztsova, A.Y., Wang, Y., Schmoyer, D.D., Kora, G.H., Park, B.H., Serres, M.H., Romine, M.F., Land, M.L., Kothe, T.B., Fredrickson, J.K., Nealson, K.H., and Uberbacher, E.C. (2010). Conserved synteny at the protein family level reveals genes underlying *Shewanella* species' cold tolerance and predicts their novel phenotypes. *Functional & Integrative Genomics* 10**,** 97-110.

Kato, Y., Sakala, R.M., Hayashidani, H., Kiuchi, A., Kaneuchi, C., and Ogawa, M. (2000). *Lactobacillus algidus* sp. nov., a psychrophilic lactic acid bacterium isolated from vacuum-packaged refrigerated beef. *International Journal of Systematic and Evolutionary Microbiology* 50**,** 1143-1149.

Kaur, M., Shang, H., Tamplin, M., Ross, T., and Bowman, J.P. (2017). Culture-dependent and culture-independent assessment of spoilage community growth on VP lamb meat from packaging to past end of shelf-life. *Food Microbiology* 68**,** 71-80.

Kautsky, H. (1939). Quenching of luminescence by oxygen. *Transactions of the Faraday Society* 35**,** 216-219.

Kern, C.C., Vogel, R.F., and Behr, J. (2014). Differentiation of *Lactobacillus brevis* strains using matrix-assisted-laser-desorption-ionization-time-of-flight mass spectrometry with respect to their beer spoilage potential. *Food Microbiology* 40**,** 18-24.

Khoo, K.S., Chew, K.W., Yew, G.Y., Leong, W.H., Chai, Y.H., Show, P.L., and Chen, W.-H. (2020). Recent advances in downstream processing of microalgae lipid recovery for biofuel production. *Bioresource Technology* 304**,** 122996.

Kim, J.U., Ghafoor, K., Ahn, J., Shin, S., Lee, S.H., Shahbaz, H.M., Shin, H.-H., Kim, S., and Park, J. (2016). Kinetic modeling and characterization of a diffusion-based time-

temperature indicator (TTI) for monitoring microbial quality of non-pasteurized angelica juice. *LWT - Food Science and Technology* 67**,** 143-150.

King, A.D., and Nagel, C.W. (1967). Growth inhibition of a *Pseudomonas* by carbon dioxide. *Journal of Food Science* 32**,** 575-579.

King Jr, A.D., and Nagel, C.W. (1975). Influence of carbon dioxide upon the metabolism of *Pseudomonas aeruginosa*. *Journal of Food Science* 40**,** 362-366.

Klees, A.G., Linder, D., and Buckel, W. (1992). 2-hydroxyglutaryl-CoA dehydratase from *Fusobacterium nucleatum* (subsp. nucleatum): an iron-sulfur flavoprotein. *Archives of Microbiology* 158**,** 294-301.

Klotz, B., Mañas, P., and Mackey, B. (2010). The relationship between membrane damage, release of protein and loss of viability in *Escherichia coli* exposed to high hydrostatic pressure. *International Journal of Food Microbiology* 137**,** 214-220.

Kolbeck, S., Behr, J., Vogel, R., Ludwig, C., and Ehrmann, M. (2019). Acid stress response of *Staphylococcus xylosus* elicits changes in the proteome and cellular membrane. *Journal of Applied Microbiology* 126.

Komiyama, C., Mendes, A.A., Takahashi, S., Moreira, J., Garcia, R., Sanfelice, C., Borba, H., Leonel, F., Almeida Paz, I., and Balog, A. (2008). Chicken meat quality as a function of fasting period and water spray. *Brazilian Journal of Poultry Science* 10.

Koutsidis, G., Elmore, J.S., Oruna-Concha, M.J., Campo, M.M., Wood, J.D., and Mottram, D.S. (2008). Water-soluble precursors of beef flavour. Part II: Effect of post-mortem conditioning. *Meat Science* 79**,** 270-277.

Koutsoumanis, K., Stamatiou, A., Skandamis, P., and Nychas, G.J.E. (2006). Development of a microbial model for the combined effect of temperature and pH on spoilage of ground meat, and validation of the model under dynamic temperature conditions. *Applied and Environmental Microbiology* 72**,** 124.

Koutsoumanis, K.P., Stamatiou, A.P., Drosinos, E.H., and Nychas, G.J. (2008). Control of spoilage microorganisms in minced pork by a self-developed modified atmosphere induced by the respiratory activity of meat microflora. *Food Microbiology* 25**,** 915-921.

Kranert, M., Hafner, G., Barabosz, J., Schuller, H., Leverenz, D., Kölbig, A., Schneider, F., Lebersorger, S., and Scherhaufer, S. (2012). "Ermittlung der Mengen weggeworfener Lebensittel und Hauptursachen für die Entstehung von Lebensmittelabfällen in Deutschland". (Berlin: https://www.bmel.de/SharedDocs/Downloads/DE/_Ernaehrung/Lebensmittelverschwendung/Studie_Lebensmittelabfaelle_Langfassung.pdf?__blob=publicationFile&v=3).

Kuswandi, B., Jayus, Oktaviana, R., Abdullah, A., and Heng, L.Y. (2014). A novel on-package sticker sensor based on methyl red for real-time monitoring of broiler chicken cut freshness. *Packaging Technology and Science* 27**,** 69-81.

Lacroce, S.J., Wilson, M.N., Romanowski, J.E., Newman, J.D., Jhanji, V., Shanks, R.M.Q., and Kowalski, R.P. (2019). *Moraxella nonliquefaciens* and *M. osloensis* are important *Moraxella s*pecies that cause ocular infections. *Microorganisms* 7**,** 163.

Lai, B., Yu, S., Bernhardt, P.V., Rabaey, K., Virdis, B., and Krömer, J.O. (2016). Anoxic metabolism and biochemical production in *Pseudomonas putida* F1 driven by a bioelectrochemical system. *Biotechnology for Biofuels* 9**,** 39-39.

Lalucat, J., Bennasar, A., Bosch, R., García-Valdés, E., and Palleroni, N.J. (2006). Biology of *Pseudomonas stutzeri*. *Microbiology and Molecular Biology reviews : MMBR* 70**,** 510-547.

Lambert, A.D., Smith, J.P., and Dodds, K.L. (1991). Shelf life extension and microbiological safety of fresh meat — a review. *Food Microbiology* 8**,** 267-297.

Lammarino, M., and Di Taranto, A. (2012). Nitrite and nitrate in fresh meats: a contribution to the estimation of admissible maximum limits to introduce in directive 95/2/EC. *International Journal of Food Science & Technology* 47**,** 1852-1858.

Larrouture, C., Ardaillon, V., Pépin, M., and Montel, M.C. (2000). Ability of meat starter cultures to catabolize leucine and evaluation of the degradation products by using an HPLC method. *Food Microbiology* 17**,** 563-570.

Laursen, B.G., Bay, L., Cleenwerck, I., Vancanneyt, M., Swings, J., Dalgaard, P., and Leisner, J.J. (2005). *Carnobacterium divergens* and *Carnobacterium maltaromaticum* as spoilers or protective cultures in meat and seafood: phenotypic and genotypic characterization. *Systematic and Applied Microbiology* 28**,** 151-164.

Laursen, B.G., Leisner, J.J., and Dalgaard, P. (2006). *Carnobacterium* species: Effect of metabolic activity and interaction with *Brochothrix thermosphacta* on sensory characteristics of modified atmosphere packed shrimp. *Journal of Agricultural and Food Chemistry* 54**,** 3604-3611.

Lechardeur, D., Cesselin, B., Fernandez, A., Lamberet, G., Garrigues, C., Pedersen, M., Gaudu, P., and Gruss, A. (2011). Using heme as an energy boost for lactic acid bacteria. *Current Opinion in Biotechnology* 22**,** 143-149.

Lee, D.A., and Collins, E.B. (1976). Influences of temperature on growth of *Streptococcus cremoris* and *Streptococcus lactis*. *Journal of Dairy Science* 59**,** 405-409.

Leisner, J.J., Greer, G.G., Dilts, B.D., and Stiles, M.E. (1995). Effect of growth of selected lactic acid bacteria on storage life of beef stored under vacuum and in air. *International Journal of Food Microbiology* 26**,** 231-243.

Leisner, J.J., Laursen, B.G., Prévost, H., Drider, D., and Dalgaard, P. (2007). *Carnobacterium*: positive and negative effects in the environment and in foods. *FEMS Microbiology Reviews* 31**,** 592-613.

Leroi, F., Cornet, J., Chevalier, F., Cardinal, M., Coeuret, G., Chaillou, S., and Joffraud, J.-J. (2015). Selection of bioprotective cultures for preventing cold-smoked salmon spoilage. *International Journal of Food Microbiology* 213**,** 79-87.

Li, X., Fang, P., Mai, J., Choi, E.T., Wang, H., and Yang, X.-F. (2013). Targeting mitochondrial reactive oxygen species as novel therapy for inflammatory diseases and cancers. *Journal of Hematology & Oncology* 6**,** 19-19.

Liang, P., Fang, X., Hu, Y., Yuan, M., Raba, D.A., Ding, J., Bunn, D.C., Sanjana, K., Yang, J., Rosas-Lemus, M., Häse, C.C., Tuz, K., and Juárez, O. (2020). The aerobic respiratory chain of *Pseudomonas aeruginosa* cultured in artificial urine media: Role of NQR and terminal oxidases. *PLoS One* 15**,** e0231965.

Liebl, W. (2006). "Corynebacterium--Nonmedical," in *The Prokaryotes,* eds. M. Dworkin, S. Falkow, E. Rosenberg, K.-H. Schleifer & E. Stackebrandt. New York: Springer, 796-818.

Lindgren, J.K., Thomas, V.C., Olson, M.E., Chaudhari, S.S., Nuxoll, A.S., Schaeffer, C.R., Lindgren, K.E., Jones, J., Zimmerman, M.C., Dunman, P.M., Bayles, K.W., and Fey,

P.D. (2014). Arginine deiminase in *Staphylococcus epidermidis* functions to augment biofilm maturation through pH homeostasis. *Journal of Bacteriology* 196**,** 2277-2289.

Line, L., Alhede, M., Kolpen, M., Kühl, M., Ciofu, O., Bjarnsholt, T., Moser, C., Toyofuku, M., Nomura, N., Høiby, N., and Jensen, P.Ø. (2014). Physiological levels of nitrate support anoxic growth by denitrification of *Pseudomonas aeruginosa* at growth rates reported in cystic fibrosis lungs and sputum. *Frontiers in Microbiology* 5**,** 554-554.

Love, J.D., and Pearson, A.M. (1971). Lipid oxidation in meat and meat products—A review. *Journal of the American Oil Chemists' Society* 48**,** 547-549.

Lu, C.D., Winteler, H., Abdelal, A., and Haas, D. (1999). The ArgR regulatory protein, a helper to the anaerobic regulator ANR during transcriptional activation of the arcD promoter in *Pseudomonas aeruginosa*. *Journal of Bacteriology* 181**,** 2459-2464.

Macaskie, L.E., Sheard, A.G., Dainty, R.H., and Henderson, P.J. (1984). Glycerol utilization by *Brochothrix thermosphacta*. *Journal of Applied Bacteriology* 56**,** 137-143.

Macé, S., Joffraud, J.-J., Cardinal, M., Malcheva, M., Cornet, J., Lalanne, V., Chevalier, F., Sérot, T., Pilet, M.-F., and Dousset, X. (2013). Evaluation of the spoilage potential of bacteria isolated from spoiled raw salmon (*Salmo salar*) fillets stored under modified atmosphere packaging. *International Journal of Food Microbiology* 160**,** 227-238.

Madamanchi, N.R., and Runge, M.S. (2007). Mitochondrial dysfunction in atherosclerosis. *Circulation Research* 100**,** 460-473.

Maloy, S.R., Bohlander, M., and Nunn, W.D. (1980). Elevated levels of glyoxylate shunt enzymes in *Escherichia coli* strains constitutive for fatty acid degradation. *Journal of Bacteriology* 143**,** 720-725.

Man, J., Rogosa, M.A., and Sharpe, M. (2008). A medium for the cultivation of *Lactobacilli*. *Journal of Applied Microbiology* 23**,** 130-135.

Mancini, R.A., and Hunt, M.C. (2005). Current research in meat color. *Meat Science* 71**,** 100-121.

Mantini, D., Petrucci, F., Pieragostino, D., Del Boccio, P., Sacchetta, P., Candiano, G., Ghiggeri, G.M., Lugaresi, A., Federici, G., Di Ilio, C., and Urbani, A. (2010). A computational platform for MALDI-TOF mass spectrometry data: Application to serum and plasma samples. *Journal of Proteomics* 73**,** 562-570.

Margesin, R., and Schinner, F. (1994). Properties of cold-adapted microorganisms and their potential role in biotechnology. *Journal of Biotechnology* 33**,** 1-14.

Marquis, R.E., Bender, G.R., Murray, D.R., and Wong, A. (1987). Arginine deiminase system and bacterial adaptation to acid environments. *Applied and Environmental Microbiology* 53**,** 198-200.

Martínez, L., Djenane, D., Cilla, I., Beltrán, J.A., and Roncalés, P. (2005). Effect of different concentrations of carbon dioxide and low concentration of carbon monoxide on the shelf-life of fresh pork sausages packaged in modified atmosphere. *Meat Science* 71**,** 563-570.

Masson, F., Johansson, G., and Montel, M.C. (1999). Tyramine production by a strain of *Carnobacterium divergens* inoculated in meat–fat mixture. *Meat Science* 52**,** 65-69.

Matamoros, S., Pilet, M.F., Gigout, F., Prévost, H., and Leroi, F. (2009). Selection and evaluation of seafood-borne psychrotrophic lactic acid bacteria as inhibitors of pathogenic and spoilage bacteria. *Food Microbiology* 26**,** 638-644.

Matindoust, S., Baghaei-Nejad, M., Abadi, M.H.S., Zou, Z., and Zheng, L. (2016). Food quality and safety monitoring using gas sensor array in intelligent packaging. *Sensor Review* 36**,** 169-183.

Mcevoy, A., Von Bueltzingsloewen, C., Mcdonagh, C., Maccraith, B., Klimant, I., and Wolfbeis, O. (2003). Optical sensors for application in intelligent food-packaging technology. *Optics and Photonics Technologies and Applications* 4876.

Mcmillin, K.W. (2008). Where is MAP Going? A review and future potential of modified atmosphere packaging for meat. *Meat Science* 80**,** 43-65.

Mcmillin, K.W., Huang, N.Y., Ho, C.P., and Smith, B.S. (1999). "Quality and shelf-life of meat in case-ready modified atmosphere packaging," in *Quality Attributes of Muscle Foods,* eds. Y.L. Xiong, H. Chi-Tang & F. Shahidi. Boston: Springer.

Mebrouk, K., Prévost, H., Henni, D., Diviès, C., and Oran, E.-S. (2008). Carbon dioxide production by *Leuconostoc mesenteroides g*rown in single and mixed culture with *Lactococcus lactis* in skimmed milk. *Scientific Research and Essays* 4.

Mellor, G.E., Bentley, J.A., and Dykes, G.A. (2011). Evidence for a role of biosurfactants produced by *Pseudomonas fluorescens* in the spoilage of fresh aerobically stored chicken meat. *Food Microbiology* 28**,** 1101-1104.

Meng, X., Kim, S., Puligundla, P., and Ko, S. (2014). Carbon dioxide and oxygen gas sensors-possible application for monitoring quality, freshness, and safety of agricultural and food products with emphasis on importance of analytical signals and their transformation. *Journal of the Korean Society for Applied Biological Chemistry* 57**,** 723-733.

Mercenier, A., Simon, J.P., Vander Wauven, C., Haas, D., and Stalon, V. (1980). Regulation of enzyme synthesis in the arginine deiminase pathway of *Pseudomonas aeruginosa*. *Journal of Bacteriology* 144**,** 159-163.

Meredith, H., Valdramidis, V., Rotabakk, B.T., Sivertsvik, M., Mcdowell, D., and Bolton, D.J. (2014). Effect of different modified atmospheric packaging (MAP) gaseous combinations on *Campylobacter* and the shelf-life of chilled poultry fillets. *Food Microbiology* 44**,** 196-203.

Meylan, S., Porter, C.B.M., Yang, J.H., Belenky, P., Gutierrez, A., Lobritz, M.A., Park, J., Kim, S.H., Moskowitz, S.M., and Collins, J.J. (2017). Carbon sources tune antibiotic susceptibility in *Pseudomonas aeruginosa* via tricarboxylic acid cycle control. *Cell Chemical Biology* 24**,** 195-206.

Mills, A. (1997). Optical oxygen sensors: Utilising the luminescence of platinum metals complexes. *Platinum Metals Review* 41**,** 115-127.

Missner, A., Kügler, P., Saparov, S.M., Sommer, K., Mathai, J.C., Zeidel, M.L., and Pohl, P. (2008). Carbon dioxide transport through membranes. *The Journal of Biological Chemistry* 283**,** 25340-25347.

Molin, G. (1983). The resistance to carbon dioxide of some food related bacteria. *European Journal of Applied Microbiology and Biotechnology* 18**,** 214-217.

Molin, G., Ternström, A., and Ursing, J. (1986). Notes: *Pseudomonas lundensis,* a new bacterial species isolated from meat. *International Journal of Systematic and Evolutionary Microbiology* 36**,** 339-342.

Morey, A., and Singh, M. (2012). Low-temperature survival of *Salmonella spp*. in a model food system with natural microflora. *Foodborne Pathogens and Disease* 9**,** 218-223.

Motoyama, M., Kobayashi, M., Sasaki, K., Nomura, M., and Mitsumoto, M. (2010). *Pseudomonas* spp. convert metmyoglobin into deoxymyoglobin. *Meat Science* 84**,** 202-207.

Nicol, D.J., Shaw, M.K., and Ledward, D.A. (1970). Hydrogen sulfide production by bacteria and sulfmyoglobin formation in prepacked chilled beef. *Appl Microbiol* 19**,** 937-939.

Nieminen, T.T., Vihavainen, E., Paloranta, A., Lehto, J., Paulin, L., Auvinen, P., Solismaa, M., and Bjorkroth, K.J. (2011). Characterization of psychrotrophic bacterial communities in modified atmosphere-packed meat with terminal restriction fragment length polymorphism. *International Journal of Food Microbiology* 144**,** 360-366.

Nopwinyuwong, A., Trevanich, S., and Suppakul, P. (2010). Development of a novel colorimetric indicator label for monitoring freshness of intermediate-moisture dessert spoilage. *Talanta* 81**,** 1126-1132.

Nortjé, G.L., Nel, L., Jordaan, E., Badenhorst, K., Goedhart, E., and Holzapfel, W.H. (1990). The aerobic psychrotrophic populations on meat and meat contact surfaces in a meat production system and on meat stored at chill temperatures. *Journal of Applied Bacteriology* 68**,** 335-344.

Nychas, G.-J.E., Marshall, D.L., and Sofos, J.N. (2007). "Meat, Poultry, and Seafood," in *Food Microbiology: Fundamentals and Frontiers,* eds. D.M. P. & L.R. Beuchat. Washington: American Society of Microbiology.

Nychas, G.-J.E., Skandamis, P.N., Tassou, C.C., and Koutsoumanis, K.P. (2008). Meat spoilage during distribution. *Meat Science* 78**,** 77-89.

O'grady, M.N., Monahan, F.J., Burke, R.M., and Allen, P. (2000). The effect of oxygen level and exogenous α-tocopherol on the oxidative stability of minced beef in modified atmosphere packs. *Meat Science* 55**,** 39-45.

Oblakova, M., Ribarski, S., Oblakov, N., and Hristakieva, P. (2016). Chemical composition and quality of turkey - broiler meat from crosses of layer light (LL) and meat heavy (MH) turkey. *Trakia Journal of Science* 14**,** 142-147.

Olivares, A., Dryahina, K., Spanel, P., and Flores, M. (2012). Rapid detection of lipid oxidation in beef muscle packed under modified atmosphere by measuring volatile organic compounds using SIFT-MS. *Food Chemistry* 135**,** 1801-1808.

Ordonez, J.A., De Pablo, B., Perez De Castro, B., Asensio, M.A., and Sanz, B. (1991). Selected chemical and microbiological changes in refrigerated pork stored in carbon dioxide and oxygen enriched atmospheres. *Journal of Agricultural and Food Chemistry* 39**,** 668-672.

Overbeek, R., Olson, R., Pusch, G.D., Olsen, G.J., Davis, J.J., Disz, T., Edwards, R.A., Gerdes, S., Parrello, B., Shukla, M., Vonstein, V., Wattam, A.R., Xia, F., and Stevens, R. (2014). The SEED and the rapid annotation of microbial genomes using subsystems technology (RAST). *Nucleic Acids Research* 42**,** D206-D214.

Özen, A.I., and Ussery, D.W. (2012). Defining the *Pseudomonas* genus: where do we draw the line with Azotobacter? *Microbial Ecology* 63**,** 239-248.

Padmaperuma, G., Kapoore, R.V., Gilmour, D.J., and Vaidyanathan, S. (2018). Microbial consortia: a critical look at microalgae co-cultures for enhanced biomanufacturing. *Critical Reviews in Biotechnology* 38**,** 690-703.

Palumbo, S., Morgan, D., and Buchanan, R. (2006). Influence of temperature, NaCl, and pH on the growth of *Aeromonas hydrophila*. *Journal of Food Science* 50**,** 1417-1421.

Panoff, J.M., Corroler, D., Thammavongs, B., and Boutibonnes, P. (1997). Differentiation between cold shock proteins and cold acclimation proteins in a mesophilic gram-positive bacterium, *Enterococcus faecalis* JH2-2. *Journal of Bacteriology* 179**,** 4451-4454.

Parasassi, T. (1990). Phase fluctuation in phospholipid membranes revealed by Laurdan fluorescence. *Biophysical Journal* 57**,** 1179.

Parasassi, T., Conti, F., and Gratton, E. (1986). Time-resolved fluorescence emission spectra of Laurdan in phospholipid vesicles by multifrequency phase and modulation fluorometry. *Cellular and Molecular Biology* 32**,** 103-108.

Parte, A.C. (2018). LPSN – List of prokaryotic names with standing in nomenclature (bacterio.net), 20 years on. *International Journal of Systematic and Evolutionary Microbiology* 68**,** 1825-1829.

Parte, A.C., Sardà Carbasse, J., Meier-Kolthoff, J.P., Reimer, L.C., and Göker, M. (2020). List of prokaryotic names with standing in nomenclature (LPSN) moves to the DSMZ. *International Journal of Systematic and Evolutionary Microbiology* 70**,** 5607-5612.

Patterson, M.J. (1996). "Chapter 13. Streptococcus," in *Medical Microbiology,* ed. S. Baron. Galveston: University of Texas Medical Branch at Galveston.

Pedersen, M.B., Gaudu, P., Lechardeur, D., Petit, M.A., and Gruss, A. (2012). Aerobic respiration metabolism in lactic acid bacteria and uses in biotechnology. *Annual Review of Food Science and Technology* 3**,** 37-58.

Pennacchia, C., Ercolini, D., and Villani, F. (2011). Spoilage-related microbiota associated with chilled beef stored in air or vacuum pack. *Food microbiology* 28**,** 84-93.

Perrella, M., Bresciani, D., and Rossi-Bernardi, L. (1975). The binding of CO_2 to human hemoglobin. *The Journal of Biological Chemistry* 250**,** 5413-5418.

Pichner, R., Schönheit, C., Kabisch, J., Böhnlein, C., Rabsch, W., Beutin, L., and Gareis, M. (2014). Assessment of microbiological quality and safety of marinated pork products from German retail during shelf life. *Food Control* 46**,** 18-25.

Pin, C., Garcia De Fernando, G.D., and Ordonez, J.A. (2002). Effect of modified atmosphere composition on the metabolism of glucose by *Brochothrix thermosphacta*. *Applied and Environmental Microbiology* 68**,** 4441-4447.

Portela, C.a.F., Smart, K.F., Tumanov, S., Cook, G.M., and Villas-Bôas, S.G. (2014). Global metabolic response of *Enterococcus faecalis* to oxygen. *Journal of Bacteriology* 196**,** 2012-2022.

Prb (2020). "World population data sheet". https://www.prb.org/2020-world-population-data-sheet/).

Prieto, M., García, M.L., García, M.R., Otero, A., and Moreno, B. (1991). Distribution and evolution of bacteria on lamb carcasses during aerobic storage. *Journal of Food Protection* 54**,** 945-949.

Qian, H., Li, W., Guo, L., Tan, L., Liu, H., Wang, J., Pan, Y., and Zhao, Y. (2020). Stress response of *Vibrio parahaemolyticus* and *Listeria monocytogenes* biofilms to different modified atmospheres. *Frontiers in Microbiology* 11.

Quintieri, L., Giribaldi, M., Giuffrida, M.G., Creanza, T.M., Ancona, N., Cavallarin, L., De Angelis, M., and Caputo, L. (2018). Proteome response of *Staphylococcus xylosus* DSM 20266T to anaerobiosis and nitrite exposure. *Frontiers in Microbiology* 9.

Rahkila, R., De Bruyne, K., Johansson, P., Vandamme, P., and Björkroth, J. (2014). Reclassification of *Leuconostoc gasicomitatum* as *Leuconostoc gelidum* subsp. *gasicomitatum* comb. nov., description of *Leuconostoc gelidum* subsp. *aenigmaticum* subsp. nov., designation of *Leuconostoc gelidum* subsp. *gelidum* subsp. nov. and emended description of *Leuconostoc gelidum*. *International Journal of Systematic and Evolutionary Microbiology* 64**,** 1290-1295.

Rahkila, R., Nieminen, T., Johansson, P., Sade, E., and Björkroth, J. (2012). Characterization and evaluation of the spoilage potential of *Lactococcus piscium* isolates from modified atmosphere packaged meat. *International Journal of Food Microbiology* 156**,** 50-59.

Raposo, A., Pèrez, E., Faria, C., Ferrús, M., and Carrascosa Iruzubieta, C. (2017). "Food Spoilage by *Pseudomonas* spp.-An Overview," in *Foodborne Pathogens and Antibiotic Resistance,* ed. O.V. Singh. New York: Wiley, 41-71.

Ravcheev, D.A., Gerasimova, A.V., Mironov, A.A., and Gelfand, M.S. (2007). Comparative genomic analysis of regulation of anaerobic respiration in ten genomes from three families of gamma-proteobacteria (*Enterobacteriaceae*, *Pasteurellaceae*, *Vibrionaceae*). *BMC Genomics* 8**,** 54.

Reitermayer, D., Kafka, T.A., Lenz, C.A., and Vogel, R.F. (2018). Interrelation between tween and the membrane properties and high pressure tolerance of *Lactobacillus plantarum*. *BMC Microbiology* 18**,** 72.

Ridell, J., and Korkeala, H. (1997). Minimum growth temperatures of *Hafnia alvei* and other *Enterobacteriaceae* isolated from refrigerated meat determined with a temperature gradient incubator. *International Journal of Food Microbiology* 35**,** 287-292.

Riedel, T.E., Berelson, W.M., Nealson, K.H., and Finkel, S.E. (2013). Oxygen consumption rates of bacteria under nutrient-limited conditions. *Applied and Environmental Microbiology* 79**,** 4921-4931.

Roberts, B.N., Chakravarty, D., Gardner, J.C., 3rd, Ricke, S.C., and Donaldson, J.R. (2020). *Listeria monocytogenes* response to anaerobic environments. *Pathogens* 9**,** 210.

Roberts, T.A., Baird-Parker, A.C., and Tompkin, R.B. (1996). "*Aeromonas*," in *Microorganisms in Foods*. New York: Springer.

Rosenfeld, E., Duport, C., Zigha, A., and Schmitt, P. (2005). Characterization of aerobic and anaerobic vegetative growth of the food-borne pathogen *Bacillus cereus* F4430/73 strain. *Canadian Journal of Microbiology* 51**,** 149-158.

Rossaint, S., Klausmann, S., and Kreyenschmidt, J. (2015). Effect of high-oxygen and oxygen-free modified atmosphere packaging on the spoilage process of poultry breast fillets. *Poultry Science* 94**,** 96-103.

Rossi, O.D., Felipe, L.M., Martineli, T.M., and Mesquita, A.J. (2011). Study of the microbiota causing "blow pack" spoilage of vacuum-packaged beef. *Ars Veterinária* 27.

Säde, E., Murros, A., and Björkroth, J. (2013). Predominant *Enterobacteria* on modified-atmosphere packaged meat and poultry. *Food Microbiology* 34**,** 252-258.

Säde, E., Penttinen, K., Björkroth, J., and Hultman, J. (2017). Exploring lot-to-lot variation in spoilage bacterial communities on commercial modified atmosphere packaged beef. *Food Microbiology* 62**,** 147-152.

Saiki, R.K., Gelfand, D.H., Stoffel, S., Scharf, S.J., Higuchi, R., Horn, G.T., Mullis, K.B., and Erlich, H.A. (1988). Primer-directed enzymatic amplification of DNA with a thermostable DNA polymerase. *Science* 239**,** 487.

Sakala, R.M., Hayashidani, H., Kato, Y., Kaneuchi, C., and Ogawa, M. (2002). Isolation and characterization of *Lactococcus piscium* strains from vacuum-packaged refrigerated beef. *Journal of Applied Microbiology* 92**,** 173-179.

Samelis, J. (2006). "Managing microbial spoilage in the meat industry," in *Food Spoilage Microorganisms,* ed. C.D.W. Blackburn. Cambridge: Woodhead Publishing 213-286.

Santos, J.-Á., García-López, M.-L., and Otero, A. (1999). "Moraxella," in *Encyclopedia of Food Microbiology,* ed. R.K. Robinson. Oxford: Elsevier, 1487-1492.

Saraoui, T., Leroi, F., Björkroth, J., and Pilet, M.F. (2016). *Lactococcus piscium*: a psychrotrophic lactic acid bacterium with bioprotective or spoilage activity in food—a review. *Journal of Applied Microbiology* 121**,** 907-918.

Savell, W., Hanna, M.O., and Smith, C.C. (1981). An Incident of predominance of *Leuconostoc* sp . in vacuum-packaged beef strip loins-- sensory and microbial profile of steaks stored in 0_2-$C0_2$-N_2 atmospheres. *Journal of Food Protection* 44**,** 742-745.

Sawsan, H., Authman, S., Zaid, R., Abbas, H., Mohammed, A., and Al-Ezee, M. (2018). Temperature effects on growth of the biocontrol agent *Pantoea agglomerans*. *Journal of Advanced Laboratory Research in Biology* 8**,** 2017-2085.

Scherf, U., Sohling, B., Gottschalk, G., Linder, D., and Buckel, W. (1994). Succinate-ethanol fermentation in *Clostridium kluyveri*: purification and characterisation of 4-hydroxybutyryl-CoA dehydratase/vinylacetyl-CoA delta 3-delta 2-isomerase. *Archives of Microbiology* 161**,** 239-245.

Schillinger, U., and Holzapfel, W.H. (1995). "The genus *Carnobacterium*," in *The Genera of Lactic Acid Bacteria,* eds. B.J.B. Wood & W.H. Holzapfel. Boston: Springer, 307-326.

Schreiber, K., Boes, N., Eschbach, M., Jaensch, L., Wehland, J., Bjarnsholt, T., Givskov, M., Hentzer, M., and Schobert, M. (2006). Anaerobic Survival of *Pseudomonas aeruginosa* by pyruvate fermentation requires an usp-type stress protein. *Journal of Bacteriology* 188**,** 659.

Schuerger, A.C., Ulrich, R., Berry, B.J., and Nicholson, W.L. (2013). Growth of *Serratia liquefaciens* under 7 mbar, 0°C, and CO_2-enriched anoxic atmospheres. *Astrobiology* 13**,** 115-131.

Schurr, B., Behr, J., and F. Vogel, R. (2013). Role of the GAD system in hop tolerance of *Lactobacillus brevis*. *European Food Research and Technology* 237**,** 199-207.

Sears, D.F., and Eisenberg, R.M. (1961). A model representing a physiological role of CO2 at the cell membrane. *Journal of General Physiology* 44**,** 869-887.

Sellars, M.J., Hall, S.J., and Kelly, D.J. (2002). Growth of *Campylobacter jejuni* supported by respiration of fumarate, nitrate, nitrite, trimethylamine-N-oxide, or dimethyl sulfoxide requires oxygen. *Journal of Bacteriology* 184**,** 4187-4196.

Shabala, L., and Ross, T. (2008). Cyclopropane fatty acids improve *Escherichia coli* survival in acidified minimal media by reducing membrane permeability to H+ and enhanced ability to extrude H^+. *Research in Microbiology* 159**,** 458-461.

Shaw, M.K., Marr, A.G., and Ingraham, J.L. (1971). Determination of the minimal temperature for growth of *Escherichia coli*. *Journal of Bacteriology* 105**,** 683-684.

Shirey, J.J., and Bissonnette, G.K. (1992). Sheen formation and growth response of groundwater bacteria to reduced oxygen concentrations during incubation of M-Endo medium. *Canadian Journal of Microbiology* 38**,** 261-266.

Signorini, M., Ponce‐Alquicira, E., and Guerrero‐Legarreta, I. (2003). Proteolytic and lipolytic changes in beef inoculated with spoilage microorganisms and bioprotective lactic acid bacteria. *International Journal of Food Properties* 6**,** 147-163.

Skandamis, P.N., and Nychas, G.J. (2002). Preservation of fresh meat with active and modified atmosphere packaging conditions. *International Journal of Food Microbiology* 79**,** 35-45.

Smiddy, M., Fitzgerald, M., Kerry, J.P., Papkovsky, D.B., O' Sullivan, C.K., and Guilbault, G.G. (2002a). Use of oxygen sensors to non-destructively measure the oxygen content in modified atmosphere and vacuum packed beef: impact of oxygen content on lipid oxidation. *Meat Science* 61**,** 285-290.

Smiddy, M., Papkovskaia, N., Papkovsky, D.B., and Kerry, J.P. (2002b). Use of oxygen sensors for the non-destructive measurement of the oxygen content in modified atmosphere and vacuum packs of cooked chicken patties; impact of oxygen content on lipid oxidation. *Food Research International* 35**,** 577-584.

Smith, J.P., Ramaswamy, H.S., and Simpson, B.K. (1990). Developments in food packaging technology. Part II. Storage aspects. *Trends in Food Science & Technology* 1**,** 111-118.

Son, M.S., Matthews, W.J., Jr., Kang, Y., Nguyen, D.T., and Hoang, T.T. (2007). In vivo evidence of *Pseudomonas aeruginosa* nutrient acquisition and pathogenesis in the lungs of cystic fibrosis patients. *Infection and Immunity* 75**,** 5313-5324.

Stanborough, T., Fegan, N., Powell, S.M., Singh, T., Tamplin, M., and Chandry, P.S. (2018). Genomic and metabolic characterization of spoilage-associated *Pseudomonas* species. *International Journal of Food Microbiology* 268**,** 61-72.

Stanbridge, L.H., and Davies, A.R. (1998). "The microbiology of chill-stored meat," in *The Microbiology of meat and poultry* ed. R. Board. London: Blackie Academic & Professional, 174-219.

Stern, N.J., Pierson, M.D., and Kotula, A.W. (1980). Effects of pH and sodium chloride on Yersinia enterocolitica growth at room and refrigeration temperatures. *Journal of Food Science* 45**,** 64-67.

Stoops, J., Maes, P., Claes, J., and Van Campenhout, L. (2012). Growth of *Pseudomonas fluorescens* in modified atmosphere packaged tofu. *Letters in Applied Microbiology* 54**,** 195-202.

Stoops, J., Ruyters, S., Busschaert, P., Spaepen, R., Verreth, C., Claes, J., Lievens, B., and Van Campenhout, L. (2015). Bacterial community dynamics during cold storage of minced meat packaged under modified atmosphere and supplemented with different preservatives. *Food Microbiology* 48**,** 192-199.

Suman, S.P., and Joseph, P. (2013). Myoglobin chemistry and meat color. *Annual Review of Food Science and Technology* 4**,** 79-99.

Sun, J., and Liu, D. (2003). Geometric models for calculating cell biovolume and surface area for phytoplankton. *Journal of Plankton Research* 25**,** 1331-1346.

Sun, X. (2012). Antimicrobial and antioxidative strategies to reduce pathogens and extend the shelf life of fresh red meats. *Comprehensive Reviews in Food Science and Food Safety* 11**,** 340-354.

Sun, X.D., and Holley, R.A. (2012). Antimicrobial and antioxidative strategies to reduce pathogens and extend the shelf life of fresh red meats. *Comprehensive Reviews in Food Science and Food Safety* 11**,** 340-354.

Talon, R., Papon, M., Bauchart, D., Duboisset, F., and Montel, M.-C. (1992). Lipolytic activity of *Brochothrix thermosphacta* on natural triglycerides. *Letters in Applied Microbiology* 14**,** 153-157.

Tang, J., Faustman, C., Hoagland, T.A., Mancini, R.A., Seyfert, M., and Hunt, M.C. (2005). Postmortem oxygen consumption by mitochondria and its effects on myoglobin form and stability. *Journal of Agricultural and Food Chemistry* 53**,** 1223-1230.

Tauch, A., and Sandbote, J. (2014). "The Family *Corynebacteriaceae*," in *The Prokaryotes,* eds. E. Rosenberg, E.F. Delong, S. Lory, E. Stackebrandt & F. Thompson. Berlin, Heidelberg: Springer, 239-277.

Thippareddi, H., and Phebus, R.K. (2007). Modified atmosphere packaging (MAP): Microbial control and quality. *National Pork Board* 4667**,** 1-5.

Thomson, W.K., and Thacker, C.L. (1973). Effect of temperature on *Vibrio parahaemolyticus* in oysters at refrigerator and deep freeze temperatures. *Canadian Institute of Food Science and Technology Journal* 6**,** 156-158.

Tielen, P., Rosin, N., Meyer, A.K., Dohnt, K., Haddad, I., Jänsch, L., Klein, J., Narten, M., Pommerenke, C., Scheer, M., Schobert, M., Schomburg, D., Thielen, B., and Jahn, D. (2013). Regulatory and metabolic networks for the adaptation of *Pseudomonas aeruginosa* biofilms to urinary tract-like conditions. *PLoS One* 8**,** e71845.

Tofteskov, J., Hansen, J.S., and Bailey, N.P. (2017). Modelling the autoxidation of myoglobin in fresh meat under modified atmosphere packing conditions. *Journal of Food Engineering* 214**,** 129-136.

Toldrá, F., and Hui, Y.H. (2014). *Handbook of fermented meat and poultry.* eds. A. Iciar, J. Sebranek & R. Talon. New York: Blackwell publishing.

Tyanova, S., Temu, T., and Cox, J. (2016a). The MaxQuant computational platform for mass spectrometry-based shotgun proteomics. *Nature Protocols* 11**,** 2301-2319.

Tyanova, S., Temu, T., Sinitcyn, P., Carlson, A., Hein, M.Y., Geiger, T., Mann, M., and Cox, J. (2016b). The Perseus computational platform for comprehensive analysis of (prote)omics data. *Nature Methods* 13**,** 731-740.

Uehlein, N., Lovisolo, C., Siefritz, F., and Kaldenhoff, R. (2003). The tobacco aquaporin NtAQP1 is a membrane CO_2 pore with physiological functions. *Nature* 425**,** 734-737.

Umezawa, K., Takeda, K., Ishida, T., Sunagawa, N., Makabe, A., Isobe, K., Koba, K., Ohno, H., Samejima, M., Nakamura, N., Igarashi, K., and Yoshida, M. (2015). A novel pyrroloquinoline quinone-dependent 2-keto-D-glucose dehydrogenase from *Pseudomonas aureofaciens*. *Journal of Bacteriology* 197**,** 1322-1329.

Vander Wauven, C., Pierard, A., Kley-Raymann, M., and Haas, D. (1984). *Pseudomonas aeruginosa* mutants affected in anaerobic growth on arginine: evidence for a four-gene cluster encoding the arginine deiminase pathway. *Journal of Bacteriology* 160**,** 928-934.

Vasilopoulos, C., Ravyts, F., De Maere, H., De Mey, E., Paelinck, H., De Vuyst, L., and Leroy, F. (2008). Evaluation of the spoilage lactic acid bacteria in modified-atmosphere-packaged artisan-type cooked ham using culture-dependent and culture-independent approaches. *Journal of Applied Microbiology* 104**,** 1341-1353.

Vihavainen, E.J., and Björkroth, K.J. (2007). Spoilage of value-added, high-oxygen modified-atmosphere packaged raw beef steaks by *Leuconostoc gasicomitatum* and *Leuconostoc gelidum*. *International Journal of Food Microbiology* 119**,** 340-345.

Vihavainen, E.J., Murros, A.E., and Björkroth, K.J. (2008). *Leuconostoc* spoilage of vacuum-packaged vegetable sausages. *Journal of Food Protection* 71**,** 2312-2315.

Von Neubeck, M., Huptas, C., Glück, C., Krewinkel, M., Stoeckel, M., Stressler, T., Fischer, L., Hinrichs, J., Scherer, S., and Wenning, M. (2016). *Pseudomonas helleri* sp. nov. and *Pseudomonas weihenstephanensis* sp. nov., isolated from raw cow's milk. *International Journal of Systematic and Evolutionary Microbiology* 66**,** 1163-1173.

Walker, S.J., Archer, P., and Banks, J.G. (1990). Growth of *Listeria monocytogenes* at refrigeration temperatures. *Journal of Applied Bacteriology* 68**,** 157-162.

Wang, G.-Y., Li, M., Ma, F., Wang, H.-H., Xu, X.-L., and Zhou, G.-H. (2017). Physicochemical properties of *Pseudomonas fragi* isolates response to modified atmosphere packaging. *FEMS Microbiology Letters* 364.

Wang, G., Ma, F., Chen, X., Han, Y., Wang, H., Xu, X., and Zhou, G. (2018a). Transcriptome analysis of the global response of *Pseudomonas fragi* NMC25 to modified atmosphere packaging stress. *Frontiers in Microbiology* 9.

Wang, G., Ma, F., Zeng, L., Bai, Y., Wang, H., Xu, X., and Zhou, G. (2018b). Modified atmosphere packaging decreased *Pseudomonas fragi* cell metabolism and extracellular proteolytic activities on meat. *Food Microbiology* 76**,** 443-449.

Wang, Y., and Pan, X. (2014). "Bacteria: *Proteus*," in *Encyclopedia of Food Safety,* ed. Y. Motarjemi. Waltham: Academic Press, 486-489.

Wei, Q., Minh, P.N.L., Dötsch, A., Hildebrand, F., Panmanee, W., Elfarash, A., Schulz, S., Plaisance, S., Charlier, D., Hassett, D., Häussler, S., and Cornelis, P. (2012). Global regulation of gene expression by OxyR in an important human opportunistic pathogen. *Nucleic Acids Research* 40**,** 4320-4333.

Werle, P., Slemr, F., Maurer, K., Kormann, R., Mücke, R., and Jänker, B. (2002). Near- and mid-infrared laser-optical sensors for gas analysis. *Optics and Lasers in Engineering* 37**,** 101-114.

Whiting, R.C., and Naftulin, K.A. (1992). Effect of headspace oxygen concentration on growth and toxin production by proteolytic strains of *Clostridium botulinum*. *Journal of Food Protection* 55**,** 23-27.

Wickramasinghe, N.N., Ravensdale, J., Coorey, R., Chandry, S.P., and Dykes, G.A. (2019). The predominance of psychrotrophic *Pseudomonads* on aerobically stored chilled red meat. *Comprehensive Reviews in Food Science and Food Safety* 18**,** 1622-1635.

Willian, K. (2013). "Lipids and lipid oxidation," in *The Science of Meat Quality,* ed. C.R. Kerth. New York: Wiley, 147-175.

Wladyka, E.J., and Dawson, L.E. (1968). Essential amino acid composition of chicken meat and drip after 30 and 90 days of frozen storage. *Journal of Food Science* 33**,** 453-455.

Wu, M., Guina, T., Brittnacher, M., Nguyen, H., Eng, J., and Miller, S.I. (2005). The *Pseudomonas aeruginosa* proteome during anaerobic growth. *Journal of Bacteriology* 187**,** 8185-8190.

Yamamoto, N., and Droffner, M.L. (1985). Mechanisms determining aerobic or anaerobic growth in the facultative anaerobe *Salmonella typhimurium*. *PNAS Proceedings of the National Academy of Sciences of the United States of America* 82**,** 2077-2081.

Yang, X. (2014). "*Moraxellaceae*," in *Encyclopedia of Food Microbiology,* eds. C.A. Batt & M.L. Tortorello. Oxford: Academic Press, 826-833.

Yoon, S.S., Hennigan, R.F., Hilliard, G.M., Ochsner, U.A., Parvatiyar, K., Kamani, M.C., Allen, H.L., Dekievit, T.R., Gardner, P.R., Schwab, U., Rowe, J.J., Iglewski, B.H., Mcdermott, T.R., Mason, R.P., Wozniak, D.J., Hancock, R.E., Parsek, M.R., Noah, T.L., Boucher, R.C., and Hassett, D.J. (2002). *Pseudomonas aeruginosa* anaerobic respiration in biofilms: relationships to cystic fibrosis pathogenesis. *Developmental Cell* 3**,** 593-603.

Zagorec, M., and Champomier-Vergès, M.C. (2017). Lactobacillus sakei: A Starter for Sausage Fermentation, a Protective Culture for Meat Products. *Microorganisms* 5.

Zaritzky, N.E., and Bevilacqua, A.E. (1988). Oxygen diffusion in meat tissues. *International Journal of Heat and Mass Transfer* 31**,** 923-930.

Zeisel, S.H., Mar, M.H., Howe, J.C., and Holden, J.M. (2003). Concentrations of choline-containing compounds and betaine in common foods. *JN the Journal of Nutrition* 133**,** 1302-1307.

Zhang, Y.M., and Rock, C.O. (2008). Membrane lipid homeostasis in bacteria. *Nature Reviews Microbiology* 6**,** 222-233.

Zotta, T., Parente, E., and Ricciardi, A. (2017). Aerobic metabolism in the genus *Lactobacillus*: impact on stress response and potential applications in the food industry. *Journal of Applied Microbiology* 122**,** 857-869.

Zwietering, M.H., Jongenburger, I., Rombouts, F.M., and Van 'T Riet, K. (1990). Modeling of the bacterial growth curve. *Applied and Environmental Microbiology* 56**,** 1875-1881.

9. Appendix

Supplementary Figures

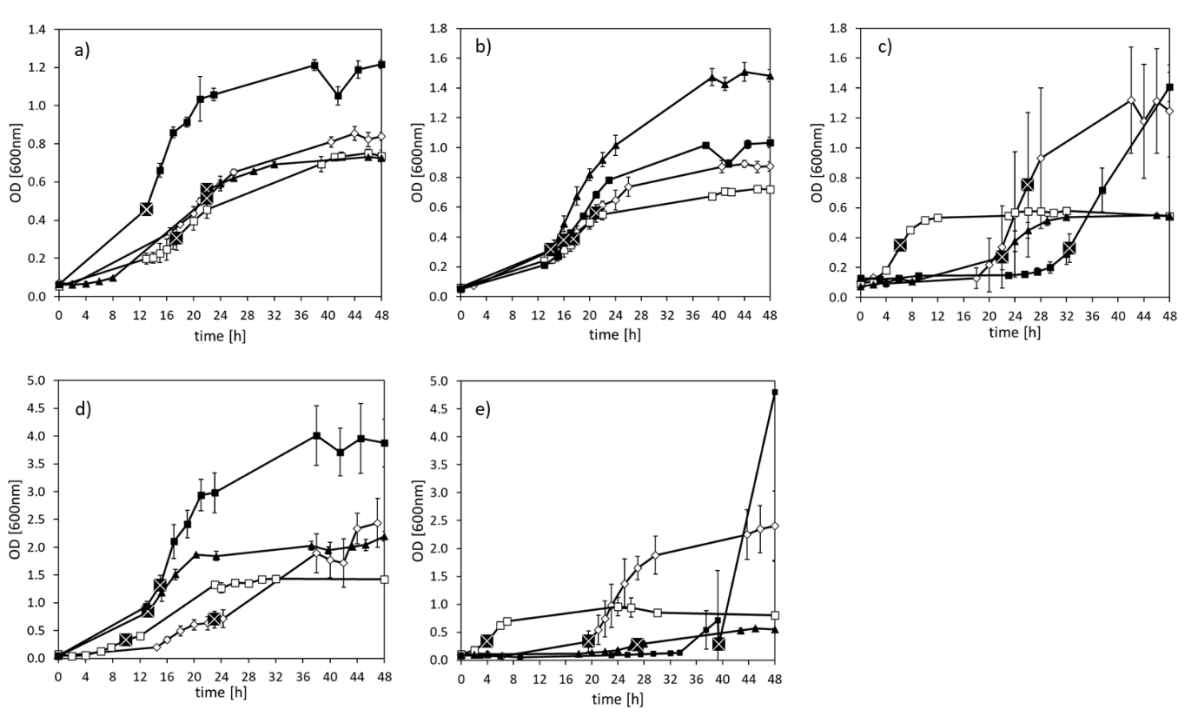

Figure S1| Growth curves of the five meat-spoiling bacteria when cultivated under four different modified atmospheres for the proteomic and single gene-transcription study. Growth curves of the five meat-spoiling bacteria (a) *L. gelidum* subsp. *gelidum* TMW2.1618 (b) *L. gelidum* subsp. *gasicomitatum* TMW2.1619 (c) *C. divergens* TMW2.1577 (d) *C. maltaromaticum* TMW2.1581 and (e) *B. thermosphacta* TMW2.2101 were recorded when cultivated under the four different gas atmospheres (◇) air, (□) N_2, (▲) 30% CO_2 / 70% N_2, (■) 30% CO_2 / 70% O_2. Time points of sample taking for proteomic analysis are marked with crossed black dots. All values are based on three independent replicates. Error bars represent calculated standard deviations.

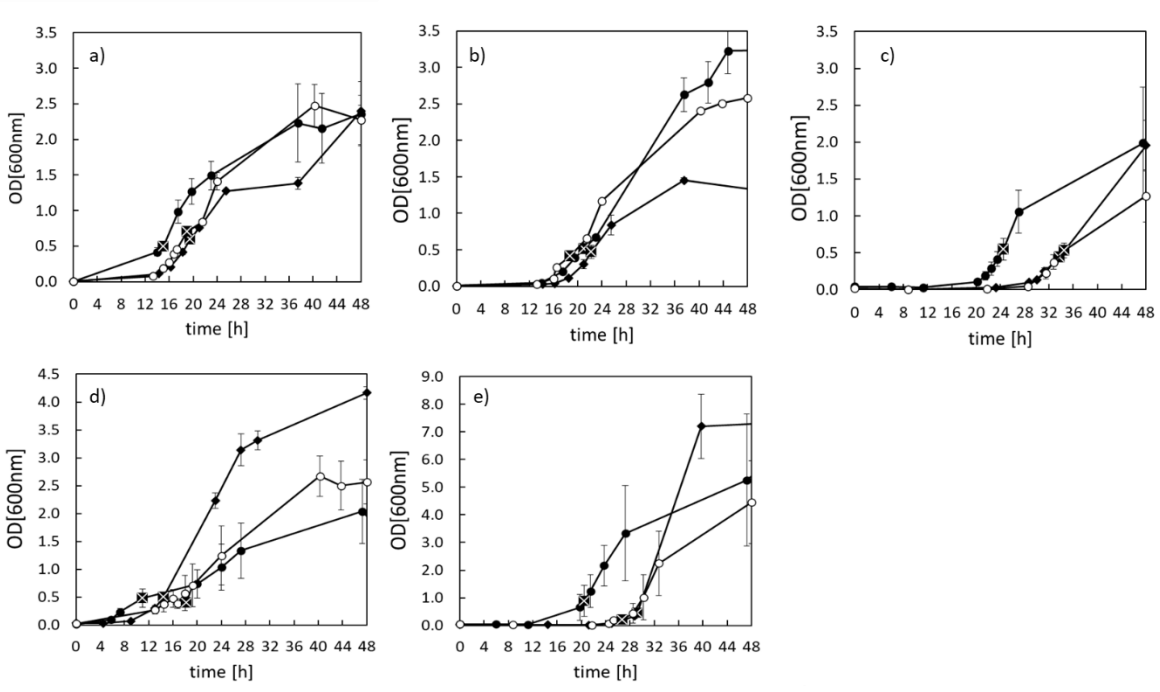

Figure S2| Growth curves of the five meat-spoiling bacteria when cultivated under three different modified atmospheres for membrane analyses. Growth curves were recorded for the five meat-spoiling bacteria (a) *L. gelidum* subsp. *gelidum* TMW2.1618 (b) *L. gelidum* subsp. *gasicomitatum* TMW2.1619 (c) *C. divergens* TMW2.1577 (d) *C. maltaromaticum* TMW2.1581 and (e) *B. thermosphacta* TMW2.2101 cultivated under the three gas atmospheres (●) air, (○) 30% CO_2 / 21% O_2 and (◆) 30% CO_2 / 70% O_2. Time points of sample taking for membrane analyses are marked with crossed black dots. All values given are means of three independent replicates. Error bars are based on calculated standard deviations.

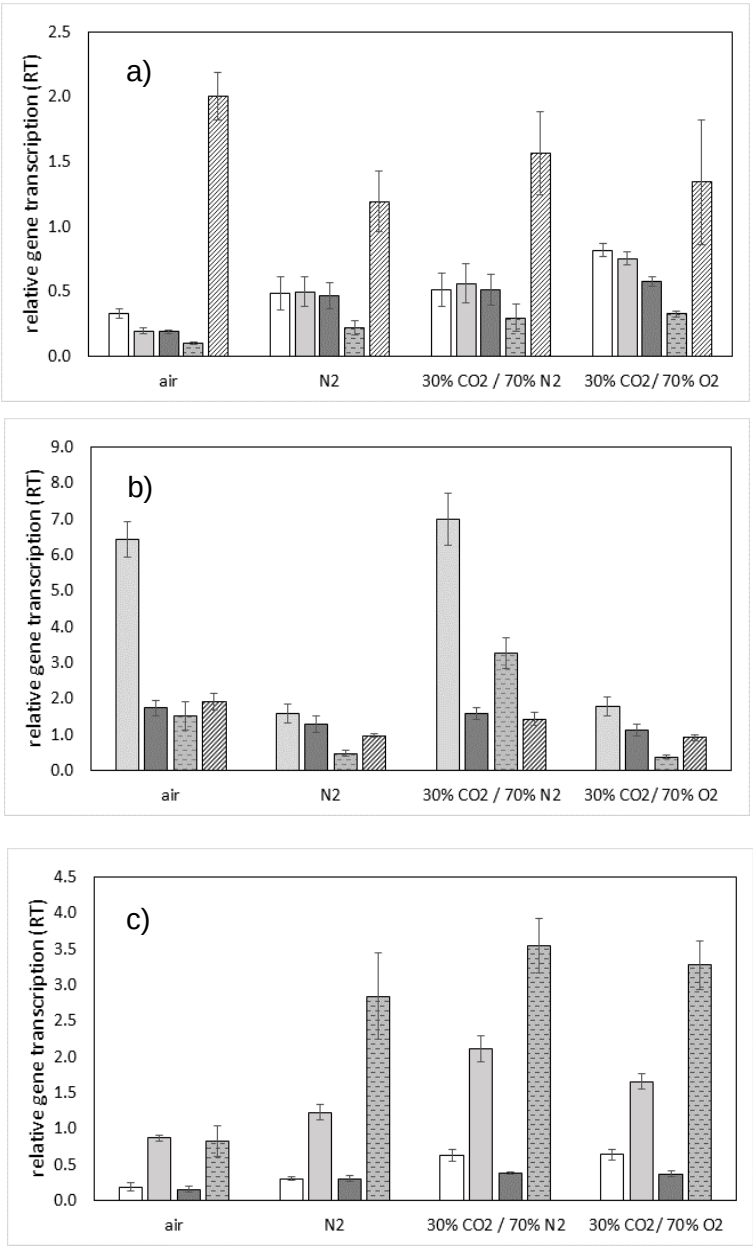

Figure S3| Relative transcription analysis of selected target genes related to O_2 consuming reaction for three meat-spoiling bacteria. An expression analysis of three representative species of the five meat-spoiling bacteria was performed with (a) *B. thermosphacta* TMW2.2101, (b) *C. divergens* TMW2.1577 and (c) *L. gelidum* subsp. *gasicomitatum* TMW2.1619. The genes pyruvate oxidase (POX) (□), glycerin-3-phosphate dehydrogenase (G3PD) (■), 2-succinyl-5-enolpyruvyl-6-hydroxy-3-cyclohexene-1-carboxylic-acid synthase (MQ) (■), NADH oxidase (NOX) (▣) and superoxide dismutase (SOD) (▨) were analyzed. All values are based on three independent biological replicates. Error bars represent calculated standard errors.

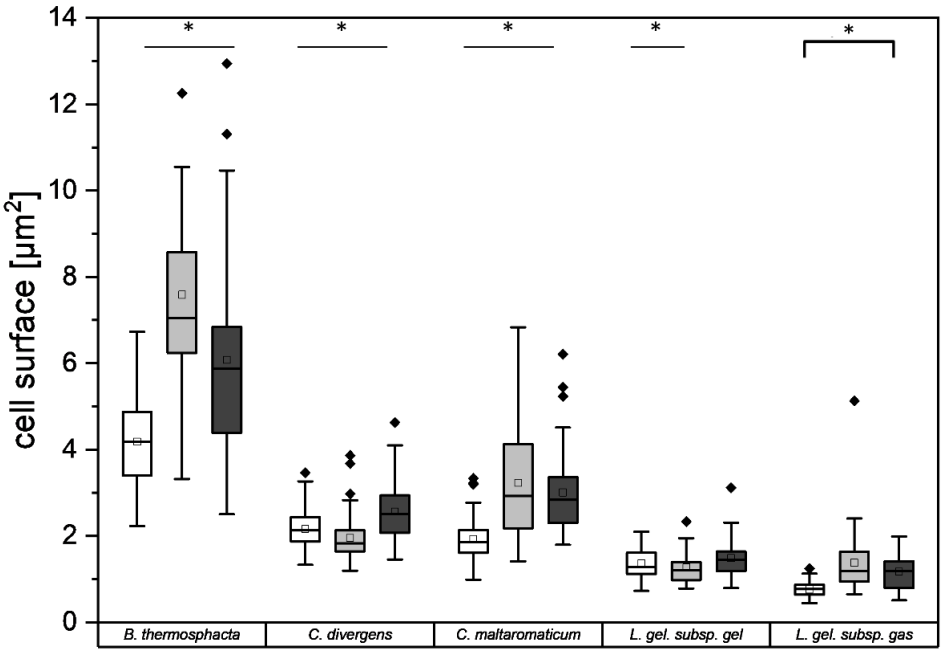

Figure S4| Analysis of the cell surface of the five meat-spoiling bacteria. The cell surface of the five meat-spoiling bacteria cultivated under the atmospheres (□) 21% O_2 / 0% CO_2 / 79% N_2 (air) (■) 20% O_2 / 30% CO_2 / 50% N_2 (■) 70% O_2 / 30% CO_2 / 0% N_2 was determined by microscopy. Values given are means of 50 measured cells. Black diamonds represent outliers of the analysis. * indicate significant differences between gas atmospheres identified by a Welch T-test with $p < 0.05$.

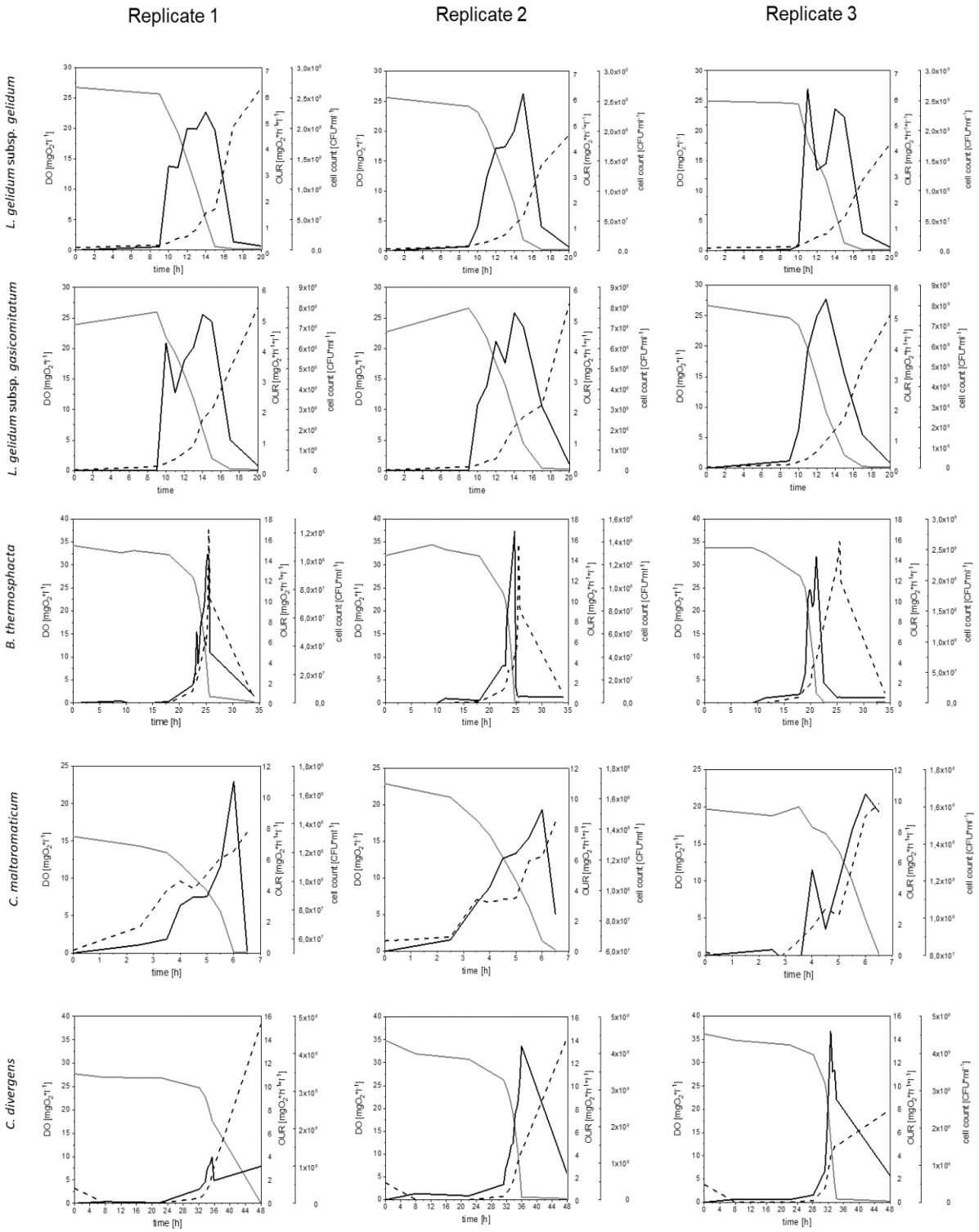

Figure S5| Record of dissolved oxygen, oxygen uptake rate and growth of the five meat-spoiling bacteria in O_2 saturated MS-media. Dissolved oxygen (DO) and cell counts of the five meat-spoiling bacteria were measured in MS-media and their corresponding oxygen uptake rate (OUR) was calculated.

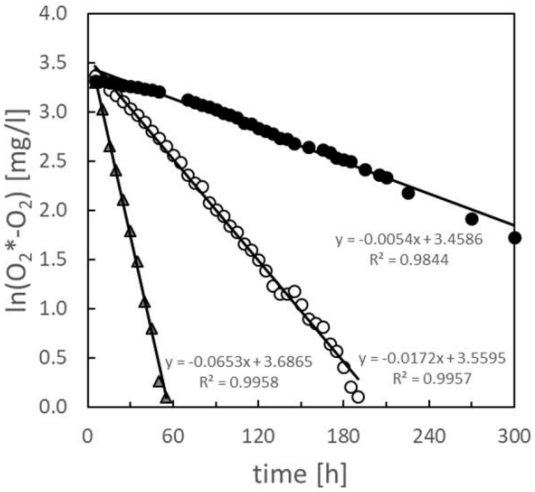

Figure S6| Analysis of the volumetric mass transfer coefficient K_La of different MS-media. The volumetric mass transfer coefficient K_La of the developed medium for *C. divergens* TMW2.1577 (▲), *B. thermosphacta* TMW2.2101 (○) and both *L. gelidum* subspecies as well as *C. maltaromaticum* TMW2.1581 (●) was calculated. K_La is defined as the negative slope of the lines. O_2* = oxygen concentration in mg/l of O_2 saturated medium.

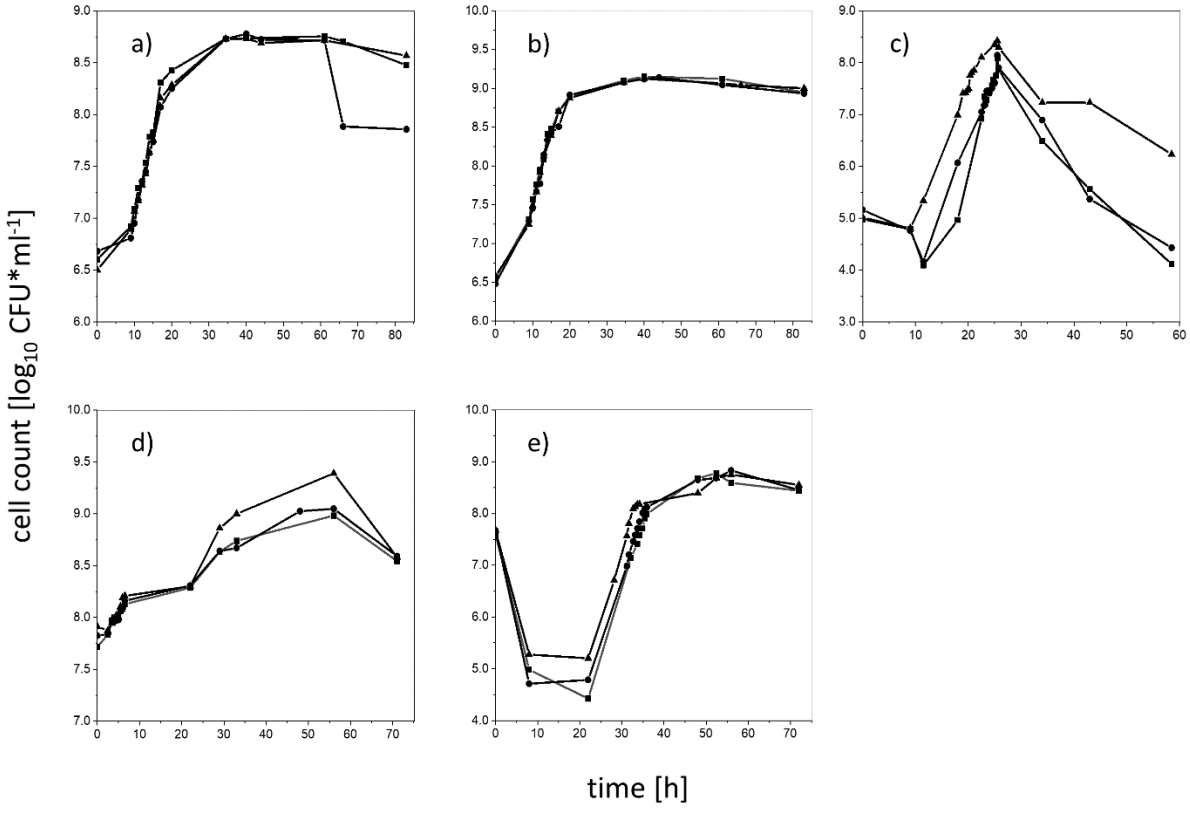

Figure S7| Analysis of the growth of the five meat-spoiling bacteria in glass bottles filled half with MS-media and half with an atmosphere of 30% CO_2 / 70% O_2. Growth of the five meat-spoiling bacteria a) *L. gelidum* subsp. *gelidum* TMW2.1618 b) *L. gelidum* subsp. *gasicomitatum* TMW2.1619 c) *B. thermosphacta* TMW2.2101 d) *C. maltaromaticum* TMW2.1581 and e) *C. divergens* TMW2.1577 was recorded over 60 hours of fermentation in 0.5-liter MS-media. All experiments were performed in triplicates: (■) replicate1, (●) replicate 2, (▲) replicate 3.

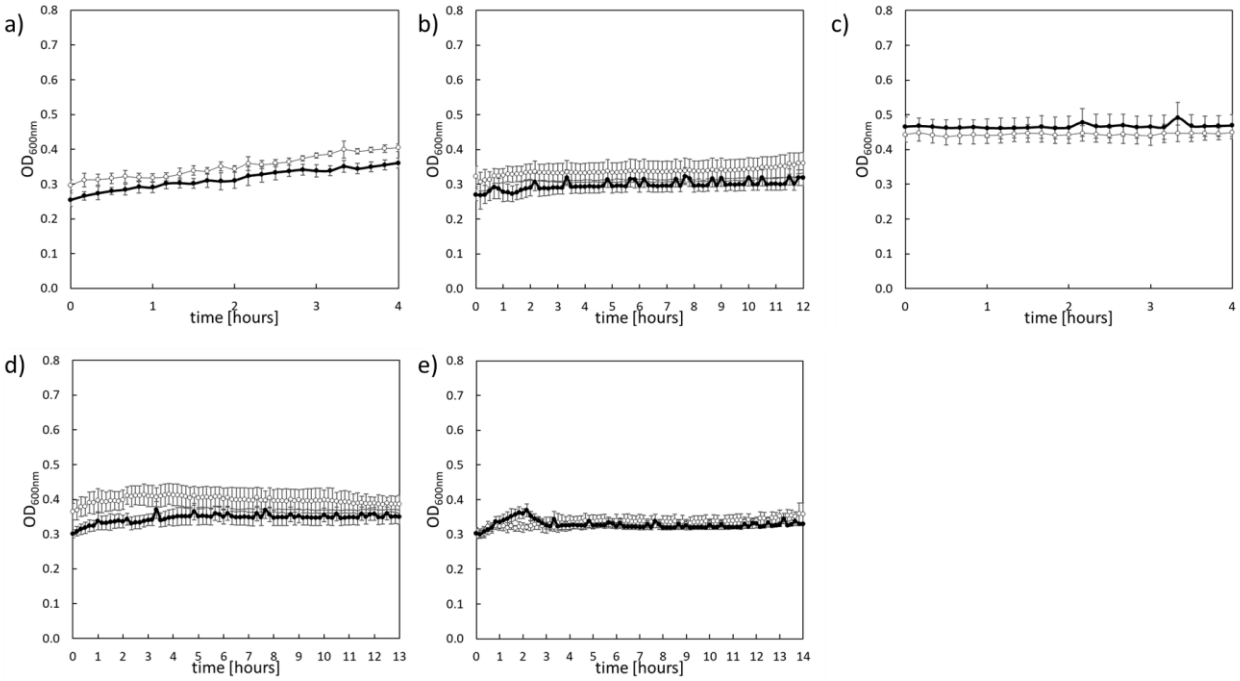

Figure S8| Growth curves of the five meat-spoiling bacteria in MS-media gassed with 30% N_2 / 70% O_2 or 30% CO_2 / 70% O_2. Growth of the five meat-spoiling bacteria a) *B. thermosphacta* TMW2.2101 b) *C. divergens* TMW2.1577 c) *C. maltaromaticum* TMW2.1581 d) *L. gelidum* subsp. *gelidum* TMW2.1618 and e) *L. gelidum* subsp. *gasicomitatum* TMW2.1619 was monitored in a 96-well plate in media previously gassed either with (○) 30% N_2 / 70% O_2 or with (●) 30% CO_2 / 70% O_2.

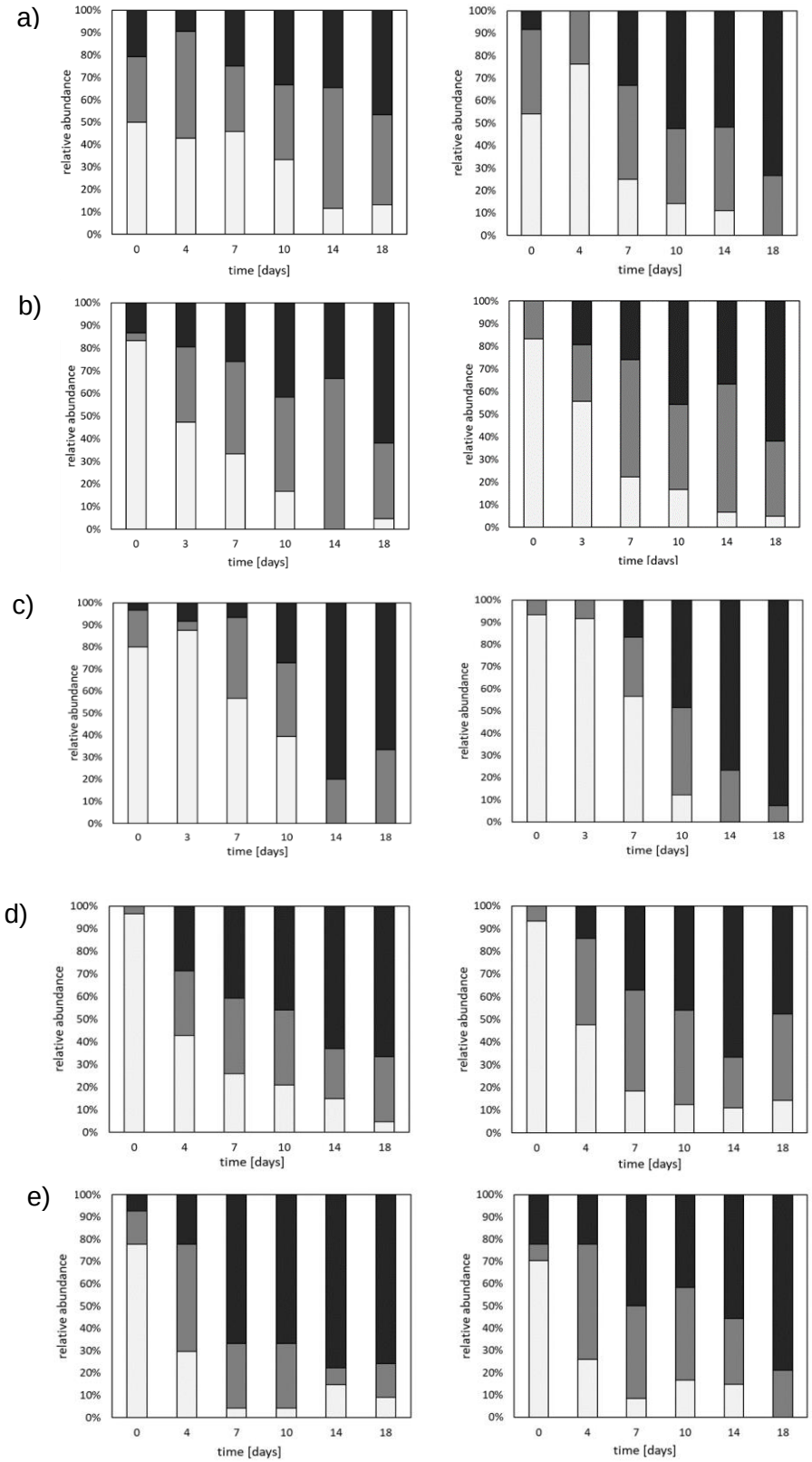

Figure S9| Validation of olfactory and visual appearance of inoculated meat by the sensory panel. Analysis of the olfactory (left graphs) and visual appearance (right graphs) of beef and chicken meat inoculated with a) *B. thermosphacta* TMW2.2101 b) *L. gelidum* subsp. *gasicomitatum* TMW2.1619 c) *L. gelidum* subsp. *gelidum* TMW2.1618 d) *C. divergens* TMW2.1577 and e) *C. maltaromaticum* TMW2.1581. Bars represent the percentage of persons, which validated the meat as "fresh" (□), "not-fresh but edible" (■) or "spoiled" (■). All values are based on three independent replicates.

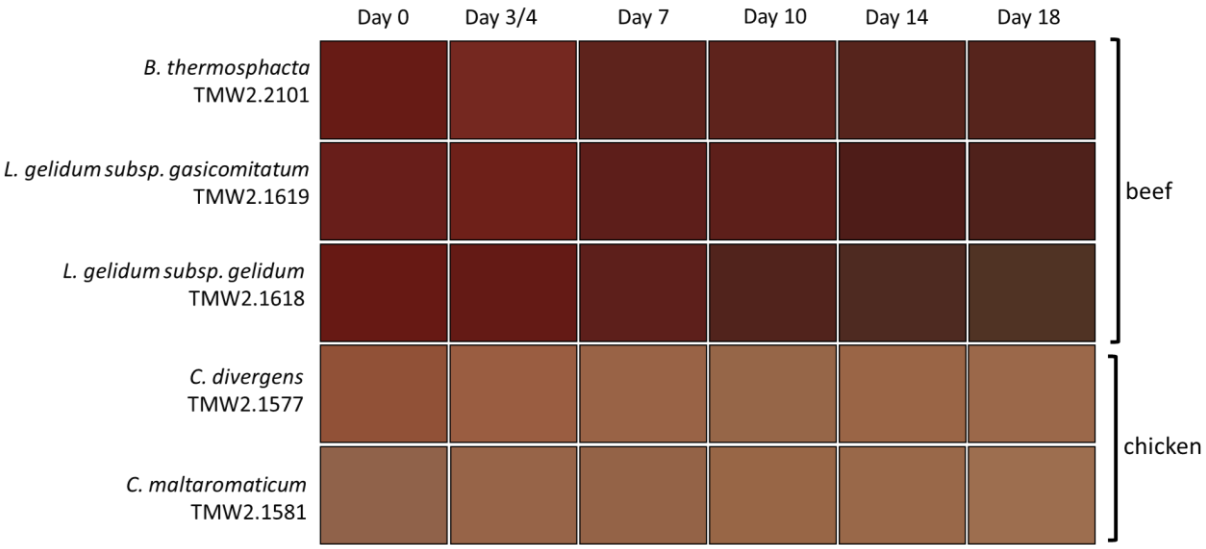

Figure S10| Analysis of the color development of inoculated meat pieces. The color of inoculated meat pieces was analyzed based on red, green and blue (RGB) values determined for each time point. Beef was inoculated with the species *B. thermosphacta* TMW2.2101, *L. gelidum* subsp. *gasicomitatum* TMW2.1619 or *L. gelidum* subsp. *gelidum* TMW2.1618 and chicken breast was inoculated with *C. divergens* TMW2.1577 or *C. maltaromaticum* TMW2.1581. Meat was stored over 18 days at 4 °C. The displayed colors are means of RGB values of three independent replicates.

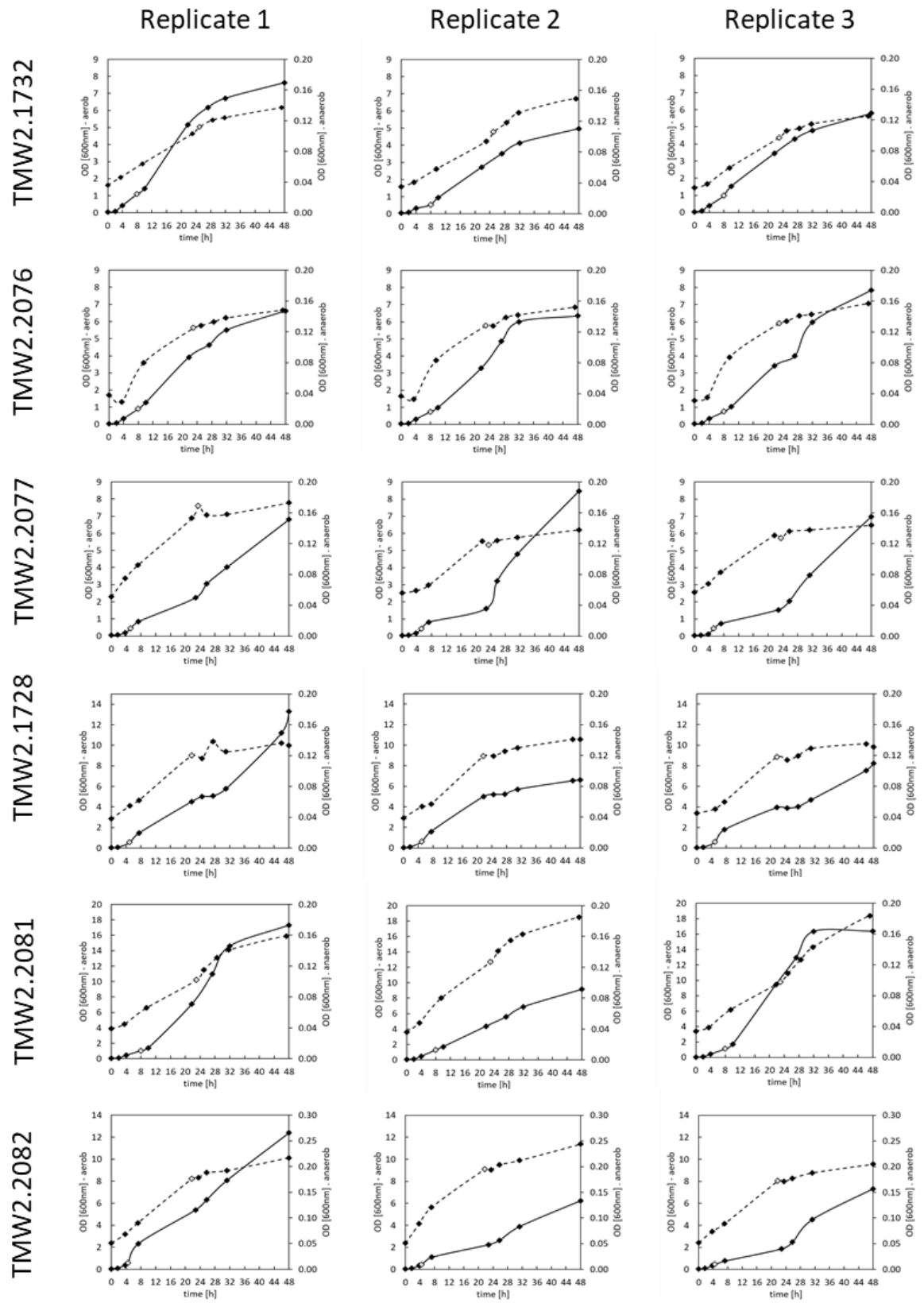

Figure S11| Growth curves recorded for the six *Pseudomonas* strains under oxic and anoxic conditions in MS-medium. Growth curves of the six *Pseudomonas* strains were recorded when growing in MS-medium under oxic (21% O_2 / 0.03% CO_2) and anoxic (100% N_2) conditions. Dotted lines: anaerobic growth (secondary axis), solid lines: aerobic growth (primary axis). White dots represent the time point of sample taking for the proteomic experiment.

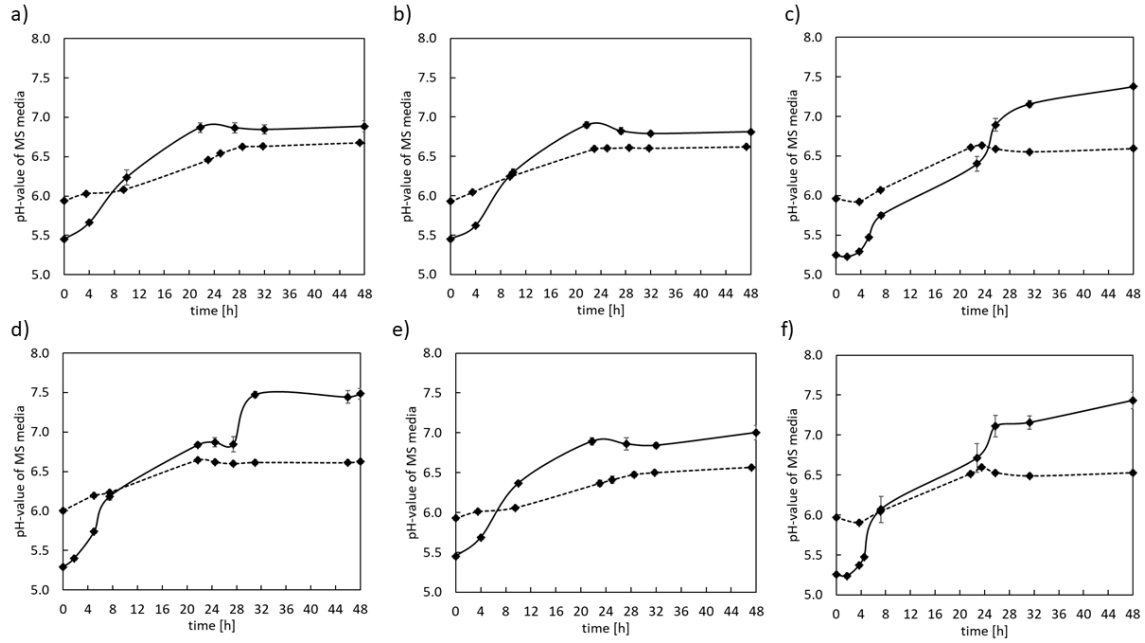

Figure S12| PH curves of the six *Pseudomonas* strains when cultivated under oxic and anoxic conditions in MS-medium. PH curves of the six species a) *P. lundensis* TMW2.1732, b) *P. lundensis* TMW2.2076, c) *P. weihenstephanensis* TMW2.2077, d) *P. weihenstephanensis* TMW2.1728, e) *P. fragi* TMW2.2081 and f) *P. fragi* TMW2.2082 were recorded in MS-medium under oxic (21% O_2 / 0.03% CO_2) and anoxic (100% N_2) conditions. Dotted lines: anaerobic pH development, solid lines: aerobic pH development. All values are based on three independent replicates. Error bars represent calculated standard errors.

Supplementary Tables

Table S1| HPLC analysis of the chemical composition of meat extract. A chemical analysis of sugars, acids, alcohols, free amino acids and biogenic amines as well as a BCA analysis of the total protein content of 100 g/l meat extract was done. Analyzed ingredients and their measured amounts are listed. All data are based on biological replicates**.** "N.d." = not detected.

	Amount
Sugar	
Glucose	6.67 mM
Glycerin	n.d.
Fructose	n.d.
Galactose	n.d.
Mannose	n.d.
Ribose	n.d.
Free amino acids	
Aspartate	0.31 mM
Glutamate	0.51 mM
Serine	0.61 mM
Histidine	0.23 mM
Glycine	0.70 mM
Threonine	0.40 mM
Arginine	0.81 mM
Alanine	0.99 mM
Tyrosine	0.12 mM
Cysteine	0.04 mM
Valine	0.55 mM
Methionine	0.22 mM
Tryptophan	n.d.
Isoleucine	0.34 mM
Leucine	0.87 mM
Lysine	0.25 mM
Proline	0.27 mM

	Amount
Acids	
Citrate	0.03 mM
Malate	0.05 mM
2,3-butanedion	0.04 mM
Lactic acid	0.02 mM
Formic acid	0.08 mM
Acetate	n.d.
Acetoin	n.d.
Isobutyric acid	n.d.
Isovaleric acid	n.d.
Alcohols	
2,3-butanediol	n.d.
Ethanol	n.d.
Biogenic amines	
Agmatine	0.40 mM
Tyramine	0.24 mM
Putrescine	n.d.
Cataverine	n.d.
Histamine	n.d.
Proteins	32.49 g/l

Table S2| Analysis of growth parameters of the five meat-spoiling bacteria cultivated under four different atmospheres in MS-media for the proteomic and single gene-transcription sample taking. The lag-phase, maximal OD and maximal growth rate was calculated for the five meat-spoiling bacteria when cultivated under the four gas atmospheres air, N_2, 30% CO_2 / 70% N_2 and 30% CO_2 / 70% O_2. Superscript letters indicate significant differences between calculated parameters comparing the cultivation conditions air vs N_2 (A), air vs 30% CO_2 / 70% N_2 (B), air vs 30% CO_2 / 70% O_2 (C), N_2 vs 30% CO_2 / 70% N_2 (D), N_2 vs 30% CO_2 / 70% O_2 (E) and 30% CO_2 / 70% N_2 vs 30% CO_2 / 70% O_2 (F). All values are based on three independent replicates.

B. thermosphacta TMW2.2101	lag-phase [h] $^{A, C-F}$	OD_{max}	μ_{max} [division/h]$^{E, F}$
air	17.78	2.06	0.15
N_2	0.00	0.96	0.08
CO_2/N_2	15.47	0.56	0.02
CO_2/O_2	38.71	4.50	0.47
C. divergens TMW2.1577	lag-phase [h] $^{A-F}$	$OD_{max}^{A,B,E,F}$	μ_{max} [division/h]$^{B, F}$
air	17.64	1.30	0.08
N_2	0	0.58	0.05
CO_2/N_2	9.65	0.56	0.03
CO_2/O_2	28.57	1.40	0.07
C. maltaromaticum TMW2.1581	lag-phase [h]$^{A-D, F}$	$OD_{max}^{A, C, E, F}$	μ_{max} [division/h]$^{C, E, F}$
air	21.16	2.44	0.09
N_2	5.46	1.44	0.07
CO_2/N_2	2.06	2.12	0.09
CO_2/O_2	7.33	4.00	0.20
L. gelidum subsp. *gelidum* TMW2.1618	lag-phase [h]$^{B-E}$	$OD_{max}^{A-C, E, F}$	μ_{max} [division/h]$^{B, C, E, F}$
air	7.40	0.84	0.04

N_2	8.50	0.75	0.03
CO_2/N_2	3.31	0.73	0.03
CO_2/O_2	3.31	1.20	0.06
L. gelidum subsp. *gasicomitatum* TMW2.1619	lag-phase [h]^{C}	$OD_{max}$$^{A-F}$	μ_{max} [division/h]$^{B-F}$
air	7.23	0.89	0.04
N_2	8.30	0.72	0.04
CO_2/N_2	9.21	1.51	0.07
CO_2/O_2	9.91	1.03	0.06

Table S3| Analysis of growth parameters of the five meat-spoiling bacteria cultivated under different gas atmospheres for membrane analysis. Growth of the five meat-spoiling bacteria was analyzed calculating the lag-phase, maximal OD and maximal growth rate when cultivated under the three gas atmospheres air, 20% O_2 / 30% CO_2 / 50% N_2 and 70% O_2 / 30% CO_2 / 0% N_2. Superscript letters indicate significant differences between calculated parameters comparing the cultivation conditions (A) air vs 20% O_2 / 30% CO_2 / 50% N_2, (B) air vs 70% O_2 / 30% CO_2 / 0% N_2 and (C) 20% O_2 / 30% CO_2 / 50% N_2 vs 70% O_2 / 30% CO_2 / 0% N_2. All data are based on three independent replicates.

B. thermosphacta TMW2.2101	lag-phase [h]$^{A-C}$	OD_{max}	μ_{max} [division/h]
air	17,35	5,56	0,31
30% CO_2 / 21% O_2	26,90	4,48	0,31
30% CO_2 / 70% O_2	23,88	7,75	0,35
C. divergens TMW2.1577	lag-phase [h]^{A,B}	OD_{max}	μ_{max} [division/h]
air	20,30	2,16	0,14
30% CO_2 / 21% O_2	28,18	1,27	0,07
30% CO_2 / 70% O_2	31,70	1,94	0,12
C. maltaromaticum TMW2.1581	lag-phase [h]^{A,B}	OD_{max}^{B,C}	μ_{max} [division/h]$^{A-C}$
air	4,21	1,94	0,05
30% CO_2 / 21% O_2	14,43	2,62	0,13
30% CO_2 / 70% O_2	10,18	4,29	0,17
L. gelidum subsp. *gelidum* TMW2.1618	lag-phase [h]^{A,B}	OD_{max}	μ_{max} [division/h]^{A,C}
air	8,97	2,45	0,11
30% CO_2 / 21% O_2	14,71	2,46	0,15
30% CO_2 / 70% O_2	13,84	2,39	0,10
L. gelidum subsp. *gasicomitatum* TMW2.1619	lag-phase [h]	OD_{max}^{B,C}	μ_{max} [division/h]^{B,C}
air	14,98	3,18	0,11
30% CO_2 / 21% O_2	15,68	2,65	0,12
30% CO_2 / 70% O_2	16,72	1,43	0,08

Table S4| Growth analysis of the five meat-spoiling bacteria cultivated on MAP meat with increasing CO_2 levels by calculating growth parameters. Growth of the five meat-spoiling bacteria under the atmospheres 15% CO_2 / 20% O_2 / 65% N_2, 30% CO_2 / 20% O_2 / 50% N_2, 50% CO_2 / 20% O_2 / 30% N_2 and 70% CO_2 / 20% O_2 / 10% N_2 was analyzed by calculating the lag-phase, maximal division rate and maximal CFU using the R package grofit. Superscript letters indicate significant differences between calculated parameters comparing the cultivation conditions (A) 15% CO_2 / 20% O_2 / 65% N_2 vs 30% CO_2 / 20% O_2 / 50% N_2, (B) 15% CO_2 / 20% O_2 / 65% N_2 vs 50% CO_2 / 20% O_2 / 30% N_2, (C) 15% CO_2 / 20% O_2 / 65% N_2 vs 70% CO_2 / 20% O_2 / 10% N_2, (D) 30% CO_2 / 20% O_2 / 50% N_2 vs 50% CO_2 / 20% O_2 / 30% N_2, (E) 30% CO_2 / 20% O_2 / 50% N_2 vs 70% CO_2 / 20% O_2 / 10% N_2, (F) 50% CO_2 / 20% O_2 / 30% N_2 vs 70% CO_2 / 20% O_2 / 10% N_2. Numbers given are means of three independent replicates.

B. thermosphacta TMW2.2101	lag-phase [h]^{C,E}	CFU_{max}^{C}	μ_{max} [division/h]^{C}
15% CO_2	-14.97	8.10	0.38
30% CO_2	-15.58	8.06	0.35
50% CO_2	-20.37	7.54	0.28
70% CO_2	-27.86	6.95	0.19
C. divergens TMW2.1577	lag-phase [h]	CFU_{max}^{E}	μ_{max} [division/h]
15% CO_2	-60.76	7.92	0.11
30% CO_2	-56.35	8.00	0.12
50% CO_2	-84.52	7.70	0.08
70% CO_2	-100.31	7.58	0.07
C. maltaromaticum TMW2.1581	lag-phase [h]	$CFU_{max}$$^{C, E, F}$	μ_{max} [division/h]^{E}

15% CO_2	-92.83	7.56	0.07
30% CO_2	-76.51	7.70	0.09
50% CO_2	-83.32	7.58	0.08
70% CO_2	-170.95	6.90	0.04
L. gelidum subsp. *gelidum* TMW2.1618	lag-phase [h]	CFU_{max}	μ_{max} [division/h]
15% CO_2	-24.33	7.07	0.20
30% CO_2	-22.36	7.18	0.22
50% CO_2	-24.60	7.11	0.20
70% CO_2	-21.47	7.20	0.22
L. gelidum subsp. *gasicomitatum* TMW2.1619	lag-phase [h]	CFU_{max}	μ_{max} [division/h]
15% CO_2	-52.04	6.27	0.10
30% CO_2	-41.75	6.50	0.12
50% CO_2	-44.30	6.51	0.11
70% CO_2	-52.51	6.23	0.09

Table S5| Growth analysis of the five meat-spoiling bacteria cultivated with increasing CO_2 levels on MAP meat by comparing the CFU after 7 days. CFU values obtained after 7 days of cultivation of the meat-spoiling bacteria under the atmospheres 15% CO_2 / 20% O_2 / 65% N_2, 30% CO_2 / 20% O_2 / 50% N_2, 50% CO_2 / 20% O_2 / 30% N_2 and 70% CO_2 / 20% O_2 / 10% N_2 are displayed. Superscript letters indicate significant differences between those values comparing the cultivation conditions (A) 15% CO_2 / 20% O_2 / 65% N_2 vs 30% CO_2 / 20% O_2 / 50% N_2 (B) 15% CO_2 / 20% O_2 / 65% N_2 vs 50% CO_2 / 20% O_2 / 30% N_2, (C) 15% CO_2 / 20% O_2 / 65% N_2 vs 70% CO_2 / 20% O_2 / 10% N_2, (D) 30% CO_2 / 20% O_2 / 50% N_2 vs 50% CO_2 / 20% O_2 / 30% N_2, (E) 30% CO_2 / 20% O_2 / 50% N_2 vs 70% CO_2 / 20% O_2 / 10% N_2, (F) 50% CO_2 / 20% O_2 / 30% N_2 vs 70% CO_2 / 20% O_2 / 10% N_2. Numbers given are means of three independent replicates.

B. thermosphacta TMW2.2101	log $(CFU/cm^2)^{B\text{-}F}$
15% CO_2	7.93
30% CO_2	7.76
50% CO_2	7.20
70% CO_2	6.80
C. divergens TMW2.1577	log $(CFU/cm^2)^{B\text{-}E}$
15% CO_2	7.80
30% CO_2	7.94
50% CO_2	7.44
70% CO_2	7.20
C. maltaromaticum TMW2.1581	log $(CFU/cm^2)^{C,E,F}$
15% CO_2	7.51
30% CO_2	7.48
50% CO_2	7.43
70% CO_2	6.69
L. gelidum subsp. *gelidum* TMW2.1618	log (CFU/cm^2)
15% CO_2	6.41
30% CO_2	6.31
50% CO_2	6.39
70% CO_2	6.30
L. gelidum subsp. *gasicomitatum* TMW2.1619	log $(CFU/cm^2)^{F}$
15% CO_2	5.84
30% CO_2	5.86
50% CO_2	6.24
70% CO_2	5.68

Table S6| Single significantly differential regulated enzymes identified by the proteomic study for the five meat-spoiling bacteria cultivated under four different gas atmospheres in MS-media. A list of all significantly regulated proteins (Welch T-test p <0.05) identified for the five meat-spoiling bacteria cultivated under the four gas atmospheres air, N_2, 30% CO_2 / 70% O_2 and 30% CO_2 / 70% N_2 is provided. Pairwise comparisons of the gas atmospheres were conducted, to reveal the effect of O_2 and CO_2 on bacterial metabolism. Colors indicate the effect of regulation with $\log_2$(diff.)= 2, $\log_2$ (diff.)= 3, $\log_2$ (diff.)= 4, $\log_2$ (diff.)= 5, $\log_2$ (diff.)= 6 and $\log_2$ (diff.)= 7 representing upregulated proteins and $\log_2$ (diff.)= 2, $\log_2$ (diff.)= 3, $\log_2$ (diff.)= 4, $\log_2$ (diff.)= 5, $\log_2$ (diff.)= 6, $\log_2$ (diff.)= 7, $\log_2$ (diff.)= 8 and $\log_2$ (diff.)= 9 representing downregulated proteins. * Functional

categories are based on NCBI, TIGR, SEED and KEGG annotation as well as manual research. All data are based on three independent replicates. Enzymes not encoded in the genome of a species are marked by a cross.

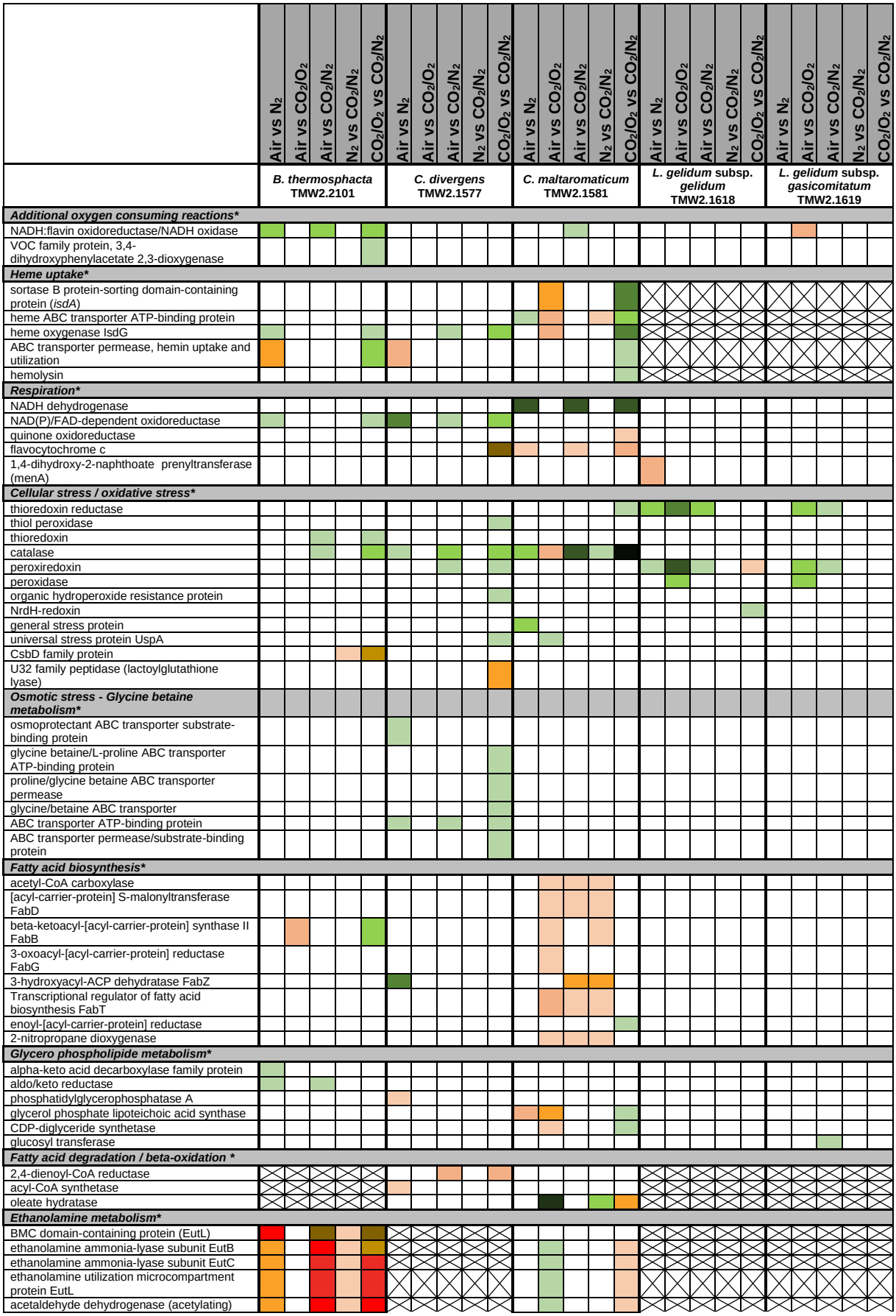

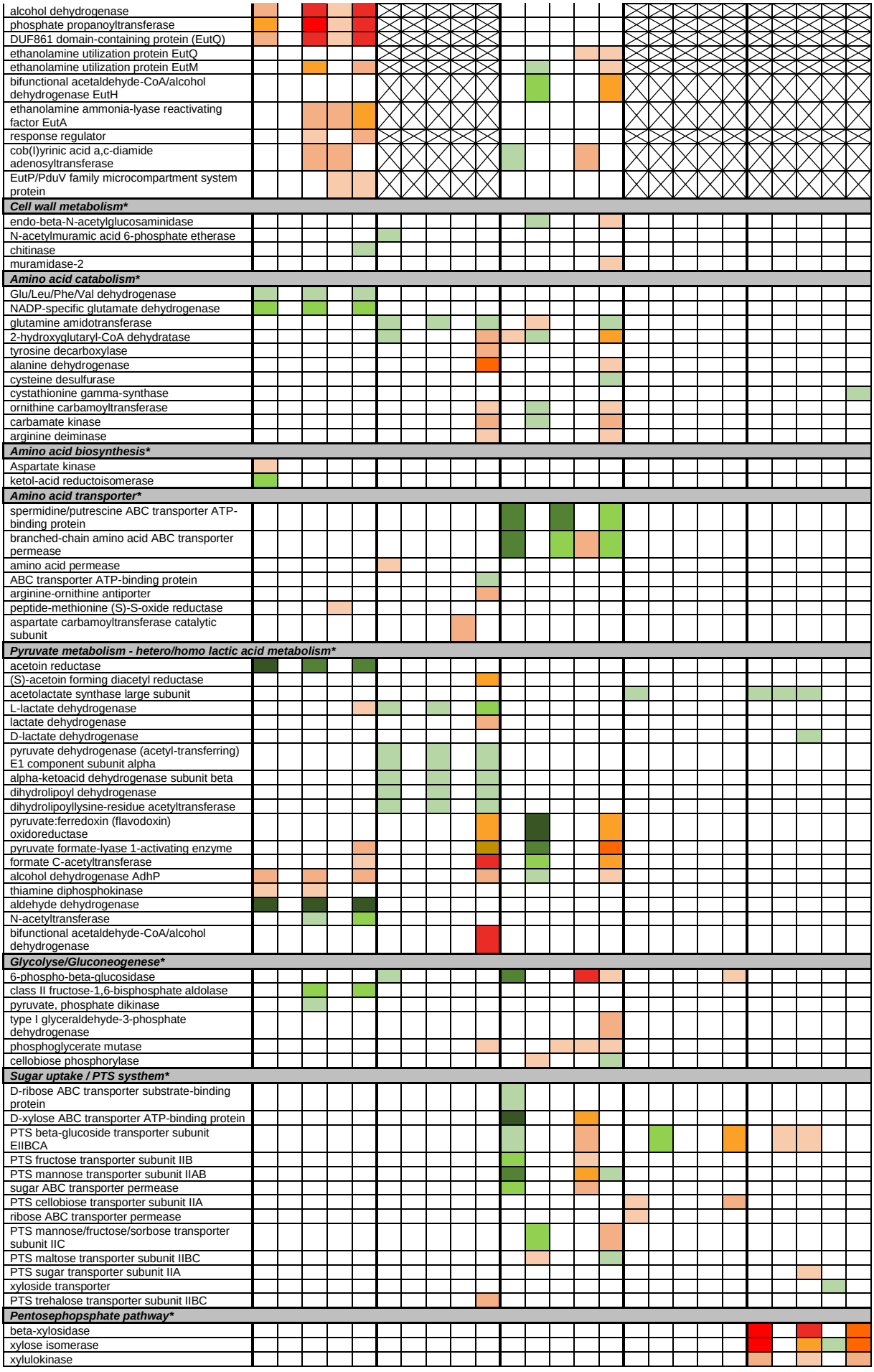
alcohol dehydrogenase
phosphate propanoyltransferase
DUF861 domain-containing protein (EutQ)
ethanolamine utilization protein EutQ
ethanolamine utilization protein EutM
bifunctional acetaldehyde-CoA/alcohol dehydrogenase EutH
ethanolamine ammonia-lyase reactivating factor EutA
response regulator
cob(I)yrinic acid a,c-diamide adenosyltransferase
EutP/PduV family microcompartment system protein
Cell wall metabolism*
endo-beta-N-acetylglucosaminidase
N-acetylmuramic acid 6-phosphate etherase
chitinase
muramidase-2
Amino acid catabolism*
Glu/Leu/Phe/Val dehydrogenase
NADP-specific glutamate dehydrogenase
glutamine amidotransferase
2-hydroxyglutaryl-CoA dehydratase
tyrosine decarboxylase
alanine dehydrogenase
cysteine desulfurase
cystathionine gamma-synthase
ornithine carbamoyltransferase
carbamate kinase
arginine deiminase
Amino acid biosynthesis*
Aspartate kinase
ketol-acid reductoisomerase
Amino acid transporter*
spermidine/putrescine ABC transporter ATP-binding protein
branched-chain amino acid ABC transporter permease
amino acid permease
ABC transporter ATP-binding protein
arginine-ornithine antiporter
peptide-methionine (S)-S-oxide reductase
aspartate carbamoyltransferase catalytic subunit
Pyruvate metabolism - hetero/homo lactic acid metabolism*
acetoin reductase
(S)-acetoin forming diacetyl reductase
acetolactate synthase large subunit
L-lactate dehydrogenase
lactate dehydrogenase
D-lactate dehydrogenase
pyruvate dehydrogenase (acetyl-transferring) E1 component subunit alpha
alpha-ketoacid dehydrogenase subunit beta
dihydrolipoyl dehydrogenase
dihydrolipoyllysine-residue acetyltransferase
pyruvate:ferredoxin (flavodoxin) oxidoreductase
pyruvate formate-lyase 1-activating enzyme
formate C-acetyltransferase
alcohol dehydrogenase AdhP
thiamine diphosphokinase
aldehyde dehydrogenase
N-acetyltransferase
bifunctional acetaldehyde-CoA/alcohol dehydrogenase
Glycolyse/Gluconeogenese*
6-phospho-beta-glucosidase
class II fructose-1,6-bisphosphate aldolase
pyruvate, phosphate dikinase
type I glyceraldehyde-3-phosphate dehydrogenase
phosphoglycerate mutase
cellobiose phosphorylase
Sugar uptake / PTS systhem*
D-ribose ABC transporter substrate-binding protein
D-xylose ABC transporter ATP-binding protein
PTS beta-glucoside transporter subunit EIIBCA
PTS fructose transporter subunit IIB
PTS mannose transporter subunit IIAB
sugar ABC transporter permease
PTS cellobiose transporter subunit IIA
ribose ABC transporter permease
PTS mannose/fructose/sorbose transporter subunit IIC
PTS maltose transporter subunit IIBC
PTS sugar transporter subunit IIA
xyloside transporter
PTS trehalose transporter subunit IIBC
Pentosephopsphate pathway*
beta-xylosidase
xylose isomerase
xylulokinase

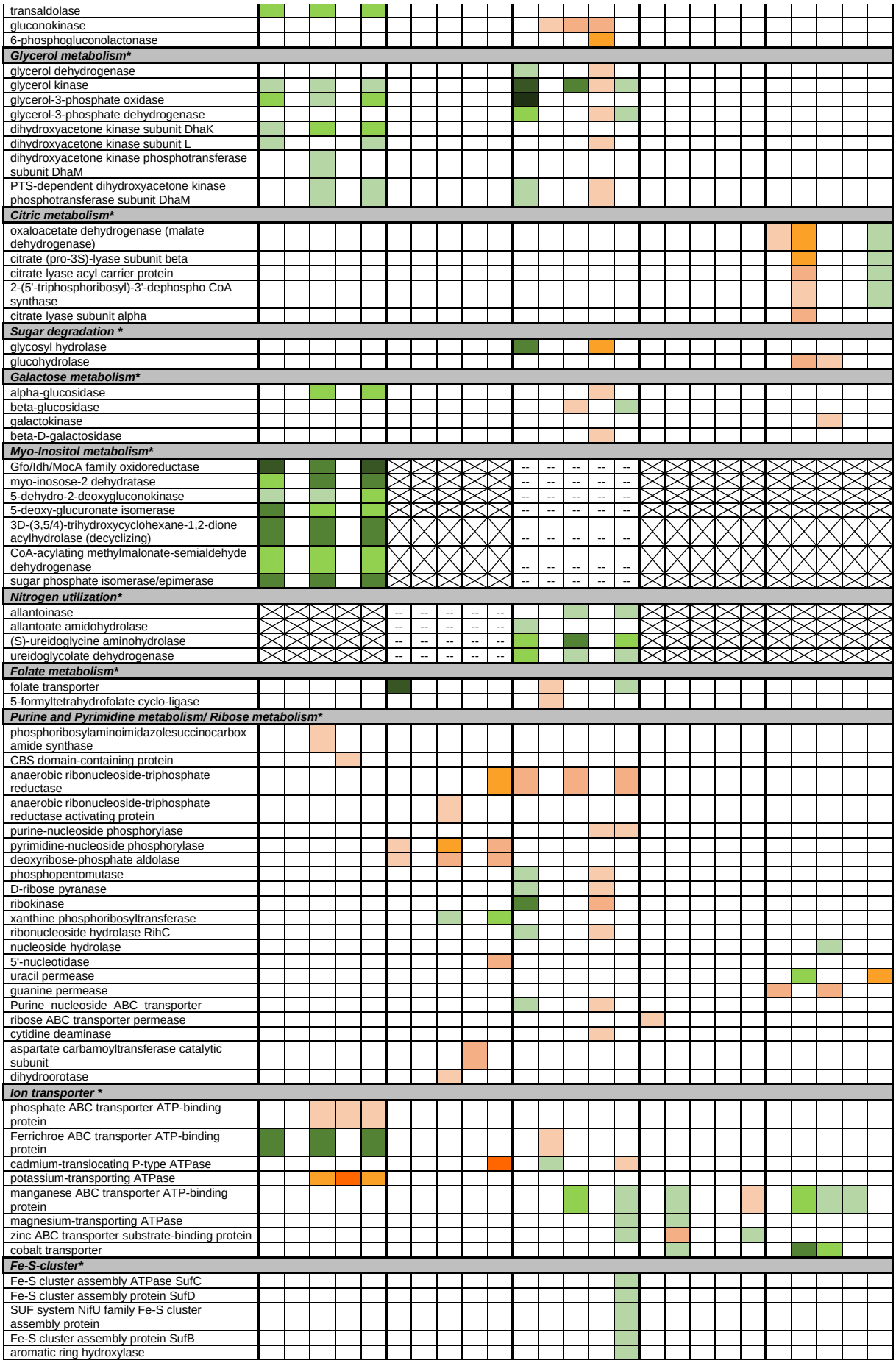
transaldolase
gluconokinase
6-phosphogluconolactonase
Glycerol metabolism*
glycerol dehydrogenase
glycerol kinase
glycerol-3-phosphate oxidase
glycerol-3-phosphate dehydrogenase
dihydroxyacetone kinase subunit DhaK
dihydroxyacetone kinase subunit L
dihydroxyacetone kinase phosphotransferase subunit DhaM
PTS-dependent dihydroxyacetone kinase phosphotransferase subunit DhaM
Citric metabolism*
oxaloacetate dehydrogenase (malate dehydrogenase)
citrate (pro-3S)-lyase subunit beta
citrate lyase acyl carrier protein
2-(5'-triphosphoribosyl)-3'-dephospho CoA synthase
citrate lyase subunit alpha
Sugar degradation *
glycosyl hydrolase
glucohydrolase
Galactose metabolism*
alpha-glucosidase
beta-glucosidase
galactokinase
beta-D-galactosidase
Myo-Inositol metabolism*
Gfo/Idh/MocA family oxidoreductase
myo-inosose-2 dehydratase
5-dehydro-2-deoxygluconokinase
5-deoxy-glucuronate isomerase
3D-(3,5/4)-trihydroxycyclohexane-1,2-dione acylhydrolase (decyclizing)
CoA-acylating methylmalonate-semialdehyde dehydrogenase
sugar phosphate isomerase/epimerase
Nitrogen utilization*
allantoinase
allantoate amidohydrolase
(S)-ureidoglycine aminohydrolase
ureidoglycolate dehydrogenase
Folate metabolism*
folate transporter
5-formyltetrahydrofolate cyclo-ligase
Purine and Pyrimidine metabolism/ Ribose metabolism*
phosphoribosylaminoimidazolesuccinocarbox amide synthase
CBS domain-containing protein
anaerobic ribonucleoside-triphosphate reductase
anaerobic ribonucleoside-triphosphate reductase activating protein
purine-nucleoside phosphorylase
pyrimidine-nucleoside phosphorylase
deoxyribose-phosphate aldolase
phosphopentomutase
D-ribose pyranase
ribokinase
xanthine phosphoribosyltransferase
ribonucleoside hydrolase RihC
nucleoside hydrolase
5'-nucleotidase
uracil permease
guanine permease
Purine_nucleoside_ABC_transporter
ribose ABC transporter permease
cytidine deaminase
aspartate carbamoyltransferase catalytic subunit
dihydroorotase
Ion transporter *
phosphate ABC transporter ATP-binding protein
Ferrichroe ABC transporter ATP-binding protein
cadmium-translocating P-type ATPase
potassium-transporting ATPase
manganese ABC transporter ATP-binding protein
magnesium-transporting ATPase
zinc ABC transporter substrate-binding protein
cobalt transporter
Fe-S-cluster*
Fe-S cluster assembly ATPase SufC
Fe-S cluster assembly protein SufD
SUF system NifU family Fe-S cluster assembly protein
Fe-S cluster assembly protein SufB
aromatic ring hydroxylase

Table S7| Analysis of the fatty acid profile of the five meat-spoiling bacteria. The fatty acid profile of the five meat-spoiling bacteria cultivated under the different gas atmospheres 21% O_2 / 0% CO_2 / 79% N_2 (air), 20% O_2 / 30% CO_2 / 50% N_2 and 70% O_2 / 30% CO_2 / 0% N_2 was analyzed by GCMS. The x-fold differential regulation of each fatty acid in response to O_2 or CO_2 is given. Results are obtained from different atmospheric comparisons: "X-fold upregulated by CO_2" Ratio of % (µg FA/g cells) identified for the gas atmosphere 21% O_2 / 0% CO_2 / 79% N_2 and 20% O_2 / 30% CO_2 / 50% N_2. "X-fold upregulated by O_2" Ratio of % (µg FA/g cells) identified for the gas atmosphere 20% O_2 / 30% CO_2 / 50% N_2 and 70% O_2 / 30% CO_2 / 0% N_2. Significantly different ($p < 0.05$) regulated fatty acids are highlighted in dark gray and bold letters. All values are based on biological replicates

Cell membrane Fatty acids	Retention time [min]	*B. thermosphacta* TMW2.2101	*C. divergens* TMW2.1577	*C. maltaromaticum* TMW2.1581	*L. gelidum* subsp. *gelidum* TMW2.1618	*L. gelidum* subsp. *gasicomitatum* TMW2.1619	*B. thermosphacta* TMW2.2101	*C. divergens* TMW2.1577	*C. maltaromaticum* TMW2.1581	*L. gelidum* subsp. *gelidum* TMW2.1618	*L. gelidum* subsp. *gasicomitatum* TMW2.1619
		x-fold upregulation by CO_2					x-fold upregulation by O_2				
C10:0	**13.64**	1.33		1.05	1.24	1.10	1.11		0.78	1.24	1.38
C12:0	**19.21**	1.27	1.40	**1.18**	1.12	**0.24**	1.02	0.76	**0.83**	**0.70**	1.14
***iso*_C13**	**22.63**	**4.20**					**1.32**				
***anteiso*_C13**	**22.96**	**3.74**					1.15				
C13:0	**24.49**	**4.60**					**1.65**				
***iso*_C14**		**2.27**					**1.42**				
C14:1 Δ9	**29.49**	1.46		1.14	1.37	**0.40**	0.87		**0.69**	0.51	0.70
14:1 isomer	**28.50**		0.92					1.39			
14:1 isomer 2	**29.25**		1.16					1.13			
C14:0	**30.32**	**1.42**	**1.29**	0.98	0.88	**2.56**	**1.35**	**0.87**	1.04	**0.75**	0.74
***iso*_C15**		1.01	0.24	1.09	1.09	0.93	1.00	3.25	0.96	0.56	**0.66**
***anteiso*_C15**		1.10	0.08	0.97	1.03	**0.79**	**0.84**	8.28	1.68	0.59	0.72
C15:0	**35.13**	1.18	1.23	1.07	1.28	**2.02**	**1.33**	0.90	1.00	**0.52**	**0.55**
***iso*_C16**	**39.58**	**0.73**		1.14	1.19	**1.69**	**1.15**		0.94	0.61	**0.58**
C16:1 isomer	**39.97**		1.00					1.25			
C16:1	**39.97**	1.01		1.06	0.94	**3.30**	1.15		0.92	**1.39**	**1.43**
C16:0	**41.22**	0.74	**1.18**	0.96	1.05	**1.43**	1.17	**0.80**	0.90	**0.74**	**0.69**
***iso*_C17**	**44.24**	**0.27**		**1.27**	1.13	0.94	**0.68**		**0.82**	0.64	0.90
***anteiso*_C17**		**0.47**	**0.50**	1.23	1.24	**1.53**	**0.62**	2.48	0.97	0.61	0.69
C17:1	**45.03**		0.74	1.14	1.08	0.96		1.11	1.16	0.60	**0.70**
C17:0	**46.21**		1.03	1.17	1.06	**0.81**		0.84	0.91	**0.78**	**0.82**
***iso*_18:2Δ9,12**	**49.18**	0.73		1.06	1.08	**0.38**	1.31		**1.61**	0.77	**0.67**
C18:1	**49.56**	0.83	**0.83**	1.01	**0.84**	**0.42**	1.16	**1.15**	**0.93**	**0.72**	0.87
C18:1 isomer	**49.92**	**0.68**	0.73	1.06	**0.95**	1.90	1.23	1.10	0.94	1.04	0.99
C18:0	**50.93**	1.12	1.30	0.71	**1.36**	**0.18**	1.43	0.57	**1.98**	0.80	0.97
18:2Δ9,12 conj		0.53	0.59	0.74	1.11	**0.07**	1.64	1.13	**3.65**	1.05	1.19
18:2Δ9,12 conj		0.48	0.60	0.76	1.18	**0.09**	1.89	1.17	**3.68**	**0.69**	0.87
C19:0 delta	**54.63**		2.60		**1.16**	**3.12**		0.61		**1.09**	1.12
C19:0 delta 2	**54.63**				1.25	**10.55**				**1.60**	1.32
C20:1+20:3n3	**58.42**		1.15		**1.37**			0.82		**0.54**	

C20:4 Δ5,8,11,14	**56.29**								**1.30**		
C20:5 Δ5,8,11,14,17	**56.51**								**1.10**		

Table S8| Summary of the genomic setting of the five meat-spoiling bacteria. A list of single genes of major metabolic pathways discussed in this study is provided for all species, including the corresponding locus tags (numbers in single cells). All data are based on genomic analysis (NCBI annotation and manual blast search). *putative gene function

		***B. thermosphacta* TMW2.2101**	***L. gelidum* subsp. *gelidum* TMW2.1618**	***L. gelidum* subsp. *gasicomitatum* TMW2.1619**	***C. divergens* TMW2.1577**	***C. maltaromaticum* TMW2.1581**
Biosample	**Gene**	**EHX26**	**BHS02**	**BHS03**	**EH150**	**BFC23**
Basic energy metabolism						
Glycolysis						
Glucose-6-phosphate isomerase	pgi	11570	01560	01545	07390	02435
6-phosphofructokinase	pfkA	07145	05585	05570	02550	05065
Fructose bisphosphate-aldolase	fbaA	06360 10495 01740	07660	07945	09365	14400 08190
Glycerinaldehyde-3-phosphate dehydrogenase	gapdh	08490	01760	01760	06845	09475
Phosphoglycerate kinase	pkg	08495	01725 03840	01710 01145 00780	06840	09470
Phosphoglycerate mutase	pgam	08505 03250	08325 03450 02715	08570 03400 02685	06830 08785	09460 04170 01895 14835 14600 13220 10905 10525
Pyruvate kinase	pk	07140	03800	03765	02545	05070
Gluconeogenesis						
Pyruvate carboxylase	pyc	01285	-------	-------	03170	04430
Phosphoenolpyruvate carboxykinase	pcka	-------	06470	06530	-------	-------
Phosphoenolpyruvate synthase	ppsa	-------	-------	-------	-------	06310 06315
Pyruvate phosphate dikinase		06325	-------	-------	-------	-------
Fructose-1,6bisphosphatase	fdp	10495	04980	05035	06685	01810
Glucose-6-phosphatase		-------	-------	-------	-------	-------
L-Lactate dehydrogenase	ldh	04585 05805 07840	00500	00440	10680	15630 00525 01270
D-Lactate dehydrogenase	ldh	-------	08445 00365 02215	07610 02180 08765 00325	03215	04385 13875
Oxidative pentose phosphate pathway						
Glucose-6-phosphat dehydrogenase	zwf	01790	08135	08375	04020	07365
6-phosphogluconolactonase (lactonase family protein)	devB	03890	04955	05015	07765	03650
6-phosphogluconate dehydrogenase	gntZ	11855	04425 02595	04495 02560	04255 08325	00260 07620
Ribulose-5-phosphate-3-epimerase	rpe	02195	02900	02840	03070 02820	04810
Ribulose-5-phosphate isomerase	rpiA	03100	08745 07630 03165	03110 07915 09480 09050	08800	00300

Citrate cycle						
Citrate synthase	citA	07125	-------	-------	03195	05995 04405
Aconitate hydratase	citB	04845	-------	-------	03200	04400
Isocitrate dehydrogenase	icdA	07120	-------	-------	03190	04410
Oxoglutarate dehydrogenase	sucAB	00960 01365	-------	-------	-------	-------
Succinyl-CoA-synthetase	sucCD	-------	-------	-------	-------	-------
Succinate dehydrogenase	sdhABCD	08370	06045	06030	-------	-------
Fumarate hydratase	fumA	01445	-------	-------	-------	03015
Malate dehydrogenase	mdh	00700	04385	08240	-------	13815
Phosphoenolpyruvate carboxylase	ppc	-------	06470	06530	-------	-------
Isocitrate lyase	ncgl	05055	-------	08230 08235 08225 08220	-------	-------
Malate synthase	aceB	-------	-------	-------	-------	-------
Amino acid metabolism						
Arginine deminiase	arcA	-------	-------	-------	00245	14805
Ornithine carbamoyltransferase	arcB	07965	05380	05445	00250	14810
Carbamate kinase	arcC	02045 02050	-------	-------	00260	14820
Arginine decarboxylase	speA	-------	-------	-------	-------	-------
Agmatinase	speB	-------	-------	-------	-------	-------
Arginase	Arg	-------	-------	-------	-------	-------
Agmatine ureohydrolase	speB	-------	-------	-------	-------	-------
Histidine decarboxylase	hdcA	-------	-------	-------	-------	-------
Lysine decarboxylase	lcdC	-------	-------	-------	-------	12280
Ornithine decarboxylase	speF	-------	-------	-------	-------	-------
Tyrosine decarboxylase	tdcA	-------	-------	-------	11100	10455
Glutamate decarboxylase	gadB	-------	-------	-------	03390	13475
Aspartate aminotransferase	aspB	-------	08670 00105 03495 05030	08920 00105 03445 05085	-------	14940
Malate dehydrogenase	mdh	-------	-------	08240	-------	13815
Glutamate dehydrogenase	gdhA	10335	-------	-------	03245	04355
Serine dehydratase	sdaAB	-------	-------	-------	-------	04835 04840
Aromatic amino acid aminotransferase	tyrB	-------	01330	01315	-------	08435
Branched-chain aa aminotransferase	ilvE	09235	04830	04900	09720	12725
Alanine dehydrogenase	ald	02725	-------	-------	06010	02035
Aspartate ammonia-lyase	aspA	11800	07635	07920	-------	-------
Aspartate oxidase	nadB	-------	-------	-------	-------	-------
Pyruvate metabolism						
Pyruvate dehydrogenase alpha E1	pdhA / aceE	01375	02405	02370	03235	04365
Pyruvate dehydrogease beta E1 / 2-oxoisovalerate Dehydrogenase	pdhB	01370 01365	02410	02375	03230	04370
Dihydrolipoamide acetyltransferase E2 / dienelactone hydrolase	pdhC	-------	02415	02380	-------	04375
Dihydrolipoyl-dehydrogenase E3	pdhD	01360 00975	02420	02385	03220	04380
Phosphotransacetylase / phosphate acetyltransferase	pta	00985 03910	03060	03005	08960	00280
Pyruvate oxidase	poxB	03750	-------	04365	-------	-------
Acetate kinase	ackA	10105	01605	03850	03495	04085
Acetaldehyde dehydrogenase / alcohol dehydrogenase	adhE	04535 04490 04310 01885 10070 05985	07945	08200	05430 04785 06040	15530 15485 04975
Pyruvate formate lyase / formate C-acetyltransferase	pflB	10215	-------	-------	02165	05535
Formate efflux transporter / formate-nitrite transporter	focA	10265	-------	-------	08795	10790
Acetolactate decarboxylase	aldC	01775	02580	02545	03765	03640
Diacetyl reductase / acetoin reductase	budC / butA / bdhA	02135	07955 02810	08255 02780	12520	-------
Heterolactic fermentation						
Phosphoketolase	xpkA	-------	07495	07745	-------	-------
Glucose-6-phosphate dehydrogenase	zwf	01790	08135	08375	04020	07365
Homolactic fermentation						
6-Phosphofructokinase	pfkA	02550	05585	05570	02550	05065
Fructose-1,6-bisphosphate aldolase	fbaA	06360 10495 01740	07660	07945	09365	14400 08190
Allantoin metabolism						
Allantoinase	hpxB	-------	-------	-------	01965	14455
Allantoate amidohydrolase	allc	-------	-------	-------	01910	06115

Ureidoglycine aminohydrolase	ylba	-------	-------	-------	01920	06105
Ureidoglycolate dehydrogenase		-------	-------	-------	01925 01930	06095 06100
Nucleoside and ribose metabolism						
Ribopyranase / D-ribose pyranase	rbsD	00875	08770	09470	01885	10570
Ribose transporter	rbsU	00865 00860	-------	09465	01895 01900	10555 10560
Putative ribose/nucleoside transporter	nubA / yngF	-------	00405	00375	09435	-------
Ribokinase	rbsK	00880	03430 08750	03380 09055 09475	01880	10575
Inosine-uridine nucleoside ribohydrolase / nucleoside hydrolase	kunH	-------	01730 06670 08790	01715 06725 09075	-------	-------
Ribonucleoside nucleosidase / ribonucleoside hydrolase	rihC	04380	08785	09070	-------	04070
Purine (deoxy)nucleoside phosphorylase	deoD	10205 09115 08635	-------	-------	08130 02250	10155 05445 05110
Pyrimidine (deoxy)nucleoside phospphorylase	deoA	09420	-------	-------	08790 08145 12005	10785 10200
Ribose1,5-phosphopentomutase	deoB	03670	-------	-------	08135	10160 05105
Ribonucleotide reductase alpha/assembly/beta	nrdA / nrdI/ nrdB	-------	01185	01165	-------	12435
Deoxyribose-phosphate aldolase / class 1b ribonucleoside-diphosphate reductase subunit beta	deoC	09430 07240 09290 09280 09285	01190	01170	12000 01605 10065 10055	10195 06445 12425

Respiration

NADH dehydrogenase						
NADH dehydrogenase	ndh	06170	01115	01095	06635	01885
Menaquinone biosynthesis						
1,4-dihydroxy-2-naphthoate prenyltransferase	menA	11995	06815	07110	09580*	01875*
1,4-dihydroxy-2-naphthoyl-CoA synthase	menB	11975	00095	00095	10860	12070
O-succinylbenzoate synthase	menC	08125	04505	04575	11290	11525
2-succinyl-5-enolpyruvyl-6-hydroxy-3- cyclohexene-1-carboxylic-acid synthase	mend	11985	04515	04585	11300	11535
O-succinylbenzoate--CoA ligase	menE	11970	00265	00210	10855	12065
isochorismate synthase	menF	11990	04520	04590	11305	11540
2-succinyl-6-hydroxy-2, 4-cyclohexadiene-1-carboxylate synthase	menH	11980	04510	04580	11295	11530
2-methoxy-6-polyprenyl-1,4-benzoquinol methylase	ubiE	08745	00270	00215	-------	00240*
Cytochrome aa_3 quinol oxidase						
Cytochrome aa3 quinol oxidase subunit I	qoxB	07625	-------	-------	-------	-------
Cytochrome aa3 quinol oxidase subunit II	qoxA	07620	-------	-------	-------	-------
Cytochrome aa3 quinol oxidase subunit III	qoxC	07630	-------	-------	-------	-------
Cytochrome aa3 quinol oxidase subunit IV	quxD	07635	-------	-------	-------	-------
Cytochrome bd ubiquinol oxidase						
Cytochrome ubiquinol oxidase subunit I	cydA	07685	02640	02605	06670	01825
Cytochrome d ubiquinol oxidase subunit II	cydB	07690	02645	02610	06665	01830
Thiol reductant ABC exporter subunit	cydC	07700	02655	02620	06655	01835
Thiol reductant ABC exporter subunit	cydD	07695	02650	02615	06660	01840
Cytochrome O ubiquinol oxidase						
Cytochrome O ubiquinol oxidase	cyo	-------	05340	05410	-------	00350
F_0F_1-ATP synthase						
F0F1 ATP synthase subunit A	atpB	08060	00690	00670	05855	01335
ATP synthase F0 subunit B	atpF	08070	00700	00680	05845	01345
F0F1 ATP synthase subunit C	atpE	08065	00695	00675	05850	01340
F0F1 ATP synthase subunit alpha	atpA	08080	00710	00690	05835	01355
F0F1 ATP synthase subunit beta	atpD	08090	00720	00700	05825	01365
F0F1 ATP synthase subunit gamma	atpG	08085	00715	00695	05830	01360
F0F1 ATP synthase subunit delta	atpH	08075	00705	00685	05840	01350
F0F1 ATP synthase subunit epsilon	atpC	08095	00725	00705	05820	01370
Heme biosynthesis						
Glutamyl-tRNA reductase	hemA	04720	-------	-------	01100	07045
Porphobilinogen synthase	hemB	04730	-------	-------	-------	-------
Hydroxymethylbilane synthase	hemC	04725	-------	-------	-------	-------
Uroporphyrinogen-III synthase	hemD	04735	-------	-------	-------	-------
Uroporphyrinogen decarboxylase	hemE	04715	-------	-------	-------	-------
Coproporphyrinogen III oxidase (oxygen independent)	hemN	11840	-------	-------	01505	06610
Protoporphyrinogen IX dehydrogenase	hemG	03920	-------	-------	00585	08360
Ferrochelatase	hemH	03925	-------	-------	07970	01065
Protoheme IX farnesyltransferase	cyoE	01275	-------	-------	-------	-------
Heme A synthase	ctaB	01280	-------	-------	-------	-------

Heme uptake and homeostasis						
Sortase B protein-sorting domain-containing protein	isdA	11590*	-------	-------	01365*	11300*
Iron surface determinant B	isdB	-------	-------	-------	-------	-------
Iron surface determinant H	isdH	-------	-------	-------	-------	-------
Iron surface determinant C	isdC	11585	-------	-------	01360	11305
Iron surface determinant E	isdE	11595	-------	-------	01370	11295
Heme ABC transporter ATP-binding protein	isdD	-------	00405	00375	01380*	07565
Iron ABC transporter permease	isdF	11600	-------	-------	01375*	11290
Iron surface determinant G	isdG	10855	-------	-------	12435	13075

Oxidative stress

Catalase	cat	11130	-------	-------	10970	11875
Superoxide dismutase (SOD)	sod	06805	-------	-------	04005	07340
2-Cys peroxiredoxin	/ prdx2	-------	07480	07730	-------	03975
Glutathione peroxidase	/ gpx	03205	04205	04195	06705	12965
Other peroxidases	--	03930 10115	01155	01135	03590	-------

Single oxygen consuming enzymes

Pyruvate oxidase	poxB	03750	-------	04365	-------	-------
Glycerol-3-phosphat oxidase / dehydrogenase	gps	08435	05735	05720	04895	09570
NADH oxidase	nox	09890	04450	04520	00705	08530 11520 10095
Acetolactate synthase (AlsS) (alpha acetolactate -> 2.3-butanedion)	alsS	01770	06300	06360	03770	03635
Pyridoxine 5'-phosphate oxidase	pdxH	-------	04395	04470	-------	-------

Fatty acid biosynthesis and conversion

SFA und UFA biosynthesis by FASII complex						
Acetyl-CoA-carboxylase (4 subunits)	acc	00675 00680 07150 07155	01810 01820 01825 01830	01810 01820 01825 01830	00980 00990 00995 01000	07135 07140 07145 07155
ACP S-malonyltransferase	fabD	02240	01795	01795	00965	07170
Beta-ketoacyl-ACP synthase III	fabH	03240	01780	01780	00950	07185
Malonyl-ACP / Condensing enzyme 3-oxoacyl-[acyl-carrier-protein] synthase II	fabF / fabB	03235	01805	01805	00975	07160
Beta-ketoacyl-ACP reductase / 3-oxoacyl-ACP-reductase	fabG	02245	01800	01800	00970	07165
3-hydroxyacyl-ACP-dehydratase	fabA / fabZ	08115	01815 01770	01815 01770	00985	07150
Enoyl-ACP reductase	fabI	11690 03110	-------	-------	00960 10575	08735
Branched chain fatty acid synthesis						
Acetolactate synthase small subunit / large subunit	ilvG / ilvM	01110 01115	06300	06360	11470 11475	13525 13530
Keto-acid reductoisomerase	ilvC	01105	02410*	02375*	11465	13520
Dihydroxy-acid dehydratase	ilvD	01120	-------	-------	11480	13535
Branched-chain aminotransferase	ilvE	09235	04830	04900	09720	12725
Branched-chain alpha-keto aicd dehydrogenase complex **E1**: 2-oxoisovalerate (lipoate) dehydrogenase / Branched chain keto acid dehydrogenase **E2**: 2-methylpropanoyl transferase / 2-oxo acid dehydrogenase / Lipoamide acyltransferase **E3**: Dehydrolipoate dehydrogenase / Dihydrolipoyl dehydrogenase	Bckdc	00960 00965 00975	02410 02420	02375 02385	03220 03230 03225	04380 04375 04370
2-isopropylmalate synthase	leuA	01100	-------	-------	11460	13515
Isopropylmalate isomerase 3-isopropylmalate dehydratase small subunit / large subunit	leuC / leuD	01085 01090	07685 07690	07970 07975	11445 11450	13500 13505
3-isopropylmalate dehydrogenase	leuB	01095	07695	07980	11455	13510
Exogenous fatty acid incorporation in FASII						
Long-chain fatty acid transport protein	fadL	-------	-------	-------	-------	-------
Fatty acid kinase subunit I: ATP binding-domain protein	fakA	02220*	02925*	02865*	02800*	04830*
Fatty acid kinase subunit I: fatty acid binding protein	fakB	04005 08215 09145	03730	03695	00195 01490 02275 02895 07075 11060	04740 05420 06625 08655 09720 14220 15230

Fatty acid incorporation in membrane						
Peripherical membrane protein / Phosphate acyltransferase	plsX	02235	02530	02495	02780	04850
Integral membrane protein Glycerol-3-phosphate acyltransferase	plsY	02495	04695 05090	04765 05145	01020*	00770
Regulators						
Quantitative amounts of fatty acids						
PpGpp synthase II	spoT	01005	05415	05480	01610	08575
Global transcriptional regulator	fabR	03235*	01775*	01775*	00945* 00935*	07005* 07190*
UFA regulators						
Transcription factor	fadR	06570	-------	-------	08330 12445	-------
Transcription factor	fabR	02230	-------	-------		-------

Conversion of existing fatty acids

Desaturation of fatty acids						
Acyl-CoA thioesterase	tesA	02485 08670	-------	--------	00185 08765	10720
Oxygen-dependent phospholipid acyl-chain desaturase (delta-5-desaturase) (membrane phospholipid desaturase)	desA	-------	-------	-------	-------	-------
Membrane phospholipid desaturase	desB	-------	-------	-------	-------	-------
Conjugation of fatty acids						
Hydratase	Cla-hy	-------	05455*	05520*	03980*	-------
Oxidoreductase	Cla-dh	-------	07695*	-------	-------	-------
Isomerase	Cla-dc	-------	-------	-------	-------	-------
Cyclisation of fatty acids						
Cyclopropane fatty acid synthase	cfas	-------	04430	04500	09690*	-------
Cis/trans isomerization of fatty acids						
Phospholipid cis/trans isomerase	cti	-------	-------	-------	-------	-------

Fatty acid degradation

Saturated medium- and long chain fatty acid degradation (beta-oxidation)						
Long-chain-CoA synthetase	fadD	07670*	07860	-------	06265 01935 12460	06090
Acyl-CoA dehydrogenase	fadE	-------	-------	-------	-------	11115**
Enoyl-CoA hydratase	fadB	-------	-------	-------	00440	03305
Acetyl-CoA C-acyltransferase	fadA	00725	07855	-------	07920	11895
Transcriptional regulator	fadR	06570	-------	-------	12445 08330	00255
Saturated short chain fatty acid degradation						
Acetyl-CoA: acetoacetyl-CoA transferase subunit alpha	atoD	00720	04600	04670	07925	11900
Acetyl-CoA: acetoacetyl-CoA transferase subunit beta	atoA	00730	01465	01450	07915	11890
2-hydroxycarboxylate transporter	atoE	10250	08045	08310	04885	01670 00580 04075
β-ketoacyl-CoA thiolase	atoB	00725	07855	-------	07920	11895
Regulator of two-component system	atoC	-------	-------	-------	07890*	11905*
Polyunsaturated fatty acid degradation (even-numbered unsaturated carbon atoms, 9-cis, 12-cis-octadienoic acid, CLA)						
2,4 Dienoyl-CoA reductase	fadH	-------	-------	-------	12560	10515
Polyunsaturated fatty acid degradation (odd-numbered unsaturated carbons atoms)						
Enyol CoA isomerase / Enoyl-CoA hydratase	fadB	-------	-------	-------	00440*	03305*

Glycerophospholipid metabolism

Glycerol degradation						
phospholipase	---	05940 12085	03465 04435 04480	03415 04505 04550	02270 02885 08770	01190 04745 05425 10595 10725 10945
glycerol transporter glycerol-3-phosphate ABC transporter	---	09885 06385 03005	00250 03105 08340 08335	03050 00195 09245 08585 08580	11340	11620 11625 11630
glycerol kinase	glpK	08430 05495	03820 06335	03785 06395	05445 04900	13905 09340 06630 02990
alpha-glycerophosphate oxidase	glpO	08435	-------	-------	04895	13910

glycerol-3-phosphate dehydrogenase	gpsA	08435 08725	06625 05735	06685 05720	11820 04895 06930	14930 13570 02995 09570
Biosynthesis of Phosphatic acid (PA) and CDP-diacylglycerol from CMP and sn-glycerol 1-Phosphat						
CDP-diacylglycerol--glycerol-3-phosphate 3-Phosphatidyltransferase	---	04695	05800	05785	04160	07525
Biosynthesis of Phosphatic acid (PA) from Glycerol 3-phosphate						
Lysophosphatic acid – acyltransferase Glycerol-3-phosphate acyltransferase	plsB / plsC	04810	04695 05090	04765 05145	02180	00770
Biosynthesis of Phosphatidylserin from PA						
Phosphatidate cytidylyltransferase CDP-diglyceride synthetase	cdsA	04875	03405	03355	01430	01075 06700
Phosphatidylserin synthase CDP-diacylglycerol--serine O-phosphatidyltransferase	pssA	03770	-------	-------	-------	06950
Degradation of Phosphatidylserin						
Phosphoserine phosphatase	psp	10010	-------	-------	-------	14515
Biosynthesis of Phosphatidylethanolamine from phosphatidylserine						
Phosphatidylserin decarboxylase	psd	03760	-------	-------	-------	00775*
Degradation of Ethanolamine						
Ethanolamine ammonia-lyase reativase	eutA	04510	-------	-------	-------	15505
Ethanoamine ammonia-lyase heavy chain	eutB	04515	-------	-------	-------	15510
Ethanolamine ammonia-lyase light chain	eutC	04520	-------	-------	-------	15515
Aldehyde dehydrogenase	eutE	04535	-------	-------	-------	15530
Alcohole dehydrogenease	eutG	04490	-------	-------	-------	15485
Ethanolamine utilization protein	eutH	04560	-------	-------	-------	15560
Ethanolamine utilization microcompartment protein	eutL	04525	-------	-------	-------	15520
Ethanolamine utilization protein	eutM	04530* 04540*	-------	-------	-------	15535 15525
Ethanolamine utilization protein	eutN	04555	-------	-------	-------	15555
Ethanolamine utilization protein	eutP	04455*	-------	-------	-------	15475
Ethanolamine utilization protein	eutQ		-------	-------	-------	15565
Response regulator	eutR	04500	-------	-------	-------	-------
Corrinoid adenosyltransferase / cobalamine	eutT	04485	-------	-------	-------	15480 15540
Biosynthesis of Phosphatidylcholine (Lecithin) from PA						
Phosphatidate phosphatase	plpp	-------	01195* 01450* 07340*	01175* 07560* 01435*	-------	02950*
Diacylglycerol cholinephosphotransferase	cpt1	-------	05525	-------	-------	-------
Biosynthesis of Phosphatidylcholine from choline (Kennedy pathway)						
Cholinkinase	ckt	-------	-------	-------	-------	-------
Phosphocholine citidyltransferase	---	-------	-------	-------	-------	-------
1,2 diacylglycerol cholinephosphotransferase	---	-------	05525	-------	-------	-------
Biosynthesis of Phosphatidylglycerolphoshate from PA						
Phosphatidate cytidylyltransferase CDP-diglyceride synthetase	cdsA	04875 04910	03405 05520 05230	03355 05300	01430	01075 06700
CDP-diacylglycerol--glycerol-3-phosphate 3-Phosphatidyltransferase	pgsA	04695	05800	05785	04160	07525
Biosynthesis of Phosphatidylglycerol from phosphatidylglycerolphoshate						
Phosphatidylglycerolphosphat phosphatase Phosphatidylglycerophosphatase A	pgpP	-------	06575 03090	06635	07435	02390
Biosynthesis of Cardiolipin from Phosphatidylglycerol						
Cardiolipin synthase	cls	08265	05820	05805	02930 08165	04710 08060
Degradation of Cardiolipin						
Lipoteichonic acid synthase LTA synthase family protein	ltaS	11125	02185	02150	00815 04570	08415
DAG kinase	dgkB	06365 07225	03820 06335	06395 03785	03395	09340 06630
Biosynthesis of Phosphatidylinositol from CDP-diacylglycerol						
Phosphatidylinositol synthase Myo-inositol 3-phosphatidyltransferase CDP-diacylglycerol--inositol 3-phosphatidyltransferase	pIS	-------	-------	-------	-------	-------
Degradation of Phosphatidylinositol						
Phospholipase C	plc	05940 12085	-------	-------	02885*	01190 04745 10595
Inositol monophosphatase	Impa1	01310	-------	-------	03205	04395
Myo-inositiol-2-dehydrogenase	IolG	10480 01725 03785 04255	-------	-------	05395 05675 08910	08205 08195
Myo-inosose-2 dehydratase	IolE	01715	-------	-------	-------	08200
3D-(3,5/4)-trihydroxycyclohexane-1,2-dione acylhydrolase (decyclizing)	IolD	01710	-------	-------	-------	08210
5-deoxy-glucuronate isomerase	IolB	01700	-------	-------	08615	08220
5-dehydro-2-deoxygluconokinase	IolC	01705	-------	-------	-------	08215
6-phospho-5-dehydro-2-deoxy-D-gluconate aldolase	IolJ	01740*	-------	-------	-------	08190*
CoA-acylating methylmalonate-semialdehyde dehydrogenase	IolA	01695	-------	-------	-------	08225

Triosephosphat isomerase	tpiA	01730 01735 08500	01245 06640	01225 06700	06835	09465 08235*

Table S9| Summary of the mass spectrometric data analysis for the six *Pseudomonas* strains. List of the total numbers of genes encoded according to the annotation pipeline of NCBI, the number of proteins detected by mass spectrometry and the number of significantly up or down regulated proteins with p <0.01 and a $\log_2$(fold change) >2 identified by Perseus analysis for the six *Pseudomonas* strains cultivated in MS-medium under oxic (21% O_2 / 0.03% CO_2) and anoxic (100% N_2) conditions.

	TMW	Encoded	Detected	Significant anaerob upregulated	Significant anaerob downregulated	**Total**
P. lundensis	2.1732	4523	2450	47	50	**97**
P. lundensis	2.2076	4215	2380	30	56	**86**
P. weihenstephanensis	2.2077	4599	2585	168	109	**277**
P. weihenstephanensis	2.1728	4270	2441	156	68	**224**
P. fragi	2.2081	4565	2440	25	50	**75**
P. fragi	2.2082	4571	2451	153	103	**256**

Table S10| Detailed list of single differentially regulated proteins of the six *Pseudomonas* strains cultivated under oxic and anoxic conditions. Summary of single enzymes significantly regulated (p <0.01, $\log_2$ >2) in the proteomic experiment for the six *Pseudomonas* strains. Colors indicate the effect of regulation with $\log_2$ (diff.)= 2, $\log_2$ (diff.)= 3, $\log_2$ (diff.)= 4, $\log_2$ (diff.)= 5, $\log_2$ (diff.)= 6, $\log_2$ (diff.)= >6 representing anoxic downregulated proteins and $\log_2$ (diff.)= 2, $\log_2$ (diff.)= 3, $\log_2$ (diff.)= 4, $\log_2$ (diff.)= 5, $\log_2$ (diff.)= 6, $\log_2$ (diff.)= >6 representing anoxic upregulated proteins. * Functional categories are based on NCBI, TIGR, SEED and KEGG annotation as well as manual research. Numbers in colored boxes are locus tags of each gene corresponding to the NCBI annotation. All data are based on three independent replicates.

	P. lundensis		*P. weihenstephanensis*		*P. fragi*	
Gene name (NCBI annotation)	2.1732	2.2076	2.2077	2.1728	2.2081	2.2082
Amino acids*						
Amino aicd transporter						
amino acid ABC transporter ATP-binding protein			05485			
amino acid ABC transporter ATP-binding protein	13790			00625		
amino acid ABC transporter substrate-binding protein					15335	
Alanine, Aspartate and Glutamine metabolism						
glutamine synthetase	07630	04210				
glutamate synthase large subunit						13245
Glu/Leu/Phe/Val dehydrogenase	15495		22005	16305		07315
glutaminase A			04370	06235		15355
type 1 glutamine amidotransferase domain-containing protein			16110	16570		04970
amidohydrolase			21730	21535		03085
ammonia-dependent NAD(+) synthetase			12565		11050	12610
N-acetylglutaminylglutamine amidotransferase			09305	02150		
glutamate decarboxylase			04375	06230		
trifunctional transcriptional regulator/proline dehydrogenase/L-glutamate gamma-semialdehyde dehydrogenase					11505	
formimidoylglutamate deiminase					11920	
asparaginase				10525	21900	19450
PLP-dependent aminotransferase family protein (Aspartate_aminotransferase_(AspB-4))	05465	12975	06810	20870	17470	19820
aspartate aminotransferase family protein		12020	11930	13615		
aspartate ammonia-lyase		05655				
asparagine synthase (glutamine-hydrolyzing)			09485	01965		
alanine transaminase		07935		17250		
Beta-alanine metabolism						
Zn-dependent hydrolase (beta-ureidopropionase)						01345
dihydropyrimidinase						01355
NAD(P)-dependent oxidoreductase (NAD-dependent_dihydropyrimidine_dehydrogenase Subunit PreT)						01360
NAD-dependent dihydropyrimidine dehydrogenase subunit PreA						01365
Arginine and Proline metabolsim						
gamma-glutamyl-gamma-aminobutyrate hydrolase family protein		04205				
ADI pahtway						

agmatine deiminase	00475	19000	13935	15555		
carbamate kinase			14660			06185
arginine deiminase				17460		
ornithine carbamoyltransferase			14655			
Arc family DNA-binding protein					17130	05750
Sonstiges						
bifunctional [glutamate--ammonia ligase]-adenylyl-L-tyrosine phosphorylase/[glutamate--ammonia-ligase] adenylyltransferase						13025
Serine und Threonine metabolism						
tryptophan synthase subunit beta				16010		
threonine dehydratase	06045					
L-serine ammonia-lyase		7690				
L-threonine dehydrogenase	19230		15890			
formylglycine-generating enzyme family protein		21360				
FAD-binding oxidoreductase, Glycine/D-amino_acid_oxidases_(deaminating)					00145	
serine/threonine protein kinase			12985			
serine O-acetyltransferase			05095			
serine kinase/phosphatase			19890	19405		
PrkA family serine protein kinase			00095	07570		08290
cysteine synthase A				21720		
Glycine cleavage system						
dihydrolipoyl dehydrogenase			07115	13320		19525
aminomethyl-transferring glycine dehydrogenase		07695	14680	17490		
glycine cleavage system protein R				14625		08535
glycine cleavage system aminomethyltransferase GcvT		07685	14690	17500		06215
glycine cleavage system protein GcvH	16225			17485		06200
glycine zipper family protein	02170			04835	07325	15845
Histidine						
imidazoleglycerol-phosphate dehydratase HisB	00645	20140	13755	15385		13690
urocanate hydratase		21675				
histidine-type phosphatase			15720	16945		05630
histidine phosphatase family protein			17520	20555		
Lysine						
4-hydroxy-tetrahydrodipicolinate reductase						21815
Val/Leu/Ileu degradation						
CoA-acylating methylmalonate-semialdehyde dehydrogenase	15045	12025	11925	13610		
3-isopropylmalate dehydratase large subunit				00945		
short chain dehydrogenase			05730	04815		20850
3-hydroxyisobutyrate dehydrogenase				20105		
3-methyl-2-oxobutanoate dehydrogenase (2-methylpropanoyl-transferring) subunit alpha				13305		
acetyl/propionyl/methylcrotonyl-CoA carboxylase subunit alpha					16065	
BCKDHC - complex (branched-chain α-keto acid catabolism)						
dihydrolipoyl dehydrogenase			07115	13320		19525
2-oxo acid dehydrogenase subunit E2			07120	13315		19520
alpha-ketoacid dehydrogenase subunit beta						19515
Methionine / Cystein						
methionine gamma-lyase			07475	12920		
S-methyl-5'-thioinosine phosphorylase					05475	
5'-methylthioadenosine/S-adenosylhomocysteine nucleosidase			16585			
GNAT family N-acetyltransferase				16235	00030	22910
GNAT family N-acetyltransferase			20760	01255	07070	04600
Respiratory chain*						
Cytochromes and function						
C-type cytochromes	07450	04390	01740	09230	08695	10085
cytochrome bc complex cytochrome b subunit			04760			
SCO family protein			01980			
copper chaperone PCu(A)C	14610	11600	12330	14010		
Anaerobic copper elektrone transfere from bc1 to Nitrit reducatse						
copper-binding protein		18525				
cupredoxin family protein				02915		
Heme metabolism						
heme biosynthesis protein HemY						14215
biliverdin-producing heme oxygenase						06155
Quinone metabolism						
2-polyprenyl-3-methyl-6-methoxy-1,4-benzoquinone monooxygenase			23155			08140
Oxygen consumption						
TauD/TfdA family dioxygenase			10790			
dioxygenase			11510			03415
Alternative electrone acceptors*						
Nitrite and Sulfite						
nitrite/sulfite reductase (CobG: precorrin-3B synthase)						18280
pseudoazurin						17330
precorrin-8X methylmutase						12330
precorrin-6A synthase (deacetylating)			16820			
Nitronate						
sigma-54-dependent Fis family transcriptional regulator			05440	05110		
response regulator transcription factor				16125		
nitronate monooxygenase			23175	07405		08120
ABC transporter substrate-binding protein (sulfate, nitrat)			07090	09960		
Redox-equivalents for respiration*						
Sulfite						
sulfite oxidase-like oxidoreductase	22960		22500			
protein-methionine-sulfoxide reductase, sulfite_DH_soxC: sulfite dehydrogenase			18605	19510		22065
Sulfide						
TIGR01244 family phosphatase, Sulfide:quinone oxidoreductase, Type II					23110	12060
Glycine						
cyanide-forming glycine dehydrogenase subunit HcnB			20955			01015
cyanide-forming glycine dehydrogenase subunit HcnA			20950			
Pyruvat						
ubiquinone-dependent pyruvate dehydrogenase			08630	02830		
Malate						
malate dehydrogenase (quinone)				01265		18575
NADPH/H2						
NADP-dependent oxidoreductase (quinone)			09555	16370		
Sorbose oxidation						
sorbosone dehydrogenase family protein			10500	03995		04155
2,5-didehydrogluconate reductase DkgB			20355	16175		
Other sugar oxidation						
PQQ-dependent sugar dehydrogenase				10755		
pyrroloquinoline quinone-dependent dehydrogenase			00790	08240		08650
Iron metabolsim*						
Iron uptake system						
deferrochelatase/peroxidase EfeB				20515		17185
iron uptake system protein EfeO			17650			17180
mercury resistance system periplasmic binding protein MerP			23025			
MerR family transcriptional regulator	20460	15285				
bacterioferritin			12475	14155		
Iron-sulfur cluster						
iron-sulfur cluster-binding protein			18930	19835		21745
(Fe-S)-binding protein			18925			
YgiQ family radical SAM protein			12585	14265		12630
hemerythrin domain-containing protein	04710					
Iron depending proteins						
Fe2+-dependent dioxygenase			04520			15225
Iron chelat complexes						

LacI family DNA-binding transcriptional regulator	04800	06940			00180	
siderophore-interacting protein	03670					
TonB-dependent siderophore receptor				01325		07285
FecR family protein				16200		
Copper metabolism*						
Copper import and export						
copper homeostasis periplasmic binding protein CopC						19495
multicopper oxidase family protein, copper-resistance protein (CopA)			05255			
Oxidative stress*						
cysteine hydrolase				01445		
peptide-methionine (S)-S-oxide reductase MsrA			22460			
NGG1p interacting factor NIF3		16340				
DNA starvation/stationary phase protection protein		13870		13110		01655
phosphate starvation-inducible protein PsiF			12460			12500
catalase		02245				
catalase HPII			01960	09440	08935	
peroxiredoxin	04180		01665	10890		17210
peroxiredoxin			16985			
thioredoxin TrxC				14780		13100
OsmC family protein (peroxiredoxin)			01705	09190		22110
OsmC family protein (peroxiredoxin)			21735	21530		10125
OsmC family protein (peroxiredoxin)						22110
DsbA family protein						13895
tannase/feruloyl esterase family alpha/beta hydrolase, S-formylglutathione hydrolase						19245
Transcriptional regulators*						
sigma-54-dependent transcriptional regulator				21335		
response regulator transcription factor			14260	15880		
response regulator transcription factor			12085			14235
response regulator transcription factor		14540	20910	01095		
response regulator		07005	01065	13820		
transcriptional regulator			21490	21815		14195
translation initiation factor 2			11265			
Lrp/AsnC family transcriptional regulator			05015			
winged helix-turn-helix transcriptional regulator					23115	12065
AraC family transcriptional regulator	11955		10300	17245		05965
AraC family transcriptional regulator			14435			
TenA family transcriptional regulator					04520	
MarR family transcriptional regulator						04925
TraR/DksA family transcriptional regulator	13985		18200	00740		01170
Membrane Transporter*						
Upregulated						
TolC family outer membrane protein		11070	12845	14500		
OmpA family protein	12425	00520	05695			06720
OmpA family protein			15155	18010		20775
transporter substrate-binding domain-containing protein					08700	
ABC transporter substrate-binding protein			07035	03665		
ABC transporter substrate-binding protein				13400		03795
ABC transporter substrate-binding protein			01885	01170		
ABC transporter ATP-binding protein			01895			
taurine ABC transporter substrate-binding protein			01675			
carbohydrate ABC transporter substrate-binding protein				17385		
efflux RND transporter permease subunit						20970
Cell wall proteins*						
Lipopolysachharide biosynthesis						
ADP-glyceromanno-heptose 6-epimerase	14110	13565	07660	12745	03485	01235
aspartyl/asparaginyl beta-hydroxylase domain-containing protein	18110					
LPS-assembly protein LptD		18265		07535		08255
LPS export ABC transporter periplasmic protein LptC			19395			
chain-length determining rotein			09435			
lipopolysaccharide heptosyltransferase I				14670		
Peptidoglycan						
D-alanyl-D-alanine endopeptidase	09505	13880	07310	13120	03960	01665
D-alanyl-D-alanine carboxypeptidase						15985
alanine racemase						23155
alanine racemase						09530
endolytic transglycosylase MltG			11180	03495		
transglycosylase SLT domain-containing protein				16405		04800
peptidoglycan-binding protein LysM			13980	15600		13950
peptidoglycan editing factor PgeF					13160	
L,D-transpeptidase family protein						19210
Murein degradation						
membrane-bound lytic murein transglycosylase MltF		16350	15400	18255		
Cellulose synthese						
cellulose synthase operon protein YhjQ						17475
Biotin metabolism*						
malonyl-ACP O-methyltransferase BioC			00325			08490
8-amino-7-oxononanoate synthase					10295	
dethiobiotin synthase				07780		
biotin synthase BioB			00340	07800		
bifunctional biotin--[acetyl-CoA-carboxylase] ligase/biotin operon repressor BirA			03090	07370		
Fatty acid metaboism*						
FASII complex						
3-oxoacyl-ACP reductase	14930		12035	13720		12095
SDR family NAD(P)-dependent oxidoreductase, 3-oxoacyl-[acyl-carrier-protein] reductase	19000					09305
acyl dehydratase	14925		12040.00	13725		12100
Biosynthesis of unsaturated fatty acids						
acyl-CoA thioesterase			15310	18165		
Fatty acid incorporation in membrane						
phosphate acyltransferase PlsX						03660
Sautrated medium-and long chain fatty acid degradation via beta-oxidation						
long-chain-fatty-acid--CoA ligase				17310		
long-chain fatty acid--CoA ligase			00750	08200		
fatty acid--CoA ligase			04695		22200	
acyl-CoA/acyl-ACP dehydrogenase	09290	14095				
acyl-CoA dehydrogenase			07605			03760
acyl-CoA dehydrogenase	16715	18085	11045	07770	10315	04615
acyl-CoA dehydrogenase			20280			
SDR family NAD(P)-dependent oxidoreductase, 3-hydroxyacyl-CoA_dehydrogenase						#######
DNA alkylation response protein			03905	06695		15870
Glycerophospholipids						
phospholipase D family protein	21810					
lipid kinase YegS			11690			
phosphatidylserine decarboxylase						12810
class I SAM-dependent methyltransferase		21365				13180
class I SAM-dependent methyltransferase			02800	00935		01240
class I SAM-dependent methyltransferase				10395		11920
Benzoat degradation*						
IclR family transcriptional regulator				00630		
carboxymuconolactone decarboxylase family protein	21600	14100	17800			02880
carboxymuconolactone decarboxylase family protein			07075			
dienelactone hydrolase family protein				02365		
putative 4-hydroxy-4-methyl-2-oxoglutarate aldolase			10730			03890
Sugar metabolism*						

Glucose oxidation						
OprD family porin		04320	01670	09155	16750	17055
OprD family porin		08510	16825		08500	10280
OprD family porin		18980			12380	13890
gluconate 2-dehydrogenase	07460		01730	09220		10095
gluconate 2 dehydrogenase			01735	09225	08690	10090
sugar kinase		06950	17365			17830
pyrroloquinoline quinone biosynthesis protein PqqF						08425
glucose/quinate/shikimate family membrane-bound PQQ-dependent dehydrogenase			05330	05225		
phosphoenolpyruvate--protein phosphotransferase			05245	05280	07750	12985
D-glycerate dehydrogenase		06960	17375			
Starch and sucrose metabolism						
extracellular solute-binding protein (maltose transporter)			08930	02525	12520	02730
4-alpha-glucanotransferase			07620	12775		
alpha/beta hydrolase			08710	21800		15760
alpha/beta hydrolase			21505	12965		22320
glycosyltransferase family 4 protein			11650	03125		
glycogen debranching protein GlgX			07610	12785		01290
glycogen/starch/alpha-glucan phosphorylase			13640	15270		
1,4-alpha-glucan branching protein GlgB			07580	12815		01300
hydrolase			17960	00980		03080
SMI1/KNR4 family protein				10450		
SMI1/KNR4 family protein				22110		
beta-glucosidase BglX		08315				05505
alpha,alpha-phosphotrehalase					07760	20145
Mannose metabolism						
mannose-1-phosphate guanylyltransferase/mannose-6-phosphate isomerase			11680			
GDP-mannose dehydrogenase	10515		21815			
Other non specific						
polysaccharide biosynthesis tyrosine autokinase					02495	
sugar phosphate isomerase/epimerase			17155			
glycosyltransferase family	08735		09470		02525	17065
alpha/beta hydrolase			04005			
alpha/beta hydrolase			15175			03070
alpha/beta hydrolase			10725	03775		
TatD family hydrolase			04480			
Pyruvate metabolism*						
Pyruvate to ethanol						
acetyl-CoA hydrolase/transferase family protein						09515
aldehyde dehydrogenase family protein			12550	14230		12595
aldehyde dehydrogenase (NADP(+)						01440
zinc-dependent alcohol dehydrogenase family protein			17145		00270	17730
zinc-binding alcohol dehydrogenase family protein			22475			
pirin family protein			17955	00985	00120	17880
pirin family protein						22105
Lactate metabolism						
glyoxalase		21335				
FAD-binding oxidoreductase (lactate dehydrogenase)		17540	18940	19845	18925	
lactate utilization protein			18935			
Pyruvate to acetaldehyde						
pyruvate dehydrogenase (acetyl-transferring), homodimeric type		10915				
aldehyde dehydrogenase		02660	03690		13840	
Citric acid cycle*						
NADP-dependent isocitrate dehydrogenase					04670	02410
ADP-forming succinate--CoA ligase subunit beta					04865	
isocitrate lyase		10075				
aconitate hydratase AcnA			09755			
bifunctional aconitate hydratase 2/2-methylisocitrate dehydratase					16355	
2-methylcitrate dehydratase			10705			
class II fumarate hydratase			09325	02130		02295
Cell division*						
Protein biosynthesis						
30S ribosomal protein S1	08665		09420		04460	02200
ribosome biogenesis GTPase			05180			
50S ribosomal protein L7/L12			03150	07310		16620
50S ribosomal protein L10			03145	07315		
50S ribosomal protein L25/general stress protein Ctc						07805
ABC-F family ATPase			17280	20790		17745
trigger factor		08975				04860
ribosome modulation factor						03855
peptidylprolyl isomerase			20065			04835
FKBP-type peptidyl-prolyl cis-trans isomerase			20800			
protease inhibitor I42 family protein			05280			
Cell division proteins						
AAA family ATPase			07805		18615	21400
cell division protein ZapE				05845	15955	04545
cell division protein ZapE						15000
cell division protein ZapA	08850				09840	08940
septal ring lytic transglycosylase RlpA family protein						15990
chromosome segregation protein			09600	19430		02005
chromosome partitioning protein ParA						08070
capsular biosynthesis protein						11175
type 1 fimbrial protein						07975
collagen-like protein	12450	00545		04875	07365	20785
transcription elongation factor GreAB			04160	06440		
DNA gyrase inhibitor YacG						15320
DNA gyrase subunit A			09390			02230
Flagella proteins						
flagellin					17930	
flagellar export chaperone FliS					17915	
flagellar hook protein FlgE					16950	
flagellar hook-associated protein FlgK						22560
flagellar biosynthesis anti-sigma factor FlgM						05605
flagellar basal body-associated protein FliL			06495			
Chemotaxis protein						
chemotaxis protein				08535	15630	
chemotaxis protein CheV					05555	
Peptidasen / Proteasen / Aminotransferasen						
aminotransferase class V-fold PLP-dependent enzyme		09370				
signal peptidase			15425			
BREX system P-loop protein BrxC						21680
peptidase						04440
M18 family aminopeptidase						02710
ATP-dependent zinc protease						13515
osmoprotectant NAGGN system M42 family peptidase			09295			
amidase					17665	
DJ-1/PfpI family protein			15840	16830		05460
Sonstiges						
lipocalin family protein			13625	15255		
lipocalin-like domain-containing protein				00960		
SpoVR family protein			00105	07580		08300
aminoacyltransferase				15840		
pilus assembly protein				13800		
Purine and Pyrimidine metabolism*						

Purine and Pyrimidine metabolism						
5-(carboxyamino)imidazole ribonucleotide mutase			02965	10555		
ribonucleotide-diphosphate reductase subunit beta		14600		01030		
nucleoside deaminase						00525
pseudouridine synthase						03325
single-stranded-DNA-specific exonuclease RecJ			15255			06845
exodeoxyribonuclease V subunit gamma			19260			21220
bifunctional GTP diphosphokinase/guanosine-3',5'-bis pyrophosphate 3'-pyrophosphohydrolase			02140			
2-oxo-4-hydroxy-4-carboxy-5-ureidoimidazoline decarboxylase					17500	
DNA replication and methylation						
replication initiation protein			22630			
type I DNA topoisomerase			11755	03020		03240
ATP-dependent DNA helicase DinG	12440		05680	04865		20795
DNA helicase II				10460		22860
DNA-directed RNA polymerase subunit beta'	19650		03160	07305		16610
RNA polymerase sigma factor RpoS		15815				
DNA-directed RNA polymerase subunit beta			03155			16615
DNA polymerase III subunit alpha			14935	17790		06500
PHP domain-containing protein						22470
nucleotidyltransferase			16595			
elongation factor			15005			07020
site-specific DNA-methyltransferase	21710					
DNA (cytosine-5-)-methyltransferase		01610	03610			
N-6 DNA methylase					18825	
BREX-1 system adenine-specific DNA-methyltransferase PglX						21670
Rsd/AlgQ family anti-sigma factor						14205
ribbon-helix-helix protein, CopG family			22965			11015
transcription/translation regulatory transformer protein RfaH						02180
Cu(I)-responsive transcriptional regulator						12050
IS66 family transposase		21660				
integrase					21825	
integrase arm-type DNA-binding domain-containing protein	19560		16215			
RNA metabolism*						
RNA translation						
ATP-dependent RNA helicase HrpA			21565	21745		22255
DEAD/DEAH box helicase	09635		21495			
DEAD/DEAH box helicase	02215		03975	21810		20085
DEAD/DEAH box helicase	18020		07435	06625		
DNA-directed RNA polymerase subunit beta'				07300		
RNA polymerase subunit sigma			14710	17520		
RNA polymerase subunit sigma				17525		
sigma-70 family RNA polymerase sigma factor						08890
class I SAM-dependent rRNA methyltransferase	13460		18750			
tRNA pseudouridine(38-40) synthase TruA	06300					
tRNA guanosine(34) transglycosylase Tgt	03375	01165	05060	05510		14560
tRNA cyclic N6-threonylcarbamoyladenosine(37) synthase TcdA			15055	17910		
valine--tRNA ligase				18315		07050
glutamate--tRNA ligase						01705
threonine--tRNA ligase				01525		19385
23S rRNA (uracil(1939)-C(5))-methyltransferase RlmD						04220
RNA degradation						
MBL fold metallo-hydrolase	21385	11940	10280		23120	04350
MBL fold metallo-hydrolase			12010			12070
DNA/RNA nuclease SfsA	13530					
CoA pyrophosphatase						06965
Riboflavin metabolism*						
GTP cyclohydrolase II		21355				
bifunctional diaminohydroxyphosphoribosylaminopyrimidine deaminase/5-amino-6-(5-phosphoribosylamino)uracil reductase RibD		21345				
WD40 repeat domain-containing protein		21350				
6,7-dimethyl-8-ribityllumazine synthase						05800
Stress resistantce*						
Chaperons						
molecular chaperone DnaJ			18865	19770		
co-chaperone HscB			05120			
Hsp20 family protein			07305			01670
Hsp70 family protein			12450	14130		12490
small heat shock protein sHSP20-GI	17105					
molecular chaperone			20200			
acid-activated periplasmic chaperone HdeA			17140	10735	00275	
DNA repair						
deoxyribodipyrimidine photo-lyase		15665				
AP endonuclease		06945				
GIY-YIG nuclease family protein		20845				
DNA repair protein RadA			04115			
DNA repair protein RecN						21795
DNA mismatch repair protein MutS						21000
DNA-3-methyladenine glycosylase						16030
Antibiotica resistance						
antibiotic biosynthesis monooxygenase			16680			
penicillin-binding protein 1B				19545		
beta-lactamase family protein						20805
Toxin-Antitoxin						
ParD-like family protein				02860		
type II toxin-antitoxin system RelE/ParE family toxin			22550		12300	
glutathione -transferase family protein			06940			17620
glutathione S-transferase family protein			00380	07840		
Other						
cold-shock protein	18715	16040	05615			
cold-shock protein			15080			
OsmC domain/YcaO domain-containing protein						00710
XRE family transcriptional regulator						11055
arsenical resistance protein ArsH		07425				
CsbD family protein				17295		
type VI secretion system tube protein Hcp				10990		
type II and III secretion system protein family protein		11830				
universal stress protein						04935
universal stress protein						02810
universal stress protein			16145	16535		03265
Virulence*						
Virulence						
LysR family transcriptional regulator			11935			
LysR family transcriptional regulator		14605	07845			09265
helix-turn-helix transcriptional regulator			14395			
virulence factor SrfB			02380			
HNH endonuclease				10365		
tryptophan 7-halogenase	01255					
Sonstiges						
metal ABC transporter ATPase	22155	20880				
metalloregulator ArsR/SmtB family transcription factor					10190	
tellurite resistance TerB family protein			15245	18100		06835
voltage-gated potassium channel protein						18775
RcnB family protein						17365
dinitro_DRAG: ADP-ribosyl-[dinitrogen reductase] hydrolase						19470

Urease*						
urease subunit alpha			20620			18740
urease subunit beta		14295	20625			
urease subunit gamma			20630			18730
urease accessory protein UreG			12505		10980	12540
urease accessory protein UreG			20605			18755
urease accessory protein UreE			20615	14175		
Sensor-histidin kinase recognizing oxygen*						
PAS domain-containing protein				21260		
PAS domain S-box protein			14465	17275	14425	
Inositol metabolism*						
inositol 2-dehydrogenase					22060	
Intracellular storage reserve material*						
phasin family protein						13345
poly(3-hydroxyalkanoate) granule-associated protein PhaF			13390	15025		
SDR family NAD(P)-dependent oxidoreductase, 3-hydroxybutyrate dehydrogenase						07720
3-hydroxybutyrate dehydrogenase				00525		######
3-hydroxybutyrate dehydrogenase						19025
acetyl-CoA C-acyltransferase			18455			19050
CoA transferase subunit B						20990
CoA transferase subunit A						######
CoA transferase subunit A						20985
CoA transferase						23075
Oxidoreductases *						
FAD-binding oxidoreductase		13245		00610	02000	00205
FAD-dependent oxidoreductase						07700
NAD(P)/FAD-dependent oxidoreductase					11615	13175
NADH:flavin oxidoreductase/NADH oxidase			15250	18105		06840
NAD(P)-dependent oxidoreductase				04210		04355
Domain containing enzymes*						
DUF1654 domain-containing protein	09385					
DUF4297 domain-containing protein	09630					
CBS domain-containing protein	16635		12950			
DUF4105 domain-containing protein		02175				
DUF3299 domain-containing protein		05690				
DUF3857 domain-containing transglutaminase family protein			17105			
DUF2288 domain-containing protein			05785			
DUF2875 domain-containing protein			16865			
DUF3800 domain-containing protein				04390		
dodecin domain-containing protein					08640	
DUF883 domain-containing protein				09050	05610	
DUF883 family protein				03325		
WYL domain-containing protein						21695
CerR family C-terminal domain-containing protein						14670
DUF4142 domain-containing protein	11620		11425			03485
DUF4136 domain-containing protein	14910	11895	12060	13740		
DUF1127 domain-containing protein	20130					
DUF2236 domain-containing protein	13470					
DUF2892 domain-containing protein	18185	12140		21600		
DUF3203 family protein	14205		07565			
heavy-metal-associated domain-containing protein	22510		11975	13660		12035
BON domain-containing protein	13450	17355	18760	19665		
STAS domain-containing protein		15000	06475	21210		22645
DUF1289 domain-containing protein		14595				
PepSY domain-containing protein		09225	20335	16195		04565
DUF3313 domain-containing protein			07680	12725		01215
DUF1289 domain-containing protein			20970	01035		
DUF4174 domain-containing protein			22255	11355		
DUF465 domain-containing protein			16685			17500
DUF924 family protein			05000			14590
DUF4398 domain-containing protein			15150	18005		06715
DUF2934 domain-containing protein			07615	12780		01285
DUF853 family protein			15945			
DUF1161 domain-containing protein			01575	09060		
DUF1269 domain-containing protein			07515	12880		01385
macro domain-containing protein			08800	02660		
PilZ domain-containing protein			04120	06480		
DUF4136 domain-containing protein				13745		12120
DUF4440 domain-containing protein				18575	15245	07210
DUF411 domain-containing protein				12765		
DUF2789 domain-containing protein				00725		14340
Ig-like domain repeat protein				02560		
CHAD domain-containing protein				02740		02950
SIMPL domain-containing protein						15120
Sonstiges*						
cupin		14610	16105			05200
ATP-binding protein			03595			
HDOD domain-containing protein			12760			09710
tetratricopeptide repeat protein				15965		
protein translocase subunit SecD					20880	
AMP-binding protein			13160			
TIM barrel protein	04805					17825
coenzyme F420 hydrogenase						11195
protease Lon-related BREX system protein BrxL						21630
PA2169 family four-helix-bundle protein	16065	07860	14515			
RidA family protein			02280	09755		09535
PhoH family protein			21795			07160
TIGR01777 family protein			19570			
YgdI/YgdR family lipoprotein			18405			
CpaF family protein			12110	13795		12170
YeaH/YhbH family protein			00100			
linear amide C-N hydrolase				12945		
thiamine-phosphate kinase					13925	
TIGR02647 family protein						09395
sel1 repeat family protein						02770
YegP family protein			15865	16805		05435
DNA binding protein			16970	10905		
molybdenum cofactor guanylyltransferase MobA			11615			03310
NAD(P)-binding protein		18155		01340		
NAD(P)-binding protein				07700		
acetyltransferase			09805			
Hypotetical proteins*						
hypothetical protein	21820	10875	20715	19420	02190	19880
hypothetical protein	05995	03240	10015	03010	02730	23315
hypothetical protein	12310	13420	02340	08435	06325	08945
hypothetical protein	18355	17820	21030	04755	09835	06010
hypothetical protein	06890	04940	05790	01245	02860	11020
hypothetical protein	22925	12910	06185	21930	-	20275
hypothetical protein	09640	20830	11765	13410		17720
hypothetical protein	05400	07305	02375	22100		03490
hypothetical protein	00385	18815	08900	09095		16385
hypothetical protein	08445		16790	15390		10040
hypothetical protein	22305		05590	21000		21725
hypothetical protein	11630		21800	09435		01940

hypothetical protein	09150		22735	03200		21325
hypothetical protein	22495		11420	20795		19390
hypothetical protein	04145		23450	12950		11030
hypothetical protein	11615		01870	09985		23160
hypothetical protein			10880	01530		
hypothetical protein			07445	19850		
hypothetical protein			01830	08910		
hypothetical protein			18945	01115		
hypothetical protein			19115	20025		
hypothetical protein			07025	21005		
hypothetical protein			01430			
hypothetical protein			22950			
hypothetical protein			09925			

Table S11| Physiological characterization of *Pseudomonas* strains based on an API 20 NE test. NO_3= reduction of nitrate to nitrite and nitrate to nitrogen, TRP= indole production, GLU= glucose fermentation, ADH= arginine dihydrolase, URE= urease, ESC= β-glucosidase hydrolysis, GEL= protease hydrolysis, PNPG= β-galactosidase, GLU= glucose, ARA= arabinose, MNE= mannose, MAN= mannitol, NAG= N-acetyl-glucosamine, MAL= maltose, GNT= potassium gluconate, CAP= capric acid, ADI= adipic acid, MLT= malate, CIT= trisodium citrate, PAC= phenylacetic acid and OX= cytochrome oxidase.

	TMW	NO_3	TRP	GLU	ADH	URE	ESC	GEL	PNPG	GLU	ARA	MNE	MAN	NAG	MAL	GNT	CAP	ADI	MLT	CIT	PAC	OX
										Assimilatory tests												
P. lundensis	2.1732	-	-	-	+	+	-	-	-	+	+	-	-	-	-	+	-	-	+	+	-	+
	2.2076	-	-	-	+	+	-	+	-	+	+	-	-	-	-	+	-	-	+	+	-	+
P. weihenstephanensis	2.2077	-	-	-	+	-	-	-	-	+	-	-	-	-	-	+	-	-	+	+	-	+
	2.1728	-	-	-	+	-	-	-	-	+	-	-	-	-	-	+	-	-	+	+	-	+
P. fragi	2.2081	-	-	-	+	+	-	-	-	+	+	-	-	-	-	+	-	-	+	+	-	+
	2.2082	-	-	-	+	+	-	-	-	+	+	-	-	-	-	+	-	-	+	+	-	+

10. Publications, presentations, collaborations and students thesis

Publications in peer-reviewed journals:

Kolbeck, S., Reetz, L., Hilgarth, M. and Vogel, R.F. (2019) „Quantitative oxygen consumption and respiratory activity of meat spoiling bacteria upon high oxygen modified atmosphere". *Frontiers in microbiology, Section food microbiology*.
https://doi.org/10.3389/fmicb.2019.02398

Kolbeck, S., Ludwig, C., Meng, C., Hilgarth, M. and Vogel, R.F. (2020) „Comparative proteomics of meat spoilage bacteria predicts drivers for their coexistence on modified atmosphere packaged meat". *Frontiers in microbiology, Section food microbiology*.
https://doi.org/10.3389/fmicb.2020.00209

Kolbeck, S., Kienberger, H., Kleigrewe, K., Hilgarth, M. and Vogel, R.F. (2021) "Effect of high levels of CO_2 and O_2 on membrane fatty acid profile and membrane physiology of meat spoilage bacteria", *European food research and technology*,
https://doi.org/10.1007/s00217-020-03681-y

Kolbeck, S., Abele, M., Hilgarth, M. and Vogel, R. F. (2021) "Comparative proteomics reveals the anaerobic lifestyle of meat-spoiling *Pseudomonas* species", *Frontiers in microbiology*, Section physiology and metabolism.
https://doi.org/10.3389/fmicb.2021.664061

Kolbeck, S., Hilgarth, M. and Vogel, R. F. (2021) "Proof of concept: "Predicting meat spoilage by an integrated oxygen sensor spot in MA-packages", *Letters in applied microbiology*,
https://doi.org/10.1111/lam.13473

Publications at the website of PreSens precision sensing GmbH

Kolbeck et al. 2019. Quantification of oxygen consumption of meat-spoiling microorganisms below 30% CO2 / 70% O2 atmosphere, PreSens precision sensing GmbH, https://www.presens.de/knowledge/publications/application-note/

Oral presentation at international symposia

Kolbeck S, Reetz L, Hilgarth M, Vogel RF. 2019. “Characterization of meat-spoiling bacteria regarding their respiratory activity and quantitative oxygen consumption in high oxygen atmosphere” Oral presentation at “3rd Innovations in food packaging, shelf-life and food safety” conference held on 09.10.2019 in Erding, Germany.

Oral presentations at meetings of the steering committee (AiF 19993N)

Kolbeck S, Hilgarth M, Vogel RF. 2020. “Contribution of single microorganisms to meat spoilage and O_2 consumption in packages with 30% CO_2 and 70% O_2.” Oral presentation at the annual AiF project meeting of the steering committee (19993N) held on 26.11.2020 per zoom online-conference.

Kolbeck S, Hilgarth M, Vogel RF. 2019. “Quantification of the oxygen consumption of meat-spoilage bacteria and their metabolic adaptation to different protective gas atmospheres.” Oral presentation at the annual AiF project meeting of the steering committee (19993N) held on 28.11.2019 in Freising, Germany.

Kolbeck S, Hilgarth M, Vogel RF. 2018. “Development of a non-destructive optical detection method for the individualized evaluation of meat spoilage in inert gas packaging with carbon dioxide and oxygen.” Oral presentation at the annual AiF project meeting of the steering committee (19993N) held on 29.11.2018 in Freising, Germany.

Students theses and contributions to this thesis

Nora Köller – Research internship: “Aerobic and anaerobic growth of *Pseudomonas* spp. on chicken breast filet”. 2021

Natalie Okan-Adjectey - Science seminar: “Effects of CO_2, as a protective gas, on growth and metabolism of meat microorganisms”. 2020

Rebecca Heigl – Master thesis: „Influence of rising concentrations of the protective gas carbon dioxide on the growth of meat spoiling bacteria”. 2020

Carina Stoll – Master thesis: “Characterization of oxygen consuming reactions of meat spoiling microorganisms at different gas atmospheres”. 2019

Leonie Reetz – Research internship: “Quantifizierung des Sauerstoffverbrauchs von fleischverderbenden Mikroorganismen unter 70% O_2 / 30% CO_2 Gasatmosphäre“. 2019

All students listed, performed their laboratory experiments and final theses under my supervision. Their results were incorporated into this thesis.

Collaborations

Mass spectrometric measurements, including proteomic (QExactive HF-X hybrid MS) and fatty acid analysis (GCMS-TQ8040), were performed by the “Bavarian center of biomolecular mass spectrometry” (BayBioMS, Freising, Germany). Sample preparation, data analysis and evaluation were conducted by me. qRT-PCR measurements using the StepOnePlus Real-Time PCR cycler were performed at the chair of plant breeding (Freising, Germany). Sample preparation, data analysis and evaluation were conducted under supervision by my master student Carina Stoll.